MONASH University

Examining PI3KC2α as an anti-thrombotic drug target

Maria Vasantha Selvadurai

(BSc(ScSchProg), BMedSc(Hons), DipLang)

A thesis submitted for the degree of Doctor of Philosophy
at Monash University in 2018
Department of Clinical Haematology

Table of Contents

Copyright Notice

Abstract

Background: Cardiovascular disease (CVD) is a significant and increasing health burden. Platelets are an essential component of thrombi, and thus are a major contributor to thrombosis and cardiovascular events. Therapeutics for the prevention and treatment of CVD generally focus on inhibiting platelet activation, however there are a number of limitations associated with anti-platelet treatments that utilise this strategy, including bleeding risks that limit dosing and a high rate of resistance. As a result, new approaches are critically needed. Two recent mouse genetic studies identified a role for the class II phosphoinositide 3-kinase, PI3KC2α, in platelet structure and function: platelets from mice deficient in PI3KC2α demonstrate structural changes to the internal membrane system sufficient to cause significant functional consequences in the setting of thrombosis. However, a number of questions remain: What is the underlying mechanism behind this effect? Does the same mechanism exist in human platelets? And, is this unique PI3KC2α-dependent mechanism drug targetable?

Aims: To define the mechanism by which PI3KC2α-deficiency is anti-thrombotic in mouse, to determine the role of PI3KC2α in human platelet structure and function, and to examine the validity of targeting PI3KC2α as an anti-thrombotic strategy.

Methods: To define the mechanism by which PI3KC2α-deficiency is anti-thrombotic in mouse platelets, platelet structure was analysed by scanning electron microscopy, transmission electron microscopy, and focused ion beam-scanning electron microscopy. Platelet lipid composition was analysed using liquid chromatography-tandem mass spectrometry. The function of the platelet membrane during platelet adhesion was examined in static activation and adhesion assays as well as shear-dependent ex vivo whole blood flow assays. To determine the role of PI3KC2α in human platelet structure and function, and to examine the validity of targeting PI3KC2α as an anti-thrombotic strategy, a rational drug design approach was used to develop a lead PI3KC2α inhibitor. The impact of pharmacological inhibition of PI3KC2α on platelet structure was examined using the various electron microscopy approaches, while function was examined in a series of standard in vitro assays, as well as ex vivo thrombosis in human blood, and in vivo thrombosis in mice.

Results: PI3KC2α deficiency leads to ultrastructural changes in mouse platelets specific to the open canalicular system, manifesting as a dilatation of the channels of this membrane network

throughout the cell including at the plasma membrane. This change in platelet membrane structure was not associated with changes to these platelets' lipid composition. Analyses of platelet membrane function revealed that PI3KC2α-deficient platelets demonstrate normal filopodia formation when activated in suspension, but markedly impaired thrombus formation in a setting known to involve membrane tether formation. A novel inhibitor of PI3KC2α was developed: MIPS-19416 had an IC_{50} of 13 nM against PI3KC2α and > 4-fold specificity over the major class I PI3K in platelets, p110β. Pharmacological inhibition of PI3KC2α with MIPS-19416 in human platelets fully recapitulated the structural and functional effects of PI3KC2α deficiency in mouse platelets. PI3KC2α inhibition did not impact upon thrombin-induced platelet activation or aggregation, or the function of the platelet receptors GPIb and $\alpha_{IIb}\beta_3$. Yet thrombus formation was significantly reduced with MIPS-19416 in two distinct in vivo mouse models, and two ex vivo human whole blood flow models, including the high shear model described above, where thrombosis has been shown to occur largely independently of canonical platelet activation.

Conclusion: These findings demonstrate that PI3KC2α is involved in the regulation of platelet membrane structure and function in both mice and humans. Inhibition of PI3KC2α has an anti-thrombotic effect that can be induced acutely, and that occurs specifically in the setting of thrombus formation under high shear forces. PI3KC2α appears to impact platelet function via a unique membrane-dependent mechanism that is independent of platelet activation. The results from this thesis suggest that targeting the platelet membrane via PI3KC2α may provide potential as a novel, thrombosis-specific anti-platelet strategy.

Publications During Enrolment

Falasca M, Hamilton JR, **Selvadurai MV**, Sundaram K, Adamska A, Thompson PE. Class II phosphoinositide 3-kinases as novel drug targets. J Med Chem. 2017 Jan 12;60(1):47-65.

Selvadurai MV, Hamilton JR. Structure and function of the open canalicular system – the platelet's internal membrane network. Platelets. 2018 Jun;29(4):319-25.

Submitted:

Selvadurai MV, Moon MJ, Zheng Z, Mountford SJ, Brazilek RJ, Iman RP, et al. Disrupting the platelet internal membrane via PI3KC2α inhibition impairs thrombosis independently of canonical platelet activation. (Submitted to *Science Translational Medicine* in December 2017, reviewed and returned with the decision 'opportunity to resubmit', estimated resubmission date November 2018).

Selvadurai MV, Brazilek RJ, Moon MJ, Rinckel J-Y, Eckly A, Gachet C, et al. The class II PI 3-kinase, PI3KC2α, regulates mouse platelet membrane structure and thrombotic function independently of membrane lipid composition. (Submitted to *Journal of Thrombosis and Haemostasis* in August 2018).

Declaration

I hereby declare that this thesis, except with the Graduate Research Committee's approval, contains no material which has been accepted for the award of any other degree or diploma at any university or equivalent institution and that, to the best of my knowledge and belief, this thesis contains no material previously published or written by another person, except where due reference is made in the text of the thesis.

This thesis includes 2 publications; 1 returned for revision and 1 submitted. The core theme of the thesis is the role of PI3KC2α in platelet structure and function, and the viability of targeting PI3KC2α as an anti-thrombotic strategy. The ideas, development and writing up of all the papers in the thesis were the principal responsibility of myself, the student, working within the Department of Clinical Haematology under the supervision of Associate Professor Justin Hamilton.

The inclusion of co-authors reflects the fact that the work came from active collaboration between researchers and acknowledges input into team-based research.

In the case of Chapters 2 and 3, my contribution to the work involved the following:

Thesis Chapter	Publication Title	Status *(published, in press, accepted or returned for revision, submitted)*	Nature and % of student contribution	Co-author name(s) Nature and % of Co-author's contribution*	Co-author(s), Monash student Y/N*
2	The Class II PI 3-kinase, PI3KC2α, regulates mouse platelet membrane structure and thrombotic function independently of membrane lipid composition	Submitted	70%	1) Rose Brazilek, data acquisition and analysis (Fig. 5), input 5% 2) Mitchell Moon, technical assistance, input 1% 3) Jean-Yves Rinckel, technical assistance, input 1% 4) Anita Eckly, experimental design, input 1% 5) Christian Gachet, experimental design, input 1% 6) Peter Meikle, data acquisition and analysis (Fig. 3), input 3% 7) Harshal Nandurkar, experimental design, input 1% 8) Warwick Nesbitt, experimental design, input 2%	Yes (Rose Brazilek, Mitchell Moon)

				9) Justin Hamilton, study conception, experimental design, writing, input 15%	
3	Disrupting the platelet internal membrane via PI3KC2α inhibition impairs thrombosis independently of canonical platelet activation	Returned for revision	50%	1) Mitchell Moon, data acquisition and analysis (Fig. 4., Fig. 5A, B, D), input 30% 2) Zhaohua Zheng, compound testing and initial experiments, input 1% 3) Simon Mountford, compound synthesis, input 1% 4) Rose Brazilek, data acquisition and analysis (Fig. 6F), input 1% 5) Rizani Iman, data acquisition (Fig. 1), input 0.5% 6) Lavika Gupta, data acquisition (Fig. 4C, D, E), input 0.5% 7) Sharelle Sturgeon, data acquisition and analysis (Fig. 5C), input 1% 8) Jean-Yves Rinckel, technical assistance, input 1% 9) Anita Eckly, experimental design, input 0.5% 10) Christian Gachet, experimental design, input 0.5% 11) Warwick Nesbitt, experimental design, input 1% 12) Ian Jennings, experimental design, input 1% 13) Philip Thompson, experimental design, input 1% 14) Justin Hamilton, study conception, experimental design, writing, input 10%	Yes (Mitchell Moon, Rose Brazilek, Rizani Iman, Lavika Gupta)

I have renumbered sections of submitted or published papers in order to generate a consistent presentation within the thesis.

Student signature: Date:

The undersigned hereby certify that the above declaration correctly reflects the nature and extent of the student's and co-authors' contributions to this work. In instances where I am not the responsible author I have consulted with the responsible author to agree on the respective contributions of the authors.

Main Supervisor signature: Date:

Acknowledgments

I would like to acknowledge the many people who have contributed to this research project, and who have enabled the completion of this thesis. In particular I would like to thank the following people:

First and foremost, my main supervisor, Associate Professor Justin Hamilton. I have learned so much over the past few years and I am very grateful for the opportunity to have been a part of your lab. Thank you for your support, encouragement, constructive criticism, patience and guidance, as well as the countless opportunities you have fostered. You have taught me skills that I will continue to use in the future, both within and outside of research, and I really could not have asked for a better supervisor.

Secondly, my co-supervisor, Professor Harshal Nandurkar. Thank you for providing me with the opportunity to undertake my PhD at the ACBD, for the valuable career advice and for your ongoing support of my work. I hope I will have the opportunity to work with you in a clinical setting in the future.

I would also like to thank the members of the Hamilton group, for their contributions to this work and assistance in the lab over the course of this project, in particular to Mitchell Moon, who performed much of the ex vivo and in vivo work in Chapter 3 of this thesis, and Shauna French, who has been an invaluable source of advice. I would also like to thank past members of the lab, whose work paved the way for this research project, and the staff and students of the ACBD, especially the student room crew, for their friendship over the last few years.

I have been lucky enough to work with a number of different research groups during the course of this project, and in particular I would like to thank the Electron Microscopy group at the Etablissement Français du Sang where I undertook the first year of this project. To Professor Christian Gachet, for the opportunity to undertake my research at the EFS, and to Anita Eckly, Jean-Yves Rinckel, Fabienne Proamer and Neslihan Ulas, for your help with all things FIB-SEM as well as your friendship, French language lessons (and all of the coffee times!). I would also like to thank the staff at the Ramaciotti Centre for Electron Microscopy for their assistance with electron microscopy work, and to Rose Brazilek and Warwick Nesbitt for their work with the microfluidic assay.

Finally I would like to thank my family, particularly Ma, Lou and Michael, for their ongoing support and encouragement, as well as my friends who have been there to celebrate the highs, commiserate the lows, and put up with my eternal busy-ness. And finally, to Imran, who against all odds has been around from the beginning of this journey to its end, for helping me to make it through. Thank you for everything – it's your turn now.

List of Abbreviations

3-PPI – 3-phosphorylated phosphoinositide

ADP – adenosine diphosphate

AFM – atomic force microscopy

ATP – adenosine triphosphate

BSS – Bernard-Soulier syndrome

CLL – chronic lymphocytic leukaemia

COX-1 – cyclo-oxygenase 1

CVD – cardiovascular disease

δR – delta opioid receptor

DAPT – dual anti-platelet therapy

DTS – dense tubular system

ECM – extracellular matrix

EGF – epidermal growth factor

EM – electron microscopy

FIB-SEM – focused ion beam-scanning electron microscopy

GP – glycoprotein

GPCR – G protein-coupled receptor

GSK3 – glycogen synthase kinase-3

mTOR – mammalian target of rapamycin

OCS – open canalicular system

PAR-1 – protease-activated receptor 1

PH – pleckstrin homology

PI – phosphatidylinositol

PI3K – phosphoinositide 3-kinase

PI(3)P – phosphatidylinositol 3-phosphate

PI(3,4)P$_2$ – phosphatidylinositol 3,4-bisphosphate

PI(3,4,5)P$_3$ – phosphatidylinositol 3,4,5-trisphosphate

PI(4)P – phosphatidylinositol 4-phosphate

PI(4,5)P$_2$ – phosphatidyl inositol 4,5-bisphosphate

PX – Phox homology

RBD – Ras-binding domain

SBI – surgical brain injury

SEM – scanning electron microscopy

T2DM – type 2 diabetes mellitus

TEM – transmission electron microscopy

TGN – trans-Golgi network

TxA$_2$ – thromboxane A$_2$

VAMP – vesicle-associated membrane protein

Vps34 – vacuolar protein sorting 34

vWF – von Willebrand factor

CHAPTER 1

Introduction

1.1 Haemostasis and Thrombosis

Cardiovascular disease (CVD) is a significant, increasing health burden both nationally and internationally. CVD is the leading cause of death in Australia[1], and atherothrombotic diseases are responsible for more than 25% of deaths worldwide[2]. Platelets are an essential component of thrombi, and thus are a major contributor to thrombosis and cardiovascular events[3].

Platelets are anuclear subcellular fragments, which represent the second most abundant cell type in the blood after red blood cells[4]. In humans, there are about 1 trillion platelets present in the circulation at any one time, and approximately 10^{11} platelets are produced from megakaryocytes in the bone marrow each day[5], with the mass of platelets in the circulation regulated by thrombopoietin[6]. Platelets circulate in the bloodstream for 7-10 days[7].

The main biological function of platelets is haemostasis, a physiological response to vascular or tissue damage, whereby a clot is formed at the side of damage to prevent excessive blood loss[4]. During thrombus formation platelets undergo three defined steps – adhesion, activation and aggregation (Figure 1.1).

When a vascular injury is sustained, extracellular matrix (ECM) proteins such as collagen become exposed. Von Willlebrand factor (vWF) in the circulation binds to this exposed collagen and uncoils, which leads to exposure of the vWF A1 domain[8]. Platelets in the bloodstream bind to the A1 domain via the glycoprotein (GP)Ib/IX/V complex, in a transient binding step, which causes platelets to slow down and roll over the site of injury[9]. vWF thus acts as a bridge between the ECM and circulating platelets.

The decreased velocity when rolling allows platelets to bind to collagen via the receptors GPVI and integrin $\alpha_2\beta_1$, and stably adhere to the site of injury[10]. GPVI is associated with the FcR γ-chain, and its binding to collagen triggers FcRγ receptor complex clustering and the initiation of signalling pathways that lead to platelet activation[11].

When platelets are activated, they lose their discoid shape and become spherical, before extending filopodia, flattening and spreading[5]. A range of soluble agonists including thromboxane A_2 (TxA$_2$) and adenosine diphosphate (ADP) are released, which stimulate platelets in an autocrine fashion to enhance thrombus formation[12]. Thrombus propagation occurs as the platelets in the developing clot spread to form a surface for the recruitment of more platelets.
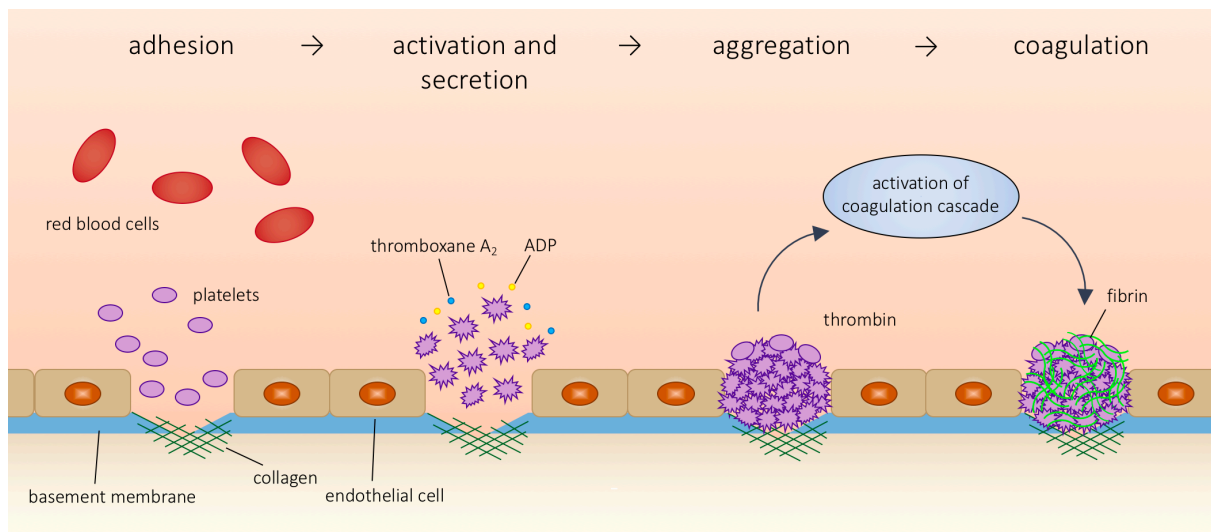
Figure 1.1. Platelets are the major mediator of haemostasis. In haemostasis, platelets first bind transiently to exposed subendothelial proteins, before adhering stably, becoming activated, secreting granule contents and finally aggregating. A fibrin mesh subsequently forms to stabilise the thrombus.

During platelet activation, the conformation of the integrin $\alpha_{IIb}\beta_3$ receptor changes from a low-affinity to a high-affinity state via inside-out signalling, which is triggered by GPIb/IX/V-vWF and GPVI-collagen interactions[13]. In its high-affinity state, integrin $\alpha_{IIb}\beta_3$ can bind soluble fibrinogen, which forms bridges between platelets, allowing platelet aggregation to occur. Integrin $\alpha_{IIb}\beta_3$ can also bind other soluble plasma proteins such as vWF, fibronectin and vitronectin in addition to fibrinogen, with the sum of these interactions forming a stably adhered haemostatic plug[14].

The platelet aggregate is stabilised via the activation of the coagulation cascade, which leads to the formation of a fibrin mesh around the thrombus (Figure 1.1). In this process, coagulation complexes such as the prothrombinase complex come together on the surface of activated platelets in the developing aggregate. This enables the generation of thrombin and fibrin, which are required for the growth and stability of the thrombus[15]. In addition to being the site at which coagulation factors convene to initiate the coagulation cascade, platelets are themselves a source of some coagulation factors, and of factors involved in the regulation of coagulation, including factors V and XIII, prothrombin and polyphosphates[16].

While haemostasis is a normal, healthy process, thrombosis is a pathological condition where occlusive blood clots form within the vasculature. Thrombosis is essentially a haemostatic response that has gone too far, as such, platelets also have a prothrombotic function by contributing to thrombosis via the same mechanisms by which they contribute to haemostasis. Platelets and fibrin are the major mediators of thrombosis[17].

1.2 Pathophysiology of Arterial Thrombosis

Arterial thrombosis is an increasingly prevalent condition and a significant health burden worldwide. It can lead to myocardial infarction and ischaemic stroke, which are the most common manifestations of CVD. Arterial thrombosis generally occurs in arteries that have been damaged by atherosclerosis, the formation of fatty plaques on the inner wall of blood vessels. These plaques are composed of lipids, cholesterol, calcium and other substances, and covered by a fibrous cap that separates the contents of the plaque from the blood within the vessel[18].

The development of atherosclerotic lesions is a slow and often clinically silent process. It begins with changes in endothelial cell permeability, that lead to the accumulation of lipids within the vessel wall. This results in the recruitment of monocytes or macrophages, which scavenge the

lipids and become lipid-filled foam cells[19]. As the plaques grow, they cause narrowing of the vessel lumen and consequent restriction of blood flow. The plaque eventually develops a fibrous cap that covers the lipid-rich core[20], as well as scattered calcifications[21]. Sites within an artery that are affected by atherosclerosis are thus subjected to local disturbances in blood flow and increased levels of shear stress.

While stable atherosclerosis does not generally produce clinical symptoms, atherosclerotic plaques may become unstable and rupture. Rupture of an atherosclerotic plaque leads to exposure of its contents and the vessel subendothelium, which contains thrombogenic substrates, and thus leads to platelet adhesion, aggregation and clot formation[22]. Thrombus formation over the ruptured plaque can cause full vessel occlusion and downstream ischaemia. Even in the absence of frank rupture, superficial erosion of the plaque surface is often sufficient to provoke thrombosis and cardiovascular events[23,24]. Plaques that have an increased risk of rupture include those where the fibrous cap is thin, and those that are heavily infiltrated with foam cells. The areas within a plaque where these conditions are most prominent are generally the points at which rupture occurs[25].

Platelets also have a proinflammatory function and can increase the recruitment of monocytes to sites of atherosclerotic plaque formation, through adhesive interactions with endothelial cells. These cell interactions are able to induce a local inflammatory response which accelerates plaque growth[26]. Furthermore, infiltration of the plaque by macrophages can reduce its stability, predisposing it to rupture and subsequent thrombosis[23].

Risk factors for the development of atherosclerotic disease include hypertension, hypercholesterolaemia, obesity, insulin resistance, diabetes, and a lack of physical activity[27]. The prevalence of these risk factors in the population has been increasing over recent decades. This underlies the growing global burden of CVD, for which pharmacological therapeutic and preventive options, although numerous, are currently limited in terms of clinical benefit and side effects.

1.3 Current Anti-Platelet Therapies

Therapies for CVD currently include both anti-platelet drugs, and anti-coagulant drugs, which target fibrin formation. As platelets are the major components of arterial thrombi, anti-platelet

agents are generally used in the prevention and treatment of acute coronary syndromes and ischaemic stroke. There are a number of anti-platelet therapies currently used clinically, however these are limited both in terms of efficacy and in terms of dose-limiting side effects, particularly with regards to bleeding risk. Anti-platelet therapies generally target the activation phase of thrombus formation, which aims to prevent thrombosis while maintaining haemostatic function, via a number of different molecular targets (Figure 1.2).

Aspirin is the oldest and most widely-used anti-platelet agent. Its active product, salicylic acid, is an irreversible inhibitor of the cyclo-oxygenase 1 (COX-1) enzyme, preventing the substrate, arachidonic acid, from accessing the enzyme's active site[3]. TxA_2, which is produced by platelet COX-1 and potentiates platelet activation, is thus not produced[3]. As the inactivation is irreversible, the effect of aspirin lasts for the lifetime of the platelet. However, aspirin use is associated with side effects including gastric ulcers, kidney failure, and bleeding[28]. Furthermore, aspirin is also ineffective at preventing thrombotic events in up to 40% of patients; and a resistance phenomenon has been observed in patients on long-term aspirin therapy[29].

A second class of anti-platelet drugs is the ADP receptor antagonists, which include clopidogrel, prasugrel and ticagrelor. The most commonly used of these, clopidogrel, is an irreversible antagonist of the ADP receptor, $P2Y_{12}$[3]. Like aspirin, it is an orally administered prodrug; it is converted into the clopidogrel active metabolite by the cytochrome P450 system in the liver. Clopidogrel covalently binds to a cysteine residue in the $P2Y_{12}$ receptor, irreversibly inactivating it, and thus preventing amplification of platelet activation and subsequent thrombus propagation[30]. Like aspirin, clopidogrel treatment is associated with a number of side effects, including cardiac events, gastrointestinal problems, neutropenia and thrombotic thrombocytopaenic purpura[31]. In addition, the conversion of the prodrug to the active metabolite is highly variable across the population, and thus patient responses vary significantly[32].

Dual anti-platelet therapy (DAPT), that is, aspirin in combination with a $P2Y_{12}$ receptor antagonist, is frequently used to reduce morbidity and mortality in certain patients with CVD, given the limitations associated with single-agent therapy. In patients with acute coronary syndromes, DAPT is more effective than single-agent therapy – the combination of clopidogrel and aspirin has been shown to reduce the risk of mortality and major vascular events[33,34].
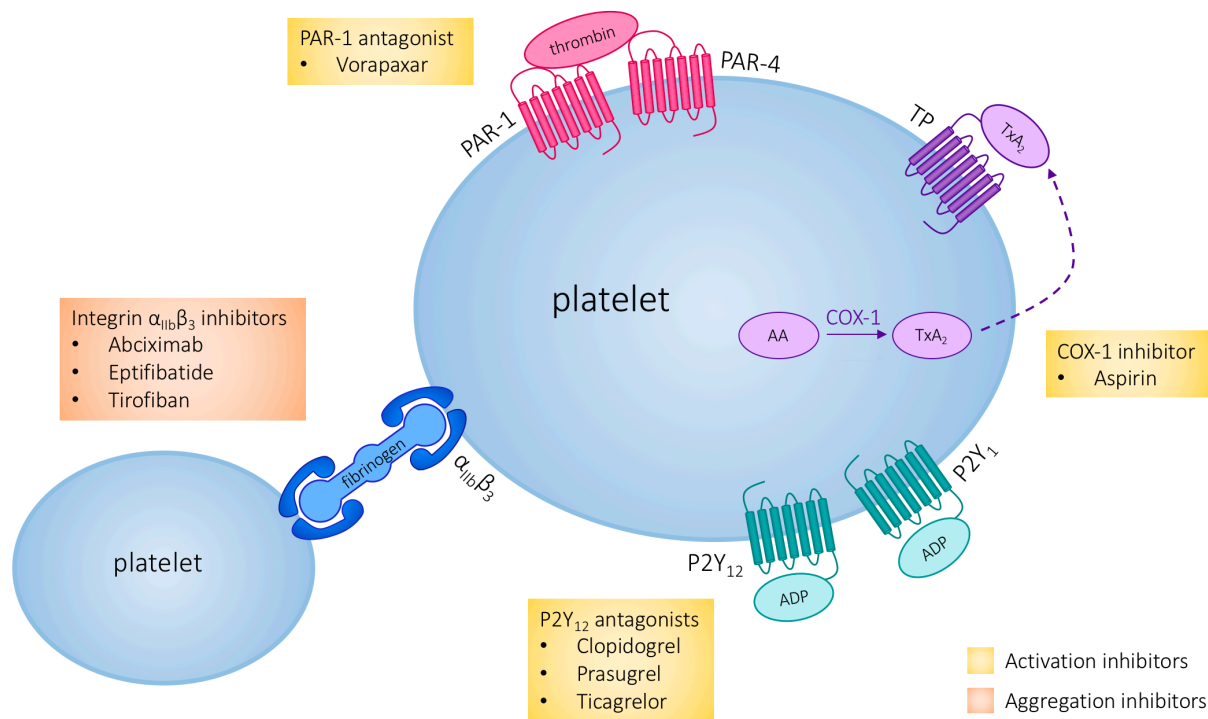
**Figure 1.2. Current anti-thrombotic agents.** Anti-platelet agents currently used clinically include the COX-1 inhibitor aspirin, P2Y$_{12}$ receptor antagonists such as clopidogrel, and the PAR-1 antagonist vorapaxar. These all inhibit the activation phase of thrombosis. Integrin $\alpha_{IIb}\beta_3$ inhibitors such as abciximab prevent platelet aggregation rather than activation and are used in limited clinical scenarios.

However, other studies have suggested that this benefit only extends to patients with established, symptomatic cardiovascular disease[35], and that there is an increased risk of bleeding with clopidogrel or ticagrelor DAPT compared to aspirin monotherapy[35,36].

The most potent anti-platelet therapeutics are the integrin $\alpha_{IIb}\beta_3$ inhibitors which, unlike other anti-platelet agents, target platelet aggregation. During this process, fibrinogen binds to integrin $\alpha_{IIb}\beta_3$ receptors on adjacent platelets, forming a bridge between the cells that leads to aggregation. Integrin $\alpha_{IIb}\beta_3$ inhibitors prevent fibrinogen from binding to the receptor, and thus prevent platelet-platelet bonds from occurring[37]. Drugs in this class include abciximab, eptifibatide and tirofiban, and these are used only in acute coronary syndromes – long term, preventive usage of these drugs is limited due to the high risk of bleeding and intravenous route of administration[38].

Finally, a protease-activated receptor 1 (PAR-1) inhibitor, vorapaxar, has in recent years been approved for therapeutic use, as the first anti-PAR-1 drug to be commercially available[39]. It is used concomitantly with aspirin or clopidogrel for the prevention of secondary cardiac events in patients with a history of heart attack or who have peripheral arterial disease[40,41]. A phase III trial found that it is able to significantly reduce the recurrence of cardiovascular events, however it increases the risk of bleeding when used in combination with other anti-platelet agents[41]. This significant increase in bleeding risk has limited the clinical use of vorapaxar to date, and it appears that its utility is restricted to patients with a high risk of ischaemic events but low risk of bleeding[42].

Despite the numerous anti-platelet agents available for the treatment and prevention of CVD, a drug that is able to adequately prevent thrombosis without significantly affecting haemostatic function remains elusive. Phosphoinositide 3-kinases (PI3Ks), in particular class I PI3Ks, have been shown to play a role in platelet activation, and inhibitors of class I PI3K isoforms are currently in development as anti-platelet agents[43]. However, it has been shown that pan-PI3K inhibitors have a greater effect on platelet function than class I-specific PI3K inhibitors, suggesting a role for a second class of these enzymes, class II PI3Ks, in platelet function[44]. Yet, to date little is known about the biological roles of the class II PI3Ks, let alone whether they could be targeted therapeutically in the context of thrombotic disease.

1.4 Phosphoinositide 3-Kinases

The PI3Ks are a family of lipid kinases, which catalyse phosphorylation at the 3'-position hydroxyl group of the inositol ring of phosphoinositides. Their products, the 3-phosphorylated phosphoinositides (3-PPIs), are second messengers that play key roles in a wide range of cellular processes, including proliferation, differentiation, migration, apoptosis, cytoskeletal organisation, membrane trafficking and autophagy.

Pathologically, the PI3K pathway is one of the most frequently dysregulated signalling pathways leading to the onset of cancer[45]. Disruptions in this pathway are also implicated in disease states such as inflammation and autoimmunity[46], while PI3K inactivation is present in some neuropathies, myopathies and ciliopathies[47].

There are eight isoforms of PI3Ks, which are divided into three classes based on structural and functional similarities (Figure 1.3). All isoforms have a PI3K core structure, made up of a C2 domain, a helical domain, and a catalytic kinase domain. Class I PI3Ks are heterodimers that consist of a catalytic subunit and a regulatory subunit, as is the sole class III PI3K, vacuolar protein sorting 34 (Vps34). Class II PI3Ks are thought to function as monomers.

PI3Ks generate three 3-PPIs – phosphatidylinositol 3,4,5-trisphosphate (PI(3,4,5)P_3), phosphatidylinositol 3,4-bisphosphate (PI(3,4)P_2), and phosphatidylinositol 3-phosphate (PI(3)P), produced from phosphatidylinositol 4,5- bisphosphate (PI(4,5)P_2), phosphatidylinositol 4-phosphate (PI(4)P), and phosphatidylinositol (PI) respectively. There is an overlap in products produced between the three classes, yet they appear to have non-redundant functions.

Class I PI3Ks have been intensively studied, and this has led to the development of inhibitors that have shown success in clinical settings. The sole class III PI3K, Vps34, is also relatively well characterised, however much less is currently known about the class II PI3Ks. This class has become a focus of scientific research in recent years, which has an uncovered a number of its biological functions.

1.4.1 Class I PI3Ks

Class I PI3Ks were the first PI3Ks to be discovered, and are the most studied and best characterised of the three classes of PI3Ks[48]. They are heterodimers of four closely related
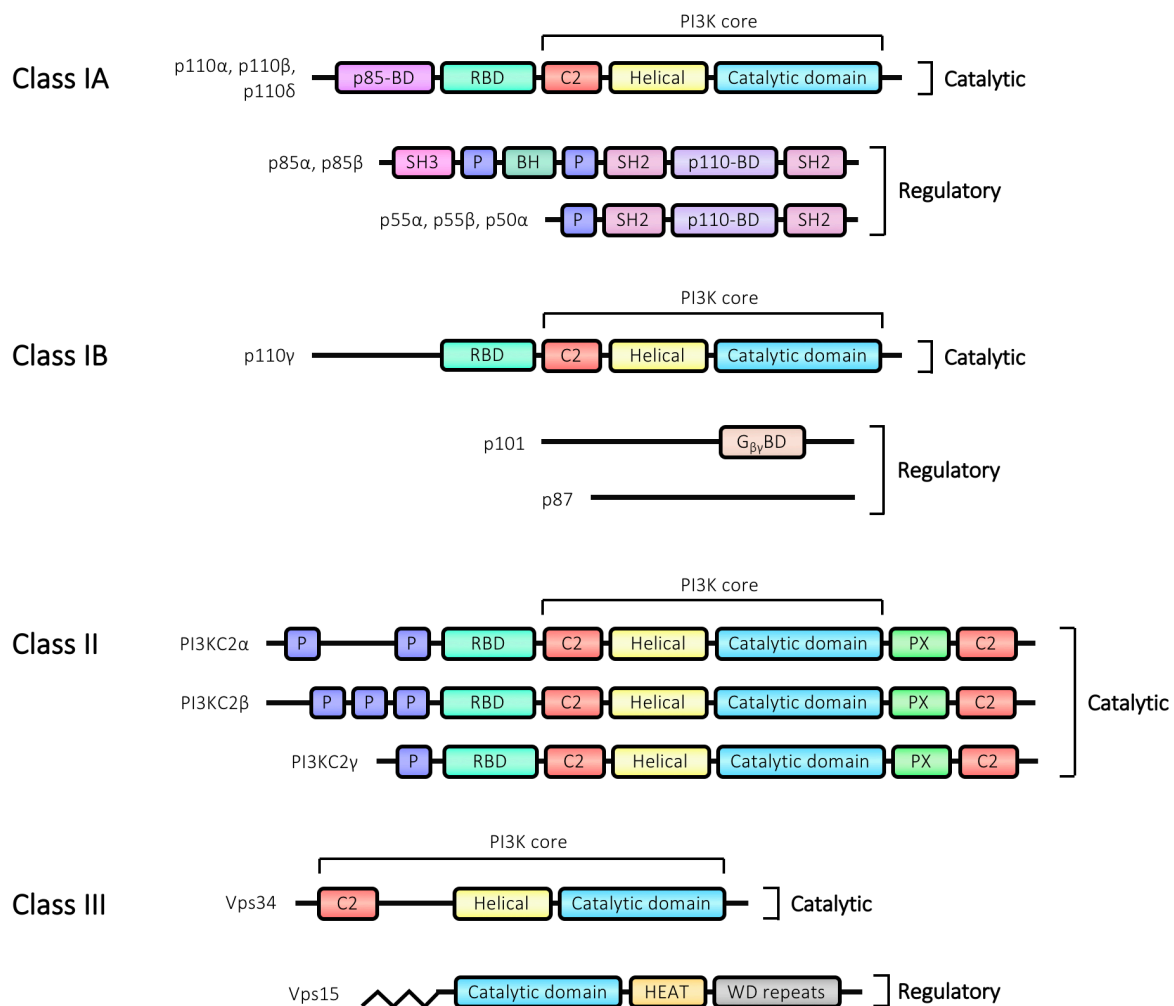
Figure 1.3. Phosphoinositide 3-kinases. There are 8 mammalian isoforms of PI3Ks, divided into 3 classes based on structural and functional similarities. In addition to the PI3K core structure, PI3KC2α contains an N-terminus clathrin-binding region, a Ras binding domain (RBD), and C-terminus extension.

catalytic subunits and two families of regulatory subunits[49]. Class I PI3Ks can be further subdivided into two groups – the Class IA PI3Ks, which comprise dimers of one of the p110α, p110β or p110δ catalytic subunits with one of the p50, p55 or p85 regulatory subunits, and the class IB PI3Ks, dimers of the p110γ catalytic subunit and either the p101 or p87 regulatory subunits (Figure 1.3). Generally, class IA PI3Ks are activated by tyrosine kinases, while class IB PI3Ks are activated by G protein-coupled receptors (GPCRs).

The four isoforms of the class I PI3Ks are named after their respective catalytic subunits. PI3Kα and PI3Kβ are ubiquitously expressed, while PI3Kδ and PI3Kγ are generally found in haematopoietic cells. Although capable of catalysing the production of all three 3-PPIs, the preferred substrate of class I PI3Ks is $PI(4,5)P_2$; they thus preferentially synthesise $PI(3,4,5)P_3$[49]. $PI(3,4,5)P_3$ produced in this way represents a major signal transduction pathway. One of the most important downstream effects of this class of PI3Ks is the activation of Akt, which regulates a number of signalling pathways, including mammalian target of rapamycin (mTOR), that have roles in cell growth and proliferation, survival, metabolism and autophagy[47].

One mechanism of action by which 3-PPIs, and thus PI3Ks, effect downstream signalling is by binding specific domains, including pleckstrin homology (PH), Phox homology (PX), and FYVE domains, of a range of effector proteins and recruiting them to the plasma membrane. Effector proteins include serine/threonine and tyrosine kinases, adaptor proteins and small GTPase regulators. These are able to form scaffolding complexes, which result in the recruitment and activation of downstream signalling proteins (Figure 1.4).

Dysregulation of the class I PI3Ks is implicated in a range of diseases. The clinical success of class I PI3K inhibitors highlights the usefulness of targeting this family of proteins, and provides a roadmap for the future development of clinically useful inhibitors of other PI3K isoforms, particularly the class II PI3Ks.

1.4.1.1 PI3Kα

PI3Kα is one of the most frequently mutated genes in cancer; with mutations leading to increased PI3Kα activity, directly or indirectly, often found in solid tumour cells[50]. These mutations are generally found in certain 'hotspots' within the gene, with changes in three particular amino acid residues accounting for around 80% of cancer-causing PI3Kα mutations[51].
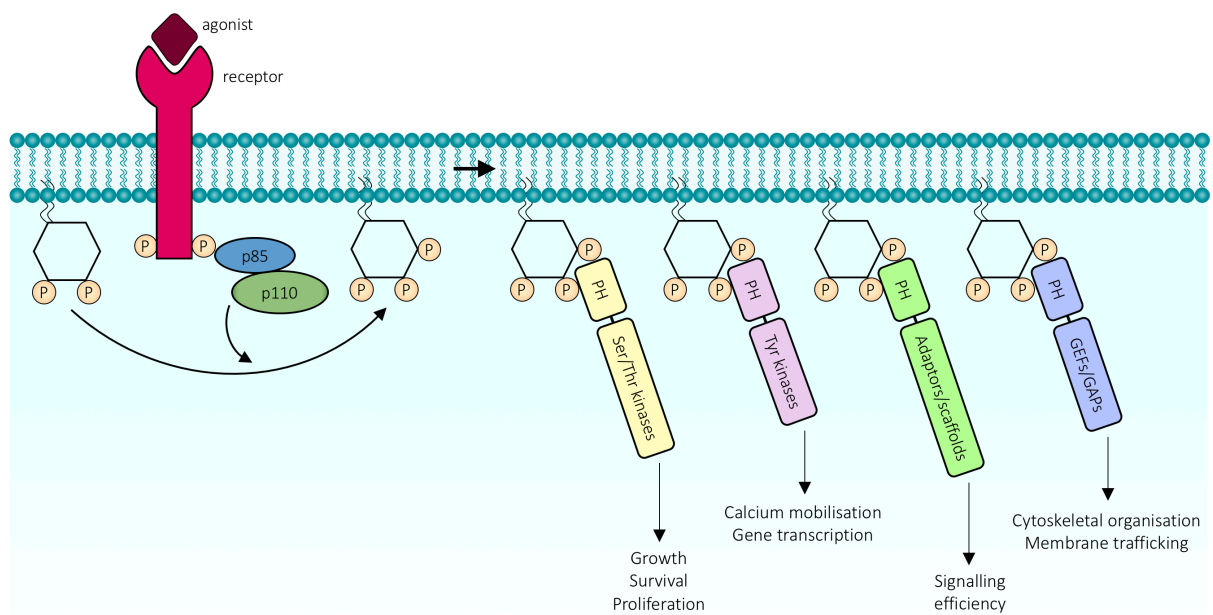
Figure 1.4. Mechanism of PI3K signalling. Activated PI3Ks phosphorylate the 3-position inositol ring of phosphoinositides to produce 3-PPIs. 3-PPIs bind to PH, FYVE or PX domains of effector proteins, recruiting them to the plasma membrane to form a scaffolding complex from which downstream signalling can occur.

As a result, selective inhibition of inhibition of PI3Kα is an emerging approach for the treatment of cancers in which PI3Kα activity is increased, and may mitigate against the severe side effect profile of a pan-PI3K inhibitor. To this end, a number of PI3Kα inhibitors are currently in clinical trials for treatment of a range of cancers. These include MLN1117, which is in a phase Ib trial for the treatment of advanced non-haematological malignancies, and BYL719, which is in a phase II trial for the treatment of squamous cell head and neck cancers[52].

A number of studies have investigated the role of PI3Kα in platelets. Inhibition of PI3Kα has been shown to attenuate the effect of insulin-like growth factor 1, which potentiates platelet responses, on platelet aggregation induced by low-dose agonists[53,54]. PI3Kα also appears to play a complementary role with PI3Kβ in signalling downstream of GPVI, with both isoforms required for full activation of the downstream target PLCγ2, calcium mobilisation and thrombus formation[55]. Finally, a very recent study has uncovered a role for PI3Kα in regulating ADP secretion, and consequently full activation of PI3Kβ and Akt, following platelet stimulation with low concentrations of GPVI agonists[56]. It was also found that PI3Kα is involved in regulating platelet adhesion to vWF under flow, leading to impaired arterial thrombus formation in ex vivo assays, however with no impact on haemostasis[56].

1.4.1.2 PI3Kβ

Perhaps the most clinically relevant function known for PI3Kβ is in thrombosis. In platelets, PI3Kβ signals downstream of the GPVI, $P2Y_{12}$ and integrin $\alpha_{IIb}\beta_3$ receptors[55,57,58]. It activates Akt[59], which results in the inhibition of glycogen synthase kinase-3 (GSK3)[60]. Inhibition of GSK3 by Akt together with protein kinase C α, promotes thrombin-mediated platelet aggregation, fibrinogen binding and release of granule contents[61]. GSK3 inhibition via PI3Kβ is necessary for thrombus growth and stability at high shear rates – thrombus stability is significantly decreased with deficiency or inhibition of PI3Kβ, yet restored with concomitant addition of a GSK3 inhibitor[62].

It has been shown that PI3Kβ regulates the activity of the integrin $\alpha_{IIb}\beta_3$ receptor, which is necessary for platelet spreading and activation[58,63]. Jackson et al. found that inhibitors specific to p110β, the catalytic subunit of PI3Kβ, were able to reduce platelet activation and impede thrombosis formation by preventing the formation of stable integrin $\alpha_{IIb}\beta_3$ bonds[58]. These studies were subsequently confirmed using a p110β knockout mouse model, with platelets

from these knockout mice demonstrating an inability to adhere to fibrinogen and a delay in fibrin clot retraction, which is mediated by integrin $\alpha_{IIb}\beta_3$ contractility[64].

A PI3Kβ-selective inhibitor, AZD6482, has been tested as an anti-platelet drug pre-clinically and in a phase I clinical trial. AZD6482 is an adenosine triphosphate (ATP)-competitive inhibitor of PI3Kβ and has an IC_{50} of 0.01 μM. In vitro studies showed that it is a potent inhibitor of platelet aggregation, particularly shear-induced platelet adhesion and aggregation[65]. In dog, AZD6482 treatment resulted in a dose-dependent anti-thrombotic effect, with no haemostatic consequences. The drug was well tolerated in humans, with inhibition of ADP- and shear-dependent platelet aggregation, and no adverse events recorded[65]. However, AZD6482 inhibits insulin-induced glucose uptake, which may raise concerns regarding insulin resistance caused by the drug[66].

1.4.1.3 PI3Kδ

Highlighting the usefulness of PI3Ks as drug targets, a PI3Kδ inhibitor, idelalisib, has recently been approved by the FDA for the treatment of relapsed chronic lymphocytic leukaemia (CLL), relapsed follicular B-cell non-Hodgkin's lymphoma and relapsed small lymphocytic lymphoma. The phase III clinical trial comparing use of idelalisib combined with rituximab, compared to rituximab monotherapy alone, in patients with relapsed or refractory CLL was stopped early due to the overwhelming efficacy of the drug. Progression free survival, response rate, and overall survival were significantly higher in idelalisib-treated patients[67].

PI3Kδ is expressed at low levels in platelets[68]. It has been shown to play a minor role in mediating platelet activation via the GPVI receptor, and in platelet spreading on fibrinogen, in in vitro assays, however loss of PI3Kδ does not impact platelet adhesion or aggregation under flow conditions[69].

1.4.1.4 PI3Kγ

PI3Kγ plays an important role in the regulation of inflammatory responses. It is highly expressed in neutrophils, eosinophils and mast cells, and is involved in the recruitment and activation of immune cells at sites of inflammation. Loss of PI3Kγ leads to impaired neutrophil and macrophage recruitment following GPCR activation. Furthermore, mouse models of PI3Kγ inactivation or deletion show protection against the development of a number of autoimmune and inflammatory conditions.

PI3Kγ is thus a clear potential anti-inflammatory drug target. A number of PI3Kγ inhibitors have been developed and used experimentally in recent years, with promising results. Bergamini et al. identified CZC24832 as a PI3Kγ-selective inhibitor that shows anti-inflammatory action in vitro and in vivo[70], and Jin et al. found that another PI3Kγ inhibitor, AS252424, inhibits mast cell degranulation and the release of inflammatory molecules[71]. Recently, Huang et al. tested the latter inhibitor in a surgical brain injury (SBI) model, and showed it was able to reduce brain inflammation following SBI in rats[72].

In platelets, PI3Kγ appears to be involved in signalling downstream of the $P2Y_{12}$ receptor, with PI3Kγ-deficient mice protected against ADP-induced thromboembolism[73]. PI3Kγ plays a cooperative role with PI3Kβ in mediating thrombus stability downstream of $P2Y_{12}$[74]. Unlike PI3Kβ, PI3Kγ appears to signal predominantly via a non-catalytic mechanism in platelets[75], and does not play a role in signalling downstream of GPVI[76].

1.4.2 Class II PI3Ks

Class II PI3Ks are the least studied and characterised PI3K isoforms, and their physiological functions are not yet well understood. However, in recent years there has been a significant increase in the amount of research performed on this group, which has begun to shed some light on this emerging area of cell biology[77,78].

Class II PI3Ks are high molecular weight monomers, which differ from their class I counterparts by extensions at both the N- and C-termini[79]. They contain a conserved, characteristic C2 domain and PX domain at the C-terminus (Figure 1.3). There are three isoforms of the class II PI3Ks – PI3KC2α, PI3KC2β, and PI3KC2γ. PI3KC2α and PI3KC2β are widely expressed in mammalian cells[78], however PI3KC2γ expression is largely restricted to exocrine glands[80].

The activation signals for Class II PI3Ks are not well understood although, like Class I isoforms, they can be activated by ligands for either receptor tyrosine kinases or GPCRs[81]. Class II PI3Ks are capable of catalysing the formation of both PI(3)P and $PI(3,4)P_2$, from PI and PI(4)P respectively, at least in vitro[82].

1.4.2.1 PI3KC2α

PI3KC2α is broadly expressed in human cells, including platelets[83]. It is a 190 kDa protein that

is structurally similar to the other members of the class, with the exception of a distinctive N-terminal region containing a clathrin-binding domain that does not appear in PI3KC2β and PI3KC2γ, and the lack of proline-rich sequence repeats found in PI3KC2β[77] (Figure 1.3). In vitro studies have shown that PI3KC2α can be activated by a range of molecules, including cytokines[84], chemokines[85], integrins, as well as insulin[86] and other growth factors[87]. One property particular to PI3KC2α is its comparably decreased sensitivity to commonly-used pan-PI3K inhibitors such as wortmannin and LY294002[88]. The reason for this is unclear, but is an important consideration when interpreting early experiments in which the relative levels of response inhibition by various PI3K inhibitors have been used to identify the responsible isoforms.

PI3KC2α is discussed in more detail in section 1.5.

1.4.2.2 PI3KC2β

PI3KC2β is widely expressed in mammalian cells, with highest expression levels found in the thymus and placenta[89]. A number of PI3KC2β mouse models have been developed in recent years, although few physiological defects have been reported. Harada et al. developed two PI3KC2β mouse models – a PI3KC2β-null model and a targeted epidermal PI3KC2β overexpression model. Mice of both strains were phenotypically and developmentally normal[90]. Similarly, Mountford et al. found no phenotypic changes in PI3KC2β knockout mice, nor any obvious physiological effects of PI3KC2β in mouse platelets. PI3KC2β knockout mice demonstrated normal platelet structure and number, and did not show any obvious functional defects in a range of in vivo and ex vivo assays, which included agonist-induced platelet aggregation and integrin $\alpha_{IIb}\beta_3$ activation[91].

However, a recent study has pointed to a role for PI3KC2β in insulin sensitivity and glucose tolerance. Alliouachene et al. created a mouse model homozygous for a knock in kinase-inactivating mutation in PI3KC2β. This approach does not remove the scaffolding function of PI3KC2β and thus enables the study of the enzyme's kinase-dependent effects alone. Mice homozygous for the knock in allele (PI3KC2β[D1212A/D1212A] mice) were developmentally normal. They demonstrated lower circulating insulin levels under fed conditions than wild type mice, and increased glucose tolerance, suggesting that PI3KC2β is a negative regulator of the insulin response[92]. Furthermore, PI3KC2β[D1212A/D1212A] mice were protected from high-fat diet-induced steatosis, indicating that this regulating role is particularly important in the liver[92]. These results

suggest that PI3KC2β may be a potential drug target for the treatment of type 2 diabetes mellitus (T2DM), as well as other insulin-resistant conditions such as non-alcoholic fatty liver disease.

In vitro, PI3KC2β has been found to regulate cell morphology and survival via interactions with the Rho family guanine nucleotide exchange factor, Dbl. PI3KC2β forms a complex with Dbl, which is then able to activate Rho GTPases RhoA and Rac1. The modulation of RhoA activity by PI3KC2β enables it to in turn regulate cytoskeletal rearrangements and protect cells from anoikis[93]. Furthermore, a number of in vitro studies have supported a role for PI3KC2β in the regulation of cell migration. Maffucci et al. found that PI3KC2β is activated by lysophosphatidic acid to generate a pool of PI(3)P at the plasma membrane, which is required for cell migration[94]. Domin et al. also showed that PI3KC2β regulates cell motility through a PI(3)P-dependent mechanism[95]. Additionally, Katso et al. found that PI3KC2β is involved in a multiprotein complex that is recruited to the epidermal growth factor (EGF) receptor following its activation by EGF. PI3KC2β regulates Rac and c-Jun N-terminal kinase activity through this complex and, as such, is involved in the regulation of membrane ruffling and cell motility[96].

PI3KC2β has also been shown to play a role in carcinogenesis. Overexpression of PI3KC2β has been reported in several tumours, including acute myeloid leukemia, glioblastoma multiforme, medulloblastoma, neuroblastoma and small cell lung cancer[97]. Pharmacological inhibition of PI3KC2β has an anti-proliferative and apoptotic effect in many cancer cell lines, and is able to sensitise cancer cells to chemotherapeutic treatments[97].

1.4.2.3 PI3KC2γ

PI3KC2γ has a much more restricted tissue expression distribution than PI3KC2α and PI3KC2β, being generally localised to exocrine glands. High levels of PI3KC2γ are found in the liver, specifically in the hepatic parenchyma, as well as the breast, prostate and in salivary glands[80]. PI3KC2γ is not expressed at detectable levels in mouse or human platelets[91].

PI3KC2γ can synthesise both PI(3)P and PI(3,4)P$_2$ in vitro, however its in vivo products have not been determined. Very little is known about the physiological functions of PI3KC2γ. However, one of the earliest studies of PI3KC2γ found that its expression levels are increased following partial hepatectomy, particularly after the period of liver regrowth, suggesting that PI3KC2γ may play a role in the maturation of hepatic cells[98].

Braccini et al. recently described the first published PI3KC2γ mouse model. PI3KC2γ knockout mice were born at expected Mendelian ratios and developed normally to adulthood. However, these mice displayed decreased insulin tolerance, and were also found to have increased fat storage and triglyceride levels, indicating altered lipid metabolism. Insulin tolerance decreased with age in these mice. In response to a high-fat diet, PI3KC2γ knockout mice exhibited higher weight gain than controls, due to an increase in fat mass, and developed insulin resistance, dyslipidaemia and fatty liver[99]. It was found that loss of PI3KC2γ results in a decrease in a pool of $PI(3,4)P_2$ specifically located on early endosomal membranes. This subsequently leads to a decrease in Akt2 activation in response to insulin, and thus downregulated glycogen synthase activity; as such, with age or exposure to a high fat diet, PI3KC2γ null mice are prone to insulin resistance and hyperlipidaemia[99].

Furthermore, an association study of polymorphisms in the gene encoding PI3KC2γ with the occurrence of T2DM in a Japanese population, found that certain single nucleotide polymorphisms in this gene were associated with an increased risk of T2DM, suggesting that PI3KC2γ is involved in its pathogenesis[100], consistent with the findings from the PI3KC2γ deficient mouse model described above.

Despite the paucity of information on PI3KC2γ to date, the links to disease that have been uncovered thus far suggest that the development of inhibitors against this protein could be useful both in further elucidating its functions, and as potential therapeutic agents.

1.4.3 Class III PI3Ks

There is only one class III PI3K – Vps34, or hVps34 for the mammalian homologue[48]. hVps34 is a monomer that consists only of the PI3K core domains. It is closely associated with and regulated by protein kinase hVps15[101]. It is the oldest and most conserved PI3K across species, being the only isoform present in yeast[102]. Vps34 exclusively catalyses the phosphorylation of PI to produce PI(3)P[101], and mediates signalling through the recruitment and binding of specific protein domains to PI(3)P, which include PX and FYVE domains[101].

Vps34 is involved in the regulation of autophagy, vesicular trafficking and protein synthesis[103]. It is required for activation of the mTOR/S6 kinase 1 pathway, which is responsible for balancing the rate of protein synthesis with the availability of nutrients[104]. To date, mutations in or

changes in expression levels of hVps34 have not been implicated in any human diseases[101].

Two very recent studies have identified a role for Vps34 in thrombosis using mouse models. Using a megakaryocyte and platelet-specific deletion of Vps34, Valet et al. showed that loss of Vps34 in platelets reduced thrombus size in an in vivo ferric chloride arterial thrombosis model. Thrombus formation was also impaired in an ex vivo whole blood flow model of thrombus formation on collagen under arterial shear rates[105]. Interestingly, haemostatic function, as measured using tail bleeding times, was not affected in these mice, suggesting that Vps34 could be a potential anti-thrombotic target[105]. Liu et al., using a similar, platelet-specific Vp34-knockout mouse model, corroborated these results, also finding that Vps34$^{-/-}$ mice had normal tail bleeding times, but impaired thrombotic function in the same in vivo ferric chloride model and ex vivo whole blood perfusion assay[106].

1.5 PI3KC2α

1.5.1 Mouse Models

A number of mouse models targeting PI3KC2α have been developed over the past five years. The first of these was a PI3KC2α hypomorphic model produced by Harris et al., which identified a role for PI3KC2α in normal growth and survival, as well as in renal function and structure. PI3KC2α hypomorphic mice retained between 10 and 20% of PI3KC2α activity, depending on the tissue examined, yet demonstrated severely diminished survival rates and heavily stunted growth when compared to wild type controls[107]. Furthermore, PI3KC2α-deficiency resulted in chronic kidney failure, as well as the development of renal lesions, including renal tubule defects, podocyte malformation and loss, and glomerulonephropathy[107].

It was subsequently shown, in at least two different studies, that complete deficiency of PI3KC2α results in absolute and early embryonic lethality. Yoshioka et al. created a mouse model with complete genetic deficiency of PI3KC2α; these mice died in utero due to severe defects in blood vessel formation, which included absent or severely disorganised major blood vessels[108]. Mountford et al. similarly found with their own PI3KC2α knockout mouse model that global PI3KC2α deficiency in mice results in early and penetrant embryonic lethality, due to impaired vascular development, with death as early as 6.5 days post conception[91]. Furthermore, Yoshioka et al. found that an endothelial cell-specific PI3KC2α deficiency is also

embryonically lethal, with the most severely affected of these mice exhibiting the same phenotype as mice with a global PI3KC2α deficiency, suggesting that endothelial cell PI3KC2α is required for normal angiogenesis and vascular development[108].

1.5.2 Functions

To circumvent the embryonic lethality of the global and endothelial cell-specific PI3KC2α knockout mouse models, Yoshioka et al. used an inducible endothelial cell-specific PI3KC2α knockout model to investigate the role of PI3KC2α in angiogenesis and vascular barrier formation. Induction of PI3KC2α deletion led to markedly reduced retinal angiogenesis, which was found to be due to impaired endothelial cell migration and proliferation[108]. Additionally, in a post-ischaemic model, revascularisation was diminished in these mice, and in a tumour angiogenesis model where tumours were implanted into the mice, both tumour volume and microvessel density within the tumour were reduced[108]. This has implications for cancer treatment, as tumours rely on the ability to develop and propagate their own blood supply in order to survive and grow, and suggests that PI3KC2α may be a potential drug target to reduce pathogenic angiogenesis.

Other known roles for PI3KC2α include its involvement in the regulation of FcεRI-triggered mast cell degranulation. Nigorikawa et al. found that knocking down PI3KC2α using an RNAi-based approach in a mast cell line caused a reduction in the release of the lysosomal enzyme β-hexosaminidase from these cells, indicating that PI3KC2α is required for normal degranulation via FcεRI[109]. In addition, the release of neuropeptide Y, a reporter for mast cell exocytosis, was also significantly slowed in these PI3KC2α-deficient cells, further supporting a role for PI3KC2α in regulating the degranulation process[109].

Additionally, Franco et al. identified a role for PI3KC2α in primary cilium elongation. Using a green fluorescent protein-tagged PI3KC2α, they found that levels of PI3KC2α are increased at the pericentriolar recycling endocytic compartment, located at the base of the growing cilium. In PI3KC2α-deficient fibroblasts, a specific pool of PI(3)P around the ciliary base is diminished, indicating that PI3KC2α regulates the production of this pool, which is required for the accumulation of proteins and the activation of pathways necessary for normal cilium elongation[110]. Using a PI3KC2α-knockout mouse model, they also found that loss of PI3KC2α

results in defects in primary cilium elongation, as well as ciliary translocation and Sonic hedgehog signalling, all of which ultimately lead to impaired embryonic development[110].

More recently, PI3KC2α has been found to play a role in the regulation of delta opioid receptor (δR) export in neuronal cells. Shiwarski et al. showed that siRNA-mediated knockdown of PI3KC2α caused retention of the receptor in the trans-Golgi network (TGN), with PI3KC2α activity required for normal receptor trafficking and surface translocation. PI3KC2α kinase activity at the TGN was able to induce δR trafficking following retention of the receptor by nerve growth factor, indicating that PI3KC2α activity is sufficient for release and subsequent surface localisation of δR[111].

Another recent study has linked PI3KC2α to leptin signalling and glucose homeostasis in mice. Alliouachene et al. found that in a mouse model with a heterozygous, kinase-inactivating mutation in PI3KC2α, male mice developed leptin resistance, as well as age-dependent obesity, hyperglycaemia and insulin resistance[112]. This, coupled with the previous study from the same group describing increased glucose sensitivity in kinase-inactivated PI3KC2β mice[92], raises the intriguing possibility that the class II PI3Ks work together to maintain a balance in regards to the regulation of glucose metabolism.

1.5.3 PI3KC2α in Thrombosis

Two recent studies have identified a role for PI3KC2α in platelet function, and suggest that PI3KC2α may be a suitable drug target for the prevention and treatment of thrombosis and CVD. Both studies found that PI3KC2α is involved in the regulation of platelet membrane structure, sufficient to cause significant platelet functional consequences in the setting of thrombosis. The first, from our laboratory, used an RNAi-based gene silencing approach to essentially abolish PI3KC2α expression in adult mouse platelets in an inducible manner. These PI3KC2α-deficient mice exhibited delayed and highly unstable in vivo arterial thrombosis that appeared due to a platelet function defect caused by a rearrangement of the structure of the platelet's internal membrane reserve, the open canalicular system (OCS)[91]. Platelets from PI3KC2α-deficient mice displayed dilatations of the OCS, leading to an increased OCS surface area in 2D transmission electron microscopy (TEM) images. A functional defect was also observed – following electrolytic injury to the carotid artery, thrombus formation was

diminished, with time to vessel occlusion increased in PI3KC2α-deficient mice, and the thrombi that formed being unstable, with an increased number of reperfusion events in these mice[91].

The second study, by Valet et al., used a mouse model in which there was a heterozygous kinase-inactivating point mutation in the PI3KC2α active site, and confirmed the membrane structural defects and impairment of in vivo thrombosis observed by Mountford et al.[113] Platelets from these PI3KC2α$^{WT/D1268A}$ mice demonstrated a rough, uneven plasma membrane morphology in addition to alterations in OCS structure and changes in alpha granule size and number when compared to platelets from wild-type mice. Membrane function was also affected, with filopodia formation in response to agonist stimulation significantly decreased in platelets from PI3KC2α$^{WT/D1268A}$ mice. These platelets also demonstrated cytoskeletal abnormalities, with decreased levels of both spectrin and myosin. These structural changes led to impaired platelet thrombotic function in both a ferric chloride in vivo model and ex vivo whole blood flow on collagen. Additional mechanistic studies indicated that PI3KC2α regulates a basal pool of PI(3)P in platelets that may lead to impaired regulation of the platelet's cytoskeletal-membrane system, and thus produce the structural defects observed[113].

Furthermore, another recent publication from our laboratory has demonstrated that the function of PI3KC2α in platelet structure and function is non-redundant, with platelets from mice deficient in both PI3KC2α and PI3KC2β structurally and functionally similar to those from mice deficient in PI3KC2α alone, and no notable phenotypic changes seen in PI3KC2β$^{-/-}$ mice. Taken together, these results point to a role for PI3KC2α in platelet prothrombotic function, and highlight the potential of this enzyme as an anti-thrombotic drug target.

1.6 Platelet Structure

Given the recently identified role of PI3KC2α in platelet structure, which will be further examined in this thesis using high resolution electron microscopy techniques, this section will provide a detailed description of platelet morphology.

Resting, or inactivated, platelets have a discoid shape, and measure approximately 0.5 x 3 μm in humans[5], with an average volume of 7 fL[114]. They do not contain any genomic DNA, however

do contain messenger RNA from the megakaryocyte from which they were derived, as well as protein synthesis machinery[115].

The discoid shape of resting platelets is achieved and maintained by an inner microtubule coil, which is located in the cytoplasm just beneath the plasma membrane[15]. These microtubules are made up of stacks of tubulin subunits, comprised of units of both α and β tubulin[116]. The main β tubulin isoform in platelets is β1 tubulin, which is exclusively expressed in megakaryocytes and platelets[117]. Platelet integrity is also maintained by the actin filament cytoskeleton. These filaments run from the centre of the cell to the plasma membrane, forming a space-filling network[5].

When platelets are activated, they lose their discoid shape and become spherical, before extending filopodia, flattening and spreading. Platelet shape change requires disassembly of the membrane skeleton, disruption of the actin filament network, and the assembly of new actin filaments from the ends of the filaments at the plasma membrane[5].

Platelets contain a variety of storage organelles, including alpha and dense granules, and lysosomes, whose contents are released upon platelet activation (Figure 1.5). Alpha granules are by far the most common secretory granule, with 50-80 being present in human platelets[118]. These granules contain the vast majority of proteins secreted by platelets, including haemostatic factors such as factor V, vWF and fibrinogen, angiogenic and anti-angiogenic factors, growth factors, proteases, necrotic factors and other cytokines[118]. Dense granules mainly contain small molecules, such as 5-hydroxytryptamine, ADP, ATP, and magnesium and calcium ions[119]. Human platelets contain on average 4-8 dense granules[120].

Platelets also contain two internal membrane systems, the OCS (Figure 1.5) and the dense tubular system (DTS), which will be discussed in more detail in the following section.

1.6.1 Open Canalicular System

The OCS is an anastomosing network of membrane channels that derives from and is continuous with the platelet plasma membrane[121]. OCS formation begins in the megakaryocyte before proplatelets develop, and is complete before the fragmentation of the megakaryocyte into platelets[122]. It is formed by invaginations of what will eventually become the platelet plasma membrane[123]. Its lipid composition is identical to that of the plasma membrane[121], and
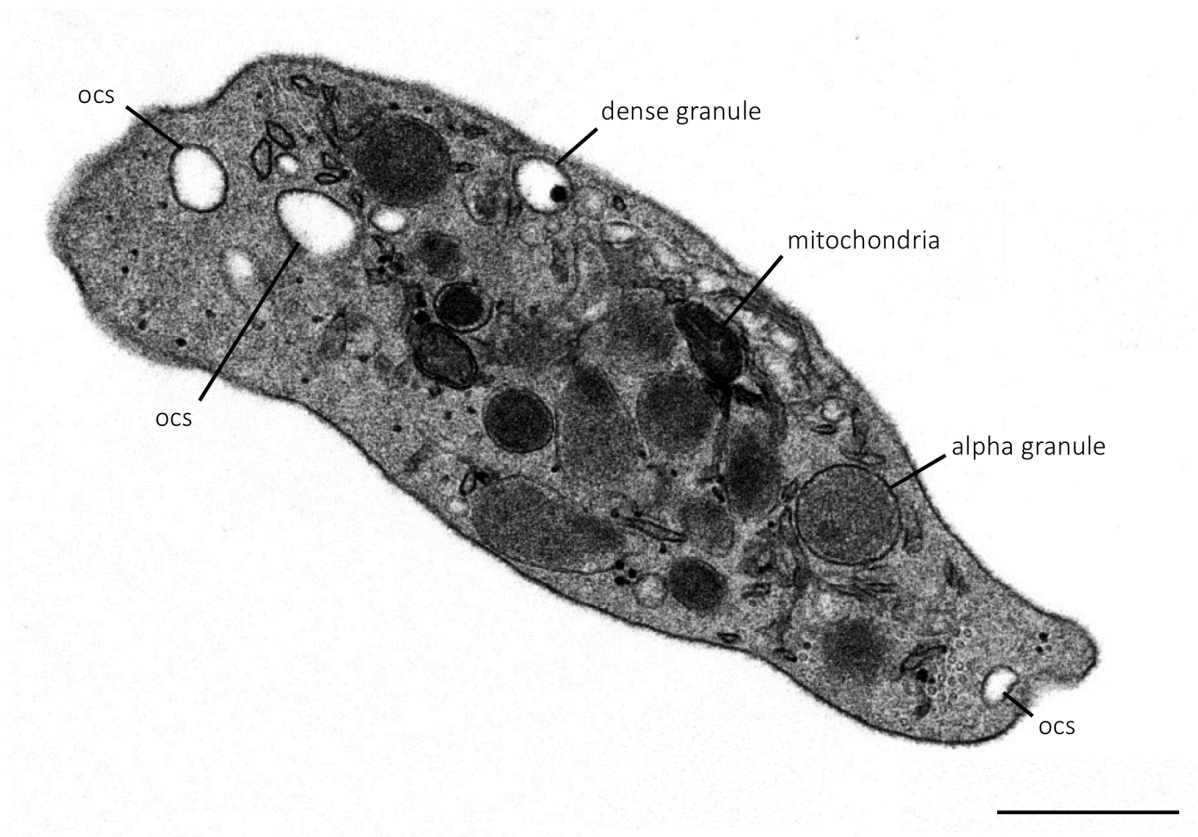
Figure 1.5. Anatomy of a platelet. TEM image of a human platelet, with the OCS, numerous alpha granules, dense granules, and mitochondria visible. Scale bar, 0.5μm.

surface glycoprotein receptors are present at similar levels across the two membranes[124,125]. The final form of the OCS is a complex, anastomosing network of interconnected and surface-connected membrane channels that spans the platelet interior. The channels of the OCS vary in diameter within individual platelets, with vacuolar sections as well as thinner tubular sections[126], and there is also variation in the amount of OCS between platelets from any one individual. On average, the channels of the OCS in human platelets occupy approximately 3-4% of the total platelet volume, as estimated from 2D TEM images[91].

The OCS was first discovered in 1967 by Olav Behnke, who identified the existence of two separate membrane systems in platelets, one of which, the OCS, was found to be continuous with the platelet plasma membrane. The second membrane system, the DTS, was not linked to either the platelet membrane or the OCS[127]. Subsequent studies of the DTS found that it is derived from the smooth endoplasmic reticulum[128], and takes the form of long, thin tubules in resting platelets[129]. It acts to regulate platelet activation by either sequestering or releasing calcium ions, thus playing an important role in platelet activation[129].

1.6.1.1 OCS Function

Uptake and Release of Platelet Contents

A major function of the OCS is the transport of substances into and out of the platelet. Platelets have very little capacity for protein synthesis and so much of their cargo is taken up from plasma sources. This uptake largely occurs via the OCS, with a number of plasma proteins including fibrinogen[130] and tissue factor[131] taken up through channels of the OCS and then subsequently distributed to organelles within the platelet (e.g. alpha or dense granules). Behnke's early studies showed that particles added to platelet-rich plasma in vitro, or infused intravenously in vivo, were subsequently found in channels of the OCS, without any change in platelet morphology[127]. This finding was soon after confirmed by James White, who showed that thorium dioxide particles added to platelet-rich plasma were observed not only in OCS channels, but also in alpha granules – even when these granules had no visible physical association with the OCS[132]. These early studies confirmed the 'open' nature of the OCS, and revealed that these internal platelet channels are essentially exposed to the same medium as the platelet exterior.

The OCS also plays an important 'delivery' role in the release of substances stored in platelets to the cell exterior. Upon platelet activation, alpha and dense granules fuse with the OCS or plasma membrane, allowing release of their contents and potentiation of platelet activation[133,134]. This process is regulated by SNARE proteins, a family of membrane-associated proteins which mediate membrane fusion. The distribution of SNARE proteins differs between granule membranes, and the plasma and OCS membranes, with the SNARE family members vesicle-associated membrane protein (VAMP) 3 and 8 primarily found on granule membranes, SNAP-23 found on plasma and OCS membranes, and syntaxins 2 and 4 evenly distributed between both types of membrane[135]. In the fusion of alpha and dense granules with OCS membranes, VAMP proteins on the granule surface interact with syntaxins 2 or 4 and SNAP-23 on the OCS membrane, linking tightly and forming an exocytic core complex[136-138]. This allows the two membranes to fuse, permitting the release of granule contents into the channels of the OCS, and subsequently the platelet exterior. The rate of secretion of alpha granule contents has been shown to be dependent on both the concentration of the stimulating agonist and the time platelets are exposed to the stimulus[139]. In platelets from species lacking an OCS, alpha granules fuse directly with the plasma membrane to release their contents[140]. Intriguingly, a simple internal channel system appears to form in thrombin-activated bovine platelets[140]. This de novo channel system, although much less extensive and complex than an OCS, connects to the exterior granules not located at the plasma membrane and thereby facilitates release of the platelet's intracellular cargo[140].

More recently, it has also been suggested that the OCS plays a role in the regulation of platelet calcium signalling. Sage et al. found that the calcium signal in agonist-stimulated platelets was generated at, and propagated through, specific areas of the platelet, that matched the broad distribution and surface-linked nature of the OCS[141]. Furthermore, impairment of the pericellular calcium signal reduced the magnitude of the agonist-induced cytosolic calcium signal as well as the rate of dense granule secretion. The authors thus proposed a model of pericellular calcium recycling, in which calcium released from the DTS following agonist stimulation moves into the OCS at specific locations – the membrane complexes where the DTS and OCS intertwine – from where it is recycled back into the platelet cytosol via calcium channels, to potentiate the calcium signal and trigger granule secretion[141].

Regulation of Adhesion Receptor Levels

The OCS also functions as a storage site for platelet membrane receptors. Glycoprotein adhesion receptors on the membrane surface, most notably the integrin $\alpha_{IIb}\beta_3$, the GPIb/IX/V complex, and GPVI, are particularly important for platelet function. It is notable then, that the total pool of $\alpha_{IIb}\beta_3$ and GPIb in a resting platelet is split evenly between the intracellular membranes of the OCS and the external plasma membrane[124,125]. This large reserve of platelet adhesion receptors becomes important during platelet activation. For example, integrin $\alpha_{IIb}\beta_3$ levels at the cell surface increase in response to platelet activation, largely due to evagination of the OCS[142]. Conversely, surface levels of the GPIb/IX/V complex are downregulated following platelet activation via sequestration into an intracellular pool in the OCS[143]. In this way, the OCS appears to contribute to platelet activation by regulating levels of important cell surface adhesion receptors.

Membrane Reserve

A further function of the OCS is to act as a membrane reserve for use during platelet activation[142]. Following initial activation, platelets undergo a defined series of morphological changes – they lose their discoid shape and become spherical before extending filopodia, flattening, and spreading – all of which require additional membrane[5]. Indeed, the surface area of a fully spread platelet is up to four-fold that of a resting platelet[118]. The importance of the OCS in these processes is evidenced by bovine platelets, which lack an OCS and do not spread in response to surface activation[144]. While bovine platelets do extend filopodia, the 'spreading' process does not proceed past this point, and flattened, spread platelets with lamellipodia are not observed[144]. Although it is possible that this could be attributable to differences in cytoskeletal organisation between bovine and human platelets[144], the most likely explanation is a lack of membrane reserve.

1.6.1.2 OCS Abnormalities in Human Platelets

Limited information on OCS function can be gleaned from human conditions. There are a number of clinical syndromes where abnormalities in the OCS have been documented, including some conditions that involve bleeding or thrombotic sequelae. However, platelets from patients with each of these conditions have a number of other structural abnormalities, making it difficult to ascertain the specific contribution of the OCS defect, if any, to any altered platelet function. For example, a dilated, hypertrophic OCS is seen in platelets from patients with Bernard-Soulier syndrome (BSS). BSS is the result of an abnormality in the gene encoding

the GPIb (or occasionally GPIX) component of the GPIb/IX/V receptor complex and manifests as a bleeding disorder[145]. Over 100 BSS-causing mutations in these genes have been identified, which impair either the expression of the receptor complex at the plasma membrane, or the ability of the receptor to interact with vWF[146]. Yet, in addition to the OCS defect, platelets from these patients are also giant, exhibit disorganised microtubules, and have sparse or even absent granulation. A similar phenotype is observed in platelets from patients with MYH9-related disorders (e.g. May-Hegglin anomaly, Epstein syndrome, Fechtner syndrome). As with BSS, platelets from these patients exhibit a dilated and hypertrophic OCS, but also a pronounced macrothrombocytopaenia and marked agranularity[124,147,148]. Intriguingly, Budd-Chiari syndrome, a rare prothrombotic condition characterised by hepatic vein or inferior vena cava thrombosis[149], also results in platelets with dilation and hypertrophy of the OCS [150]. Yet, again, multiple other platelet ultrastructural defects are observed, including a general lack of organelle content. Finally, abnormal linkage of storage granules to the OCS has been implicated in alpha-delta platelet storage pool deficiency. In an ultrastructural study of multiple familial cases of the disease, it was found that alpha and dense granules were replaced by empty vacuolar structures in platelets from these patients, and that many of these vacuoles were connected to the OCS, suggesting that extraneous connections between the granules and OCS result in the loss of granule contents to the cell exterior in the absence of platelet activation[151].

1.6.1.3 Tools for Studying the OCS

2D Electron Microscopy

Detailed study of OCS structure is generally performed using electron microscopy, indeed, the discovery of the OCS was enabled by the advent of TEM. Standard TEM allows indications of the relative amount of OCS in a platelet, the size of the channels of the OCS, and can show surface openings, while the surface-linked nature of the OCS was determined using TEM imaging of platelets stained with cell-impermeable membrane dyes such as ruthenium red. Scanning electron microscopy (SEM) can also be used to image aspects of the OCS – specifically to look at OCS openings by examining the surface topology of the platelet's plasma membrane. However, there are a number of limitations of using two-dimensional imaging techniques to visualise the OCS. SEM provides only surface level information, and is therefore limited to examination of the number, size, and potential distribution of OCS openings, as well as general plasma membrane morphology. TEM looks at only one slice through the platelet interior, at a

random orientation, so does not infer what the entire internal membrane system in a given platelet may look like. As a result, changes in the distribution of the OCS or in the number or size of surface openings may be missed. These limitations in two-dimensional imaging techniques have led to more recent studies using three-dimensional approaches.

3D Electron Microscopy

The development of automated, serial-section, electron microscopy (EM)-based techniques has allowed a more sophisticated reconstruction of OCS structure in three dimensions and throughout the entire cell. The first of these methods to be used in platelet imaging, EM tomography, involves a series of images taken at different angular orientations of the sample; which are then aligned and merged to create a 3D representation of the sample (electron tomogram). Specific aspects within the sample, such as the OCS within a platelet, can be manually reconstructed from the tomogram. The first and most comprehensive EM tomography study of platelets to date was performed by van Nispen tot Pannerden et al., in which the authors used this technique to perform intricate reconstructions of OCS-DTS membrane complexes, as well as detailed analyses on the various subtypes of alpha granule present in the platelet[126]. While EM tomography can provide much useful information on platelet ultrastructure, limitations on the thickness of sections that can be imaged and the largely manual nature of the reconstruction limit the capacity of this approach to produce accurate reconstructions of an entire platelet. For these reasons, with regards to the OCS, electron tomography may be most useful for examining specific parts of the OCS within a platelet, as exploited to great effect by van Nispen tot Pannerden et al., such as its interactions with, or proximity to, other organelles.

A second 3D imaging technique, which is able to produce detailed whole-cell reconstructions of the platelet and its OCS, is focused ion beam-scanning electron microscopy (FIB-SEM), as recently published by Eckly et al.[152] FIB-SEM is an automated microscopy technique involving the combined use of a scanning electron microscope and focused ion beam technology[153]. This approach produces a series of sectional images, of comparable quality to traditional TEM, by sequentially using a gallium ion beam to remove thin layers of tissue from a sample and an electron beam to image each new block face (Figure 1.6)[153,154]. Components across these serial sections can be reconstructed to produce three-dimensional images of cell ultrastructure and subcellular structures. In the case of a platelet, these whole-cell 3D reconstructions produced

| Milling and imaging | Stack of serial 2D images | 3D whole cell reconstruction |
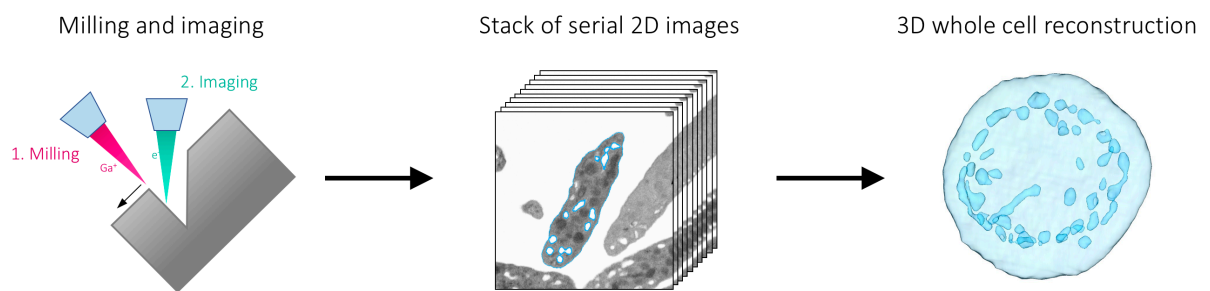
Figure 1.6. Whole cell OCS analysis via focused ion beam-scanning electron microscopy (FIB-SEM). In FIB-SEM, the sample is sequentially milled with a gallium ion beam and imaged with an electron beam. Each milling step removes 10 nm of embedded sample. This stack of serial 2D images at 10 nm intervals is then segmented. Shown here is the segmentation of the OCS and plasma membrane of one platelet in cell suspension. A typical image stack for a whole-cell platelet reconstruction comprises 200-300 images. In this way, a whole-cell, 3D platelet reconstruction is produced. The reconstruction here shows the platelet plasma membrane and OCS.

using FIB-SEM show the entire OCS within any particular platelet, including both its network of connected channels within the cell and its openings at the plasma membrane (Figure 1.6). Organelles and smaller components can also be analysed in detail. For example, Eckly et al. have, in addition to whole-cell platelet reconstruction, used FIB-SEM to show detailed changes in the ultrastructure of alpha and dense granules, and mitochondria, at various stages of platelet activation[152]. As such, FIB-SEM provides more information than both traditional TEM and SEM combined, allowing quantitative information about the internal membranes of the whole cell, such as accurate determination of the total OCS volume. However, both the imaging and reconstructive analysis of FIB-SEM are very time consuming, making it impractical for analysing large numbers of cells. A further limitation is the resolution of current approaches such that, as with TEM, particularly narrow channels of the OCS may be missed resulting in a likely underestimate of the true interconnectivity of the system.

1.7 Rationale and Aims

Given the global burden of CVD, and the limitations of currently available treatments, new anti-platelet approaches are critically needed. Early evidence has suggested that targeting the class II PI3K isoform, PI3KC2α, may provide some potential toward this goal. We have previously shown that inducible genetic deficiency of PI3KC2α in mice results in changes to the structure of the platelet internal membrane that are sufficient to cause functional impairment in the setting of arterial thrombosis. However, the mechanisms linking these structural and functional alterations remain unknown.

Furthermore, we have recently developed a first-in-class PI3KC2α inhibitor, enabling the examination of the role of PI3KC2α in human platelet structure and function. The focus of this thesis therefore is to further characterise the role of PI3KC2α in mouse platelets, to determine whether PI3KC2α plays a role in human platelet structure and function, and to assess the utility of targeting PI3KC2α as a potential anti-thrombotic strategy. This research is of interest both in terms of defining the biological function of PI3KC2α and in the greater context of thrombosis and cardiovascular disease.

The specific aims of this work are as follows:

1) Determine the mechanism by which PI3KC2α deficiency is anti-thrombotic in mice (Chapter 2)
2) Determine the role of PI3KC2α in human platelets and the validity of targeting PI3KC2α as an anti-thrombotic strategy (Chapter 3)

Sections of this chapter have been published as:

Falasca M, Hamilton JR, **Selvadurai MV**, Sundaram K, Adamska A, Thompson PE. Class II phosphoinositide 3-kinases as novel drug targets. J Med Chem. 2017 Jan 12;60(1):47-65.

Selvadurai MV, Hamilton JR. Structure and function of the open canalicular system – the platelet's internal membrane network. Platelets. 2018 Jun;29(4):319-25.

(See Appendices I and II)

CHAPTER 2

Determining the Mechanism by which PI3KC2α Deficiency is Anti-Thrombotic in Mice

Previous work identified a structural and functional defect in platelets from PI3KC2α-deficient mice – a dilation of the internal membrane system, the OCS, and an impairment in arterial thrombosis[91]. However, it remains unclear how the structural change in the OCS is linked to reduced thrombus propagation in vivo. As such, further examination of the role of PI3KC2α in mouse platelet structure and function is warranted in order to identify any potential mechanism linking OCS dilation and impaired thrombosis.

The dilatations of the OCS previously identified in 2D TEM images are not uniform, nor are they present in every PI3KC2α-deficient mouse platelet. Furthermore, TEM images capture only a thin slice at a random orientation through the cell, and do not provide a comprehensive representation of the structure of the internal membrane network throughout the platelet. This drove a desire to examine the three-dimensional structure of the entire OCS. Moreover, given that changes in alpha granule structure have previously been identified in a model of PI3KC2α deficiency[113], a more detailed ultrastructural analysis seemed necessary. Here, high-resolution electron microscopy techniques were used to perform a detailed analysis of the whole cell structural changes induced by PI3KC2α deficiency in mouse platelets. FIB-SEM was used to create 3D reconstructions of PI3KC2α-deficient and wild-type mouse platelets, allowing comprehensive examination of the channels of the OCS, as well as other platelet organelles. A second aspect of OCS architecture, its openings at the plasma membrane, was examined using traditional SEM.

It was also unknown how loss of PI3KC2α led to the change in OCS structure. Given that one of the most important contributors to membrane structure is the lipid content of the membrane, whether these dilations were driven by alterations to the lipid composition of the membrane induced by PI3KC2α deficiency was determined. This approach also has the potential to provide clues as to whether the phenotype can be induced acutely (in either mouse or human cells) with a small molecule inhibitor. For example, if membrane lipid content was the determinant of the phenotype, this would suggest that the phenotype would not be acutely inducible with pharmacological inhibitors. Here, we used liquid chromatography-tandem mass spectrometry to profile and compare the lipid composition of the plasma membrane in PI3KC2α-deficient and wild-type mouse platelets.

Finally, an effort was made to determine how the alteration in platelet internal membrane structure leads to the functional phenotype of impaired arterial thrombosis, and begin to

uncover the mechanism underlying the effect seen with loss of PI3KC2α. Given that the phenotype was that of an altered membrane structure, analyses of platelet membrane function were performed, in both in the absence and presence of shear forces. SEM was used to visualise the formation of filopodia in suspension-activated platelets, and a microfluidic whole blood flow assay in which thrombus formation is largely membrane-dependent was used to assess platelet prothrombotic capacity.

These studies found that the structural changes in PI3KC2α-deficient platelets are limited to the membrane and occur independently of membrane composition. Furthermore, the functional defect in PI3KC2α-deficient platelets occurs specifically under the high shear forces present during thrombus formation, suggesting that if a similar role exists for PI3KC2α in human platelet structure and function, it may have significant potential as an anti-thrombotic target.

The PI 3-kinase, PI3KC2α, regulates the membrane structure and thrombotic function of mouse platelets independently of membrane lipid composition

M.V. Selvadurai[1], R.J. Brazilek[1], M.J. Moon[1], J.-Y. Rinckel[2], A. Eckly[2], C. Gachet[2], P.J. Meikle[3], H.H. Nandurkar[1], W.S. Nesbitt[1,4], and J.R. Hamilton[1]*

Affiliations:

[1]Australian Centre for Blood Diseases, Monash University, Melbourne, VIC 3004, AUSTRALIA

[2]Université de Strasbourg, INSERM, EFS GEST, BPPS UMR_S1225, FMTS, F-67000 Strasbourg, FRANCE

[3]Metabolomics Laboratory, Baker IDI Heart and Diabetes Institute, Melbourne, Victoria, AUSTRALIA

[4]Microplatforms Research Group, School of Engineering, RMIT University, Melbourne, AUSTRALIA

*To whom correspondence should be addressed:
Justin R. Hamilton
Australian Centre for Blood Diseases
Monash University
L1 AMREP Building
99 Commercial Road
Melbourne, VIC 3004
AUSTRALIA

Telephone: +61-3-9903-0125
Email: justin.hamilton@monash.edu

Keywords: platelets, thrombosis, phosphoinositide 3-kinase, open canalicular system

Essentials

- The phosphoinositide 3-kinase, PI3KC2α, regulates platelet function via an unknown mechanism.

- We examined the effect of PI3KC2α deficiency on platelet membrane structure and function.

- PI3KC2α-deficiency altered platelet membrane structure independently of lipid composition.

- PI3KC2α-deficiency selectively impaired platelet adhesion when dependent on membrane tethering.

Abstract

Background: The class II phosphoinositide 3-kinase, PI3KC2α, is a lipid kinase with a recently reported role in platelet function. Platelets from PI3KC2α-deficient mice exhibit an altered internal membrane structure and an impaired thrombotic capacity, yet how this change in membrane structure impacts platelet function remains unknown.

Objectives: To examine the effect of PI3KC2α deficiency on platelet membrane structure and function.

Methods & Results: We used focused ion beam-scanning electron microscopy to examine the whole cell ultrastructure of PI3KC2α-deficient platelets. Analysis of the major organelles revealed a specific increase in internal membrane volume of PI3KC2α-deficient platelets due to dilation of open canalicular system channels throughout the cell, including at the plasma membrane. Profiling of 294 lipid species across the 22 most abundant lipid classes using liquid chromatography-tandem mass spectrometry indicated these membrane structure changes were not due to variations in lipid composition. Analyses of membrane function showed normal filopodia formation in PI3KC2α-deficient platelets activated in suspension but impaired thrombosis under conditions involving membrane tethering.

Conclusions: These studies indicate the structural changes in PI3KC2α-deficient platelets are limited to the membrane and are independent of membrane lipid composition. The impaired function of the cell membrane in PI3KC2α-deficient platelets occurs specifically in the setting of thrombus formation, suggesting PI3KC2α regulates platelet function via a unique membrane-dependent mechanism that may be targetable for anti-thrombotic benefit.

Introduction

The phosphoinositide 3-kinases (PI3Ks) are a family of lipid kinases that catalyse the phosphorylation of the 3' hydroxyl group of the inositol ring of phosphoinositides to produce the 3-phosphorylated phosphoinositides (3-PPIs) – important second messengers for a wide range of processes in cells [1, 2]. There are eight mammalian PI3K isoforms, divided into three classes based on structural and functional similarities: four class I, three class II, and one class III PI3K. The class I PI3Ks are comfortably the most widely studied and have well-defined roles in range of cells, including platelets [3]. More recently, mouse genetic models have been used to uncover the importance of one of the class II PI3Ks, PI3KC2α, and the sole class III PI3K, Vps34, in platelet function. While Vps34 appears to play a modest role in platelet production and function [4, 5], PI3KC2α regulates the thrombotic function of mouse platelets by a unique and as-yet-undefined mechanism that may involve the structure of the cell membrane [6-8]. Specifically, we used an inducible shRNA-based approach to deplete PI3KC2α protein in the platelets of adult mice to show that PI3KC2α regulates the structure of the platelet internal membrane system (the open canalicular system; OCS) [6, 7]. Here, transmission electron microscopy (TEM) revealed that PI3KC2α-deficient platelets exhibit dilatations of the channels of the OCS. Perhaps surprisingly, platelets from PI3KC2α-deficient mice displayed normal function in all in vitro function tests performed (aggregation, granule secretion, integrin activation, and adhesion and spreading on activating surfaces), yet have impaired platelet thrombotic function in both *in vitro* and *in vivo* models [6, 7]. A subsequent study confirmed this role for PI3KC2α in platelet structure and function in a distinct mouse model involving heterozygosity of a kinase-inactivating point mutation in the PI3KC2α active site [8]. These intriguing findings suggest PI3KC2α links regulation of the platelet internal membrane

structure to the cell's prothrombotic function. However, the mechanism by which this occurs remains unknown.

One potential mechanism by which alterations in the platelet membrane structure might impair platelet function is provided by the observation that PI3KC2α-deficient platelets exhibit reduced expression of a number of proteins important for linking the cell membrane with its cytoskeleton, most notably spectrin and myosin [8]. If the reduction in these proteins is sufficient to impair communication between the membrane and cytoskeleton, one prediction is that this may lead to impaired filopodia formation in activated platelets. Yet how such an impact would result in the observed selective impairment of platelet function in the setting of thrombosis – and not a global impairment of platelet function in, for example, standard assays of aggregation, granule secretion, or platelet spreading [6], remains unclear.

Given this uncertainty regarding the mechanism by which PI3KC2α regulates platelet membrane structure and function, we have further examined the structural changes to the platelet membrane induced by PI3KC2α-deficiency and have investigated how these structural changes affect the function of the platelet membrane. Here, we use focused ion beam-scanning electron microscopy (FIB-SEM) [9], as well as traditional scanning electron microscopy (SEM), to perform a detailed, three-dimensional ultrastructural analysis of platelets from PI3KC2α-deficient mice. This analysis indicates PI3KC2α-deficient platelets exhibit specific changes to the structure of the OCS. These changes occur without major alterations in the lipid composition of these platelets. Surprisingly, the structural changes to the platelet OCS membrane have no impact on the formation of filopodia by platelets activated in suspension, yet markedly impacts on the ability of these platelets to form thrombi in a blood

flow environment involving a prominent shear gradient that produces membrane tether formation [10-12]. Together, these findings indicate that PI3KC2α modulates the structure of the platelet internal membrane (OCS) independently of changes to membrane composition. These structural changes to the OCS appear to compromise platelet membrane function specifically in the setting of thrombus formation. If this regulation of membrane structure by PI3KC2α is acute, these studies reveal the potential for a novel approach toward thrombosis-specific anti-platelet therapy.

Methods

Mice

All animal experiments were approved by the Alfred Medical Research and Education Precinct Animal Ethics Committee (approvals E/1465/2014/M and E/1644/2016/M). Mice were backcrossed ≥ 5 generations on a C57BL/6 genetic background (i.e. ≥ 98%) and maintained on a 12 h light/dark cycle with food and water *ad libitum*. All genetic studies were littermate controlled and were performed with mice at 6 to 20 weeks of age of either sex. Mice deficient in PI3KC2α (CMV-rtTA;TRE-GFP-shPI3KC2α) were generated using an inducible shRNA-based gene-silencing approach, as reported previously [6]. Control mice consisted of either pooled wild-type and monotransgenic littermates or were mice with similar transgenes but with a control shRNA targeting Renilla luciferase (CMV-rtTA;TRE-GFP-shControl). To induce shRNA-based knockdown of PI3KC2α expression, mice were placed on a doxycycline diet (600 mg/kg, Speciality Feeds, Australia), for at least 10 days prior to experimentation.

Platelet isolation

Blood was drawn from the inferior vena cava of anaesthetised mice into enoxaparin (40 U/ml, final concentration) using a 25-gauge needle. Platelets were isolated as previously described [6]. Briefly, blood was treated with acid-citrate-dextrose and platelet wash buffer (4.3 mM K_2HPO_4, 4.3 mM Na_2HPO_4, 24.3 mM NaH_2PO_4, 113 mM NaCl, 5.5 mM D-glucose and 10 mM theophylline; pH 6.5; containing 0.5% BSA, 20 U/ml enoxaparin and 0.01 U/ml apyrase), platelets isolated via centrifugation, and resuspended in Tyrode's buffer containing 0.5% BSA, 1.8 mM Ca^{2+} and 0.02 U/ml apyrase.

Focused ion beam-scanning electron microscopy

Isolated mouse platelets were fixed in 2.5% glutaraldehyde, post-fixed in 1% osmium tetroxide and 1.5% potassium ferrocyanide, incubated in 4% uranyl acetate, then dehydrated through a series of graded ethanol concentrations before being embedded in Epon resin. Samples were imaged using a Helios NanoLab microscope (FEI). Stacks of approximately 1000 images with a field size of 15 µm x 15 µm were generated. Samples were milled with the FIB (20 kV) at a thickness of 20 nm per section. Three dimensional models were computed using the imaging software Amira (FEI).

Scanning electron microscopy

Isolated mouse platelets were activated with ADP under constant stirring in the presence of eptifibatide (40 µg/ml) and then fixed with the addition of glutaraldehyde (2.5%, final concentration). Fixed platelets were seeded on glass coverslips pre-coated with 0.01% poly-L-lysine; coverslips were then rinsed, dehydrated, and coated with a 10 nm layer of platinum/palladium or gold using a sputter coater (Cressington 208-HR). Imaging was performed using a Nova NanoSEM 450 scanning electron microscope (FEI) at 5 kV, and analysis completed using FIJI software.

Platelet lipid composition

Platelet lipid composition analyses were performed as previously described [13, 14]. Briefly, lipids were extracted using a single-phase chloroform:methanol extraction. Isolated mouse platelets in suspension were added to equal volumes of internal standard mix, comprising known concentrations of all lipid classes measured. A 2:1 ratio of chloroform:methanol was added to each sample. Samples were mixed with a rotary mixer for 10 min, sonicated for 30

min, and rested for 20 min at room temperature. Samples were then centrifuged at 16,000*g* for 10 min and the resulting supernatant removed and dried with nitrogen gas at 40°C. Samples were dissolved in water-saturated butanol and sonicated for 10 min prior to addition of an equal volume of methanol with 10 mM ammonium formate. The lipid extracts were centrifuged at 3350*g* for 5 min and the supernatant removed for analysis.

Lipid analysis was performed using liquid chromatography electrospray ionisation – tandem mass spectrometry, as previously described in detail [13, 14], using an Agilent 1200 UHPLC coupled to an AB Sciex Q/TRAP 4000 mass spectrometer with a turbo-ionspray source (350 °C) and Analyst 1.5 and Multiquant data systems. Separation by liquid chromatography was performed on a Zorbax C18 column (1.8 μm, 50 x 2.1 mm; Agilent Technologies), again as previously described [13, 14]. In total, 294 lipids were detected and quantitated.

The total lipid concentration for each class measured was determined by summing the concentrations of individual species in that class. Univariate comparisons were conducted comparing lipid classes between PI3KC2α-deficient (CMV-rtTA;TRE-GFP-shPI3KC2α) and littermate control mice, using Welch's *t* test followed by Bonferroni correction to account for multiple comparisons.

Microfluidic assay

Platelet aggregation was performed using a previously described method modified for use in the present study with mouse whole blood [11]. Briefly, a microfluidic device consisting of 200 μm wide channels with inset 40 μm stenosis was fabricated using standard photolithography techniques [10]. Microchannels were selectively coated at the stenosis geometry with human

vWF (10 μg/ml - isolated from Biostate® CSL Ltd) for 10 min, blocked with BSA (2 μg/ml) for 10 min, then coated with botrocetin (2.5 μg/ml) for 10 min, before being flushed with Tyrode's buffer prior to sample perfusion. Hirudin-anticoagulated mouse whole blood was perfused through the microfluidic at 45 μl/min (equating to a shear rate at the stenosis geometry of 11,500 s^{-1}) and platelet deposition at the stenosis monitored in real time via epifluorescence (Nikon Ti-U microscope - Plan Fluor 20x/0.50 objective with Andor Zyla sCMOS detector). Mid-plane platelet aggregate size was analysed in ImageJ following thresholding (Huang's fuzzy image thresholding method). Maximal aggregation, expressed as cross-sectional area (μm^2), was extrapolated from non-linear curve fitting following 300 s perfusion time.

Analyses

Statistical analyses were performed using GraphPad Prism. Statistical significance was defined at $P < 0.05$ and was determined with an unpaired, two-tailed Student's *t*-test, followed by Bonferroni correction to account for multiple comparisons where appropriate and as indicated in the figure legends.

Results

PI3KC2α regulates platelet membrane structure

We have previously used 2-dimensional TEM imaging to demonstrate that PI3KC2α-deficiency results in a dilation of the channels of the OCS within mouse platelets [6]. In order to examine this and any other potential ultrastructural change caused by PI3KC2α-deficiency in more detail, we used FIB-SEM to create whole-cell, three-dimensional reconstructions of PI3KC2α-deficient mouse platelets. These reconstructions allow for visualisation and quantitation of various intracellular compartments, which in this case comprised the OCS and plasma membrane, as well as alpha and dense granules. In agreement with our previous 2-dimensional findings, we observed dilation of the OCS in platelets from PI3KC2α-deficient mice when compared with platelets from littermate controls (Figure 1A). Areas of OCS dilation in PI3KC2α-deficient platelets were more evident at certain points in a given cell (Figure 1A, red arrows) and the total volume of OCS in platelets isolated from PI3KC2α-deficient mice was 48% greater than in platelets from littermate control mice (3.6 ± 0.5 vs 5.4 ± 0.6% of total cell volume for control and PI3KC2α-deficient cells, respectively; Figure 1B). Despite this OCS dilation, no obvious differences were observed in the spatial distribution of the OCS throughout the cell (Figure 1A). In contrast to the OCS, the total volume of either alpha or dense granules was not different between control and PI3KC2α-deficient platelets (Figure 1C).

Given the OCS dilatation observed here and previously [6, 7], we next examined the external aspect of the OCS – its openings at the plasma membrane – via SEM (Figure 2A). There were similar numbers of OCS openings in the visible plasma membrane of cells examined in these studies (Figure 2B). However, in a near-identical finding to the OCS measurements inside

platelets, the diameter of OCS openings at the plasma membrane were significantly increased by 46% in platelets from PI3KC2α-deficient mice versus littermate controls (37 ± 4 vs 54 ± 3 nm, respectively; Figure 2C).

PI3KC2α does not regulate platelet membrane lipid composition

One of the most important contributors to membrane structure is the lipid content of the membrane. Therefore, we next examined whether the observed structural changes to the OCS were caused by or associated with alterations in the lipid profile of the platelet. We performed a detailed analysis of 294 lipids across the 22 most abundant lipid classes and subclasses using liquid chromatography electrospray ionisation-tandem mass spectrometry. This analysis revealed an unchanged lipid profile in PI3KC2α-deficient when compared with littermate control platelets (Figure 3), with no significant differences in molar abundance observed in any of the lipid classes analysed.

PI3KC2α does not regulate filopodia formation in platelets in suspension

We next examined whether the structural alteration in the platelet internal membrane impacts on platelet membrane function by imaging filopodia formation in platelets activated in suspension. Isolated platelets were stimulated with ADP (in the presence of eptifibatide to prevent aggregation), then fixed and imaged by SEM (Figure 4A). No differences were detected in either the number or length of filopodia between platelets isolated from PI3KC2α-deficient or littermate control mice (Figure 4B,C).

PI3KC2α regulates platelet adhesion and thrombus formation

Given the impaired arterial thrombus formation previously observed in PI3KC2α-deficient mice, we examined platelet function in a microfluidic whole blood flow assay known to be dependent on membrane tether formation [10-12]. Mouse blood was perfused through a von Willebrand factor-coated microfluidic channel incorporating a shear force gradient-inducing stenosis [10-12]. Platelet aggregation occurred downstream of the stenosis and the size of these platelet aggregates was quantified using the epifluorescent signal of the GFP-positive platelets (Figure 5). The extent of platelet deposition was significantly lower in blood from PI3KC2α-deficient mice (838 ± 314 μm^2) versus that in blood from control mice (2194 ± 485 μm^2) – a 62% reduction (Figure 5).

Together, these findings suggest loss of PI3KC2α leads to a specific structural change in the platelet membrane that occurs independently of membrane lipid composition. This membrane modification is sufficient to selectively impact upon platelet function in the setting of thromboses formed downstream of a shear gradient-inducing stenosis and dependent on membrane tethering.

Discussion

We performed an analysis of the structural and functional consequences of the loss of PI3KC2α in mouse platelets in order to gain insights into the mechanism by which PI3KC2α deficiency leads to the previously observed anti-thrombotic phenotype. We showed that PI3KC2α deficiency leads to an ultrastructural change in platelets that is limited to the internal membrane (OCS) of these cells. Specifically, the OCS in platelets from PI3KC2α-deficient mice was dilated throughout the cell, including at the plasma membrane. This structural change in the platelet membrane occurred independently of the cell's lipid composition. Yet inspection of platelet membrane function revealed PI3KC2α deficiency had selective effects under pro-thrombotic conditions: filopodia formation was unaffected in a static assay performed on cells in suspension, but platelet deposition and aggregation was significantly impaired in an ex vivo whole blood flow thrombosis model.

We and others have previously shown that platelets from PI3KC2α-deficient mice exhibit an increased surface area occupied by the channels of the OCS in TEM images [6, 8]. Here we add to those findings to show that the enlargements previously reported in 2D TEM images are reflective of a widespread and largely uniform dilation of membrane channels throughout the cell, including at the plasma membrane. Our detailed three-dimensional analysis of PI3KC2α-deficient platelets revealed this structural change was specific to the OCS: its volume was significantly increased in PI3KC2α-deficient platelets while the volumes of alpha and dense granules were unaffected, despite the occasional change in granule number or shape. Furthermore, the size of the openings of the OCS at the plasma membrane were significantly larger in PI3KC2α-deficient platelets. Despite this OCS dilation throughout the cell, no gross change in the spatial distribution of the OCS across the cell was observed.

Given that the biggest predictor of any membrane structure is its lipid composition, we performed a comprehensive analysis of the lipidome of both PI3KC2α-deficient and wild-type platelets. This analysis revealed the lipid profile of PI3KC2α-deficient platelets was indistinguishable to that of wild-type platelets, indicating the observed internal membrane dilatation is unlikely driven by compositional changes to the membrane. This is, to our knowledge, the first comprehensive lipidomic analysis of the mouse platelet. On this, it is interesting to note some potential differences in the relative abundance of some lipids between mouse platelets and similar lipidomic analyses of human platelets [15]. For example, while phospholipids are the predominant component in both mouse and human platelet membranes, there is a notably higher abundance of sterol lipids and a relative paucity of glycerolipids in mouse platelets when compared with human [15]. Whether these differences are important in terms of membrane function remains to be determined.

Previous studies have demonstrated an in vivo anti-thrombotic phenotype conferred by loss of PI3KC2α [6, 8]. Given that platelets from these PI3KC2α-deficient mice have a structural defect that is specific to the OCS – a reserve of membrane thought to be utilised for platelet shape change and spreading during activation and aggregation [16] – we examined platelet membrane function in both static and blood flow environments. We found that platelet membrane function is affected specifically in the presence of the forces of flowing blood. Here, filopodia production in suspension-activated platelets was unaffected by loss of PI3KC2α, yet in a microfluidic assay incorporating a high shear gradient-inducing stenosis, PI3KC2α-deficiency led to a marked reduction in platelet deposition. We utilised this microfluidic blood flow assay because of its incorporation of a pronounced stenosis that has been shown to cause a substantial shear gradient (from very high at the point of stenotic narrowing, to very low

immediately downstream of the stenosis) [10-12]. Importantly, in vivo studies of platelet behaviour following exposure to such a shear gradient environment (via a vascular stenosis) have shown that initial platelet deposition occurs largely independently of cellular activation by soluble agonists [12]. Indeed, such shear gradients appear to drive initial platelet deposition via the formation of membrane tethers [10-12]. As a result, the significant reduction in platelet deposition in this system using blood from PI3KC2α mice may suggest that PI3KC2α is important for the earliest stages of platelet adhesion, where membrane tethers, presumably derived from the OCS, are pulled from platelets without detectable cell activation via an interaction between von Willebrand factor and the platelet adhesion receptor GPIbα [17]. Alternatively, PI3KC2α may be involved in the subsequent propagation of platelet aggregates, since incoming platelets that tether to the surface of forming thrombi are discoid and demonstrate low levels of activation markers and minimal calcium flux, in sharp contrast to the initial core of the thrombus where platelets are generally fully activated [12, 18]. The lack of effect of PI3KC2α deficiency on platelet filopodia production in response to cell activation may suggest that the involvement of PI3KC2α is most prevalent where changes in shear stress sustain and drive thrombus propagation, potentially in the absence of conspicuous agonist-induced activation. The surprising lack of effect of PI3KC2α deficiency in standard assays of agonist-induced in vitro platelet function [6, 8] supports this hypothesis.

The intriguing link between the PI3KC2α-dependent modulation of platelet internal membrane structure and impaired platelet function specifically in the setting of blood flow suggests targeting PI3KC2α and/or the platelet internal membrane system may have utility as an anti-thrombotic strategy. However it remains unknown whether this function of PI3KC2α translates to human platelets. In addition, the relevance of changes in platelet membrane structure to

human platelet function are completely unexplored. There are a number of clinical syndromes in which abnormalities in the OCS are observed, including some with either bleeding or thrombotic consequences [19-21]. Yet platelets from patients with these conditions demonstrate a number of structural abnormalities in addition to OCS changes, making it difficult to determine how much, if any, contribution the OCS defect has to the clinical phenotype. The development of PI3KC2α inhibitors would be a useful step forward in determining the role of this enzyme in human platelets and in addressing any validity of this target as an anti-thrombotic approach. If PI3KC2α function is conserved in human platelets and acute inhibition of this enzyme is able to reproduce the phenotype observed in mouse platelets, this opens the possibility of manipulating the platelet membrane structure via PI3KC2α as a novel, thrombosis-specific, anti-platelet strategy.

Declarations of interest

The authors declare no competing financial interests.

Author contributions

MVS performed research, analysed data and wrote the manuscript; RJB, MJM and J-YR performed research; AE, CG, PJM, HHN and WSN contributed to study design, data analysis and interpretation of results; JRH designed the study, interpreted results and wrote the manuscript.

References

1.   Jean S, Kiger AA. Classes of phosphoinositide 3-kinases at a glance. *J Cell Sci* 2014; **127**: 923-8.

2.   Vanhaesebroeck B, Stephens L, Hawkins P. PI3K signalling: the path to discovery and understanding. *Nat Rev Mol Cell Biol* 2012; **13**: 195-203.

3.   Valet C, Severin S, Chicanne G, Laurent PA, Gaits-Iacovoni F, Gratacap MP, Payrastre B. The role of class I, II and III PI 3-kinases in platelet production and activation and their implication in thrombosis. *Adv Biol Regul* 2016; **61**: 33-41.

4.   Valet C, Levade M, Chicanne G, Bilanges B, Cabou C, Viaud J, Gratacap MP, Gaits-Iacovoni F, Vanhaesebroeck B, Payrastre B, Severin S. A dual role for the class III PI3K, Vps34, in platelet production and thrombus growth. *Blood* 2017; **130**: 2032-42.

5.   Liu Y, Hu M, Luo D, Yue M, Wang S, Chen X, Zhou Y, Wang Y, Cai Y, Hu X, Ke Y, Yang Z, Hu H. Class III PI3K Positively Regulates Platelet Activation and Thrombosis via PI(3)P-Directed Function of NADPH Oxidase. *Arterioscler Thromb Vasc Biol* 2017; **37**: 2075-86.

6.   Mountford JK, Petitjean C, Putra HW, McCafferty JA, Setiabakti NM, Lee H, Tonnesen LL, McFadyen JD, Schoenwaelder SM, Eckly A, Gachet C, Ellis S, Voss AK, Dickins RA, Hamilton JR, Jackson SP. The class II PI 3-kinase, PI3KC2alpha, links platelet internal membrane structure to shear-dependent adhesive function. *Nat Commun* 2015; **6**: 6535.

7.   Petitjean C, Setiabakti NM, Mountford JK, Arthur JF, Ellis S, Hamilton JR. Combined deficiency of PI3KC2alpha and PI3KC2beta reveals a nonredundant role for PI3KC2alpha in regulating mouse platelet structure and thrombus stability. *Platelets* 2016; **27**: 402-9.

8.   Valet C, Chicanne G, Severac C, Chaussade C, Whitehead MA, Cabou C, Gratacap MP, Gaits-Iacovoni F, Vanhaesebroeck B, Payrastre B, Severin S. Essential role of class II PI3K-C2alpha in platelet membrane morphology. *Blood* 2015; **126**: 1128-37.

9.   Eckly A, Heijnen H, Pertuy F, Geerts W, Proamer F, Rinckel JY, Leon C, Lanza F, Gachet C. Biogenesis of the demarcation membrane system (DMS) in megakaryocytes. *Blood* 2014; **123**: 921-30.

10.   Tovar-Lopez FJ, Rosengarten G, Westein E, Khoshmanesh K, Jackson SP, Mitchell A, Nesbitt WS. A microfluidics device to monitor platelet aggregation dynamics in response to strain rate micro-gradients in flowing blood. *Lab Chip* 2010; **10**: 291-302.

11.   Brazilek RJ, Tovar-Lopez FJ, Wong AKT, Tran H, Davis AS, McFadyen JD, Kaplan Z, Chunilal S, Jackson SP, Nandurkar H, Mitchell A, Nesbitt WS. Application of a strain rate gradient microfluidic device to von Willebrand's disease screening. *Lab Chip* 2017; **17**: 2595-608.

12.   Nesbitt WS, Westein E, Tovar-Lopez FJ, Tolouei E, Mitchell A, Fu J, Carberry J, Fouras A, Jackson SP. A shear gradient-dependent platelet aggregation mechanism drives thrombus formation. *Nat Med* 2009; **15**: 665-73.

13.   Weir JM, Wong G, Barlow CK, Greeve MA, Kowalczyk A, Almasy L, Comuzzie AG, Mahaney MC, Jowett JB, Shaw J, Curran JE, Blangero J, Meikle PJ. Plasma lipid profiling in a large population-based cohort. *J Lipid Res* 2013; **54**: 2898-908.

14.	Giles C, Takechi R, Mellett NA, Meikle PJ, Dhaliwal S, Mamo JC. The Effects of Long-Term Saturated Fat Enriched Diets on the Brain Lipidome. *PloS One* 2016; **11**: e0166964.

15.	Slatter DA, Aldrovandi M, O'Connor A, Allen SM, Brasher CJ, Murphy RC, Mecklemann S, Ravi S, Darley-Usmar V, O'Donnell VB. Mapping the Human Platelet Lipidome Reveals Cytosolic Phospholipase A2 as a Regulator of Mitochondrial Bioenergetics during Activation. *Cell Metab* 2016; **23**: 930-44.

16.	Escolar G, Leistikow E, White JG. The fate of the open canalicular system in surface and suspension-activated platelets. *Blood* 1989; **74**: 1983-8.

17.	Savage B, Saldivar E, Ruggeri ZM. Initiation of platelet adhesion by arrest onto fibrinogen or translocation on von Willebrand factor. *Cell* 1996; **84**: 289-97.

18.	Stalker TJ, Traxler EA, Wu J, Wannemacher KM, Cermignano SL, Voronov R, Diamond SL, Brass LF. Hierarchical organization in the hemostatic response and its relationship to the platelet-signaling network. *Blood* 2013; **121**: 1875-85.

19.	Maldonado JE, Gilchrist GS, Brigden LP, Bowie EJ. Ultrastructure of platelets in Bernard-Soulier syndrome. *Mayo Clin Proc* 1975; **50**: 402-6.

20.	Dayal S, Pati HP, Pande GK, Sharma P, Saraya AK. Platelet ultra-structure study in Budd-Chiari syndrome. *Eur J Haematol* 1995; **55**: 294-301.

21.	White JG, Krumwiede MD, Escolar G. Glycoprotein Ib Is Homogeneously Distributed on External and Internal Membranes of Resting Platelets. *Am J Path* 1999; **155**: 2127-34.

Figures and legends:

Fig.1
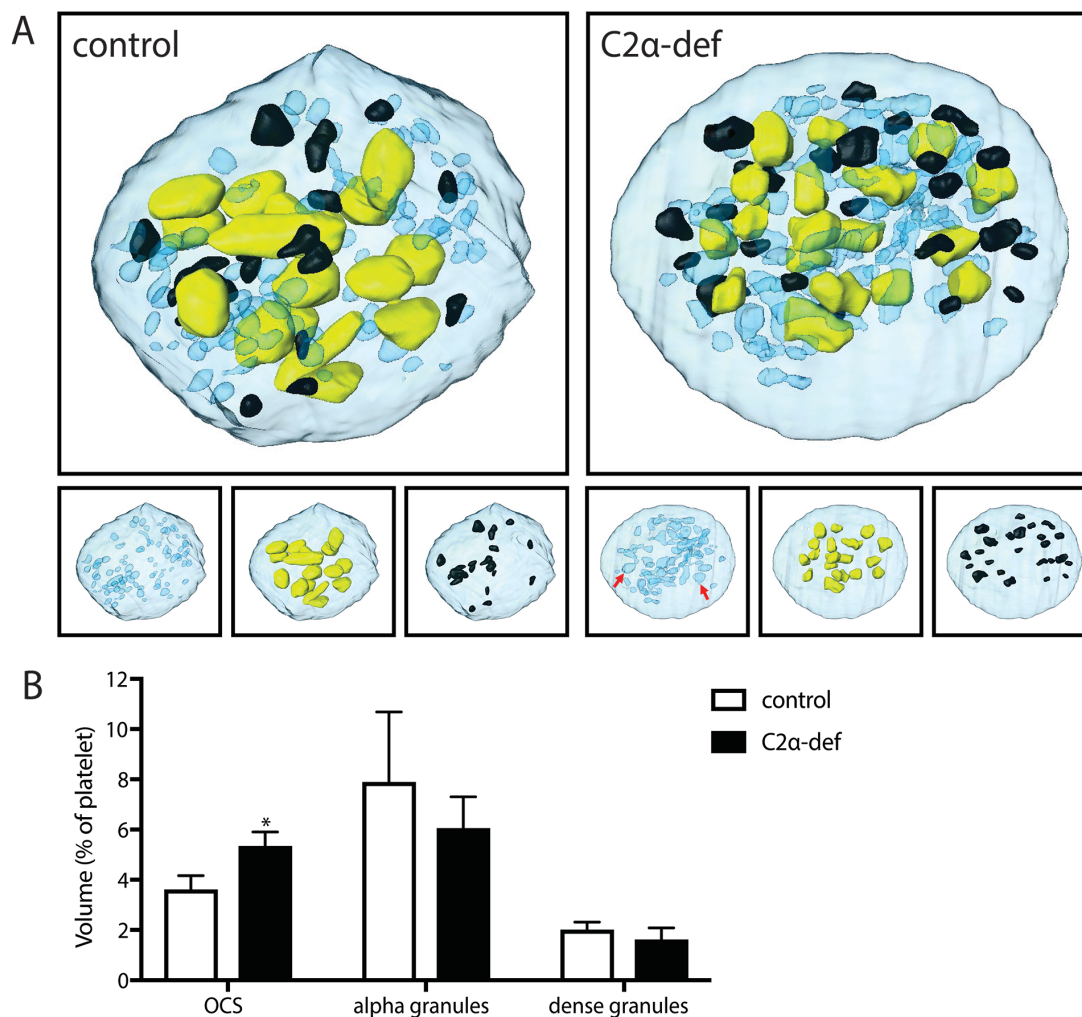
Figure 1. PI3KC2α regulates internal platelet membrane structure. (A) Representative 3-dimensional whole-cell FIB-SEM reconstructions of a platelet from a CMV-rtTA;TRE-GFP-shPI3KC2α bi-transgenic mouse (C2α-def) and a monotransgenic littermate (control) mouse, showing the OCS (blue), alpha granules (yellow), dense granules (black), and plasma membrane (light blue). Bottom panels show reconstructions with individual components only for clarity. Note dilation of the OCS in the PI3KC2α-deficient platelet (red arrows). (B) Quantitation of the volume of each organelle measured (as a percentage of the total platelet volume). Data are mean ± SEM from n=6 platelets. *, $P<0.05$ (unpaired, two-tailed, Student's t test).

Fig. 2
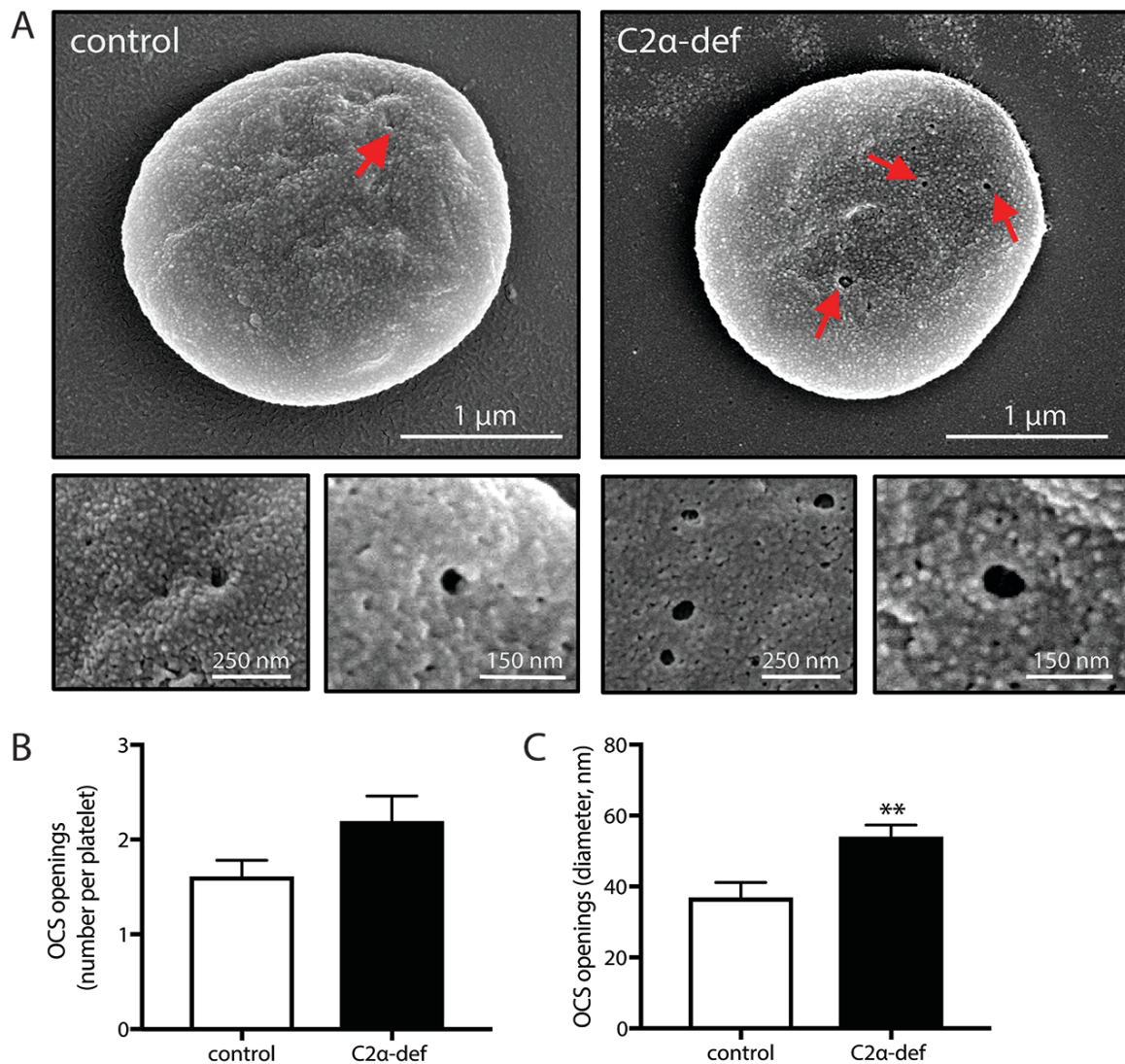
Figure 2. PI3KC2α regulates external platelet membrane structure. (A) Representative SEM images of resting platelets isolated from CMV-rtTA;TRE-GFP-shPI3KC2α bi-transgenic mice (C2α-def) or their wild-type and monotransgenic littermates (control), showing OCS surface openings (red arrows and the focus of the increased magnification images). (B) Number and (C) size of OCS openings. Data are mean ± SEM from n=112-116 platelets from n=4 mice per genotype. **, $P<0.01$ (unpaired, two-tailed, Student's t test).

Fig. 3
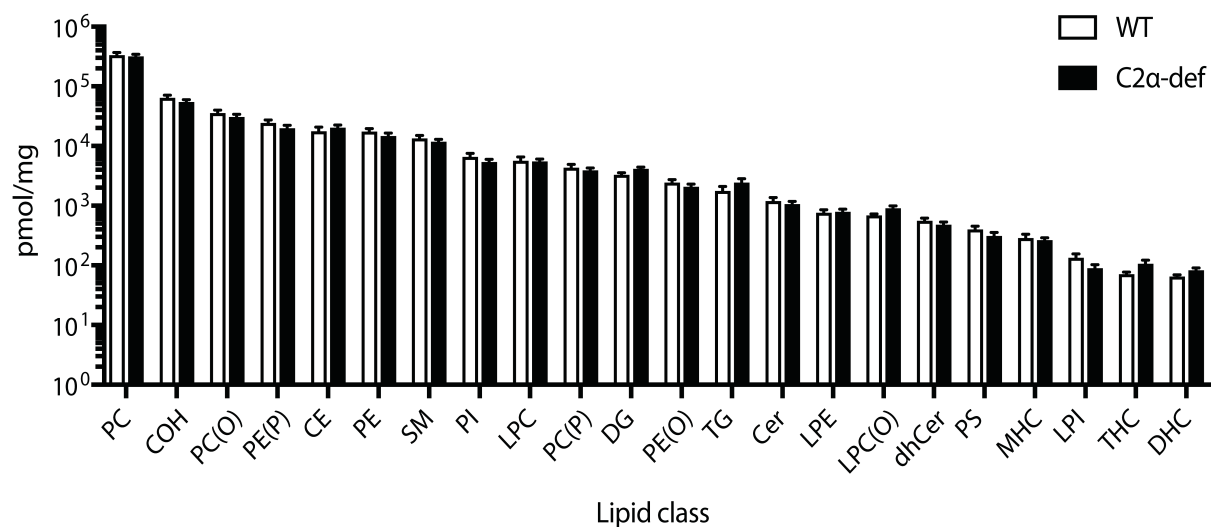
Figure 3. PI3KC2α does not regulate platelet lipid composition. Concentration of the 22 most abundant lipid classes in platelets isolated from CMV-rtTA;TRE-GFP-shPI3KC2α bi-transgenic mice (C2α-def) or their wild-type and monotransgenic littermates (control), via LC-ESI-MS/MS. Lipid classes are phosphatidylcholine (PC), free cholesterol (COH), alkylphosphatidylcholine (PC(O)), alkenylphosphatidylethanolamine (PE(P)), cholesterol ester (CE), phosphatidylethanolamine (PE), sphingomyelin (SM), phosphatidylinositol (PI), lysophosphatidylcholine (LPC), alkenylphosphatidylcholine (PC(P)), diacylglycerol (DG), alkylphosphatidylethanolamine (PE(O)), triacylglycerol (TG), ceramide (Cer), lysophosphatidylethanolamine (LPE), lysoalkylphosphatidylcholine (LPC(O)), dihydroceramide (dhCer), phosphatidylserine (PS), monohexosylceramide (MHC), lysophosphatidylinositol (LPI), trihexosylceramjde (THC) and dihexosylceramide (DHC). Molar abundance of each class is the total of the individual species within each class. Data are mean ± SEM from n=10-13 mice per genotype. No significant differences were observed (P>0.05 by unpaired, two-tailed, *t*-test with Bonferroni correction for multiple comparisons).

Fig. 4
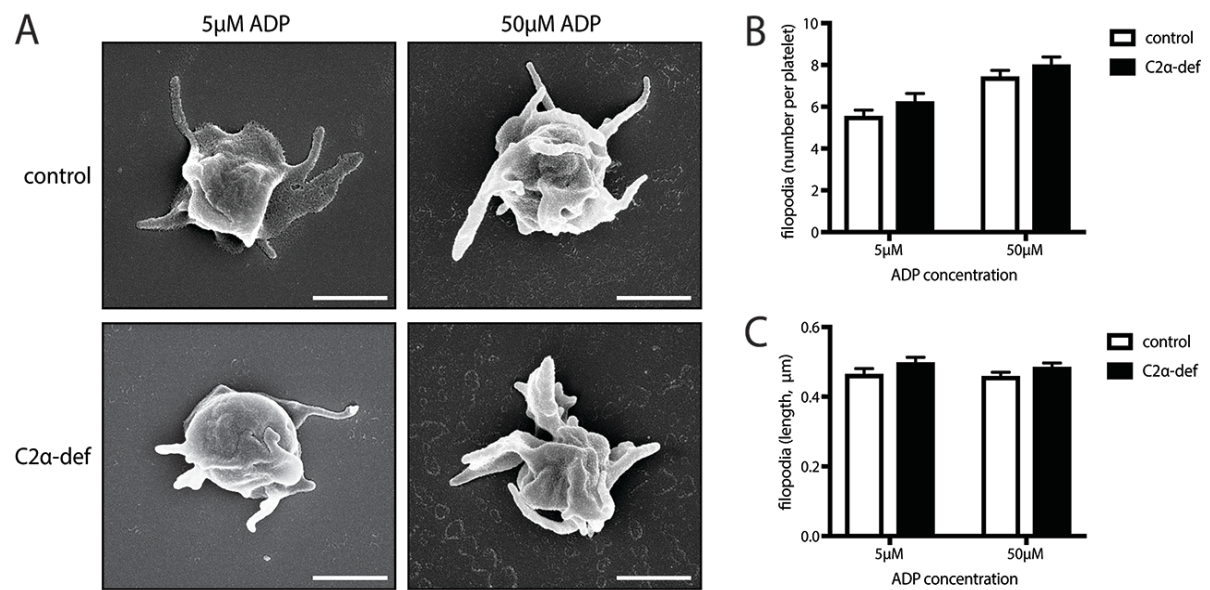
**Figure 4. PI3KC2α does not regulate filopodia formation in the absence of shear forces.** (A) Representative SEM images of platelets isolated from CMV-rtTA;TRE-GFP-shPI3KC2α bi-transgenic mice (C2α-def) or monotransgenic littermates (control) and activated in suspension with 5 or 50 µM ADP (in the presence of eptifibatide to prevent aggregation). All scale bars are 1 µm. (B) Number and (C) length of filopodia per platelet. Data are mean ± SEM from n=119-122 platelets from n=6 mice per genotype. No significant differences were observed in any comparison (P>0.05 by unpaired, two-tailed, *t* test).

Fig. 5
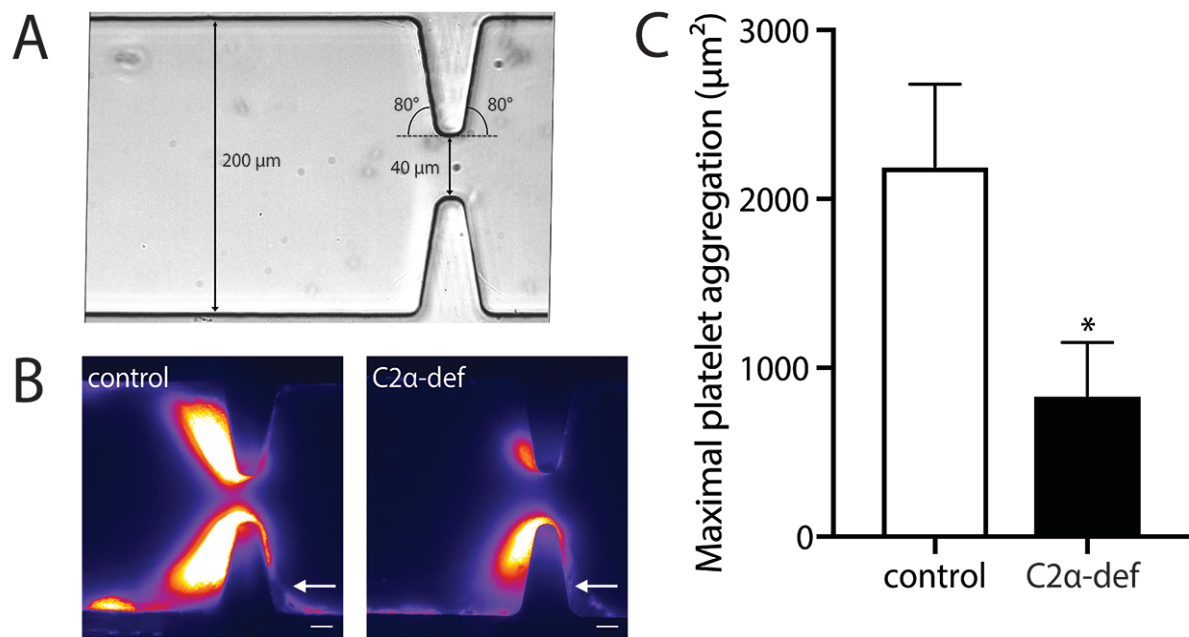
Figure 5. PI3KC2α regulates platelet adhesion and deposition driven by a shear gradient. (A) DIC image showing the geometry of the microfluidic flow cell used in the whole blood flow assay. The channel has a width of 200 μm narrowing to 40 μm at the stenosis, with side-wall entry and exit angles of 80°. (B) Representative fluorescence images following perfusion of blood taken from CMV-rtTA;TRE-GFP-shPI3KC2α (C2α-def) or CMV-rtTA;TRE-GFP-shControl (control) mice through the flow cell shown in (A), with platelet aggregates seen forming downstream of the stenosis. Arrows indicate direction of flow. Scale bars, 10 μm. (C) Maximal platelet aggregation measured in these experiments (expressed as aggregate area). Data are mean ± SEM from n=5-6 mice per genotype. *, $P<0.05$ (unpaired, two-tailed, Student's t test).

Determining the Role of PI3KC2α in Human Platelets and the Validity of Targeting PI3KC2α as an Anti-Thrombotic Strategy

The studies in Chapter 2, building upon our and other groups' previous research[91,113], showed that PI3KC2α regulates platelet function in mice specifically under conditions of blood flow and shear stress, suggesting that the enzyme may have potential as an anti-thrombotic drug target. However, several key questions remained. It was unknown whether PI3KC2α plays a role in human platelet structure and function, nor whether, if it did, the phenotype would be acute and inducible, rather than inherited, and thus targetable with a small molecule inhibitor. Furthermore, significant questions remained regarding the mechanism by which the changes in platelet structure gave rise to the functional impairment.

We have previously shown that PI3KC2α is present in human platelets at similar levels to those found in mouse platelets[91], yet its function in these cells was unknown. In order to examine the role of PI3KC2α in human platelets, a pharmacological inhibitor of PI3KC2α was required. However, no drugs targeting the enzyme have been reported. Therefore, our laboratory, in conjunction with the Monash Institute of Pharmacological Sciences, developed a small molecule inhibitor of PI3KC2α using a rational drug design approach. This compound, MIPS-19416, is a potent inhibitor of PI3KC2α, albeit, as the first-in-class compound identified, with less than desirable specificity. Careful controlling for these off-target effects using a number of other PI3K inhibitors was performed in all experiments here.

First, whether MIPS-19416 could acutely induce the structural changes in the platelet OCS seen in our mouse genetic model was determined. Initial studies were performed using TEM, testing various concentrations of MIPS-19416, the specificity of the structural phenotype, and the acuity and reversibility of the effect. A 3D analysis of the OCS in 19416-treated human platelets using FIB-SEM, similar to that undertaken previously in mouse, was also performed.

Next, the effect of PI3KC2α inhibition on a number of different aspects of platelet function was examined, in order to determine if there were any impacts on these that were contributing to the mechanism of action of PI3KC2α inhibition. Platelet membrane reserves were examined, given that the OCS functions as a source of extra membrane for platelet shape change and spreading. Platelet adhesion to vWF was also examined, and therefore the function of the platelet receptors GPIb and integrin $\alpha_{IIb}\beta_3$, as well as components of the platelet cytoskeleton, to determine if any changes to these were contributing to or associated with the membrane structural change.

Finally, whether PI3KC2α inhibition in human samples was able to acutely induce the functional impact of PI3KC2α deficiency seen in mouse was tested. This was assessed via platelet activation and aggregation using standard in vitro assays, as well as the impact on platelet deposition in a microfluidic whole blood thrombosis assay.

These studies found that inhibition of PI3KC2α in human samples acutely reproduced the structural and functional defects observed with PI3KC2α deficiency in mice. Inhibition of PI3KC2α is anti-thrombotic in human blood but does not impact on platelet activation or aggregation. This anti-thrombotic effect occurred via a unique, membrane-dependent mechanism, and was restricted to conditions where thrombus formation is driven by mechanisms outside of platelet activation.

Disrupting the platelet internal membrane via PI3KC2α inhibition impairs thrombosis independently of canonical platelet activation

M.V. Selvadurai[1], M.J. Moon[1], Z. Zheng[2], S.J. Mountford[2], R.J. Brazilek[1], R.P. Iman[1], L. Gupta[1], S.A. Sturgeon[1], J.-Y. Rinckel[3], A. Eckly[3], C. Gachet[3], W.S. Nesbitt[1,4], I.G. Jennings[2], P.E. Thompson[2] and J.R. Hamilton[1]*

Affiliations:

[1]Australian Centre for Blood Diseases, Monash University, Melbourne, VIC 3004, AUSTRALIA

[2]Medicinal Chemistry, Monash Institute of Pharmaceutical Sciences, Monash University, Parkville, VIC 3052, AUSTRALIA

[3]Université de Strasbourg, INSERM, EFS GEST, BPPS UMR_S949, FMTS, F-67000 Strasbourg, France

[4]Microplatforms Research Group, School of Engineering, RMIT University, Melbourne, Australia

*To whom correspondence should be addressed:

Justin R. Hamilton
Australian Centre for Blood Diseases
Monash University
L1 AMREP Building
99 Commercial Road
Melbourne, VIC 3004
AUSTRALIA

Telephone: +61-3-9903-0125
Email: justin.hamilton@monash.edu

One Sentence Summary: PI3KC2α inhibition selectively impairs platelet function during thrombosis by disrupting the structure of the internal membrane and blocking prothrombotic platelet function independently of canonical activation.

Abstract:

Arterial thrombosis causes heart attacks and most strokes and is the most common cause of death in the world. Platelets are the cells that form arterial thrombi, and anti-platelet drugs are the mainstay of heart attack and stroke prevention. Yet current drugs have limited efficacy, preventing fewer than 25% of lethal cardiovascular events without clinically significant effects on bleeding. The key limitation on the ability of all current drugs to impair thrombosis without causing bleeding is that they block global platelet activation, thereby indiscriminately preventing platelet function in hemostasis and thrombosis. Here, we identify an approach that overcomes this limitation by preventing platelet function independently of canonical platelet activation and that appears relevant specifically in the setting of thrombosis. Genetic or pharmacological targeting of the Class II PI3-kinase, PI3KC2α, dilates the internal membrane reserve (open canalicular system) of platelets but does not affect activation-dependent platelet function. Inhibition of PI3KC2α is potently anti-thrombotic in human blood *ex vivo* and mice *in vivo*, but does not impact hemostasis. Mechanistic studies reveal that this anti-thrombotic effect occurs via a unique mechanism involving the regulation of membrane-dependent platelet adhesive function in the presence of hemodynamic forces. These findings demonstrate an important role for PI3KC2α in regulating platelet structure and function via a unique membrane-dependent mechanism, and suggest that drug targeting the platelet internal membrane may be a suitable approach for novel anti-thrombotic therapies with an improved therapeutic window.

Introduction

PI3Ks are a family of broadly-expressed enzymes that catalyse the formation of the intracellular signalling molecules PI(3)P, PI(3,4)P$_2$, and PI(3,4,5)P$_3$. These membrane-bound lipids influence the location and activity of signalling complexes by scaffolding key signalling proteins *via* specialised lipid-binding domains (*1*). Mammals have eight PI3Ks that are separated into three classes defined by substrate specificity and use of regulatory subunits: four Class Is (p110α, p110β, p110δ, and p110γ), three Class IIs (PI3KC2α, PI3KC2β, and PI3KC2γ), and one Class III (Vps34). The Class I PI3Ks are by far the most widely studied and have well-defined roles in a number of cell types (*2-4*). In marked contrast, the cellular functions of Class II PI3Ks have only begun to emerge in recent years, in large part due to the recent development of genetically modified mouse models and selective pharmacological inhibitors of these enzymes (*5, 6*).

We and others have recently reported an important role for PI3KC2α in mouse platelet function (*7-9*). We have shown that platelets from mice and humans express PI3KC2α and PI3KC2β, but not PI3KC2γ (*7*). We generated mice deficient in PI3KC2α or PI3KC2β and found no platelet defect in PI3KC2β$^{-/-}$ mice and 100% embryonic lethality in PI3KC2α$^{-/-}$ mice (*7*). To overcome this, we developed an inducible RNAi-based approach to reduce gene expression in platelets of adult mice (*10*). We used a CMV-driven and tet-regulated system to induce expression of microRNA-based short hairpin RNAs (shRNAs) (*11, 12*) against PI3KC2α. We have shown that this system induces knockdown of target proteins in a wide range of cells and is highly effective in platelets (*10*). Treating these mice with doxycycline (600 mg/kg in food for ≥ 10 days) resulted in undetectable platelet PI3KC2α expression and led to marked protection against arterial thrombosis without any impact on bleeding (*7*). These findings were confirmed using a distinct mouse model in which a kinase-inactivating point mutation was

introduced into the active site of PI3KC2α (*8*). Intriguingly, the *in vivo* platelet dysfunction of PI3KC2α-deficient mice appears due to a novel mechanism related to the regulation by PI3KC2α of the structure of the internal membrane reserves of platelets (open canalicular system; OCS) (*7-9*). Together, these studies defined an unexpected role for PI3KC2α in regulating the structure of the platelet internal membrane, and provide the first evidence linking the OCS to the thrombotic function of platelets. This initial work suggests that drug targeting of platelet internal membrane structure and function via pharmacological inhibition of PI3KC2α may represent a viable approach for novel anti-platelet therapy. However, in the absence of PI3KC2α inhibitors, whether or not a similar function occurs in human platelets remained unknown.

Here, we develop a first generation PI3KC2α inhibitor and show that it reproduces in human platelets the structural and functional anti-platelet effects observed in PI3KC2α-deficient mouse platelets. Further, PI3KC2α inhibition provides potent anti-thrombotic effects in mice and humans via a mechanism involving the function of the platelet membrane. Our studies indicate PI3KC2α inhibition is a viable target for unique anti-platelet drug therapy and identify an approach for targeting the platelet internal membrane structure and function for therapeutic benefit.

Results

Identification of a potent inhibitor of PI3KC2α.

There are no reported isoform-selective PI3KC2α inhibitors, and the literature relating to PI3KC2α inhibition in general is sparse. As a starting point for the development of such inhibitors, we drew on a report by Knight et al., that described "off-target" PI3KC2α inhibition induced by a range of compounds from the patent literature. Among them was PIK-90 (Fig. 1), which has an IC_{50} against PI3KC2α of 47 nM (versus 11 nM against PI3K p110α), with IC_{50} values determined in *in vitro* kinase assays using purified enzymes (*13*). We also identified the analogue copanlisib (Fig. 1) as a potent inhibitor of all class I isoforms (< 10 nM for each) but substantially more moderate against PI3KC2α (> 1000 nM) (*14*). We confirmed these potencies in our own hands using activity assays of recombinant PI3K enzymes and sought to make more potent inhibitors (Table 1). The x-ray structures of PIK-90 and copanlisib bound to the Class I PI3K, p110γ, show that the C5-amide of each molecule projects into the affinity pocket (*13, 14*). This region is conserved across the PI3K isoforms except for PI3KC2α, where there is both a Phe for Tyr substitution and a Glu for Asp substitution. Therefore, we considered that changes in structure may enhance the potency or selectivity of PIK-90 for PI3KC2α.

To this end, modification of PIK-90 at the C5-nicotinamide yielded several compounds with comparable potency versus PI3KC2α. The 4-amino-nicotinamide, MIPS-19416, was the most potent of these, with an IC_{50} against PI3KC2α of 13 nM, which was equal to or more potent than against any of the Class I isoforms (IC_{50}s against p110α, p110β, p110γ and p110δ of 12, 53, 94 and 20 nM, respectively) or against PI3KC2β (15 nM; Table 1). We also developed the unrelated compound MIPS-19417 (Fig. 1), which exhibited potency against PI3KC2β (IC_{50} 278 nM) but not PI3KC2α (IC_{50} > 10 μM; Table 1). Together, this formed a suite of compounds that provided either potency against PI3KC2α (MIPS-19416) or acted as a control for the non-

PI3KC2α PI3K activity of MIPS-19416 (e.g. MIPS-19417 for PI3KC2β; copanlisib for all Class I PI3Ks; Table 1).

PI3KC2α inhibition reproduces the platelet cell biology effects of PI3KC2α-deficiency

Having uncovered a series of compounds with varying potency and specificity against PI3KC2α, we first examined whether pharmacological inhibition of PI3KC2α reproduces the phenotypes observed in PI3KC2α-deficient mice. We have previously reported that genetic deficiency of PI3KC2α causes dilation of the open canalicular system (OCS) in platelets that appears linked to an *in vivo* platelet dysfunction sufficient to impair arterial thrombosis (*7, 9*). Therefore, we examined whether PI3KC2α inhibition mimicked these effects. Here, MIPS-19416 accurately reproduced the changes in OCS structure observed in PI3KC2α-deficient mouse platelets, both qualitatively and quantitatively, in platelets isolated from either mice or humans. Ultrastructure analysis by transmission electron microscopy revealed that exposure of mouse platelets to MIPS-19416 (10 µM, 3 h) induced a similar pattern of OCS dilation to that observed in platelets from PI3KC2α-deficient mice (Fig. 2A). Both PI3KC2α-deficient and MIPS-19416-treated mouse platelets displayed regions of dilated OCS, with a cross-sectional surface area that was 30 – 40% larger than in platelets from their littermate or vehicle-treated controls respectively (Fig. 2B). Importantly, the same treatment of human platelets with MIPS-19416 (10 µM, 3 h) resulted in a near-identical effect (Fig. 2A,B). A concentration-response curve to MIPS-19416 revealed concentrations of 1 µM were sufficient to induce a significant effect in this assay (Fig. 2C). Note that treatment of platelets from PI3KC2α-deficient mice with MIPS-19416 caused no additional effect (Fig. 2A,B).

As MIPS-19416 is potent but not PI3KC2α isoform-specific, we examined the effects of an array of PI3K inhibitors with reduced PI3KC2α inhibitory potency (Fig. 2D). No effect on the OCS was observed following treatment with copanlisib (IC_{50}s [nM] against PI3KC2α > 1000;

PI3KC2β > 1000; p110α = 0.5), pictilisib (IC$_{50}$s [nM] against PI3KC2α > 10000; PI3KC2β = 590; p110δ = 6) dactolisib (IC$_{50}$s [nM] against PI3KC2α = 155; PI3KC2β = 44; p110α = 4), or MIPS-19417 (Compound 13, Miller et al. (*15*), IC$_{50}$s [nM] against PI3KC2α >10000; PI3KC2β = 278; p110β = 775, p110δ = 52). Together, this genetic and pharmacological evidence strongly suggests that it is inhibition of PI3KC2α that leads to dilation of the OCS in mouse and human platelets.

The OCS dilation induced by PI3KC2α inhibition occurred rapidly, with a significant increase in OCS surface area in as little as 5 min of MIPS-19416 treatment and with no greater dilation occurring beyond this time out to 3 h of drug treatment (Fig. 2E). In addition, the OCS effects induced by MIPS-19416 were fully reversible; pretreatment of human isolated platelets for 5 min followed by drug washout resulted in a marked reduction in OCS dilation after 5 min and a return to control levels after 60 min (Fig. 2E). Together, these findings indicate the regulation of OCS structure by PI3KC2α is surprisingly dynamic.

To extend on this 2-dimensional analysis of OCS dilation in response to genetic deficiency or pharmacological inhibition of PI3KC2α, we next examined the complete architecture of the OCS using focused ion bean-scanning electron microscopy (FIB-SEM) (*16*). Whole cell 3D reconstructions of wildtype versus PI3KC2α-deficient mouse platelets and vehicle- versus PI3KC2α inhibitor-treated human platelets revealed a similar pattern of OCS dilation as observed in our 2-dimensional analysis (Fig. 3A). In both cases, a near-uniform OCS dilation was observed throughout the cells, without any major change in its distribution (Fig. 3A). Quantitation revealed a strikingly similar ~ 40% increase in OCS volume in PI3KC2α-deficient mouse platelets or PI3KC2α-inhibitor treated human platelets when compared with their respective control (Fig. 3B). Taken together, these studies indicate that pharmacological inhibition of PI3KC2α accurately reproduces the effects of PI3KC2α deficiency relating to the

structure of the internal membrane reserves of platelets, and that this effect extends to human platelets.

PI3KC2α inhibition is anti-thrombotic in human blood ex vivo *independently of canonical platelet activation mechanisms*

Pretreatment of human platelets with MIPS-19416 had no effect on thrombin-induced platelet aggregation (Fig. 4A) or $\alpha_{IIb}\beta_3$ activation (Fig. 4B), even at concentrations 100-fold above that required to induce marked changes in OCS structure under identical treatment conditions. The rank order of potency for inhibition of both aggregation and $\alpha_{IIb}\beta_3$ activation was copanlisib > MIPS-19417 >> MIPS-19416, which suggests inhibition of platelet activation observed here is largely dependent on Class I PI3Ks and is decoupled from PI3KC2α.

We next examined the anti-thrombotic potential of PI3KC2α inhibition. Platelet-dependent thrombus formation was examined in human blood *ex vivo* by perfusing anticoagulated whole blood over an immobilised Type I fibrillar collagen substrate (*17, 18*). Here, we observed that pretreatment of human whole blood with MIPS-19416 (10 µM, 10 min) was sufficient to provide striking anti-thrombotic effects, markedly impairing platelet-dependent thrombus growth on a collagen surface (Fig. 4C,D). 3D reconstructions of thrombi indicated that the platelet deposition on the collagen surface was not significantly different at its base level (platelet-collagen interaction), but that subsequent platelet-platelet interaction-dependent growth was markedly impaired (Fig. 4C). As was observed in the platelet cell biology experiments, the anti-thrombotic effects induced by MIPS-19416 occurred rapidly (10 min pre-treatment).

We next examined the effects of PI3KC2α inhibition directly against the effects of the two most commonly-used anti-platelet strategies, aspirin (50 µM acetylsalicylic acid) and $P2Y_{12}$ receptor inhibition (100 µM 2-MeSAMP). As previously observed (*19, 20*), the anti-thrombotic

effects of both aspirin and 2-MeSAMP were dependent on the blood shear rate present during thrombogenesis. As expected, both aspirin and 2-MeSAMP effectively impaired human thrombus formation at 1800 s^{-1}, but not at the elevated shear rate of 3000 s^{-1} (Fig. 4E). In contrast, the anti-thrombotic effects of MIPS-19416 were retained at 3000 s^{-1} (Fig. 4E). These findings indicate that inhibition of PI3KC2α provides robust anti-thrombotic effects in human blood that occur in the absence of overt inhibition of canonical platelet activation. Further, this anti-thrombotic activity persisted in the face of elevated blood shear forces that are sufficient to overcome the anti-thrombotic effects of gold-standard approaches to platelet function inhibition.

PI3KC2α inhibition is anti-thrombotic in mice in vivo *but has no effect on hemostasis*

Having established the anti-thrombotic effects of PI3KC2α inhibition in humans *ex vivo*, we next examined the *in vivo* effects of MIPS-19416 on thrombosis and hemostasis. Electrolytic injury-induced thrombosis of the mouse carotid artery was significantly impaired by pre-treatment of mice with as little as 0.1 mg/kg MIPS-19416 and almost abolished by 1 mg/kg MIPS-19416 (Fig. 5A). Histological analyses of thrombi formed in the damaged carotid arteries in these experiments showed occlusive platelet-rich thrombi in vehicle-treated mice, non-occlusive thrombi in mice treated with 0.1 mg/kg MIPS-19416, and markedly smaller fibrin-rich thrombi with very few platelets in mice treated with 1 mg/kg MIPS-19416 (Fig. 5B). Similarly striking anti-thrombotic activity was observed in a distinct mouse model of occlusive thrombus formation. In the Folts model of recurrent occlusive thrombotic events in the mouse carotid artery damaged by physical trauma (*17, 21*), intravenous administration of MIPS-19416 (1 mg/kg) abolished the stable recurrent occlusive thromboses in this model inside 15 min (Fig. 5C). This absolute protection against thrombosis remained for the entirety of the 60 min observation period (Fig. 5C). Despite striking anti-thrombotic effects in these two models, the same dose of MIPS-19416 (1 mg/kg) had no impact on bleeding when compared to vehicle-

treated control mice in an *in vivo* model of hemostasis (Fig. 5D). Notably, a therapeutic dose of the gold-standard anti-platelet drug, aspirin (200 mg/kg – sufficient to cause modest anti-thrombotic effects in the two *in vivo* models examined here (*19, 21, 22*)), significantly prolongs bleeding time under these conditions (Fig. 5D). These *in vivo* findings support our *ex vivo* human thrombosis studies and indicate PI3KC2α inhibition prevents *in vivo* thrombosis and affords an improved therapeutic window over that provided by the current leading anti-platelet approaches.

The anti-platelet effects provided by PI3KC2α inhibition are due to a unique impact on membrane-dependent platelet adhesion under high shear

We next examined the mechanism by which modulation of the OCS structure may link to the prothrombotic function of platelets. The OCS is the specialized internal membrane reserve of platelets and its mobilization is important for the increased platelet surface area that occurs during platelet shape change and spreading (*23*). Our previous observations in mice revealed that, despite their dilated OCS, PI3KC2α-deficient platelets do not have additional membrane reserves nor cytoskeletal abnormalities, yet they fail to form robust and stable thrombi under the hemodynamic shear forces of flowing blood (*7*). Here, we observed the same holds true for PI3KC2α-inhibited human platelets. First, MIPS-19416 pretreatment (10 μM, 10 min) had no effect on the surface area of human platelets spread on glass (Fig. 6A) nor on tether-dependent platelet adhesion to von Willebrand factor (Fig. 6B), despite the latter being dependent on both GPIb and $\alpha_{IIb}\beta_3$ – as indicated by a 3-fold increase in platelet translocation velocity with the $\alpha_{IIb}\beta_3$ inhibitor, integrilin (Fig. 6B). Second, MIPS-19416 had no effect on the structure of the platelet microtubule ring at rest nor on the formation of filamentous actin in activated platelets (Fig. 6C). Given 1) the similarities between PI3KC2α-deficient mouse platelets and PI3KC2α-inhibited human platelets in both structure and function and 2) that, in both cases, anti-thrombotic effects are observed only in the presence of hemodynamic forces, we focused on

the utilization of membrane reserves under such conditions. Therefore, we next established a microfluidic system in which the prothrombotic function of platelets occurs largely independently of traditional platelet activation mechanisms (*24, 25*). Specifically, we examined real time platelet aggregation in human blood perfused through a von Willebrand factor-coated microfluidic channel that incorporates a high-shear-inducing stenosis (Fig. 6D,E). The perturbed blood flow that occurs as a result of this shear gradient, specifically the deceleration in shear immediately after the stenosis, leads to the deposition and aggregation of unactivated discoid platelets via the formation of membrane tethers (*26*). As such, under these conditions, platelet deposition is resistant to inhibitors of platelet activation; combined treatment with drugs to block $P2Y_1$ (10 µM MRS2179), $P2Y_{12}$ (100 µM 2-MeSAMP), ADP (2 U/ml apyrase), COX (10 µM indomethacin), and thrombin (800 U/ml hirudin) only partially impaired platelet deposition (~30%) in these channels ('amplification loops blocked', ALB; Fig. 6F). Remarkably, pretreatment of human blood with MIPS-19416 alone (10 µM, 10 min) inhibited platelet deposition to a greater extent than with amplification loop blockade, and nearly abolished platelet deposition when added to the cocktail of platelet activation inhibitors (Fig. 6F). Together, these experiments suggest PI3KC2α regulates the utilization of platelet membrane reserves that drives activation-independent platelet adhesion in the setting of pronounced hemodynamic shear stress.

Discussion

We have described here an approach to prevent thrombosis without inhibition of canonical platelet activation. We developed a small molecule inhibitor of PI3KC2α that was an effective anti-thrombotic in mice and humans but did not affect agonist-induced platelet activation *in vitro* – even at concentrations 100-fold greater than those required for thrombosis prevention. Intriguingly, and in contrast to all known anti-platelet approaches, this effect appears to involve a structural change in the platelet's OCS that leads to impaired platelet function only under conditions where thrombus formation is promoted independently of platelet activation.

We have previously reported that PI3KC2α-deficiency in mouse platelets results in impaired thrombus formation (*7*). Specifically, we used an inducible RNAi-based approach to deplete PI3KC2α in adult mouse platelets. These mice exhibited delayed and unstable thrombosis in an *in vivo* model, yet platelet function in standard *in vitro* function tests (aggregation, alpha and dense granule secretion, phosphotidylserine exposure, adhesion and spreading on various surfaces) remained unchanged. Indeed, the only change we observed in PI3KC2α-deficient platelets was a previously undescribed and marked dilation of the OCS that was apparent in circulating platelets. These previous studies led us to hypothesize a link between the OCS and *in vivo* prothrombotic platelet function. Our initial observations were supported by a subsequent study, using a distinct model of PI3KC2α-deficiency in mouse platelets, but in which strikingly similar effects on platelet OCS structure and prothrombotic function were reported (*8*). However, in the absence of pharmacological inhibitors of PI3KC2α, whether or not a similar mechanism existed in human platelets remained unknown. Indeed, in the studies from both us (*7*) and others (*8*), a modest effect on megakaryocyte structure was also observed, indicating the likelihood that the OCS structural abnormalities of PI3KC2α-deficient mouse platelets may have been inherited at the time of their production. However, the pharmacological studies described here not only reveal that the regulation of OCS structure by

PI3KC2α in mouse platelets is conserved in human platelets, but they also indicate that the regulation of OCS structure by PI3KC2α can occur acutely and is surprisingly dynamic.

There is little information indicating the possibility of rapidly and acutely altering OCS structure. Cholesterol depletion has been suggested to collapse the OCS (*27*), presumably through a direct effect on membrane composition. To our knowledge, the only pharmacological manipulation of OCS structure reported to date involves the use of amphiphilic cationic agents, such as the calmodulin inhibitor W-7, which have been shown to dilate the megakaryocyte DMS and platelet OCS (*28*). It has been proposed that this dilation of internal membrane reserves in these cells occurs via a mechanism that may involve interference with phospholipid signaling, most likely PI(4,5)P_2 (*28*). Our studies show that inhibition of Class II PI3K function can similarly dilate the OCS of mouse and human platelets, and that this can impact on platelet function. While the PI3KC2α-dependent effects observed here are unlikely to be due to a direct effect on PI(4,5)P_2, phospholipid signaling may still be involved. Previous studies have shown that the Class II PI3K, PI3KC2α, is responsible for producing a basal pool of PI(3)P in mouse platelets (*8*). This same study also showed reduced expression of key cytoskeletal proteins in PI3KC2α-deficient mouse platelets (*8*). The rapid effect of PI3KC2α inhibition on platelet structure observed here (< 5 min) suggests changes in cytoskeletal protein expression are unlikely causative of the structural and functional changes in PI3KC2α-inhibited platelets. However, whether or not continued PI(3)P production is necessary for the maintenance of OCS structure remains unknown, and is certainly plausible. Using standard approaches for the analysis of phospholipid production, we have not yet observed any basal or induced changes in PI levels in PI3KC2α-deficient platelets (*7, 9*). The rapid nature of the effects of PI3KC2α inhibition are suggestive of this mechanism, but will require approaches with improved sensitivity for detecting changes in intracellular PI levels (*8, 29*), including the possibility of

small, localized changes in PI(3)P in and around the OCS beyond the detection limits of current approaches.

Regardless of the level of involvement of PI signaling, the specificity of the effect for PI3KC2α is clear: pharmacological targeting acutely reproduced the genetic effects; PI3KC2α inhibition produced no additional effects over PI3KC2α-deficiency; and only drugs with significant activity against PI3KC2α were with effect. Together, these findings strongly suggest further drugs targeting PI3KC2α are likely to produce the potent anti-thrombotic effects observed here, and further improvements in potency and, more particularly, specificity, for PI3KC2α are keenly sought.

Finally, the translation here of previous studies in mice to humans is the first demonstration of drug targeting the OCS for anti-thrombotic benefit. It is far too early to say whether this novel approach is a viable strategy for anti-thrombotic therapy. However, it is noteworthy that the anti-thrombotic effects observed here in response to PI3KC2α inhibition occur independently of known platelet activation mechanisms. One potential advantage of such an approach is that PI3KC2α-inhibited platelets function normally in all situations we have examined – except when forming thrombi under pathological conditions. One major limitation on the efficacy of all current anti-platelet drugs is that they all block global platelet activation and thus indiscriminately prevent platelet function in the setting of hemostasis and thrombosis. Our prediction is that the unique mechanism by which PI3KC2α-deficiency or -inhibition prevents platelet function underlies the lack of bleeding observed in PI3KC2α-deficient or PI3KC2α-inhibited mice, since the platelets are not circulating in an inhibited state. Whether or not this will enable a widening of the therapeutic window between hemostasis and thrombosis remains to be seen, but is of obvious appeal. In addition, the targeting of a distinct mechanism of action within the cell provide an opportunity for additive effects over standard–of-care. Such additive effects are most readily observed in our microfluidic assay in which significant platelet

deposition occurs independently of platelet activation (*24, 25*). Much of the platelet aggregation and deposition under these conditions is not inhibited by drugs blocking global platelet activation mechanisms, and yet is highly sensitive to PI3KC2α inhibition. The ability to target this aspect of thrombosis that is relatively resistant to current therapies is of obvious interest. It is notable that such deposition of unactivated platelets is largely favored by the presence of a region of stenosis (high shear) followed by a rapid expansion (low shear), with platelet accumulation occurring almost exclusively in the low shear zone immediately downstream of the stenosis. This anatomy resembles that observed in, for example, large arteries burdened with significant deposits of atherosclerotic plaque – a major site of arterial thrombosis. In this regard, it is tempting to speculate that PI3KC2α inhibition may improve thrombosis prevention in the setting of such pathologies.

Materials and Methods

Study Design

This study was designed to determine the feasibility and impact of pharmacological inhibition of PI3KC2α in the context of arterial thrombosis. Our first-in-class small molecule inhibitor of PI3KC2α, MIPS-19416, was identified using a rational drug design approach, and chosen due to its high potency (IC_{50} = 13 nM). The effect of MIPS-19416 on human and mouse platelet membrane structure was examined using transmission electron microscopy for 2D imaging and focused ion beam-scanning electron microscopy for 3D modelling. Functional anti-thrombotic effects were examined in human blood from healthy volunteers using *ex vivo* thrombosis assays, and in mice *in vivo* using the electrolytic thrombosis and Folts models.

Mouse generation and use

All animal experiments performed in this study were approved by the Alfred Medical Research and Education Precinct Animal Ethics Committee (approvals E/1465/2014M and E/1644/2016/M). All mice used in this study were backcrossed ≥ 5 generations on a C57BL/6 genetic background (i.e., ≥ 98%) and maintained on a 12-h light/dark cycle with food and water given *ad libitum*. PI3KC2α-deficient mice were generated using our previously published shRNA-based inducible and reversible gene-silencing approach (*7*). To induce gene knockdown, mice were placed on a doxycycline diet (600 mg/kg, Speciality Feeds, Australia), for at least 10 days prior to experimentation.

For mouse whole blood and platelet isolation, blood was drawn from the inferior vena cava of anaesthetised mice, using a 25-gauge needle, into enoxaparin (40 U/ml, final concentration). Platelets were isolated as previously described (*7*).

Human platelet preparation

All human studies were approved by the Monash University Human Research Ethics Committee. Blood from healthy volunteers was withdrawn using a 19-gauge butterfly needle into syringes containing either acid citrate dextrose (7:1 v/v, final concentration) for platelet isolation, or hirundine (800 U/ml, final concentration) or enoxaparin (40 U/ml, final concentration), for *ex vivo* whole blood flow experiments.

Platelets were isolated as previously described (*17, 18*). Briefly, platelet-rich plasma (PRP) was obtained by centrifuging blood at 200 g for 15 min. Following 10 min of rest, the PRP was centrifuged at 1700 g. The platelet-poor plasma was removed by aspiration, and the pellet resuspended in platelet wash buffer (4.3 mM K_2HPO_4, 4.3 mM Na_2HPO_4, 24.3 mM NaH_2PO_4, 113 mM NaCl, 5.5 mM D-glucose and 10 mM theophylline; pH 6.5; containing 0.5% BSA, 20 U/ml enoxaparin and 0.01 U/ml apyrase). After a second 10 min rest period, centrifugation at 1500 g produced a platelet pellet, which was resuspended at the required concentration in Tyrode's buffer containing 0.5% BSA, 1.8 mM Ca^{2+} and 0.02 U/ml apyrase.

Transmission electron microscopy and OCS analysis

Platelet ultrastructure was analysed via TEM as described (*30*). Briefly, isolated platelets were fixed in 2% glutaraldehyde and 2.5% paraformaldehyde, post-fixed in 2% osmium tetroxide, dehydrated through an ethanol series, and embedded in Spurr's resin. Ultrathin sections were cut with a diamond knife (Diatome) on an ultramicrotome (Leica) and stained with methanolic uranyl acetate and lead citrate before TEM imaging (JEOL 1011). Images were recorded with a MegaView III CCD (Soft Imaging Systems) and were analysed using FIJI software. A common threshold was applied to all images used to quantify the surface area of the OCS, which was expressed as a percentage of the total surface area of the cell.

Focused ion beam-scanning electron microscopy

Isolated mouse platelets, and human platelets pretreated with dimethylsulfoxide (DMSO, 0.1% v/v), or 10 μM MIPS-19416 for 30 min, were fixed in 2.5% glutaraldehyde, postfixed in 1% osmium tetroxide and 1.5% potassium ferrocyanide, incubated in 4% uranyl acetate, then dehydrated through a series of graded ethanol concentrations before being embedded in Epon resin. Samples were imaged using a Helios NanoLab 600i microscope (FEI). Stacks of approximately 1000 images, with a field size of 15 μm x 15 μm, were generated. Samples were milled with the FIB (20 kV) at a thickness of 20 nm per section, allowing the OCS (45 < diameter < 150 nm) to be followed in the Z-dimension. 3D models were computed using the imaging software Amira (FEI).

Ex vivo *thrombosis and platelet adhesion assays*

Glass microslides (0.1 × 1.0 mm, VitroCom) were washed in nitric acid, rinsed with dH_2O and coated with bovine type 1 collagen (250 μg/ml diluted in 10 mM acetic acid, overnight at 4 °C), or vWF (100 μg/ml, 10 min). For thrombus formation on collagen, human whole blood collected in hirudin (800 U/ml) or enoxaparin (40 U/ml) was pretreated with $DiOC_6$ (0.01% v/v) and either dimethylsulfoxide (DMSO, 0.1% v/v), 10 μM MIPS-19416, 10 μM MIPS-19417, 10 μM copanlisib, 100μM 2-MeSAMP, saline (0.009% v/v), or 50 μM aspirin (acetylsalicylic acid, ASA). Blood was then perfused through coated microslides at 37 °C for 10 min at 1800 s^{-1} or 3000 s^{-1}, and thrombus formation monitored in real time using a Nikon A1r confocal microscope with a 25x water objective. Thrombus volume was analyzed using NIS-Element confocal imaging software, and was quantified by applying a constant threshold to all Z-stack images obtained and summing the resultant surface areas.

Analysis of spread platelet area was performed on acid-washed glass coverslips. Washed platelets were resuspended in Tyrode's buffer at 3 x 10^7/ml and pretreated with DMSO (0.1% v/v), 10 μM MIPS-19416, or 10 μM copanlisib (all 10 min). Platelet suspensions were placed on the coverslips and allowed to spread for 15 min. Non-adherent platelets were then removed

with a Tyrode's buffer wash and adherent platelets fixed using 4% PFA. Platelets were imaged using a Nikon Ti-E motorized inverted microscope with a 60x water objective, and analyzed using ImageJ software.

For platelet translocation, microslides were coated with vWF (100 µg/ml, 10 min) and blocked with BSA (2%, 10 min). Enoxaparin-anticoagulated human whole blood (40 U/ml) was pretreated with dimethylsulfoxide (DMSO, 0.1% v/v), 10 µM MIPS-19416, or 20 µg/ml integrilin (all 10 min). Blood was then perfused through coated microslides at 1800 s^{-1} for 2.5 min. Platelet translocation across the substrate was monitored in real time using a Nikon Ti-E motorized inverted microscope with a 60x water objective. Videos were analyzed offline using ImageJ software for platelet translocation velocity.

Cytoskeletal analyses

Isolated platelets were pretreated with DMSO (0.1% v/v), 10 µM MIPS-19416, or 10 µM copanlisib (10 min). Some platelets were activated with 1U/ml thrombin (10 min) prior to fixation with 2% PFA. Fixed platelets were seeded on poly-L-lysine coated coverslips, and then permeabilized (0.1% Triton X-100, 15 min), blocked (1% BSA in 0.1% Triton X-100, 15 min), stained (α-tubulin Alexa Fluor 488 antibody, 0.5 µg/ml, and Alexa Fluor 647 phalloidin, 40U/ml, 45 min) and mounted with Dako fluorescent mounting media. Images were taken using a Nikon A1r confocal microscope with a 60x oil objective.

Microfluidic ex vivo *thrombosis assay*

Platelet aggregation was performed as described (*25*). Briefly, a microfluidic device consisting of 200 µm wide channels with inset 40 µm stenosis was fabricated using standard photolithography techniques (*24*). Microchannels were selectively derivitized at the stenosis geometry with human vWF (10 µg/ml - isolated from Biostate® CSL Ltd) for 10 min and subsequently blocked with BSA (2 µg/ml) for 10 min prior to sample perfusion. Human whole

blood was pretreated with $DiOC_6$ (1 µg/ml) and either vehicle (DMSO, 0.1% v/v), amplification loop blockers (ALB: 10 µM MRS2179, 100 µM 2-MeSAMP, 2 U/ml apyrase, 10 µM indomethacin and 800 U/ml hirudin), MIPS-19416 (10 µM), MIPS-19416 + ALB, MIPS-19417 (10 µM), or MIPS-19417 + ALB for 10 mins. Blood was then perfused through the microfluidic at Q = 45 µl/min (equating to a shear rate at the stenosis geometry of 11,500 s^{-1}) and platelet aggregation at the stenosis monitored via epifluorescence at 1 fps for 210 s (Nikon Ti-U microscope - Plan Fluor 20x/0.50 objective with Andor Zyla sCMOS detector). Mid-plane platelet aggregate size was analysed in ImageJ following thresholding (Huang's fuzzy image thresholding method). Maximal aggregation, expressed as cross-sectional area (μm^2) was extrapolated from non-linear curve fitting following 210 s perfusion time. Statistical significance was determined using one-way ANOVA where appropriate.

Platelet aggregation

Platelet aggregation was performed as previously described (*7*). Briefly, human platelets were incubated with MIPS-19416, MIPS-19417, copanlisib (all 0.01 – 100 µM), or DMSO (0.1% v/v) for 10 min. Platelets were stimulated with thrombin (0.1 U/ml). Aggregation was measured as a change in optical density over 60 min.

PAC-1 binding

Flow cytometry was used to measure $\alpha_{IIb}\beta_3$ activation by PAC-1 binding. Washed human platelets were incubated with MIPS-19416, MIPS-19417, copanlisib (all 0.01 – 10 µM) or DMSO (0.1% v/v) for 10 min. Platelets were stimulated with thrombin (0.1 U/ml) and incubated with FITC-PAC1 (BD Biosciences) for 10 min at 37 °C. Samples were analyzed using a FACS Calibur flow cytometer and FlowJo software (Becton Dickinson).

In vivo *thrombosis models*

The electrolytic model of thrombosis was performed essentially as described (*19, 21*). Mice were anaesthetized via intraperitoneal injection using a combination of ketamine (85 mg/kg) and xylazine (15 mg/kg), and a flow probe (0.5 mm inner diameter) linked to a flow meter (TS420, Transonic Systems) placed around the exposed left carotid artery to record blood flow using PowerLab Chart (v. 5.0, AD Instruments). MIPS-19416 (1 mg/kg, and 0.1 mg/kg) or vehicle (volume-matched DMSO) was administered intravenously via the right jugular vein, and blood flow allowed to stabilise for 10 min prior to injury. A constant current lesion maker (53500, Ugo Basile) was used to deliver 22 mA for 2.75 min to the carotid artery via a platinum electrode—the minimal current required to reliably produce a stable occlusive thrombotic event in untreated, wild type mice. Blood flow was monitored for 30 min post-injury.

The Folts-like model of thrombosis was performed essentially as previously described (*21*). A suture was tied around the carotid artery and tightened until blood flow was decreased by 50%. The section of vessel under stenosis was pinched with forceps five times to induce injury and blood flow was measured until vessel occlusion. After 30 s the site of injury was agitated to induce embolization and restore blood flow. The number of these cyclic flow reductions (CFRs) was recorded for 15 min. MIPS-19416 (1 mg/kg) or vehicle (volume-matched DMSO) was injected via the jugular vein and CFRs were measured in 15 min periods for 60 min.

In vivo *hemostasis assay*

Tail transection bleeding times were performed as described (*7*). Briefly, mice were anaesthetised via intraperitoneal injection using a combination of ketamine (85 mg/kg) and xylazine (15 mg/kg). MIPS-19416 (1 mg/kg, and 0.1 mg/kg) or vehicle (volume-matched DMSO) was administered via the right jugular vein 10 min prior to tail transection. In some cases, mice were instead gavaged with aspirin (200 mg/kg) or volume-matched saline 24 h and 2 h prior to experimentation. The tail was transected 5 mm from the tip with a scalpel blade.

The bleeding end was immediately immersed in warmed saline (37 °C) and time to bleeding cessation (stoppage for > 2 min) was measured.

Histological analysis

Following *in vivo* thrombosis assays, carotid arteries were excised and fixed in 4% paraformaldehyde at room temperature for at least 24 h. Fixed tissues were embedded in paraffin and kept at room temperature until sectioning. 2 μm thick transverse sections were prepared using a microtome (microTec CUT-4060) and stained with Carstairs' stain (*31*) for platelets, collagen, fibrin and red blood cells. Slides were imaged using a Nikon Eclipse TS100 with a 10x objective, and images captured using NIS-Elements software.

Statistical analyses

Statistical analyses were performed using GraphPad Prism. Statistical significance ($P < 0.05$) was determined with either an unpaired, two-tailed Student's *t*-test, a one-way ANOVA with Dunnett's multiple comparisons test, or by plotting the data as Kaplan-Meier survival curves and analyzing by log-rank test versus the relevant vehicle, as indicated in the relevant figure legends.

References

1.   A. Toker, L. C. Cantley, Signalling through the lipid products of phosphoinositide-3-OH kinase. *Nature* **387**, 673-676 (1997).

2.   L. Stephens, R. Williams, P. Hawkins, Phosphoinositide 3-kinases as drug targets in cancer. *Curr. Opin. Pharmacol.* **5**, 357-365 (2005).

3.   E. Hirsch, C. Costa, E. Ciraolo, Phosphoinositide 3-kinases as a common platform for multi-hormone signaling. *J. Endocrinol.* **194**, 243-256 (2007).

4.   E. Hirsch, E. Ciraolo, A. Ghigo, C. Costa, Taming the PI3K team to hold inflammation and cancer at bay. *Pharmacol. Ther.* **118**, 192-205 (2008).

5.   M. Falasca, T. Maffucci, Regulation and cellular functions of class II phosphoinositide 3-kinases. *Biochem. J.* **443**, 587-601 (2012).

6.   T. Maffucci, M. Falasca, New insight into the intracellular roles of class II phosphoinositide 3-kinases. *Biochem. Soc. Trans.* **42**, 1378-1382 (2014).

7.   J. K. Mountford, C. Petitjean, H. K. Kusuma Putra, J. A. McCafferty, N. M. Setiabakti, H. Lee, L. L. Tonnesen, J. D. McFadyen, S. M. Schoenwaelder, A. Eckly, C. Gachet, S. Ellis, A. K. Voss, R. A. Dickins, J. R. Hamilton, S. P. Jackson, The Class II PI 3-Kinase, PI3KC2a Links Platelet Internal Membrane Structure to Shear-dependent Adhesive Function. *Nat. Commun.* **6:6536**, (2015).

8.   C. Valet, G. Chicanne, C. Severac, C. Chaussade, M. A. Whitehead, C. Cabou, M. P. Gratacap, F. Gaits-Iacovoni, B. Vanhaesebroeck, B. Payrastre, S. Severin, Essential role of class II PI3K-C2alpha in platelet membrane morphology. *Blood* **126**, 1128-1137 (2015).

9.   C. Petitjean, N. M. Setiabakti, J. K. Mountford, J. F. Arthur, S. Ellis, J. R. Hamilton, Combined deficiency of PI3KC2alpha and PI3KC2beta reveals a nonredundant role for PI3KC2alpha in regulating mouse platelet structure and thrombus stability. *Platelets* **27**, 402-409 (2016).

10.   M. Takiguchi, C. James, E. C. Josefsson, C. L. Carmichael, P. K. Premsrirut, S. W. Lowe, J. R. Hamilton, D. C. Huang, B. T. Kile, R. A. Dickins, Transgenic, inducible RNAi in megakaryocytes and platelets in mice. *J. Thromb. Haemost.* **8**, 2751-2756 (2011).

11.   R. A. Dickins, K. McJunkin, E. Hernando, P. K. Premsrirut, V. Krizhanovsky, D. J. Burgess, S. Y. Kim, C. Cordon-Cardo, L. Zender, G. J. Hannon, S. W. Lowe, Tissue-specific and reversible RNA interference in transgenic mice. *Nat. Genet.* **39**, 914-921 (2007).

12.   R. A. Dickins, M. T. Hemann, J. T. Zilfou, D. R. Simpson, I. Ibarra, G. J. Hannon, S. W. Lowe, Probing tumor phenotypes using stable and regulated synthetic microRNA precursors. *Nat. Genet.* **37**, 1289-1295 (2005).

13.   Z. A. Knight, B. Gonzalez, M. E. Feldman, E. R. Zunder, D. D. Goldenberg, O. Williams, R. Loewith, D. Stokoe, A. Balla, B. Toth, T. Balla, W. A. Weiss, R. L. Williams, K. M. Shokat, A pharmacological map of the PI3-K family defines a role for p110alpha in insulin signaling. *Cell* **125**, 733-747 (2006).

14. W. J. Scott, M. F. Hentemann, R. B. Rowley, C. O. Bull, S. Jenkins, A. M. Bullion, J. Johnson, A. Redman, A. H. Robbins, W. Esler, R. P. Fracasso, T. Garrison, M. Hamilton, M. Michels, J. E. Wood, D. P. Wilkie, H. Xiao, J. Levy, E. Stasik, N. Liu, M. Schaefer, M. Brands, J. Lefranc, Discovery and SAR of Novel 2,3-Dihydroimidazo[1,2-c]quinazoline PI3K Inhibitors: Identification of Copanlisib (BAY 80-6946). *ChemMedChem.* **11**, 1517-1530 (2016).

15. M. S. Miller, S. J. Mountford, J. A. Pinson, Z. Zheng, M. Kunzli, V. Patel, S. J. Hogg, J. Shortt, I. G. Jennings, P. E. Thompson, Development of single and mixed isoform selectivity PI3Kdelta inhibitors by targeting Asn836 of PI3Kdelta. *Bioorg. Med. Chem. Lett.* **26**, 4790-4794 (2016).

16. A. Eckly, H. Heijnen, F. Pertuy, W. Geerts, F. Proamer, J. Y. Rinckel, C. Leon, F. Lanza, C. Gachet, Biogenesis of the demarcation membrane system (DMS) in megakaryocytes. *Blood* **123**, 921-930 (2013).

17. H. Lee, S. A. Sturgeon, S. P. Jackson, J. R. Hamilton, The contribution of thrombin-induced platelet activation to thrombus growth is diminished under pathological blood shear conditions. *Thromb. Haemost.* **107**, 328-337 (2012).

18. A. Ono, E. Westein, S. Hsiao, W. S. Nesbitt, J. R. Hamilton, S. M. Schoenwaelder, S. P. Jackson, Identification of a fibrin-independent platelet contractile mechanism regulating primary hemostasis and thrombus growth. *Blood* **112**, 90-99 (2008).

19. H. Lee, S. A. Sturgeon, J. K. Mountford, S. P. Jackson, J. R. Hamilton, Safety and efficacy of targeting platelet proteinase-activated receptors in combination with existing anti-platelet drugs as antithrombotics in mice. *Br. J. Pharmacol.* **166**, 2188-2197 (2012).

20. K. B. Neeves, S. F. Maloney, K. P. Fong, A. A. Schmaier, M. L. Kahn, L. F. Brass, S. L. Diamond, Microfluidic focal thrombosis model for measuring murine platelet deposition and stability: PAR4 signaling enhances shear-resistance of platelet aggregates. *J. Thromb. Haemost.* **6**, 2193-2201 (2008).

21. S. A. Sturgeon, C. Jones, J. A. Angus, C. E. Wright, Adaptation of the Folts and electrolytic methods of arterial thrombosis for the study of anti-thrombotic molecules in small animals. *J. Pharmacol. Toxicol. Methods* **53**, 20-29 (2006).

22. H. J. Daykin, S. A. Sturgeon, C. Jones, C. E. Wright, Arterial antithrombotic effects of aspirin, heparin, enoxaparin and clopidogrel alone, or in combination, in the rat. *Thromb. Res.* **118**, 755-762 (2006).

23. J. G. White, C. C. Clawson, The surface-connected canalicular system of blood platelets--a fenestrated membrane system. *Am. J. Pathol.* **101**, 353-364 (1980).

24. F. J. Tovar-Lopez, G. Rosengarten, E. Westein, K. Khoshmanesh, S. P. Jackson, A. Mitchell, W. S. Nesbitt, A microfluidics device to monitor platelet aggregation dynamics in response to strain rate micro-gradients in flowing blood. *Lab Chip* **10**, 291-302 (2010).

25. R. J. Brazilek, F. J. Tovar-Lopez, A. K. T. Wong, H. Tran, A. S. Davis, J. D. McFadyen, Z. Kaplan, S. Chunilal, S. P. Jackson, H. Nandurkar, A. Mitchell, W. S. Nesbitt, Application of a strain rate gradient microfluidic device to von Willebrand's disease screening. *Lab Chip* **17**, 2595-2608 (2017).

26. W. S. Nesbitt, E. Westein, F. J. Tovar-Lopez, E. Tolouei, A. Mitchell, J. Fu, J. Carberry, A. Fouras, S. P. Jackson, A shear gradient-dependent platelet aggregation mechanism drives thrombus formation. *Nat. Med.* **15**, 665-673 (2009).

27. S. Grgurevich, R. Krishnan, M. M. White, L. K. Jennings, Role of in vitro cholesterol depletion in mediating human platelet aggregation. *J. Thromb. Haemost.* **1**, 576-586 (2003).

28. S. Osman, K. A. Taylor, N. Allcock, R. D. Rainbow, M. P. Mahaut-Smith, Detachment of surface membrane invagination systems by cationic amphiphilic drugs. *Sci. Rep.* **6**, 18536 (2016).

29. A. Kielkowska, I. Niewczas, K. E. Anderson, T. N. Durrant, J. Clark, L. R. Stephens, P. T. Hawkins, A new approach to measuring phosphoinositides in cells by mass spectrometry. *Adv. Biol. Regul.* **54**, 131-141 (2014).

30. M. P. McCormack, M. A. Hall, S. M. Schoenwaelder, Q. Zhao, S. Ellis, J. A. Prentice, A. J. Clarke, N. J. Slater, J. M. Salmon, S. P. Jackson, S. M. Jane, D. J. Curtis, A critical role for the transcription factor Scl in platelet production during stress thrombopoiesis. *Blood* **108**, 2248-2256 (2006).

31. K. C. Carstairs, The identification of platelets and platelet antigens in histological sections. *J. Pathol. Bacteriol.* **90**, 225-231 (1965).

Author contributions:

M.V.S. and M.J.M. performed experiments, analyzed data and co-wrote the paper; Z.Z., S.J.M., R.J.B., R.P.I., and J.-Y.R. performed experiments and analyzed data; A.E. and C.G. designed experiments and provided intellectual input; W.S.N., I.G.J. and P.E.T. designed and performed experiments and provided intellectual input; and J.R.H. designed and supervised the study and wrote the paper.

Competing interests: The authors declare no competing financial interests.

Figures and legends:

Fig. 1
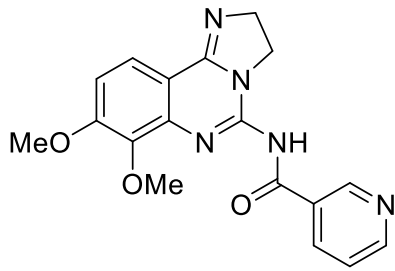
PIK-90
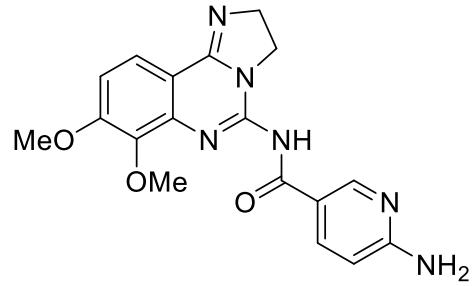
MIPS-19416
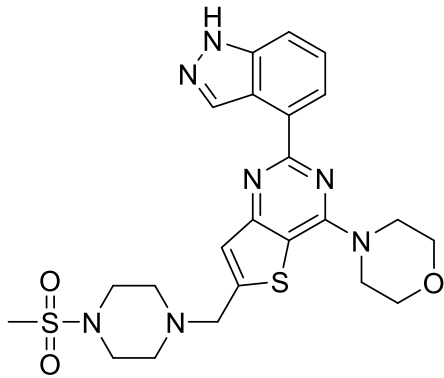
Pictilisib, GDC-0941
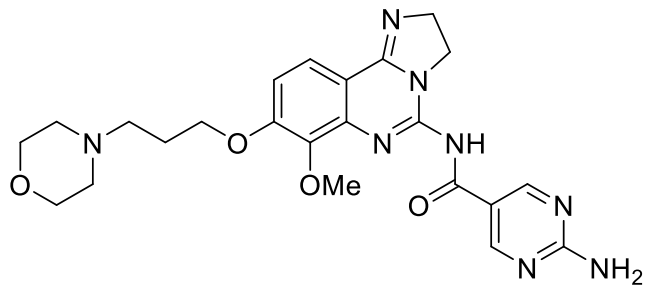
Copanlisib, BAY80-6946
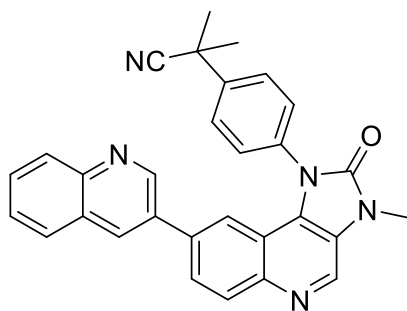
Dactolisib (NVP-BEZ235)
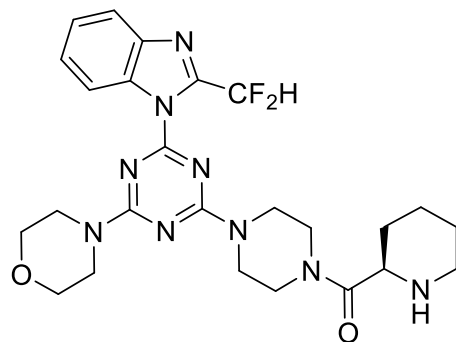
MIPS-19417

Figure 1. Class I and Class II PI3K inhibitors. Molecular structures of PIK-90, MIPS-19416, pictilisib, copanlisib, dactolisib and MIPS-19417. MIPS-19416 was synthesized from PIK-90 (Suppl. Methods) and is a potent inhibitor of PI3KC2α. MIPS-19417 is a PI3KC2β inhibitor, however both MIPS-19416 and MIPS-19417 also have significant effects at the class I PI3Ks. Copanlisib is an analogue of PIK-90 and is a pan-class I PI3K inhibitor, and pictilisib and dactolisib are broad spectrum inhibitors across the class I and II PI3Ks. IC$_{50}$s for each molecule against various PI3K isoforms are shown in Table 1.

Fig. 2
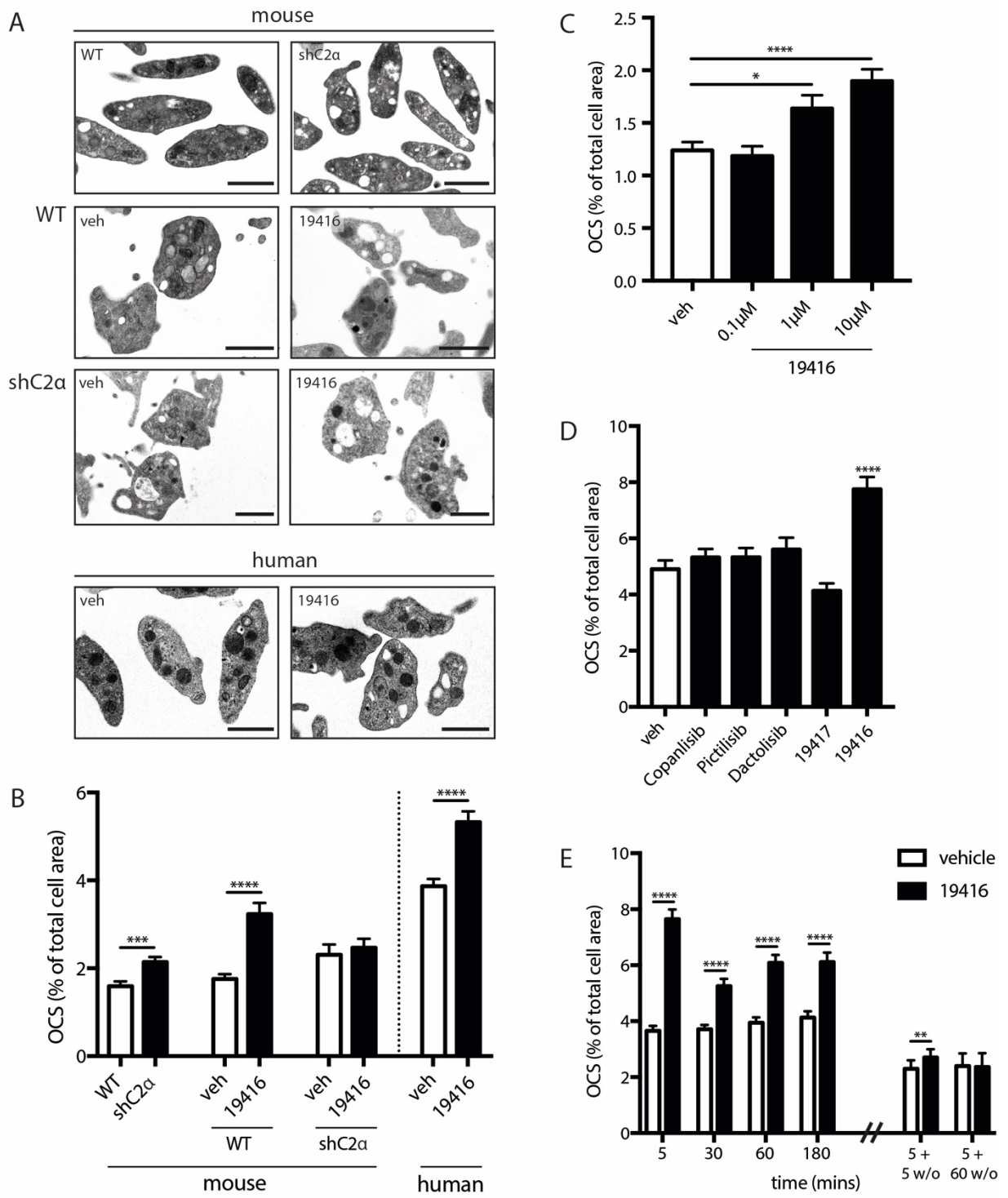
Figure 2. PI3KC2α inhibition reproduces the platelet cell biology effects of PI3KC2α deficiency. (**A**) Representative TEM images of platelets. Top panels: untreated platelets from wild-type (WT) or PI3KC2α-deficient (shC2α) mice. Middle: platelets from WT or shC2α mice treated with vehicle (DMSO, 0.1% v/v, 3 h) or MIPS-19416 (19416, 10 µM, 3h). Bottom: human platelets treated with vehicle (DMSO, 0.1% v/v, 3 h) or MIPS-19416 (10 µM, 3h). Note dilated OCS in PI3KC2α-deficient and MIPS-19416-treated platelets (red arrows). Scale bars = 1 µm. (**B-E**) Quantification of OCS surface area from TEM images, showing: (**B**) Mouse and human platelets as described in (**A**); (**C**) The concentration-response of MIPS-19416 in human platelets; (**D**) The specificity of the OCS dilation to MIPS-19416 over inhibitors of other PI3Ks (all at 10 µM for 3 h); (**E**) The time course of response to MIPS-19416 (10 µM), and its reversibility in cells treated for 5 min before drug washout (w/o) for a further 5 or 60 min. All data are percentage OCS of total cell area and are mean ± SEM of n=81-455 cells from n=3-6 experiments per condition. *, $P<0.05$; **, $P<0.01$; ***, $P< 0.001$; ****, $P<0.0001$ (unpaired, two-tailed, Student's *t*-test versus indicated control in **B** and **E** and one-way ANOVA with Dunnett's multiple comparison test against vehicle in **C** and **D**).

Fig. 3
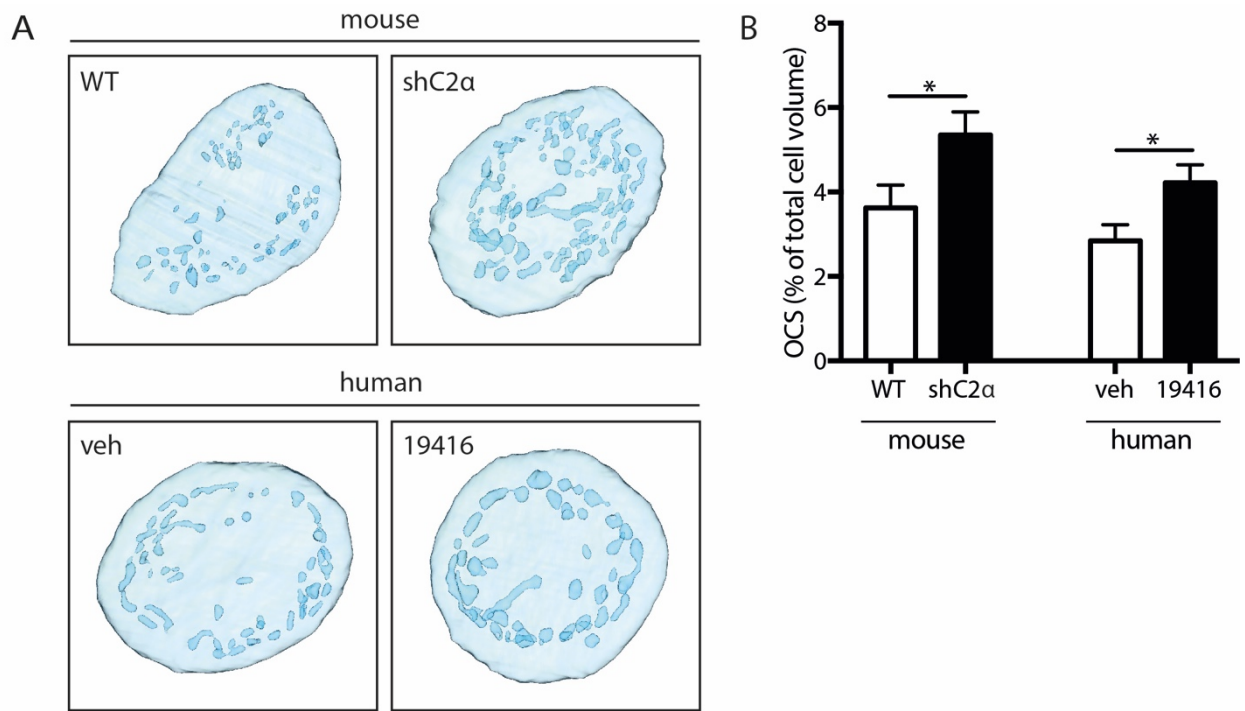
Figure 3. Genetic deficiency or pharmacological inhibition of PI3KC2α similarly dilate the platelet internal membrane system throughout the entire cell. (A,B) FIB-SEM analyses of the whole-of-cell platelet membrane. (**A**) Representative 3D reconstructions of membranes of platelets from wild-type (WT) or PI3KC2α-deficient (shC2α) mice (top panels), and human platelets treated with MIPS-19416 (10μM, 30 min) or vehicle (DMSO, 0.1% v/v, 30 min), showing plasma (light blue) and internal (dark blue) membrane. Note the even dilation of the OCS throughout both PI3KC2α-deficient mouse platelets and MIPS-19416-treated human platelets. (**B**) Quantification of OCS volume from 3D reconstructions. Data are mean ± SEM from n=10-12 platelets per group. *, P<0.05 (unpaired, two-tailed, Student's t test).

Fig. 4
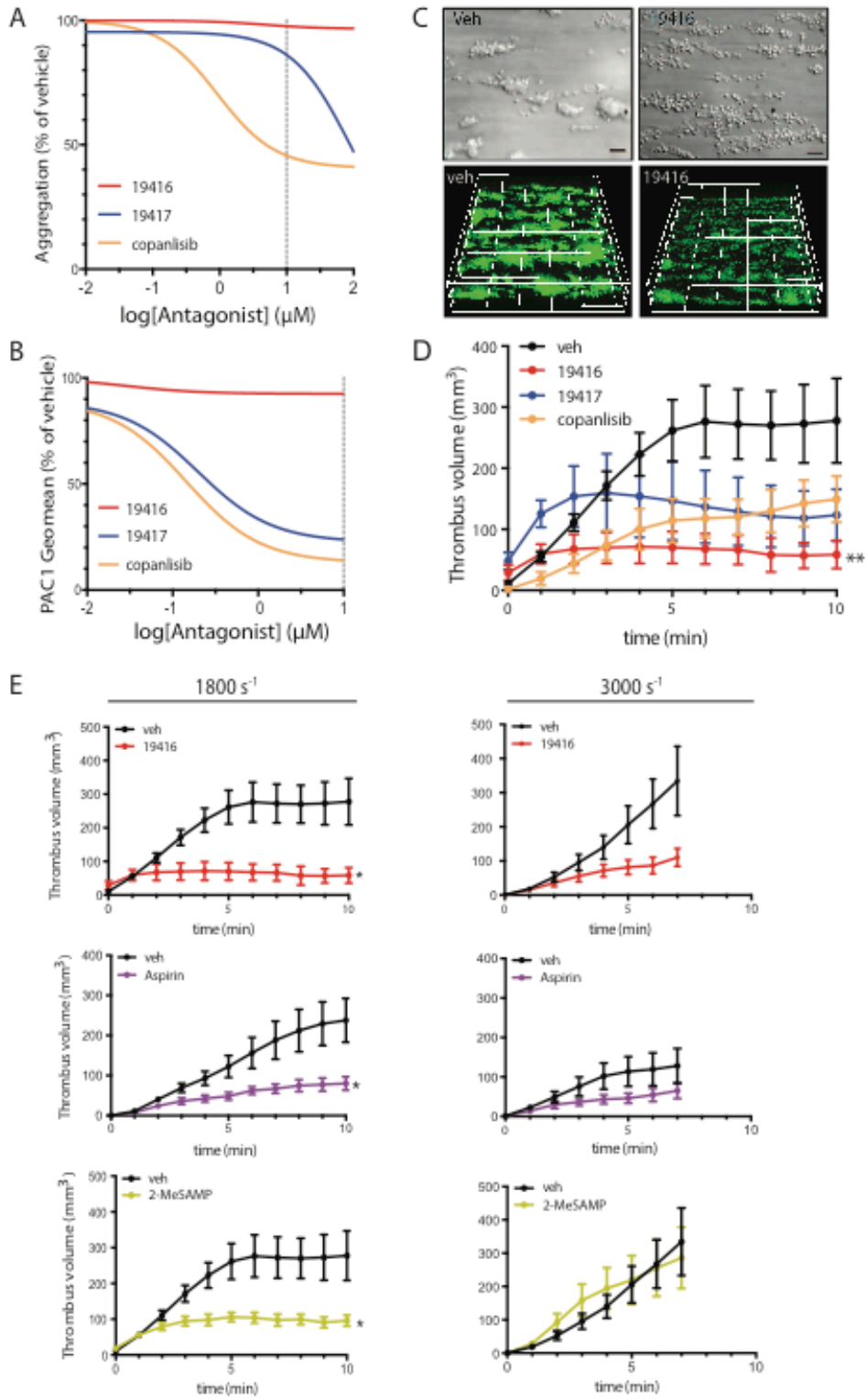
Figure 4. PI3KC2α inhibition is anti-thrombotic in human blood independently of canonical platelet activation. (**A,B**) Concentration-inhibition curves for MIPS-19416, MIPS-19417, or copanlisib against (**A**) aggregation or (**B**) $\alpha_{IIb}\beta_3$ activation (PAC-1 binding) in thrombin (0.1 U/ml)-stimulated human platelets. Shown are curve fits generated from mean ± SEM data expressed as a percentage of vehicle from 8 experiments (individuals) in **A** and 3 in **B**. (**C,D**) Thrombus formation in anticoagulated human blood flowed over a collagen surface at 1800 s^{-1} in the presence of MIPS-19416, MIPS-19417, copanlisib (all 10 μM), or vehicle (DMSO, 0.1% v/v). (**C**) Representative bright field images (top, scale bars = 10 μm) and 3D reconstructions (bottom, graticules = 50 μm) at the 10 min endpoint. (**D**) Total thrombus volume determined in real time every min for 10 min. Mean ± SEM of n=6 experiments (individuals). **, $P<0.01$ (one-way ANOVA with Dunnett's multiple comparison test against vehicle). (**E**) Thrombus volume in anticoagulated human blood flowed over a collagen surface at 1800 or 3000 s^{-1}, in the presence of MIPS-19416 (10 μM, top row), aspirin (50 μM, middle row), or the P2Y$_{12}$ antagonist 2-MeSAMP (100 μM, bottom row) versus relevant vehicle (DMSO, 0.1% v/v for MIPS-19416 and 2-MeSAMP; saline, 0.009% v/v for aspirin). Data are mean ± SEM from n=6-13 experiments (individuals). Data is only shown up to 7 min in experiments performed at 3000 s^{-1} because gross embolization occurred in > 50% of cases after this time in these experiments. Note the data in the left graph of the top row is taken from the experiments shown in **D**. *, $P<0.05$; **, $P<0.01$ (unpaired, two-tailed, Student's *t*-test).

Figure 5.
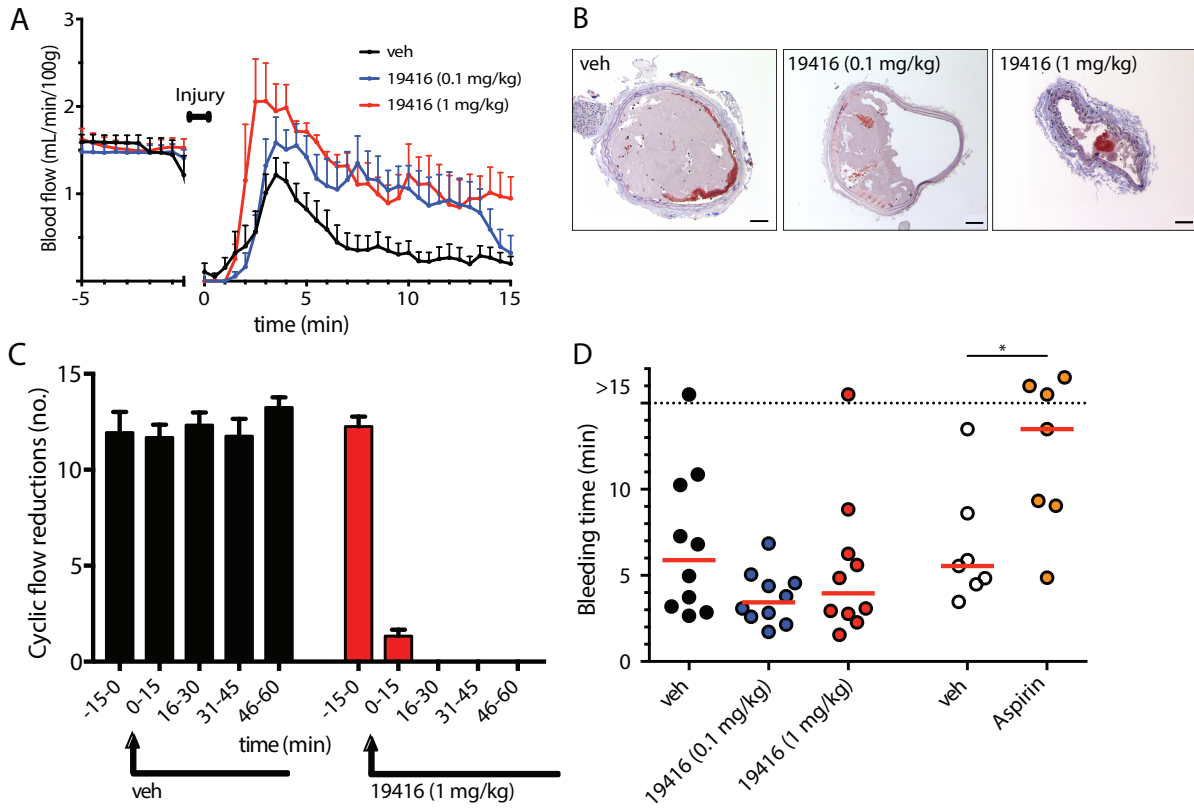
Figure 5. PI3KC2α inhibition is anti-thrombotic in mice *in vivo* but has no effect on hemostasis. (**A-C**) Thrombosis and (**D**) hemostasis in *in vivo* mouse models in the absence and presence of PI3KC2α inhibition. (**A**) Carotid artery blood flow before and after electrolytic injury of the vessel in wild-type mice treated with MIPS-19416 (0.1 or 1 mg/kg; n=8 each) or vehicle (volume-matched DMSO; n=11). Mean ± SEM. (**B**) Representative histological images of transverse sections of carotid arteries containing Carstair's-stained thrombi from experiments in **A**, showing platelets (purple), fibrin (red), and collagen (blue). All scale bars are 50 μm. (**C**) Cyclic flow reductions in carotid arteries of mice in a Folts-like model of recurrent occlusive thrombosis in the absence and presence of MIPS-19416 (1 mg/kg; n=4) or vehicle (volume-matched DMSO; n=3). Shown are the number (mean ± SEM) of reformed occlusive thrombi (cyclic flow reductions) per 15 min period before and after drug administration (arrow). (**D**) Tail bleeding time in wild-type mice treated with MIPS-19416 (0.1 or 1 mg/kg) or its vehicle (DMSO), or aspirin (200 mg/kg) or its vehicle (0.9% saline). Data points represent time to cessation of bleeding in an individual mouse. Experiments were terminated after 15 min and mice still bleeding at this time are shown above the dotted line. Red bars are medians. *, $P<0.05$ with significance determined by plotting the data as Kaplan-Meier survival curves and analyzing by log-rank test versus the relevant vehicle.

Fig. 6
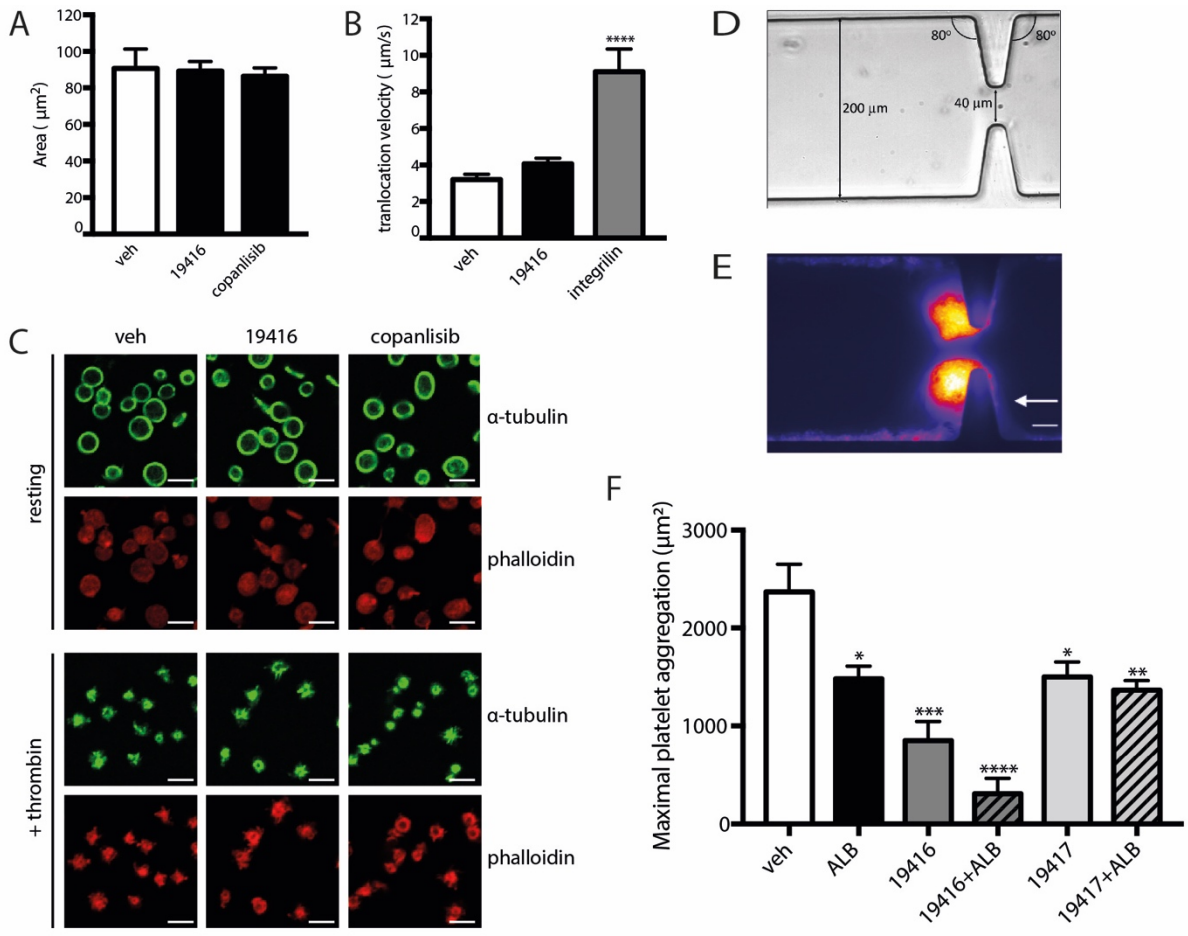
Figure 6. The anti-platelet effects provided by PI3KC2α inhibition are due to a unique impact on membrane-dependent platelet adhesion under high shear. (A) Surface area of human platelets pre-treated for 10 min with vehicle (0.1% DMSO) or MIPS-19416 (10 µM) and spread on glass for 15 min. Data are mean ± SEM of n=60 cells from n=3 independent experiments. **(B)** Translocation velocity of platelets in human blood flowed over vWF (100 µg/ml) at 1800 s^{-1} in the presence of vehicle (0.1% DMSO), MIPS-19416 (10 µM) or integrilin (20 µg/ml). Data are mean ± SEM of n=35-89 cells from n=3-6 independent experiments. ****, $P<0.0001$ (one-way ANOVA with Dunnett's multiple comparisons test against vehicle). **(C)** Representative immune-fluorescence images (n=3) of human platelets treated with vehicle (0.1% DMSO), MIPS-19416 (10 µM) or copanlisib (10 µM) and stained with an α-tubulin antibody (green) or phalloidin (red). Platelets were either unactivated (top) or activated in suspension with thrombin (1 U/ml; bottom). Scale bars are 5 µm. **(D)** DIC image (20x) of a PDMS microfluidic flow channel used here. **(E)** Representative fluorescence image during blood perfusion through the channel in (D), showing platelet aggregation downstream of the stenosis. Arrow indicates direction of blood flow. Scale bar is 25 µm. **(F)** Maximal platelet aggregation following device perfusion with human blood for 260 s. Blood was pretreated for 10 min with vehicle (0.1% DMSO), amplification loop blockers (ALB: 10 µM MRS2179, 100 µM 2-MeSAMP, 2 U/ml apyrase, 10 µM indomethacin and 800 U/ml hirudin), MIPS-19416 (10 µM), MIPS-19416 + ALB, MIPS-19417 (10 µM), or MIPS-19417 + ALB. Mean ± SEM of n=3 experiments (individuals). *, $P<0.05$; **, $P<0.01$; ***, $P<0.001$; ****, $P<0.0001$ (one-way ANOVA with Dunnett's multiple comparisons test against vehicle).

Tables:

Table 1.

	IC$_{50}$ (μM)					
Compound	*PI3KC2α*	*PI3KC2β*	*p110α*	*p110β*	*p110γ*	*p110δ*
PIK-90	0.047	0.064	0.011	0.350	0.018	0.058
MIPS-19416	0.013	0.015	0.012	0.053	0.094	0.020
Pictilisib	> 10	0.590	0.003	0.003	0.075	0.033
Copanlisib	> 10	> 10	0.0005	0.0037	0.0064	0.0007
Dactalosib	0.155	0.044	0.004	0.075	0.005	0.007
MIPS-19417	> 10	0.278	2.371	0.775	3.594	0.052

Table 1. Potency and specificity of PI3K inhibitors. IC$_{50}$ values (μM) of PI3K inhibitors used in this study, at the class II isoforms PI3KC2α and PI3KC2β, and the class I isoforms p110α, p110β, p110γ and p110δ.

CHAPTER 4

General Discussion

4.1 Key Findings from this Thesis

The class II phosphoinositide 3-kinase, PI3KC2α, is a lipid kinase with emerging biological roles. Recent studies have identified a role for PI3KC2α in mouse platelet structure and function – mice deficient in PI3KC2α demonstrate a dysregulated internal membrane system which is sufficient to cause significant platelet functional impairment in the setting of arterial thrombosis[91,113]. The studies of this thesis build upon those initial studies to investigate the mechanism linking the alteration in platelet structure to this functional attenuation, and use a novel pharmacological inhibitor to determine whether a similar role for PI3KC2α exists in the regulation of human platelet structure and function.

The key findings from this thesis are:

1) Deficiency of PI3KC2α in mice leads to structural changes that are specific to the platelet open canalicular system and are not associated with alterations in membrane lipid composition. These structural changes lead to impaired platelet membrane function specifically in the setting of thrombus formation.

2) PI3KC2α regulates human platelet structure and function. Pharmacological inhibition of PI3KC2α in human samples acutely reproduces the structural and functional effects seen with PI3KC2α deficiency in mouse, with inhibitor-treated cells exhibiting dilatations of the OCS and impaired thrombosis in two ex vivo models.

3) The mechanism of action of deficiency and inhibition of PI3KC2α appears to be largely independent of platelet activation. The effects of loss of PI3KC2α on platelet function are observed only under conditions involving blood flow and are most pronounced where platelets are exposed to high levels of shear stress.

These findings demonstrate that loss of PI3KC2α alters the structure of the platelet internal membrane in both mouse and human, with functional consequences of this change manifesting specifically in the setting of the high shear forces experienced by platelets during thrombus formation in flowing blood. These effects can be induced acutely with a small molecule inhibitor of PI3KC2α. Targeting the platelet membrane via PI3KC2α may thus represent a novel anti-thrombotic strategy.

4.2 Targeting Thrombosis but not Haemostasis

Current strategies for the treatment and prevention of arterial thrombosis largely aim to curb inappropriate platelet activation, in order to prevent pathological clot formation and vessel occlusion. However, the processes of platelet activation and aggregation are common to both thrombosis and haemostasis. As such, anti-platelet agents that act on platelet activation pathways can also lead to bleeding, which limits dosing and consequently limits their anti-thrombotic effect. Furthermore, although drugs such as aspirin and clopidogrel have been shown to have benefit in preventing cardiovascular events, a significant proportion of patients are not adequately protected from thrombosis despite therapeutic doses of these anti-platelet agents[155]. Given this, targeting mechanisms outside of the common pathway of platelet activation may be a useful strategy in widening the therapeutic window for the prevention and treatment of thrombosis. However, our knowledge of the mechanisms that distinguish thrombosis from haemostasis remains limited.

It has been shown that there are distinct populations of platelets within a forming thrombus. Platelets surrounding the vessel injury stably adhere and demonstrate high levels of activation[156]. However, this core region of activated platelets is surrounded by a shell of discoid platelets that extends downstream of the vessel injury site, and which forms part of the aggregate without undergoing demonstrable activation[156]. Calcium flux, another measure of platelet activation, is similarly sustained within the core region, but decreases towards the periphery of the forming thrombus[157]. Since the core region surrounds the vascular injury, it would appear that the little-activated platelets that continue to aggregate to form the shell are not required for haemostasis.

This concept may underscore the lack of efficacy of current anti-platelet strategies, given that this discoid platelet aggregation has been shown to be largely insensitive to inhibitors of platelet activation[157]. It is unclear exactly why the thrombus continues to propagate in the absence of sustained platelet activation, when previously exposed thrombogenic substrates have been covered by the core of the haemostatic plug. However, this is likely linked to dysregulated blood flow and increased levels of shear stress around the forming thrombus – the conditions that occur in blood vessels affected by the presence of atherosclerotic plaques. The inappropriate recruitment of non- or minimally-activated platelets to a growing thrombus under altered blood flow conditions may thus be a target for novel anti-thrombotic strategies,

and would be unlikely to have a significant effect on haemostatic function. Cellular targets currently being investigated that appear to fit this model include PI3Kβ[58] and protein disulfide-isomerase[158]. Given our findings here showing that the functional defect seen with loss of PI3KC2α occurs specifically under flow and high shear stress, and that in vitro platelet activation and in vivo haemostasis is unaffected, it would appear that PI3KC2α can be added to this growing list of putative thrombosis-specific anti-platelet targets.

4.3 The Role of the OCS in Platelet Function and Thrombosis

The studies in this thesis have revealed a previously unrecognised link between the structure of the platelet's internal membrane network, the OCS, and platelet function in the setting of thrombosis, in both mouse and human. The OCS has a number of known functions, including the uptake and release of platelet contents, the regulation of levels of adhesion receptors on the platelet surface, and as a membrane reserve for platelet shape change and spreading during activation and aggregation[142]. However, dysregulation of OCS structure has not been directly associated with a specific impairment of platelet function.

Intriguingly, deficiency or inhibition of PI3KC2α does not appear to impact on any of the known functions of the OCS. We have found no differences in release of platelet granule contents, levels of the platelet adhesion receptors GPIb or integrin $\alpha_{IIb}\beta_3$, nor in the amount of membrane reserve available, in the absence of PI3KC2α activity[91]. The widespread dilation of OCS channels in PI3KC2α-deficient mouse platelets and MIPS-19416-treated human cells thus does not appear to be reflective of global membrane functional dysregulation. However, the consistent observation of a platelet functional defect specifically in in vivo arterial thrombosis and high-shear ex vivo assays, points to a subtle alteration in membrane function that manifests overtly only when platelets are under flow in a whole blood system.

The current studies have shown that both the channels of the OCS within the platelet, as well as its external openings at the plasma membrane, are dilated with loss of PI3KC2α. These widened surface openings may have implications for the entry of large plasma proteins. For example, fibrinogen is normally stored in platelet alpha granules, and is present in plasma, however does not enter the resting platelet due to the size of the pores of the OCS. Upon platelet activation, extrinsic fibrinogen binds to platelet receptors and enters OCS channels,

while fibrinogen in alpha granules is released to the exterior via binding of alpha granules to the OCS[139]. The average size of OCS openings in PI3KC2α-deficient mouse platelets was 54 nm, compared to 37 nm in wild-type platelets, and given that the length of the fibrinogen molecule is approximately 47 nm[159], it is possible that the enlarged OCS pores seen with loss of PI3KC2α permit premature entry of fibrinogen into the resting platelet. In a whole blood system, this could result in pre-exposure of low-affinity integrin $\alpha_{IIb}\beta_3$ receptors to their substrate, and in turn lead to modulation of platelet behaviour, such as an attenuation of the platelet response to exposed thrombogenic substrates. This may also explain the lack of effect seen with loss of PI3KC2α in standard in vitro platelet assays, which use isolated platelets with plasma, and thus extrinsic fibrinogen, removed from the system prior to the assay.

Another possible explanation for the markedly specific functional defect seen in our studies is that the dilatations of the channels of the OCS reflect, or are associated with, a mechanical change in the membrane. While we have shown that the lipid composition of PI3KC2α-deficient mouse platelets is unaltered compared to wild-type mice, and it is unlikely that any change in lipid composition is induced acutely with our pharmacological inhibitor, loss of PI3KC2α activity may nonetheless impact upon the mechanical properties of the membrane. Indeed, Valet et al., using atomic force microscopy (AFM), found that the membrane of platelets from mice with a heterozygous kinase-inactivating mutation in PI3KC2α was significantly more rigid than that of control mice[92]. This increased membrane rigidity may alter platelet behaviour – for example, a more rigid membrane may be less susceptible to the effects of dysregulated blood flow and high levels of shear. Predictive computational simulations of platelet adhesion at sites of vascular injury have shown that platelet membrane stiffness significantly affects adhesion[160]. However, the effect of platelet membrane rigidity on functional behaviour is not well studied, and further investigation of membrane dynamics, using techniques such as AFM, micropipette aspiration[161] or fluorescence anisotropy[162], would be required to determine whether this plays a role in the phenotype seen here.

4.4 PI3K Signalling in Platelets – Where Does PI3KC2α Fit In?

In the past fifteen years, a number of roles for the PI3Ks in platelet function have been revealed. Until very recently, this has been restricted to the class I PI3Ks. The PI3Kβ isoform is the

dominant player from this class in terms of platelet function, with PI3Kα and PI3Kγ having less critical roles. PI3Kβ signals downstream of the GPVI, P2Y$_{12}$ and integrin α$_{IIb}$β$_3$ receptors[55,57,58]. It activates Akt[59], which results in the inhibition of GSK3[60], promoting thrombin-mediated platelet aggregation, fibrinogen binding and release of granule contents[61]. PI3Kα and PI3Kγ signal downstream of GPVI and P2Y$_{12}$ respectively and play a cooperative role with PI3Kβ[55,74].

Downstream signalling of the class II PI3Ks is much less well understood. Our previous studies have not identified any signalling consequences of PI3KC2α deficiency, with levels of the cellular products of PI3KC2α comparable in wild-type and PI3KC2α-deficient cells[91]. However, using a more sensitive PI(3)P mass assay, Valet et al. were able to identify a significant reduction in the basal, but not agonist-induced, pool of PI(3)P in their heterozygous model of PI3KC2α-deficiency[113]. It is possible that this alteration in PI(3)P levels contributes to the functional defect. That pharmacological inhibition of PI3KC2α is able to acutely induce the structural and functional phenotype of PI3KC2α deficiency adds weight to the suggestion of PI3K signalling playing a role. Very recent unpublished data from our group indicates that this is indeed the case – using the same PI(3)P mass assay, PI3KC2α inhibition with MIPS-19416 led to a significant reduction in PI(3)P levels in human platelets at rest. However the role of PI(3)P in platelet signalling is unknown, and further investigation of this with suitably sensitive techniques would be required to correlate the phenotype to a specific signalling alteration.

4.5 PI3KC2α as an Anti-Thrombotic Target

4.5.1 PI3KC2α vs. PI3Kβ

Among the PI3Ks, PI3Kβ has an established role in platelet function, and has been well-characterised as an anti-thrombotic target. As discussed above, PI3Kβ is involved in signalling downstream of a number of major platelet receptors, and it has a known role in platelet activation[58]. Yet studies show minimal to no increase in cutaneous bleeding time with inhibition of PI3Kβ in both animal models and in humans despite a clear anti-thrombotic effect[65,163], marking it as a promising thrombosis-specific anti-platelet target. However, the evidence to date suggests that PI3KC2α may have just as much potential in the effort to prevent thrombosis without impacting upon haemostasis, and may even afford certain advantages over targeting PI3Kβ.

Neither deficiency nor inhibition of PI3KC2α impact upon platelet activation, and the anti-thrombotic effect of loss of PI3KC2α appears to be membrane-dependent and shear-specific. As such, given the lack of impact on canonical platelet activation pathways, PI3KC2α may prove to be an even more thrombosis-specific target than PI3Kβ, and may provide a superior therapeutic window. Furthermore, PI3Kβ is known to regulate thrombus stability under conditions of high shear[62], likely due to its role in regulating the integrin $\alpha_{IIb}\beta_3$ receptor and therefore its inactivation preventing the formation of stable integrin $\alpha_{IIb}\beta_3$ bonds[58,63]. It has thus been suggested that inhibition of PI3Kβ could lead to an increased risk of embolisation and secondary downstream ischaemia[164]. It remains to be seen whether this would be the case with inhibition of PI3KC2α, but the evidence to date suggests that platelet-platelet bonds via integrin $\alpha_{IIb}\beta_3$, which mediate the stability of platelet aggregates, are not affected by loss of PI3KC2α. A third consideration is that although PI3KC2α and PI3Kβ are both ubiquitously expressed, long-term use of a PI3Kβ inhibitor may have a more severe side effect profile than a PI3KC2α inhibitor given the well-established role for the class I PI3Ks in cell growth and differentiation.

Appealingly, given the differing mechanisms by which inhibition of PI3Kβ and PI3KC2α appear to be anti-thrombotic, it is possible that inhibitors of the two could be used in combination, and may produce a synergistic anti-thrombotic effect without an increase in bleeding. Studies examining the effect of concurrent inhibition of PI3Kβ and PI3KC2α would be useful in determining the feasibility and clinical utility of this combination.

4.5.2 Potential Off-Target Effects

In terms of future drug development, it is important to consider the possible off-target effects that may result from therapeutic use of a pharmacological inhibitor of PI3KC2α. Although speculative, the results from published mouse models of PI3KC2α deficiency may provide clues as to the potential effects of PI3KC2α inhibitors on cells other than platelets in humans. Encouragingly, while loss of PI3KC2α is embryonically lethal in mice due to impaired vascular development[91,108], unpublished observations by our laboratory have shown that long-term suppression of PI3KC2α in adult mice of up to one year in duration does not appear to produce any obvious phenotypic changes, nor increase morbidity or mortality.

Loss of PI3KC2α activity has been shown to lead to age-dependent obesity, hyperglycaemia and insulin resistance in mice[112]. This raises the possibility that long-term inhibition of PI3KC2α could lead to metabolic syndrome conditions, which increase CVD risk in their own right, and would somewhat nullify any anti-thrombotic benefit of an inhibitor. It has also been found that PI3KC2α has a role in renal function, with a hypomorphic mouse model of PI3KC2α deficiency producing chronic renal failure secondary to the development of renal lesions including glomerular crescent formation, podocyte effacement and renal tubule defects[107]. If PI3KC2α has a similar role in human kidney function, this would likely limit the use of PI3KC2α inhibitors clinically.

Furthermore, PI3KC2α has an important role in endothelial cell proliferation and angiogenesis[108]. This suggests that inhibition of PI3KC2α may be detrimental in situations where angiogenesis is beneficial, such as post myocardial infarction or ischaemic stroke – although, of course, these are the precise conditions that a PI3KC2α inhibitor would aim to prevent. However, a reduction in angiogenesis may be clinically useful in certain settings, such as in oncology – it is possible that a PI3KC2α inhibitor could provide benefit both in terms of addressing the increased risk of arterial thrombosis in patients with cancer[165], and in preventing further tumour growth via the inhibition of pathological angiogenesis.

4.6 Future Directions

One significant limitation of this study was the lack of specificity of the PI3KC2α inhibitor. The first-in-class compound used here, MIPS-19416, is a potent inhibitor of PI3KC2α, with an IC_{50} of 13 nM. However, it has a number of off-target effects, including at PI3KC2β (IC_{50} of 15 nM) and PI3Kβ (IC_{50} of 53 nM). The pan-class I inhibitor copanlisib was used in many of our experiments to control for off-target effects at PI3Kβ, and the compound MIPS-19417 to control for effects at PI3KC2β. Off-target effects at PI3Kβ were particularly important to control for in our experiments given the well-known anti-thrombotic effects of PI3Kβ inhibition.. Furthermore, it must be noted that the activity of MIPS-19416 against the class III PI3K Vps34, which has recently been shown to have a role in thrombosis[105,106], was not measured.

While it is possible that a proportion of the significant anti-thrombotic effect seen in our experiments is due to off-target activity at PI3Kβ or other targets that were not examined, the results in human samples using MIPS-19416 closely mirror those using our PI3KC2α-deficient mouse model, suggesting that the contribution of any off-target effects is minimal. Future work is aimed at developing more targeted inhibitors of PI3KC2α that retain the potency of MIPS-19416 but improve specificity, particularly by taking advantage of the unique structural features of PI3KC2α compared to the other PI3Ks.

Furthermore, although we have made insights into the mechanism by which loss of PI3KC2α function leads to structural and functional changes in platelets, much is left to be determined regarding exactly how the inhibition of PI3KC2α activity drives the changes to OCS structure, and how in turn this altered membrane structure leads to the attenuation of platelet prothrombotic function in the setting of high-shear whole blood flow. Further investigation into the molecular details of this mechanism would be useful both in further defining the role of PI3KC2α in platelet biology and in adding to the scientific repertoire of the potentially targetable factors that distinguish thrombosis from haemostasis.

4.7 Conclusion

The studies performed in this thesis have characterised in detail the phenotype of PI3KC2α deficiency in mouse, and identified a role for PI3KC2α in the regulation of human platelet structure and function. The results obtained here reveal that loss of PI3KC2α results in structural changes that are specific to the platelet internal membrane system, are independent of membrane lipid composition, can be acutely induced, and that perturb platelet function specifically under conditions of high shear blood flow. PI3KC2α appears to impact platelet function via a unique membrane-dependent mechanism that is independent of platelet activation. The findings of this thesis suggest that targeting the platelet membrane via PI3KC2α may represent a novel, thrombosis-specific, anti-platelet strategy.

References

1. National Heart Foundation of Australia. Data and Statistics. (2014).

2. Lozano, R. et al. Global and regional mortality from 235 causes of death for 20 age groups in 1990 and 2010: a systematic analysis for the Global Burden of Disease Study 2010. *Lancet* **380**, 2095-2128 (2012).

3. Barrett, N.E. et al. Future innovations in anti-platelet therapies. *Br. J. Pharmacol.* **154**, 918-939 (2008).

4. Davi, G. & Patrono, C. Platelet activation and atherothrombosis. *N. Engl. J. Med.* **357**, 2482-2494 (2007).

5. Hartwig, J.H. The platelet: form and function. *Semin. Hematol.* **43**, S94-100 (2006).

6. Hitchcock, I.S. & Kaushansky, K. Thrombopoietin from beginning to end. *Br. J. Haematol.* **165**, 259-268 (2014).

7. Harker, L.A. The kinetics of platelet production and destruction in man. *Clin. Haematol.* **6**, 671-693 (1977).

8. Ju, L. et al. Von Willebrand factor-A1 domain binds platelet glycoprotein Ibα in multiple states with distinctive force-dependent dissociation kinetics. *Thromb. Res.* **136**, 606-612 (2015).

9. Savage, B., Saldivar, E. & Ruggeri, Z.M. Initiation of platelet adhesion by arrest onto fibrinogen or translocation on von Willebrand factor. *Cell* **84**, 289-297 (1996).

10. Savage, B., Almus-Jacobs, F. & Ruggeri, Z.M. Specific Synergy of Multiple Substrate–Receptor Interactions in Platelet Thrombus Formation under Flow. *Cell* **94**, 657-666 (1998).

11. Watson, S.P., Herbert, J.M.J. & Pollitt, A.Y. GPVI and CLEC-2 in hemostasis and vascular integrity. *J. Thromb. Haemost.* **8**, 1456-1467 (2010).

12. Offermanns, S. Activation of platelet function through G protein-coupled receptors. *Circ. Res.* **99**, 1293-1304 (2006).

13. Huang, J. et al. Platelet integrin αIIbβ3: signal transduction, regulation, and its therapeutic targeting. *J. Hematol. Oncol.* **12**, 26 (2019).

14. Bennett, J.S. Structure and function of the platelet integrin αIIbβ3. *J. Clin. Investig.* **115**, 3363-3369 (2005).

15. Semple, J.W., Italiano, J.E., Jr. & Freedman, J. Platelets and the immune continuum. *Nat. Rev. Immunol.* **11**, 264-274 (2011).

16. Golebiewska, E.M. & Poole, A.W. Platelet secretion: From haemostasis to wound healing and beyond. *Blood Rev.* **29**, 153-162 (2015).

17. Furie, B. & Furie, B.C. Mechanisms of thrombus formation. *N. Engl. J. Med.* **359**, 938-949 (2008).

18. Geer, J.C., McGill, H.C., Jr. & Strong, J.P. The fine structure of human atherosclerotic lesions. *Am. J. Pathol.* **38**, 263-287 (1961).

19. Faruqi, R.M. & DiCorleto, P.E. Mechanisms of monocyte recruitment and accumulation. *Br. Heart J.* **69**, S19-S29 (1993).

20. Kragel, A.H., Reddy, S.G., Wittes, J.T. & Roberts, W.C. Morphometric analysis of the composition of atherosclerotic plaques in the four major epicardial coronary arteries in acute myocardial infarction and in sudden coronary death. *Circulation* **80**, 1747-1756 (1989).

21. Stary, H.C. The development of calcium deposits in atherosclerotic lesions and their persistence after lipid regression. *Am. J. Cardiol.* **88**, 16e-19e (2001).

22. Fuster, V. et al. Atherosclerotic plaque rupture and thrombosis. Evolving concepts. *Circulation* **82**, II47-59 (1990).

23. van der Wal, A.C., Becker, A.E., van der Loos, C.M. & Das, P.K. Site of intimal rupture or erosion of thrombosed coronary atherosclerotic plaques is characterized by an inflammatory process irrespective of the dominant plaque morphology. *Circulation* **89**, 36-44 (1994).

24. Farb, A. et al. Coronary plaque erosion without rupture into a lipid core. A frequent cause of coronary thrombosis in sudden coronary death. *Circulation* **93**, 1354-1363 (1996).

25. Falk, E. Why do plaques rupture? *Circulation* **86**, III30-42 (1992).

26. Jackson, S.P. Arterial thrombosis--insidious, unpredictable and deadly. *Nat. Med.* **17**, 1423-1436 (2011).

27. Rafieian-Kopaei, M., Setorki, M., Doudi, M., Baradaran, A. & Nasri, H. Atherosclerosis: Process, Indicators, Risk Factors and New Hopes. *Int. J. Prev. Med.* **5**, 927-946 (2014).

28. Awtry, E.H. & Loscalzo, J. Aspirin. *Circulation* **101**, 1206-1218 (2000).

29. Gum, P.A. et al. Profile and prevalence of aspirin resistance in patients with cardiovascular disease. *Am. J. Cardiol.* **88**, 230-235 (2001).

30. Pereillo, J.M. et al. Structure and stereochemistry of the active metabolite of clopidogrel. *Drug Metab. Dispos.* **30**, 1288-1295 (2002).

31. Elmi, F., Peacock, T. & Schiavone, J. Isolated profound thrombocytopenia associated with clopidogrel. *J. Invasive Cardiol.* **12**, 532-535 (2000).

32. Jiang, X.L., Samant, S., Lesko, L.J. & Schmidt, S. Clinical pharmacokinetics and pharmacodynamics of clopidogrel. *Clin. Pharmacokinet.* **54**, 147-166 (2015).

33. Yusuf, S. et al. Effects of clopidogrel in addition to aspirin in patients with acute coronary syndromes without ST-segment elevation. *N. Engl. J. Med.* **345**, 494-502 (2001).

34. Chen, Z.M. et al. Addition of clopidogrel to aspirin in 45,852 patients with acute myocardial infarction: randomised placebo-controlled trial. *Lancet* **366**, 1607-1621 (2005).

35. Bhatt, D.L., et al. Clopidogrel and aspirin versus aspirin alone for the prevention of atherothrombotic events. *N. Engl. J. Med.* **354**, 1706-1717 (2006).

36. Bonaca, M.P. et al. Long-term use of ticagrelor in patients with prior myocardial infarction. *N. Engl. J. Med.* **372**, 1791-1800 (2015).

37. Kristensen, S.D. et al. Contemporary use of glycoprotein IIb/IIIa inhibitors. *Thromb. Haemost.* **107**, 215-224 (2012).

38. Kastrati, A. et al. Abciximab in patients with acute coronary syndromes undergoing percutaneous coronary intervention after clopidogrel pretreatment: the ISAR-REACT 2 randomized trial. *JAMA* **295**, 1531-1538 (2006).

39. French, S.L., Arthur, J.F., Tran, H.A. & Hamilton, J.R. Approval of the first protease-activated receptor antagonist: Rationale, development, significance, and considerations of a novel anti-platelet agent. *Blood Rev.* **29**, 179-189 (2015).

40. Lam, S. & Tran, T. Vorapaxar: A Protease-Activated Receptor Antagonist for the Prevention of Thrombotic Events. *Cardiol Rev.* **23**, 261-267 (2015).

41. Magnani, G. et al. Efficacy and safety of vorapaxar as approved for clinical use in the United States. *J. Am. Heart Assoc.* **4**, e001505 (2015).

42. Gryka, R.J., Buckley, L.F. & Anderson, S.M. Vorapaxar: The Current Role and Future Directions of a Novel Protease-Activated Receptor Antagonist for Risk Reduction in Atherosclerotic Disease. *Drugs R. D.* **17**, 65-72 (2017).

43. Laurent, P.A., Severin, S., Gratacap, M.P. & Payrastre, B. Class I PI 3-kinases signaling in platelet activation and thrombosis: PDK1/Akt/GSK3 axis and impact of PTEN and SHIP1. *Adv. Biol. Regul.* **54**, 162-174 (2014).

44. Eisenreich, A. & Rauch, U. PI3K inhibitors in cardiovascular disease. *Cardiovasc. Ther.* **29**, 29-36 (2011).

45. Hennessy, B.T., Smith, D.L., Ram, P.T., Lu, Y. & Mills, G.B. Exploiting the PI3K/AKT pathway for cancer drug discovery. *Nat. Rev. Drug Discov.* **4**, 988-1004 (2005).

46. Rommel, C., Camps, M. & Ji, H. PI3Kδ and PI3Kγ: partners in crime in inflammation in rheumatoid arthritis and beyond? *Nat. Rev. Immunol.* **7**, 191-201 (2007).

47. Vanhaesebroeck, B., Stephens, L. & Hawkins, P. PI3K signalling: the path to discovery and understanding. *Nat. Rev. Mol. Cell Biol.* **13**, 195-203 (2012).

48.   Jean, S. & Kiger, A.A. Classes of phosphoinositide 3-kinases at a glance. *J. Cell Sci.* **127**, 923-928 (2014).

49.   Hawkins, P.T., Anderson, K.E., Davidson, K. & Stephens, L.R. Signalling through Class I PI3Ks in mammalian cells. *Biochem. Soc. Trans.* **34**, 647-662 (2006).

50.   Samuels, Y. et al. High frequency of mutations of the PIK3CA gene in human cancers. *Science* **304**, 554 (2004).

51.   Gabelli, S.B., Mandelker, D., Schmidt-Kittler, O., Vogelstein, B. & Amzel, L.M. Somatic mutations in PI3Kα: structural basis for the enzyme activation and drug design. *Biochim. Biophys. Acta* **1804**, 533 (2010).

52.   Stark, A.-K., Sriskantharajah, S., Hessel, E.M. & Okkenhaug, K. PI3K inhibitors in inflammation, autoimmunity and cancer. *Curr. Opin. Pharmacol.* **23**, 82-91 (2015).

53.   Hers, I. Insulin-like growth factor-1 potentiates platelet activation via the IRS/PI3Kα pathway. *Blood* **110**, 4243-4252 (2007).

54.   Kim, S., Garcia, A., Jackson, S.P. & Kunapuli, S.P. Insulin-like growth factor-1 regulates platelet activation through PI3-Kα isoform. *Blood* **110**, 4206-4213 (2007).

55.   Gilio, K. et al. Non-redundant roles of phosphoinositide 3-kinase isoforms α and β in glycoprotein VI-induced platelet signaling and thrombus formation. *J. Biol. Chem.* **284**, 33750-33762 (2009).

56.   Laurent, P.A. et al. Impact of PI3Kα (Phosphoinositide 3-Kinase α) Inhibition on Hemostasis and Thrombosis. *Arterioscler. Thromb. Vasc. Biol.* **38**, 2041-2053 (2018).

57.   O'Brien, K.A., Gartner, T.K., Hay, N. & Du, X. ADP-stimulated activation of Akt during integrin outside-in signaling promotes platelet spreading by inhibiting glycogen synthase kinase-3β. *Arterioscler. Thromb. Vasc. Biol.* **32**, 2232-2240 (2012).

58.   Jackson, S.P. et al. PI 3-kinase p110β: a new target for antithrombotic therapy. *Nat. Med.* **11**, 507-514 (2005).

59.   Kim, S. et al. Role of Phosphoinositide 3-Kinase β in Glycoprotein VI-mediated Akt Activation in Platelets. *J. Biol. Chem.* **284**, 33763-33772 (2009).

60.   Cross, D.A., Alessi, D.R., Cohen, P., Andjelkovich, M. & Hemmings, B.A. Inhibition of glycogen synthase kinase-3 by insulin mediated by protein kinase B. *Nature* **378**, 785-789 (1995).

61.   Moore, S.F. et al. Dual Regulation of Glycogen Synthase Kinase 3 (GSK3)α/β by Protein Kinase C (PKC)α and Akt Promotes Thrombin-mediated Integrin α(IIb)β(3) Activation and Granule Secretion in Platelets. *J. Biol. Chem.* **288**, 3918-3928 (2013).

62.   Laurent, P.A. et al. Platelet PI3Kβ and GSK3 regulate thrombus stability at a high shear rate. *Blood* **125**, 881-888 (2015).

63. Schoenwaelder, S.M. et al. Phosphoinositide 3-kinase p110β regulates integrin $\alpha_{IIb}\beta_3$ avidity and the cellular transmission of contractile forces. *J. Biol. Chem.* **285**, 2886-2896 (2010).

64. Martin, V. et al. Deletion of the p110β isoform of phosphoinositide 3-kinase in platelets reveals its central role in Akt activation and thrombus formation in vitro and in vivo. *Blood* **115**, 2008-2013 (2010).

65. Nylander, S. et al. Human target validation of phosphoinositide 3-kinase (PI3K)β: effects on platelets and insulin sensitivity, using AZD6482 a novel PI3Kβ inhibitor. *J. Thromb. Haemost.* **10**, 2127-2136 (2012).

66. Jackson, S.P. & Schoenwaelder, S.M. Antithrombotic phosphoinositide 3-kinase β inhibitors in humans: a 'shear' delight! *J. Thromb. Haemost.* **10**, 2123-2126 (2012).

67. Furman, R.R. et al. Idelalisib and rituximab in relapsed chronic lymphocytic leukemia. *N. Engl. J. Med.* **370**, 997-1007 (2014).

68. Zhang, J. Vanhaesebroeck, B. & Rittenhouse, S.E. Human platelets contain p110δ phosphoinositide 3-kinase. *Biochem. Biophys. Res. Commun.* **296**, 178-181 (2002).

69. Senis, Y.A. et al. Role of the p110δ PI 3-kinase in integrin and ITAM receptor signalling in platelets. *Platelets* **16**, 191-202 (2005).

70. Bergamini, G. et al. A selective inhibitor reveals PI3Kγ dependence of TH17 cell differentiation. *Nat. Chem. Biol.* **8**, 576-582 (2012).

71. Jin, M. et al. AS252424, a PI3Kγ Inhibitor, Downregulates Inflammatory Responsiveness in Mouse Bone Marrow-Derived Mast Cells. *Inflammation* **37**, 1254-1260 (2014).

72. Huang, L. et al. Phosphoinositide 3-kinase γ contributes to neuroinflammation in a rat model of surgical brain injury. *J. Neurosci.* **35**, 10390-10401 (2015).

73. Hirsch, E. et al. Resistance to thromboembolism in PI3Kγ-deficient mice. *FASEB J.* **15**, 2019-2021 (2001).

74. Cosemans, J.M. et al. Continuous signaling via PI3K isoforms β and γ is required for platelet ADP receptor function in dynamic thrombus stabilization. *Blood* **108**, 3045-3052 (2006).

75. Schoenwaelder, S.M. et al. Identification of a unique co-operative phosphoinositide 3-kinase signaling mechanism regulating integrin $\alpha_{IIb}\beta_3$ adhesive function in platelets. *J. Biol. Chem.* **282**, 28648-28658 (2007).

76. Canobbio, I. et al. Genetic evidence for a predominant role of PI3Kβ catalytic activity in ITAM- and integrin-mediated signaling in platelets. *Blood* **114**, 2193-2196 (2009).

77. Mazza, S. & Maffucci, T. Class II phosphoinositide 3-kinase C2α: what we learned so far. *Int. J. Biochem. Mol. Biol.* **2**, 168-182 (2011).

78. Mountford, S.J. et al. Class II but Not Second Class-Prospects for the Development of Class II PI3K Inhibitors. *ACS Med. Chem. Lett.* **6**, 3-6 (2015).

79. Falasca, M. & Maffucci, T. Role of class II phosphoinositide 3-kinase in cell signalling. *Biochem. Soc. Trans.* **35**, 211-214 (2007).

80. Rozycka, M. et al. cDNA cloning of a third human C2-domain-containing class II phosphoinositide 3-kinase, PI3K-C2γ, and chromosomal assignment of this gene (PIK3C2G) to 12p12. *Genomics* **54**, 569-574 (1998).

81. C Campa, C.C., Franco, I. & Hirsch, E. PI3K-C2α: One enzyme for two products coupling vesicle trafficking and signal transduction. *FEBS Lett.* **589**, 1552-1558 (2015).

82. Vanhaesebroeck, B., Guillermet-Guibert, J., Graupera, M. & Bilanges, B. The emerging mechanisms of isoform-specific PI3K signalling. *Nat. Rev. Mol. Cell. Biol.* **11**, 329-341 (2010).

83. Domin, J. et al. Cloning of a human phosphoinositide 3-kinase with a C2 domain that displays reduced sensitivity to the inhibitor wortmannin. *Biochem. J.* **326**, 139-147 (1997).

84. Ktori, C., Shepherd, P.R. & O'Rourke, L. TNF-α and leptin activate the α-isoform of class II phosphoinositide 3-kinase. *Biochem. Biophys. Res. Commun.* **306**, 139-143 (2003).

85. Turner, S.J., Domin, J., Waterfield, M.D., Ward, S.G. & Westwick, J. The CC chemokine monocyte chemotactic peptide-1 activates both the class I p85/p110 phosphatidylinositol 3-kinase and the class II PI3K-C2α. *J. Biol. Chem.* **273**, 25987-25995 (1998).

86. Brown, R.A., Domin, J., Arcaro, A., Waterfield, M.D. & Shepherd, P.R. Insulin activates the α isoform of class II phosphoinositide 3-kinase. *J. Biol. Chem.* **274**, 14529-14532 (1999).

87. Arcaro, A. et al. Class II Phosphoinositide 3-Kinases Are Downstream Targets of Activated Polypeptide Growth Factor Receptors. *Mol. Cell. Biol.* **20**, 3817-3830 (2000).

88. Knight, Z.A. et al. A pharmacological map of the PI3-K family defines a role for p110α in insulin signaling. *Cell* **125**, 733-747 (2006).

89. Brown, R.A., Ho, L.K., Weber-Hall, S.J., Shipley, J.M. & Fry, M.J. Identification and cDNA cloning of a novel mammalian C2 domain-containing phosphoinositide 3-kinase, HsC2-PI3K. *Biochem. Biophys. Res. Commun.* **233**, 537-544 (1997).

90. Harada, K., Truong, A.B., Cai, T. & Khavari, P.A. The Class II Phosphoinositide 3-Kinase C2β Is Not Essential for Epidermal Differentiation. *Mol. Cell. Biol* **25**, 11122-11130 (2005).

91. Mountford, J.K. et al. The class II PI 3-kinase, PI3KC2α, links platelet internal membrane structure to shear-dependent adhesive function. *Nat. Commun.* **6**, 6535 (2015).

92.   Alliouachene, S. et al. Inactivation of the Class II PI3K-C2β Potentiates Insulin Signaling and Sensitivity. *Cell Rep.* **13**, 1881-1894 (2015).

93.   Blajecka, K. et al. Phosphoinositide 3-kinase C2β regulates RhoA and the actin cytoskeleton through an interaction with Dbl. *PLoS One* **7**, e44945 (2012).

94.   Maffucci, T. et al. Class II phosphoinositide 3-kinase defines a novel signaling pathway in cell migration. *J. Cell Biol.* **169**, 789-799 (2005).

95.   Domin, J. et al. The class II phosphoinositide 3-kinase PI3K-C2β regulates cell migration by a PtdIns(3)P dependent mechanism. *J. Cell. Physiol.* **205**, 452-462 (2005).

96.   Katso, R.M. et al. Phosphoinositide 3-Kinase C2β regulates cytoskeletal organization and cell migration via Rac-dependent mechanisms. *Mol. Biol. Cell* **17**, 3729-3744 (2006).

97.   Boller, D. et al. Targeting PI3KC2β impairs proliferation and survival in acute leukemia, brain tumours and neuroendocrine tumours. *Anticancer Res..* **32**, 3015-3027 (2012).

98.   Ono, F. et al. A Novel Class II Phosphoinositide 3-Kinase Predominantly Expressed in the Liver and Its Enhanced Expression during Liver Regeneration. *J. Biol. Chem.* **273**, 7731-7736 (1998).

99.   Braccini, L. et al. PI3K-C2γ is a Rab5 effector selectively controlling endosomal Akt2 activation downstream of insulin signalling. *Nat. Commun.* **6**, 7400 (2015).

100.   Daimon, M. et al. Association of the PIK3C2G gene polymorphisms with type 2 DM in a Japanese population. *Biochem. Biophys. Res. Commun.* **365**, 466-471 (2008).

101.   Backer, J.M. The regulation and function of Class III PI3Ks: novel roles for Vps34. *Biochem. J.* **410**, 1-17 (2008).

102.   Brown, J.R. & Auger, K.R. Phylogenomics of phosphoinositide lipid kinases: perspectives on the evolution of second messenger signaling and drug discovery. *BMC Evol. Biol.* **11**, 4 (2011).

103.   Simonsen, A. & Tooze, S.A. Coordination of membrane events during autophagy by multiple class III PI3-kinase complexes. *J. Cell Biol.* **186**, 773-782 (2009).

104.   Jaber, N. et al. Class III PI3K Vps34 plays an essential role in autophagy and in heart and liver function. *Proc. Natl. Acad. Sci. USA* **109**, 2003-2008 (2012).

105.   Valet, C. et al. A dual role for the class III PI3K, Vps34, in platelet production and thrombus growth. *Blood* **130**, 2032-2042 (2017).

106.   Liu, Y. et al. Class III PI3K Positively Regulates Platelet Activation and Thrombosis via PI(3)P-Directed Function of NADPH Oxidase. *Arterioscler. Thromb. Vasc. Biol.* **37**, 2075-2086 (2017).

107.   Harris, D.P. et al. Requirement for class II phosphoinositide 3-kinase C2α in maintenance of glomerular structure and function. *Mol. Cell. Biol.* **31**, 63-80 (2011).

108. Yoshioka, K. et al. Endothelial PI3K-C2α, a class II PI3K, has an essential role in angiogenesis and vascular barrier function. *Nat. Med.* **18**, 1560-1569 (2012).

109. Nigorikawa, K., Hazeki, K., Guo, Y. & Hazeki, O. Involvement of class II phosphoinositide 3-kinase α-isoform in antigen-induced degranulation in RBL-2H3 cells. *PLoS One* **9**, e111698 (2014).

110. Franco, I. et al. PI3K class II α controls spatially restricted endosomal PtdIns3P and Rab11 activation to promote primary cilium function. *Dev. Cell* **28**, 647-658 (2014).

111. Shiwarski, D.J., Darr, M., Telmer, C.A., Bruchez, M.P. & Puthenveedu, M.A. PI3K class II α regulates δ-opioid receptor export from the trans-Golgi network. *Mol. Biol. Cell* (2017).

112. Alliouachene, S. et al. Inactivation of class II PI3K-C2α induces leptin resistance, age-dependent insulin resistance and obesity in male mice. *Diabetologia* **59**, 1503-1512 (2016).

113. Valet, C. et al. Essential role of class II PI3K-C2α in platelet membrane morphology. *Blood* **126**, 1128-1137 (2015).

114. von Hundelshausen, P. & Weber, C. Platelets as immune cells: bridging inflammation and cardiovascular disease. *Circ. Res.* **100**, 27-40 (2007).

115. Macaulay, I.C. et al. Platelet genomics and proteomics in human health and disease. *J. Clin. Investig.* **115**, 3370-3377 (2005).

116. Kenney, D.M., Weiss, L.D. & Linck, R.W. A novel microtubule protein in the marginal band of human blood platelets. *J. Biol. Chem.* **263**, 1432-1438 (1988).

117. Schwer, H.D. et al. A lineage-restricted and divergent β-tubulin isoform is essential for the biogenesis, structure and function of blood platelets. *Curr. Biol.* **11**, 579-586 (2001).

118. Blair, P. & Flaumenhaft, R. Platelet α-granules: Basic biology and clinical correlates. *Blood Rev.* **23**, 177-189 (2009).

119. Masliah-Planchon, J., Darnige, L. & Bellucci, S. Molecular determinants of platelet delta storage pool deficiencies: an update. *Br. J. Haematol.* **160**, 5-11 (2013).

120. Hayward, C.P. et al. Results of an external proficiency testing exercise on platelet dense-granule deficiency testing by whole mount electron microscopy. *Am. J. Clin. Pathol.* **131**, 671-675 (2009).

121. Kosaki, G. Platelet production by megakaryocytes: protoplatelet theory justifies cytoplasmic fragmentation model. *Int. J. Hematol.* **88**, 255-267 (2008).

122. Patel, S.R., Hartwig, J.H. & Italiano, J.E., Jr. The biogenesis of platelets from megakaryocyte proplatelets. *J. Clin. Investig.* **115**, 3348-3354 (2005).

123. Choi, E., Nichol, J., Hokom, M., Hornkohl, A. & Hunt, P. Platelets generated in vitro from proplatelet-displaying human megakaryocytes are functional. *Blood* **85**, 402-413 (1995).

124. White, J.G., Krumwiede, M.D. & Escolar, G. Glycoprotein Ib Is Homogeneously Distributed on External and Internal Membranes of Resting Platelets. *Am. J. Pathol.* **155**, 2127-2134 (1999).

125. Cramer, E.M. et al. Alpha-granule pool of glycoprotein IIb-IIIa in normal and pathologic platelets and megakaryocytes. *Blood* **75**, 1220-1227 (1990).

126. van Nispen tot Pannerden, H. et al. The platelet interior revisited: electron tomography reveals tubular alpha-granule subtypes. *Blood* **116**, 1147-1156 (2010).

127. Behnke, O. Electron microscopic observations on the membrane systems of the rat blood platelet. *Anat. Rec.* **158**, 121-137 (1967).

128. White, J.G. Interaction of membrane systems in blood platelets. *Am. J. Pathol.* **66**, 295-312 (1972).

129. Ebbeling, L., Robertson, C., McNicol, A. & Gerrard, J.M. Rapid ultrastructural changes in the dense tubular system following platelet activation. *Blood* **80**, 718-723 (1992).

130. Harrison, P. et al. Uptake of plasma fibrinogen into the alpha granules of human megakaryocytes and platelets. *J. Clin. Investig.* **84**, 1320-1324 (1989).

131. Escolar, G., Lopez-Vilchez, I., Diaz-Ricart, M., White, J.G. & Galan, A.M. Internalization of tissue factor by platelets. *Thromb. Res.* **122**, S37-41 (2008).

132. White, J.G. The transfer of thorium particles from plasma to platelets and platelet granules. *Am. J. Pathol.* **53**, 567-575 (1968).

133. White, J.G. & Krumwiede, M. Further studies of the secretory pathway in thrombin-stimulated human platelets. *Blood* **69**, 1196-1203 (1987).

134. Fogelson, A.L. & Wang, N.T. Platelet dense-granule centralization and the persistence of ADP secretion. *Am. J. Physiol.* **270**, H1131-1140 (1996).

135. Feng, D., Crane, K., Rozenvayn, N., Dvorak, A.M. & Flaumenhaft, R. Subcellular distribution of 3 functional platelet SNARE proteins: human cellubrevin, SNAP-23, and syntaxin 2. *Blood* **99**, 4006-4014 (2002).

136. Flaumenhaft, R. Molecular basis of platelet granule secretion. *Arterioscler. Thromb. Vasc. Biol.* **23**, 1152-1160 (2003).

137. Flaumenhaft, R., Croce, K., Chen, E., Furie, B. & Furie, B.C. Proteins of the exocytotic core complex mediate platelet alpha-granule secretion. Roles of vesicle-associated membrane protein, SNAP-23, and syntaxin 4. *J. Biol. Chem.* **274**, 2492-2501 (1999).

138. Polgár, J., Chung, S.-H. & Reed, G.L. Vesicle-associated membrane protein 3 (VAMP-3) and VAMP-8 are present in human platelets and are required for granule secretion. *Blood* **100**, 1081-1083 (2002).

139. White, J.G. & Escolar, G. The blood platelet open canalicular system: a two-way street. *Eur. J. Cell. Biol.* **56**, 233-242 (1991).

140. White, J.G. The secretory pathway of bovine platelets. *Blood* **69**, 878-885 (1987).

141. Sage, S.O., Pugh, N., Farndale, R.W. & Harper, A.G. Pericellular Ca(2+) recycling potentiates thrombin-evoked Ca(2+) signals in human platelets. *Physiol. Rep* **1**, e00085 (2013).

142. Escolar, G., Leistikow, E. & White, J.G. The fate of the open canalicular system in surface and suspension-activated platelets. *Blood* **74**, 1983-1988 (1989).

143. Hourdillé, P. et al. Thrombin induces a rapid redistribution of glycoprotein Ib-IX complexes within the membrane systems of activated human platelets. *Blood* **76**, 1503-1513 (1990).

144. Grouse, L.H., Rao, G.H., Weiss, D.J., Perman, V. & White, J.G. Surface-activated bovine platelets do not spread, they unfold. *Am. J. Pathol.* **136**, 399-408 (1990).

145. Maldonado, J.E., Gilchrist, G.S., Brigden, L.P. & Bowie, E.J. Ultrastructure of platelets in Bernard-Soulier syndrome. *Mayo Clin. Proc.* **50**, 402-406 (1975).

146. Savoia, A. et al. Spectrum of the mutations in Bernard-Soulier syndrome. *Hum. Mutat.* **35**, 1033-1045 (2014).

147. Jantunen, E. Inherited giant platelet disorders. *Eur. J. Haematol.* **53**, 191-196 (1994).

148. White, J.G. Giant Platelet Disorders. *Haematologica* **87**, 85-92 (2002).

149. Ludwig, J., Hashimoto, E., McGill, D.B. & van Heerden, J.A. Classification of hepatic venous outflow obstruction: ambiguous terminology of the Budd-Chiari syndrome. *Mayo Clin. Proc.* **65**, 51-55 (1990).

150. Dayal, S., Pati, H.P., Pande, G.K., Sharma, P. & Saraya, A.K. Platelet ultra-structure study in Budd-Chiari syndrome. *Eur. J. Haematol.* **55**, 294-301 (1995).

151. White, J.G., Keel, S., Reyes, M. & Burris, S.M. Alpha–delta platelet storage pool deficiency in three generations. *Platelets* **18**, 1-10 (2007).

152. Eckly, A. et al. Respective contributions of single and compound granule fusion to secretion by activated platelets. *Blood* **128**, 2538-2549 (2016).

153. Merchan-Perez, A., Rodriguez, J.R., Alonso-Nanclares, L., Schertel, A. & Defelipe, J. Counting Synapses Using FIB/SEM Microscopy: A True Revolution for Ultrastructural Volume Reconstruction. *Front. Neuroanat.* **3**, 18 (2009).

154. Bennett, A.E. et al. Ion-abrasion scanning electron microscopy reveals surface-connected tubular conduits in HIV-infected macrophages. *PLoS Pathog* **5**, e1000591 (2009).

155. Ben-Dor, I., Kleiman, N.S. & Lev, E. Assessment, mechanisms, and clinical implication of variability in platelet response to aspirin and clopidogrel therapy. *Am. J. Cardiol.* **104**, 227-233 (2009).

156. Stalker, T.J. et al. Hierarchical organization in the hemostatic response and its relationship to the platelet-signaling network. *Blood* **121**, 1875-1885 (2013).

157. Nesbitt, W.S. et al. A shear gradient-dependent platelet aggregation mechanism drives thrombus formation. *Nat. Med.* **15**, 665-673 (2009).

158. Cho, J., Furie, B.C., Coughlin, S.R. & Furie, B. A critical role for extracellular protein disulfide isomerase during thrombus formation in mice. *J. Clin. Investig.* **118**, 1123-1131 (2008).

159. Hall, C.E. & Slayter, H.S. The Fibrinogen Molecule: Its Size, Shape, and Mode of Polymerization. *J. Biophys. Biochem. Cytol.* **5**, 11-27 (1959).

160. Wu, Z., Xu, Z., Kim, O. & Alber, M. Three-dimensional multi-scale model of deformable platelets adhesion to vessel wall in blood flow. *Philos. Trans. A Math. Phys. Eng. Sci.* **372**, 1-23 (2014).

161. McGrath, B., Mealing, G. & Labrosse, M.R. A mechanobiological investigation of platelets. *Biomech. Model. Mechanobiol.* **10**, 473-484 (2011).

162. Popov, V.M. et al. Membrane Fluidity's Role In Platelet Function In Patients with Myeloproliferative Neoplasms. *Blood* **116**, 5125-5125 (2010).

163. Zheng, Z. et al. Discovery and antiplatelet activity of a selective PI3Kβ inhibitor (MIPS-9922). *Eur. J. Med. Chem.* **122**, 339-351 (2016).

164. Torti, M. PI3Kβ inhibition: all that glitters is not gold. *Blood* **125**, 750-751 (2015).

165. Aronson, D. & Brenner, B. Arterial thrombosis and cancer. *Thromb. Res.* **164**, S23-s28 (2018).

Appendix I

Class II Phosphoinositide 3-Kinases as Novel Drug Targets

Miniperspective

Marco Falasca,*,[†] Justin R. Hamilton,[‡] Maria Selvadurai,[‡] Krithika Sundaram,[§] Aleksandra Adamska,[†] and Philip E. Thompson[§]

[†]Metabolic Signalling Group, School of Biomedical Sciences, CHIRI Biosciences, Curtin University, Perth, Western Australia 6845, Australia

[‡]Australian Centre for Blood Diseases and Department of Clinical Haematology, Monash University, 99 Commercial Road, Melbourne, Victoria 3004, Australia

[§]Medicinal Chemistry, Monash Institute of Pharmaceutical Sciences, Monash University (Parkville Campus), 381 Royal Parade, Parkville, Victoria 3052, Australia

ABSTRACT: The phosphoinositide 3-kinases (PI3Ks) are a family of lipid kinases central to regulating a wide range of important intracellular processes. Despite the vast knowledge around class I PI3Ks, the class II PI3Ks have been neglected, seemingly only due to the chronology of their discovery. Here we focus on the cellular functions of the three class II PI3K isoforms, PI3KC2α, PI3KC2β, and PI3KC2γ, in different cell systems and underline the emerging importance of these enzymes in different physiological and pathological contexts. We provide an overview on the current development of class II PI3 kinase inhibitors and outline the potential use for such inhibitors. The field is in its infancy as compared to their class I counterparts. Nevertheless, recent advances in understanding the roles of class II PI3 kinases in different pathological contexts is leading to an increased interest in the development of specific inhibitors that can provide potential novel pharmacological tools.
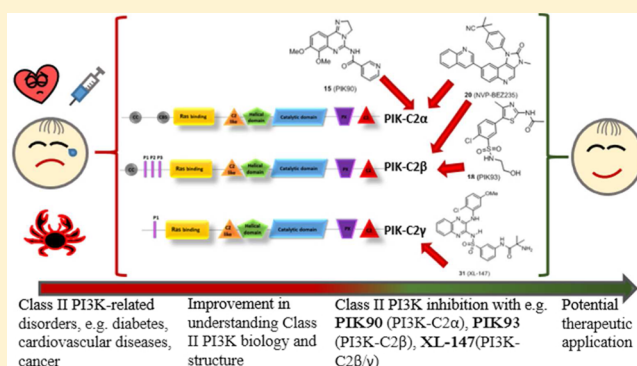
■ INTRODUCTION

Phosphoinositide 3-kinases (PI3Ks) are lipid kinases that catalyze the phosphorylation of the D3 position within the inositol ring of phosphoinositides. The resulting lipid products, PtdIns3P, PtdIns(3,4)P2, and PtdIns(3,4,5)P3, can in turn bind and modulate the activation of several signaling molecules, ultimately regulating many cellular functions.[1−4] Since their discovery, the interest in PI3Ks has been constantly fueled by the identification of the many physiological roles of these enzymes and the establishment of the central role that deregulation of PI3K-dependent pathways plays in many human diseases.[5−7] Eight PI3K isoforms exist in mammalian cells, which are grouped into three classes according to their structure and substrate specificity (Figure 1). For a long time, class II isoforms have been the least investigated of all PI3Ks, and our knowledge of their intracellular roles, mechanisms of regulation, and downstream effectors has been very limited.

Work from our laboratories demonstrated that class II PI3Ks are involved in glucose transport, insulin secretion, cell migration, platelet activation, and endothelial cell remodeling.[8] Our work has also clearly shown that the mechanisms of action of these enzymes are distinct from other PI3Ks.[8,10,11]

Simultaneous activation of class II isoforms and other PI3Ks has been reported in some cellular processes, such as regulation of glucose disposal into muscle cells and insulin secretion in pancreatic β-cells. Additional in vitro evidence has appeared recently, supporting the conclusion that class II PI3Ks play distinct intracellular roles and that different PI3K isoforms may cooperate in the regulation of critical cellular functions.[11] Overall, data so far have confirmed that class II PI3Ks are not redundant and that signaling downstream these enzymes are distinct from those of class I PI3Ks.

Functionally, the class I PI3Ks produce the bulk of the cell's PtdIns(3,4,5)P3. The sole class III PI3K, Vps34, appears limited to producing PtdIns3P. It is becoming increasingly clear that the class IIs are capable of producing PtdIns3P and possibly, PtdIns(3,4)P2, albeit under distinct conditions. Structurally, all eight PI3K isoforms have a PIK core region that comprises a C2 domain, helical domain, and catalytic (kinase) domain. However, one key point of distinction in the class II PI3Ks is that they function as monomers. This is in contrast to the sole class III and all four class I PI3Ks, which function as heterodimers between a catalytic and regulatory subunit.
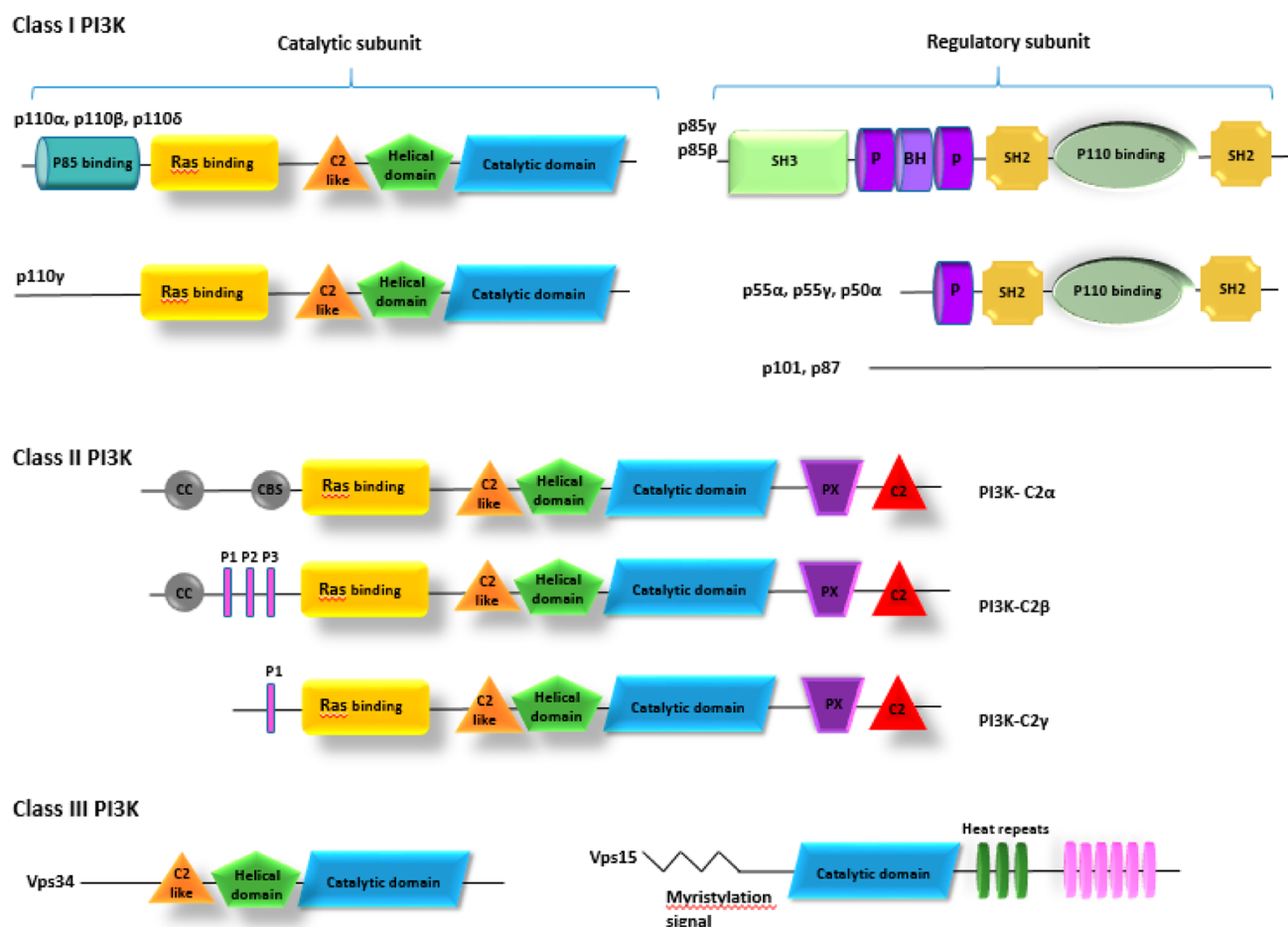
Figure 1. Structures of the isoforms of the three classes of PI3Ks. Adapted from refs 8 and 9.

PI3K function has been heavily studied over several decades, predominantly in the context of class I function in cancer, since the PI3K pathway is one of the most frequently dysregulated signaling pathways in oncogenesis and progression. However, dysregulation of PI3K signaling, either directly or indirectly, has also been implicated in disease states involving inflammation and autoimmunity,[12] as well as neuropathies, myopathies, and ciliopathies.[4] Indeed, isoform-specific inhibitors of various class I PI3Ks have been successful in a range of preclinical settings and provide a valuable roadmap for similar development of class II isoform-specific inhibitors.

Much is known about the functions of the class I PI3Ks, and drug targeting of each of the four class I isoforms has been examined in specific pathological settings. The class II PI3Ks are by far the least well studied isoforms, in large part due to a lack of pharmacological inhibitors and genetically modified mouse models. However, recent developments have begun to address this knowledge gap, leading to the discovery of some of the physiological roles of class II PI3Ks. Here, we discuss these recently discovered cellular functions of class II PI3Ks, the rationale for targeting each of these enzymes for drug therapy, and the early progress with the development of the first isoform-specific class II PI3K inhibitors.

Class I PI3Ks as Drug Targets: A Model for Class II PI3Ks? Due to their early discovery and dysregulation in human pathologies, class I PI3Ks have been heavily studied and well characterized.[13] The class consists of four closely related catalytic subunits that form functional heterodimers with two families of regulatory subunits.[3] The class IA PI3K subgroup comprises any one of the p110α, p110β, or p110δ catalytic subunits in combination with one of the p50, p55, or p85 regulatory subunits. The class IB PI3K subgroup comprises dimers of the p110γ catalytic subunit with either of the p101 or p84 regulatory subunits. The central difference between the class I subgroups is that class IA PI3Ks are activated downstream of receptor tyrosine kinases while class IB PI3Ks are activated downstream of G-protein-coupled receptors. The class I PI3K isoforms are named after their catalytic subunits: PI3Kα, PI3Kβ, PI3Kδ, and PI3Kγ. PI3Kα and PI3Kβ are ubiquitously expressed, while PI3Kδ and PI3Kγ are expressed in hematopoietic cells. Although capable of catalyzing the production of all three 3-phosphoinositides, the preferred substrate of the class I PI3Ks is PtdIns(4,5)P2, resulting in the production of PtdIns(3,4,5)P3.[3] Intracellular signaling effectors are recruited in response to this rise in localized PtdIns(3,4,5)P3 production via binding through specialized and highly specific lipid binding domains within effector proteins, such as pleckstrin homology (PH) and Phox homology (PX) domains, enabling efficient recruitment of these effector proteins to the plasma membrane and assembly into signaling complexes. For example, one of the most important cell signaling processes mediated by PtdIns(3,4,5)P3 is the activation of Akt, which regulates a number of signaling pathways, including the mammalian target of rapamycin (mTOR) pathway that is central to cell growth and proliferation, survival, metabolism, and autophagy.[4]
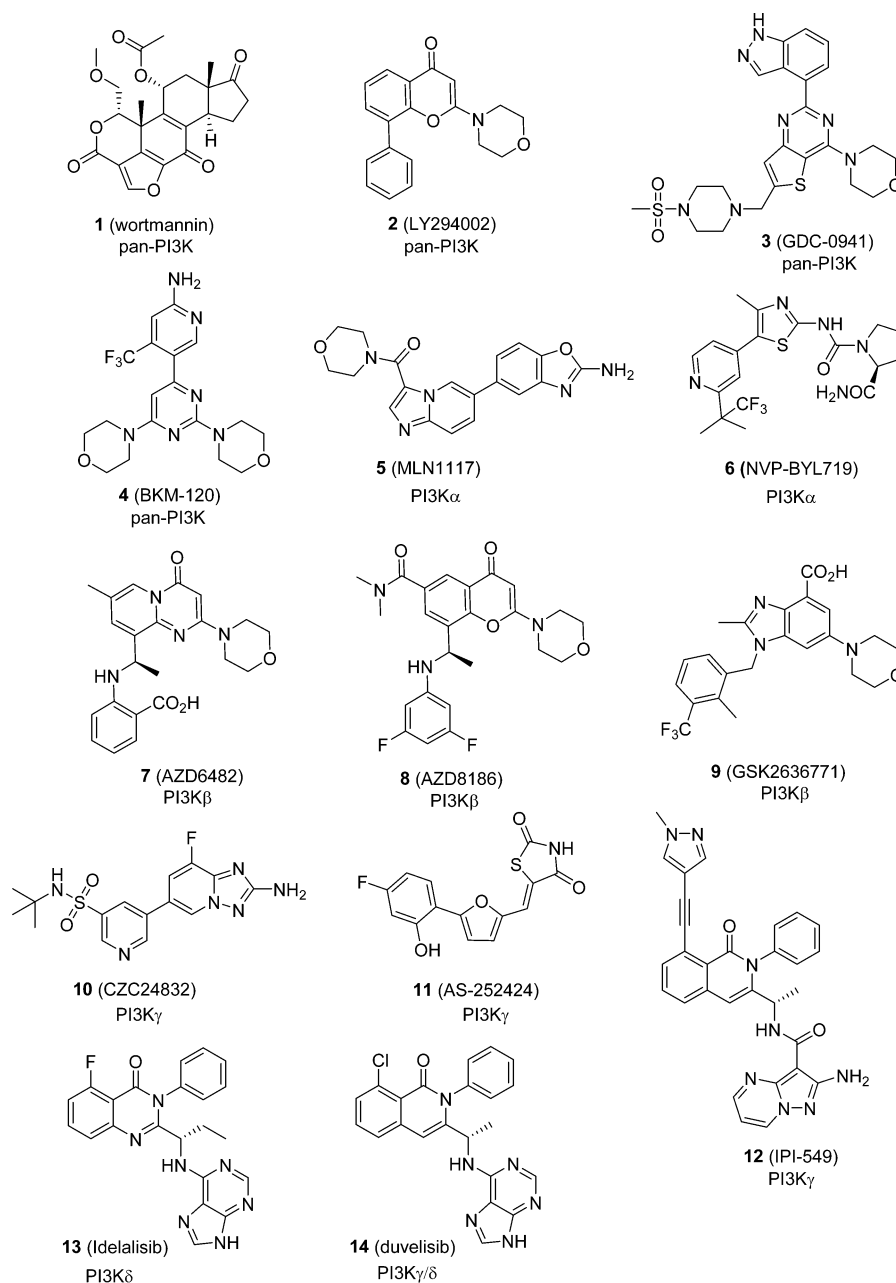
Figure 2. Selected class I PI3 kinase inhibitors **1−14**.

Class I PI3Ks in Disease and Class I PI3K Inhibitors.

Dysregulation of class I PI3K signaling is observed in a range of diseases, and each of the class I isoforms has been targeted as a therapeutic option in distinct pathologies. The identification of the first class I inhibitors, **1** (wortmannin,[14] Figure 2) and **2** (LY294002),[15] prefaced the development of current pan-PI3K clinical candidates such as **3** (GDC-0941)[16] and **4** (BKM-120),[17] and the subsequent development of class I isoform-specific PI3K inhibitors (compounds **5−14**, Figure 2) underscores the usefulness of targeting this family of proteins and may provide a useful model for any future development of class II PI3K inhibitors.

PI3Kα. PI3Kα is one of the most frequently mutated genes in certain cancers, with mutations leading to increased PI3Kα activity, directly or indirectly, often found in solid tumor cells.[18] These mutations are generally found in defined "hotspots" within the gene, with mutations in the region encoding three particular amino acid residues accounting for around 80% of cancer-causing PI3Kα mutations.[18] As a result of this, selective inhibition of PI3Kα is an emerging approach for the treatment of cancers in which PI3Kα activity is increased and may mitigate against the side effect profile of a pan-PI3K inhibition. To this end, a number of PI3Kα inhibitors are currently in clinical trials for treatment of a range of cancers. For example, two novel, potent, selective PI3Kα inhibitors are currently in clinical trials: **5** (MLN1117), which has an IC_{50} of 15 nM,[19] is in a phase Ib trial for the treatment of advanced non-hematological malignancies, and the 2-aminothiazole derivative **6** (BYL719) (IC_{50} = 4.6 nM)[20] is in a phase II trial for the treatment of squamous cell head and neck cancers.[21]

PI3Kβ. Perhaps the most clinically relevant function known for PI3Kβ is in thrombosis. Specifically, PI3Kβ has been shown to regulate the activity of the major platelet integrin $\alpha_{IIb}\beta_3$ in the setting of platelet adhesion and aggregation.[22,23] Pharmaco-

Table 1. Mouse Models of Class II PI3K Deficiency and Their Phenotypes

isoform	mouse model	phenotype	ref
PI3KC2α	Hypomorph (global but variable)	Stunted growth, decreased survival, renal abnormalities	Harris et al.[48]
	Global deficiency	Embryonic lethality	Yoshioka et al.[49]
			Mountford et al.[50]
			Franco et al.[51]
	Endothelial-cell-specific deficiency	Embryonic lethality, phenocopying the effects of global deficiency	Yoshioka et al.[49]
	Induced endothelial-cell-specific deficiency	Decreased retinal angiogenesis. Impaired revascularization following ischemic injury	Yoshioka et al.[49]
	Induced global deficiency	Impaired platelet function during thrombosis	Mountford et al.[50]
	Heterozygous kinase-dead inactivating mutation	Impaired platelet function during thrombosis	Valet et al.[52]
PI3KC2β	Global deficiency	None reported	Harada et al.,[53] Mountford et al.[50]
	Heterozygous kinase-dead inactivating mutation	Decreased circulating insulin levels, increased glucose tolerance, and protection against steatosis	Alliouachene et al.[54]
PI3KC2γ	Global deficiency	Hyperlipidemia, adiposity, insulin resistance	Braccini et al.[55]

logical inhibition of PI3Kβ impairs platelet activation and thrombosis in animal models[22] and in ex vivo human assays. These studies led to the clinical development of the PI3Kβ-selective inhibitor, **7**, (AZD6482), which has been examined in a phase I trial. **7** is an ATP-competitive inhibitor of PI3Kβ with an IC$_{50}$ of 0.01 μM. In vitro studies showed that it is a potent inhibitor of platelet aggregation.[24] In dog, treatment with **7** resulted in a dose-dependent antithrombotic effect, with no hemostatic consequences. The drug was well tolerated in humans, with potent in vivo inhibition of platelet aggregation and no adverse events recorded.[24] However, **7** inhibits insulin-induced glucose uptake, which may raise concerns regarding insulin resistance caused by the drug.[25]

It has been recently shown that inhibition of PI3Kβ signaling with isoform-specific inhibitors such as **8** (AZD8186) inhibits growth of PTEN-deficient breast and prostate tumors alone and in combination with drugs like docetaxel, and clinical trials on PI3Kβ inhibitors **8** and **9** (GSK263771) are currently ongoing.[26,27]

PI3Kγ. PI3Kγ is a potential target for anti-inflammatory drugs. PI3Kγ is strongly expressed in neutrophils, eosinophils, and mast cells and appears to play an important role in the regulation of inflammatory responses by regulating the recruitment and activation of immune cells at sites of inflammation. Mice in which PI3Kγ is either absent or inactivated are protected against the development of a number of autoimmune and inflammatory conditions. As a result, a number of PI3Kγ inhibitors have been developed and examined in experimental models in recent years and with promising results. For example, **10** (CZC24832) is a PI3Kγ-selective inhibitor that exhibits anti-inflammatory activity in vitro and in vivo.[28] The PI3Kγ-selective inhibitor **11** (AS252424) has been shown to inhibit mast cell degranulation and the release of inflammatory molecules in vitro[29] and to impair the inflammatory response to surgical brain injury in rats in vivo.[30] Interestingly, a role has been suggested for p110γ in tumor angiogenesis[31] and drug resistance of chronic myeloid leukemia cells.[32] Recently, work from our group has demonstrated that p110γ has a key role in pancreatic and liver cancer.[33,34] In particular, we reported data from an extensive screening for constitutive expression of the different PI3K isoforms in human tissues from pancreatic and liver cancer and normal counterparts and showed a clear over-expression of p110γ in pancreatic and liver cancer tissues. Further, we demonstrated that specific chemical inhibition of

p110γ or downregulation by siRNAs blocks pancreatic cancer cell proliferation with no effect on cell apoptosis, indicating that p110γ has a specific role in cell growth and proliferation.[35] In this respect, it is noteworthy that the transforming activity of the p110γ isoform has been suggested to be dependent on Ras binding. An p110γ-isoform selective inhibitor **12** (IPI-549) has entered phase I studies as an immune-oncology agent.[36]

PI3Kδ. Further highlighting the usefulness of targeting PI3Ks as therapy, the PI3Kδ inhibitor **13** (idelalisib) was recently approved by the FDA for the treatment of relapsed chronic lymphocytic leukemia (CLL), relapsed follicular B-cell non-Hodgkin's lymphoma, and relapsed small lymphocytic lymphoma. The phase III clinical trial comparing use of **13** combined with rituximab compared to rituximab monotherapy alone in patients with relapsed or refractory CLL was terminated early due to the overwhelming efficacy of the drug. Progression free survival, response rate, and overall survival were significantly higher in patients treated with **13**,[37] although the FDA has recently published an alert regarding increased rate of adverse events, including deaths, in clinical trials with combination therapies. The dual PI3Kγ/δ inhibitor **14** (duvelisib) has recently completed phase II studies.

■ CLASS II PI3Ks

Until very recently, the physiological functions of class II PI3Ks remained almost entirely unknown. However, a number of recent mouse genetic studies and some initial pharmacological studies have begun to shed some light on this emerging area of cell biology.[8,38,39]

Class II PI3 Kinase Architecture. There are three class II PI3Ks: PI3KC2α, PI3KC2β, and PI3KC2γ. PI3KC2α and PI3KC2β are widely expressed, while PI3KC2γ expression appears largely restricted to exocrine glands. The activation signals for class II PI3Ks are not well understood, although like class I isoforms they can be activated by ligands for either receptor tyrosine kinases or GPCRs.[40] Class II PI3Ks are capable of catalyzing the formation of both PtdIns3P and PtdIns(3,4)P2, from PtdIns and PtdIns4P, respectively, at least in vitro.[41]

In common with all PI3Ks, the class II PI3Ks have a core containing a C2 domain, helical domain, and the catalytic domain, as well as having a Ras-binding domain in common with the class I isoforms. What is notably different about the class II proteins is that they contain a conserved, characteristic C-terminal extension comprising a PX-domain and a second

C2-domain. At the N-terminus there are no binding sites for the regulatory partners as found in class I isoform but chain extensions that in PI3KC2α and PI3KC2β facilitate binding to clathrin; while in PI3KC2β the Pro-rich N terminus also allows interaction with partners such as intersectin. The molecular details governing these domains remain largely unknown. The structure of the PX-domain of PI3KC2α was deposited in 2006 (PDB code 2AR5), but little other detail has been revealed.

PI3KC2α. PI3KC2α is broadly expressed in human cells.[42] It is a 190 kDa protein that is structurally similar to the other members of the class, with the exception of a distinctive N-terminal region containing a clathrin-binding domain that does not appear in PI3KC2β and PI3KC2γ and the lack of proline-rich sequence repeats found in PI3KC2β.[38] In vitro studies have shown that PI3KC2α can be activated by a range of molecules, including cytokines,[43] chemokines,[44] integrins, as well as insulin[45] and other growth factors.[46] One property particular to PI3KC2α is its comparably decreased sensitivity to commonly used pan-PI3K inhibitors such as **1** and **2**.[47] The reason for this is unclear but this is an important consideration when interpreting early experiments in which the relative levels of response inhibition by various PI3K inhibitors have been used to identify the responsible isoforms.

Mouse Models of PI3KC2α Deficiency. A number of mouse models targeting PI3KC2α have been developed over the past 5 years (Table 1). The first of these was a gene trap-induced truncation that resulted in a hypomorphic allele and identified a role for PI3KC2α in overall growth and survival, as well as in renal structure and function.[48] Specifically, PI3KC2α hypomorphic mice retained between 10% and 20% of PI3KC2α activity, depending on the tissue examined, yet still exhibited significantly diminished survival rates and heavily stunted growth.[48] Furthermore, PI3KC2α hypomorphs presented chronic kidney failure, with the development of renal lesions and glomerulonephropathy.[48]

It was subsequently shown by several groups that complete deficiency of PI3KC2α results in absolute and early embryonic lethality.[49−51] The first of these was the study by Yoshioka et al., in which global and constitutive genetic deletion of PI3KC2α resulted in a mid-gestational embryonic lethality due to defective vasculogenesis.[49] Using a distinct genetic model, Mountford et al. also found that global PI3KC2α deficiency in mice resulted in an early and penetrant embryonic lethality, although this occurred slightly earlier.[50] Given that the third separate homozygous inactivation of *Pik3c2a* revealed a phenotype similar to the first,[51] the reasons for this discrepancy remain unknown. However, regardless of these differences, it is arguably the additional phenotypes investigated in each of these three papers that hold the most interest. Specifically, Yoshioka et al. detailed the involvement of endothelial cell PI3KC2α in angiogenesis and vascular development.[49] Mountford et al. uncovered a role for platelet PI3KC2α in thrombosis,[50] while Franco et al. reported that PI3KC2α is important in cilia function.[51]

PI3KC2α in Diabetes. It has been shown that PI3KC2α has a role in glucose transport and secretion.[56−60] We have recently reported that PI3KC2α mRNA is downregulated in islets from type 2 diabetic patients compared to nondiabetic individuals.[58] Recent work reported a sex-dependent role for PI3KC2α in the modulation of hypothalamic leptin action and systemic glucose homeostasis.[61]

Indeed, while homozygosity for kinase-dead PI3KC2α was embryonic lethal, heterozygous PI3KC2α KI mice were viable and fertile, with no significant histopathological findings. However, male heterozygous mice showed early onset leptin resistance, with a defect in leptin signaling in the hypothalamus, correlating with a mild, age-dependent obesity, insulin resistance, and glucose intolerance. Recently, a whole genome sequencing study of the Goto-Kakizaki rat, a nonobese animal model of type 2 diabetes, compared to normal Wistar rats reveals *Pik3c2a* among other mutant genes.[62]

PI3KC2α in Angiogenesis and Cancer. Limited data are available relating to the possible role of PI3KC2α in carcinogenesis. The expression of PI3KC2α was observed in several pancreatic cancer specimens, as well as normal pancreatic tissues, both in acini and in ducts.[33] In the same conditions, PI3KC2β isoform was barely detected in just a few pancreatic samples. Amplification of *Pik3c2a* has also been observed in colon, cervical, ovarian, thyroid, and non-small-cell lung cancers,[18,63−66] and alterations in *Pik3c2a* have been found in medulloblastomas[67] and anaplastic oligodendrioglomas.[68]

An increase in PI3KC2α mRNA levels has been observed in a subset of B-positive hepatocellular cancer samples when compared to nontumorigenic tissues.[69] The expression of PI3KC2α has also been attributed to the survival of HeLa cells.[70] Additionally, a significant increase in PI3KC2α expression has been observed in a population of MCF7 cells, enriched in cancer stemlike cells, compared to normal breast cells.[71] These data suggest a possible involvement of PI3KC2α in breast cancer development.

A potential involvement of PI3KC2α in tumor angiogenesis favoring lung cancer and melanoma has also been proposed. Indeed, in PIK3C2A knockout mice injected with Lewis lung carcinoma or B16-BL6 melanoma a significant reduction in microvessel density, tumor weight, and volume could be observed, compared to control mice.[49]

In a recent study, repression of PI3KC2α by miR-30e-3p has been indicated at mRNA levels in DLD1 CRC cells.[72] Importantly, the same authors also demonstrated that the levels of miR-30e-3p are considerably downregulated in CRC tissues, most probably at the early stages of CRC carcinogenesis. Taken together, these two studies suggest that in CRC, downregulation of miR-302-3p may increase PI3KC2α levels, promoting CRC cell growth and contributing to cancer development. On the other hand, inhibition of the Wnt pathway is involved in the upregulation of miR-30e-3p levels in the same cell line, suggesting another possible mechanism of regulation of PI3KC2α levels.

Importantly, a recent study has identified PI3KC2α as a key in angiogenesis, an important process in carcinogenesis. Yoshioka et al. demonstrated a role of this enzyme in the maintenance of vascular barrier integrity and mural-cell recruitment.[49] Endothelial-cell-specific deficiency of PI3KC2α in mice results in markedly reduced retinal angiogenesis and postischemic hindlimb revascularization due to impaired endothelial cell migration and proliferation. Furthermore, the microvessel density and overall volume of solid tumors implanted into the mice were reduced in a mouse model.[49] Taken together, these observations suggest that PI3KC2α inhibition may have some value as a therapeutic strategy for the treatment of solid tumors, with PI3KC2α as a potential drug target for reducing pathologic tumor angiogenesis and growth/survival.

PI3KC2α in Thrombosis. Two recent studies identified a role for PI3KC2α in platelet function and suggested that PI3KC2α may be a suitable drug target for the prevention and treatment

of thrombosis and cardiovascular disease. Using a series of distinct mouse models of PI3KC2α-deficiency, Mountford et al.[39] and Valet et al.[52] both observed that PI3KC2α is involved in the regulation of platelet membrane structure that is sufficient to cause significant platelet functional consequences in the setting of thrombosis. Here, an RNAi-based gene silencing approach was used to essentially abolish PI3KC2α expression in adult mouse platelets in an inducible manner. These PI3KC2α-deficient mice exhibited impaired delayed and highly unstable in vivo arterial thrombosis that appeared to be caused by a platelet function defect due to a rearrangement of the structure of the platelet's internal membrane reserve, the open canalicular system (OCS).[50] In support of this study, Valet et al.[52] used a mouse model in which there was a heterozygous kinase-inactivating point mutation in the PI3KC2α active site and confirmed the membrane structural defects and impairment of in vivo thrombosis observed by Mountford et al.[39]

Additional mechanistic studies performed by Valet et al.[52] indicated that PI3KC2α regulates a basal pool of PtdIns3P in platelets that may lead to impaired regulation of the platelet's cytoskeletal-membrane system. Taken together, these two studies point to a key role for PI3KC2α in platelet function and highlight the potential of this enzyme as an antithrombotic drug target. Given the global burden of cardiovascular diseases and the limitations of currently available treatments, new antiplatelet approaches are critically needed. The early evidence from these two studies suggests that targeting PI3KC2α may provide some potential toward this goal.

Additional Roles for PI3KC2α. Franco et al. have recently identified a role for PI3KC2α in primary cilium elongation.[51] By use of a series of in vitro and in vivo approaches, the levels of PI3KC2α were observed to increase at the pericentriolar recycling endocytic compartment at the base of growing cilium. The pool of PtsIns3P around the ciliary base was diminished in PI3KC2α-deficient cells indicating that, as in platelets, PI3KC2α regulates the production of a PtdIns3P pool. In the setting of cilia, this appears important for the accumulation of proteins and the activation of pathways necessary for normal cilium elongation.[51]

Other suggested roles for PI3KC2α include an involvement in the regulation of FcεRI-triggered mast cell degranulation. Nigorikawa et al. found that knocking down PI3KC2α using an RNAi-based approach in a mast cell line caused a reduction in the release of the lysosomal enzyme β-hexosaminidase from these cells, indicating that PI3KC2α is required for normal degranulation via FcεRI.[73] In addition, the release of neuropeptide Y, a reporter for mast cell exocytosis, was also significantly slowed in these PI3KC2α-deficient cells, further supporting a role for PI3KC2α in regulating the degranulation process.[73]

PI3KC2β. *PI3KC2β in Diabetes.* As with PI3KC2α, a number of PI3KC2β-deficient mouse models have been recently developed, although fewer physiological defects have been reported. Harada et al.[53] developed the first reported PI3KC2β-null mouse (as well as an overexpression model in which elevated PI3KC2β levels were targeted to the epidermis). Mice of both strains were phenotypically normal, and no spontaneous phenotypes were reported. Similarly, Mountford et al.[50] reported no phenotypic changes in PI3KC2β-deficient mice, including a lack of effect of PI3KC2β-deficiency in mouse platelets. This was recently extended to an examination of the first mouse model in which there is combined deficiency of

both PI3KC2α and PI3KC2β,[74] suggesting that at least some of the key functions of these two highly related enzymes do not overlap.

The first significant phenotype observed in PI3KC2β-deficient mice came from a very recent study and points to a role for PI3KC2β in insulin sensitivity and glucose tolerance. Here, a homozygous "knock-in" kinase-inactivating mutation in PI3KC2β (PI3KC2β^D1212A/D1212A mice), analogous to that used by Valet et al.[52] for PI3KC2α, demonstrated diminished circulating insulin levels after feeding and increased glucose tolerance, suggesting that PI3KC2β is a negative regulator of the insulin response.[54] Furthermore, PI3KC2β^D1212A/D1212A mice were protected from high-fat diet-induced steatosis, indicating that this regulatory role of insulin signaling is particularly important in the liver.[54] These results suggest that PI3KC2β may be a potential drug target for the treatment of type 2 diabetes, as well as other insulin-resistant conditions such as nonalcoholic fatty liver diseases.

PI3KC2β in Cancer. Involvement of PI3Ks in carcinogenesis has been described before as one of the key factors in this process. It was indicated that inhibition of PI3Ks signaling pathways was able to facilitate cell apoptosis and sensitize cells to cytotoxic drugs.[65]

Amplification of the gene encoding PI3KC2β, *PIK3C2B*, has been reported in several tumors.[75] A genome-wide analysis revealed the amplification of *PIK3C2B*, together with *MDM4*, in glioblastoma multiforme.[76] An increase in the copy number of these genes has also been detected by the analysis of whole-genome studies of glioblastoma histological sections.[77] Furthermore, the assessment of almost 90 ovarian cancer specimens pointed to a similar, significant increase in *PIK3C2B* copy number in these cells.[78] Importantly, the observed increase in PI3KC2β expression in ovarian cancer cells was significantly higher than of other PI3K classes. Amplification of *PIK3C2B*, together with *MDM4*, was also detected (using fluorescence in situ hybridization) in 1 out of 14 oligodendroglia tumors.[79]

Furthermore, overexpression of PI3KC2β has been observed in different cancer cell lines and specimens, such as acute myeloid leukemia,[80,81] medulloblastoma,[82] and glioblastoma multiforme.[83] In a study based on screening and sequencing of 31 samples, *PIK3C2B* was identified as one of the genes mutated in non-small-cell lung cancer samples, compared to nontumorigenic tissues.[84] Furthermore, overexpression of negative PI3KC2β considerably inhibited growth and growth-factor-induced Akt activation in small cell lung cancer.[85] Increased expression of PI3KC2β was also demonstrated in myeloid leukemia and acute lymphocytic leukemia. Its inhibition showed high antiproliferative activity, especially in AML cell lines, in which reduced proliferation, as well as considerable increase in apoptosis, was observed.[82] Furthermore, it was indicated that PI3KC2β and its activator intersectin 1 (ITSN1) are upregulated in primary neuroblastoma tumors and cell lines.[86,87] It was suggested that PI3KC2β plays an essential role in neuroblastoma development by mediating functions of ITSN1 and by stabilizing metylocytomatosis viral oncogene (MYCN),[88] an oncogene found in 20% of neuroblastoma cases and a marker for poor prognosis.[89] Moreover, downregulation of PI3KC2β resulted in the inhibition of early stage neuroblastoma formation.[86] The requirement for ITSN1, one of PI3KC2β activators, has been also proposed for glioblastoma tumorigenesis,[90] suggesting possible contribution of PI3KC2β in this process; however this

aspect was not addressed in that study. A correlation between a cluster of variants localized in the *PIK3C2B* promotor region and prostate cancer risk has been observed, especially in patients with familial disease.[91] Substantial recurrent mutations (12.9%) have been also identified in the *PIK3C2B* gene in lung cancer.[84] More recently, whole-exome sequencing revealed several candidate mutations for gastric cancer peritoneal carcinomatosis including recurrent mutations in *PIK3C2B*. Moreover, increased PI3KC2β mRNA levels have been found in several cancers, such as pancreatic cancer[92] and mixed lineage leukemia.[85] It was demonstrated as well that over-expression of PI3KC2β contributes to oncogenic trans-formation of colonic epithelial cells.[93]

Recently, a study of esophageal squamous-cell carcinoma (ESCC) tissues from more than 60 patients demonstrated that PI3KC2β was expressed in 45.9% of ESCC, whereas normal stratified squamous epithelial cells did not show any expression of this protein.[94] Furthermore, a correlation between PI3KC2β expression levels and ESCC metastasis was established.[94] Almost 70% of ESCC cases, in which the expression of this protein could be detected, showed metastasis.

Recent studies, based on genomic analysis, have identified PI3KC2β as an important factor in breast cancer development.[95] Through the analysis of COSMIC database it was demonstrated that a substantial increase in gene copy number of *PIK3C2B* occurs in a significant number of breast cancer cases. Moreover, this amplification correlated with a loss in copy number of tumor suppressor genes, such as PTEN or TP53. Furthermore, in the same study, survey of the Human Protein Atlas revealed that the expression of class II PI3Ks occurs mainly in ductal carcinomas. Importantly, PI3K genes that were found to be deregulated in this study are localized on 1q chromosome. Interestingly, abnormalities of this chromo-some are reported in 50−60% of breast cancer cases.[96−98]

Contribution of PI3KC2β in breast carcinogenesis was confirmed in a very recent study. It was shown that this enzyme is overexpressed in several human breast cancer cell lines and breast primary tumors when compared with normal breast tissues. PI3KC2β has been demonstrated to be an essential factor in breast cancer growth, by regulation of growth factor-induced cell proliferation, anchorage-independent growth, as well as breast cancer cell invasion in vitro.[99] Moreover, its expression has been linked to the proliferative status of the tumor. A possible mechanism of PI3KC2β action in breast cancer has also been proposed. It was suggested that PI3KC2β regulates cyclin B1 levels, influencing cell cycle progression. Furthermore, miR-449a has been proposed as a molecule that links PI3KC2β and cyclin B1 activity. Importantly, both cyclin B1 and miR-449 play key roles in various breast cancer cell lines[100] and their expression has been elevated in highly proliferative breast cancer samples[101] and is associated with poor prognosis.[102,103]

Moreover, accumulation of PI3KC2β could be clearly detected in lymph-node breast cancer metastases, indicating the role of this isoform in metastasis. More importantly, a significant increase in mice survival after PI3KC2β depletion was observed in an in vivo model of lung metastasis, PI3KC2β-deficient mice decreased number of metastases and reduced metastatic burden.[99]

Overall, the data from our study indicate that the PI3KC2β/miR-449s pathway is an important factor in the regulation of breast cancer cell proliferation, tumor growth, and metastasis.

In another study, the same authors highlighted the important role of PI3KC2β in prostate cancer (PCa).[104] As was stated before, almost 40% of primary and 70% of metastatic PCa samples showed alterations in *PIK3C2B*.[105] Interestingly, in this study,[104] PC3 and LNCaP cell lines, which showed increased PI3KC2β expression, are lacking the suppressor gene PTEN, an antagonist of PI3K action. The decrease in PTEN copy number is observed in a large percentage of both primary and metastatic tumors.[106,107] This gene was also associated with increased progression of prostate cancer in mice.[106]

The data from the aforementioned study revealed that PI3KC2β is involved in the regulation of cell invasion in PCa cells, partly by activation of MEK/ERK pathways and partly by regulation of cell migration through regulation of Slug protein. This protein is essential for epithelial−mesenchymal transition (EMT), a process which enables cells to gain migratory and invasive properties.[108,109] Slug activity has previously been shown to be specifically implicated in the regulation of cell invasion.[110,111] Interestingly, it was demonstrated that PI3KC2β has no influence on PCa cell proliferation. However, it plays crucial roles in cell motility, migration, and invasion. Taken together, this study highlighted the role of class II PI3Ks in the regulation of cell migration and invasion, suggesting its involvement in cancer metastasis.

A number of additional studies have also shown that PI3KC2β is involved in the regulation of cell migration and invasion in different cancers.[112−114] Implication of PI3KC2β in metastasis has been demonstrated in breast, prostate, and ovarian cancers. In a recent study, it has been demonstrated that this enzyme has a key role in lamellipodia formation in ovarian cancer SKOV3 cells, allowing for the increase in cell motility.[115] In fact, serum-dependent lamellipodia formation has been significantly reduced in cells lacking PI3KC2β, suggesting a specific role for this enzyme in ovarian cancer cell motility and, as a consequence, in cancer metastasis. Inhibition of PI3KC2β significantly reduced ovarian cancer metastasis in mice. Importantly, selective inhibition of PI3KC2β with ceramide has been shown to diminish PI3KC2β-dependent lamellipodia formation, reducing ovarian cancer cell mobility. Therefore, ceramide has been proposed as an antitumorigenic lipid that may be used in the treatment of metastatic cancers. Considering these results, further focus needs to be placed on the investigation of ceramide and its derivatives as novel anticarcinogenic agents.

The importance of PI3KC2β in ovarian cancer cell migration was initially proposed by Maffucci et al.,[112] who found that LPA is able to activate PI3KC2β in SKOV3 cells, which in turn generate PtdIns3P at the plasma membrane that may further act as a secondary messenger. This process is necessary for LPA-dependent cell migration and has been reported in many cancers,[116−118] suggesting that blocking of PI3KC2β pathway results in the impairment of SKOV3 cell migration.

Overexpression of PI3KC2β has been also found to enhance migration of A-431 epidermoid carcinoma cells, HeLa and ovarian cancer cells, whereas overexpression of the negative PI3KC2β was able to reduce this process.[113]

Recently, another possible mechanism of contribution of PI3KC2β in cancer cell migration and metastasis has been proposed.[119] Using RNA-seq analysis, it has been suggested that PIK3C2B is regulated by miR-515-5p, which plays a role in the control of cancer cell migration and metastasis. Over-expression of miR-515-5p has been shown to downregulate PIK3C2B, among others, binding directly to its 3′UTR region.

Increased miR-515-5p expression was correlated to reduced tumor dissemination in mice, as well as to a reduction in metastasis, assessed by in vivo xenograft studies. These data suggest once more the role of PI3KC2β in metastasis; however in this study overexpression of this protein has been only found in metastatic cells derived from brain and adrenal glands.

In yet another study,[82] treatment of highly invasive epithelial cells reduced the migratory capacity (assessed by wound-healing assay) of these cells, highlighting once again the relevance of PI3KC2β in the regulation of cancer cell migration.

Another important implication of PI3KC2β in cancer is the suggestion that its expression may contribute to chemo-resistance. It was reported that the expression levels of PI3KC2β were correlated with the sensitivity of glioblastoma cells to erlotinib.[120] This possibility was then confirmed in another study, which examined the response of MCF7, a breast cancer cell line, to tamoxifen treatment and concluded that PI3KC2β may be involved in the resistance of breast cancer cells to tamoxifen.[121] Furthermore, it was recently shown that upregulation of PI3KC2β in a human ESCC cell line highly decreased cell sensitivity to cisplatin, whereas its down-regulation was able to restore that sensitivity, pointing once again to the possible role of this protein in chemoresistance.[94]

Accordingly, targeting of PI3KC2β with specific inhibitors can enhance the sensitivity of cancer cells to chemotherapy. The use of these inhibitors resulted in decreased resistance of human AML and GBM cancer cells to chemotherapeutics such as etoposide or doxorubicin.[82]

On the other hand, a different study suggested that in leukemia cells, depletion of PI3KC2β can increase resistance of cells to chemotherapeutics.[122] It was demonstrated that upon *PIK3C2B* knockdown, CEM human leukemia cells gained resistance to thioguanine and mercaptopurine treatment. Therefore, more studies need to be conducted in order to gain more insight into the role of class II PI3Ks in chemoresistance in different contexts.

Additional Roles for PI3KC2β. PI3KC2β has been found to regulate cell morphology and survival via interactions with the Rho family guanine nucleotide exchange factor, Dbl. PI3KC2β forms a complex with Dbl, which is then able to activate Rho GTPases RhoA and Rac1. The modulation of RhoA activity by PI3KC2β enables it to in turn regulate cytoskeletal rearrangements and protect cells from anoikis.[123] Furthermore, a number of studies have supported a role for PI3KC2β in the regulation of cell migration. Work from our group has found that PI3KC2β is activated by lysophosphatidic acid and sphingosine 1-phosphate to generate a pool of PtdIns3P at the plasma membrane, which is required for cell migration.[112,124] Domin et al.[114] similarly observed that PI3KC2β regulates cell motility through a PtdIns3P-dependent mechanism, while Katso et al. reported that PI3KC2β signaling downstream of EGFR activation regulates membrane ruffling and cell motility.[113] Whether or not these in vitro findings will translate to in vivo functions of PI3KC2β in the setting of inflammatory conditions and/or cancers remains unknown but is of clear therapeutic interest.

PI3KC2γ. PI3KC2γ in Diabetes. PI3KC2γ has a much more restricted tissue expression distribution than PI3KC2α and PI3KC2β, being generally localized to exocrine glands. High levels of PI3KC2γ are found in the liver, specifically in the hepatic parenchyma, as well as the breast, prostate, and salivary glands.[125] As with the other class II PI3Ks, PI3KC2γ is capable of synthesizing both PtdIns3P and PtdIns$(3,4)P_2$ in vitro,

although its in vivo products have not been determined and even less is known about the physiological functions of PI3KC2γ than is known about PI3KC2α and PI3KC2β. One of the earliest studies of PI3KC2γ found that its expression levels are increased following partial hepatectomy, particularly after the period of liver regrowth, suggesting that PI3KC2γ may play a role in the maturation of hepatic cells.[126] This list of in vivo functions may grow with the recent publication of the first PI3KC2γ-deficient mouse model.[127] Of interest, PI3KC2γ-deficient mice were born at expected rates and developed normally but displayed decreased insulin tolerance and increased fat storage and triglyceride levels, indicating altered lipid metabolism. Insulin tolerance decreased with age, and in response to a high-fat diet, PI3KC2γ-deficient mice gained significantly more weight than controls. This was suggested to be due to the development of insulin resistance and the subsequent dyslipidemia, increase in fat mass, and fatty liver.[127] It has been suggested that the mechanism by which this occurs may be directly via the decreased pool of PtdIns$(3,4)P_2$ in early endosomal membranes, which leads to a decrease in Akt2 activation in response to insulin, and downregulation of glycogen synthase activity, with the end result that PI3KC2γ null mice are prone to insulin resistance and hyperlipidemia with age or exposure to a high fat diet.[127] This mouse study is supported by a human genetic study, in which polymorphisms in the gene encoding PI3KC2γ were associated with the occurrence of type 2 diabetes mellitus in a Japanese population.[128] Specifically, a single nucleotide polymorphism in *PIK3C2G* led to a significantly (OR: 2.2) increased risk of diabetes, suggesting PI3KC2γ may be involved in the pathogenesis of the disease.[128] Together, this intriguing link suggests that the development of inhibitors against PI3KC2γ will be useful in further elucidating the specific cell functions of the enzyme and for determining the potential of PI3KC2γ as a therapeutic target in diabetes. However, a genome-wide association study in an Australian aboriginal population recently found that *PIK3C2G* was associated with body mass index but not with type 2 diabetes.

PI3KC2γ in Cancer. Recent evidence suggested that *PIK3C2G*, the gene encoding PI3KC2γ, acts mainly as a tumor suppressor gene. Low PI3KC2γ expression has been shown to influence colorectal cancer (CRC) development,[129] with low copy number of *PIK3C2G* associated with a 2.5-fold increase in the risk of death. It has been demonstrated that this decrease in *PIK3C2G* copy number is also correlated with clinical outcomes for stage III CRC patients, independent of gender, age, or tumor site. This observation places PI3KC2γ as a potential novel biomarker, whose expression levels may predict CRC recurrence and patient survival.

■ MEDICINAL CHEMISTRY CONSIDERATIONS FOR DEVELOPMENT OF CLASS II PI3K INHIBITORS

The PI3K Catalytic Site. No crystal structure of a class II PI3K catalytic domain has been solved, so in order to understand the characteristics of ligand binding at class II PI3Ks, homology-based analysis is required. The extensive crystallographic studies of class I PI3Ks and more recently the class III PI3K, Vps34, and class IV, mTOR, provide a reliable starting point.[130−134] While there is relatively modest homology in the protein sequences overall (~30%), sequence alignment shows the capacity of the catalytic domain of the class II PI3K isoforms to adopt a common fold with a canonical ATP binding

site architecture. Plausible homology models can be derived from class I or class III PI3Ks without difficulty.

ATP and Substrate Binding. The binding of ATP in the active site is comparable to protein kinases in general and relies on the adenine moiety binding into a backbone amide at the so-called hinge region of the kinase and positioning of phosphate binding residues via the p-loop for presentation to the lipid substrate by the activation loop (Figure 3).[135] The residues that
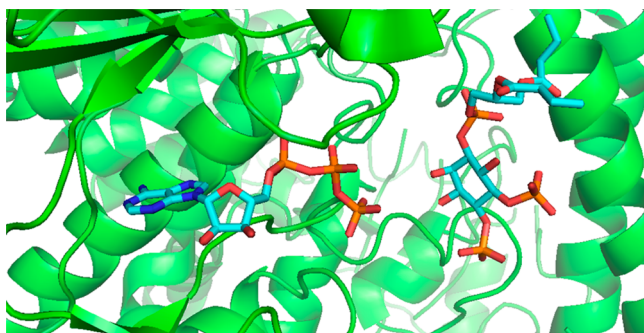

Figure 3. PI3K binding site: representation taken from crystal structure of PI3Kα (4OVV) with phosphoinositide bound (4OVV);[138] ATP modeled by using coordinates from 1e8x.[136]

interact directly with ATP in the class I PI3K crystal structure are largely conserved, but within 6 Å of ATP, which encompasses 26 residues, there is significant heterogeneity.[136] The lipid binding site does vary between PI3K classes consistent with the different lipid substrate preferences. In class I PI3Ks, basic residues adjacent to the activation loop are

key mediators of presentation phosphoinositide 4,5-bis-phosphate lipids (PIP3) but not in the class II isozymes (Figure 3) which utilize PtdIns or PtdIns4P as substrates.[137,138] The P-loop structures, as well presenting the β-phosphate of ATP, have also involvement in phosphoinositide engagement. In class I PI3Ks, this loop is strongly basic, while in class II and III PI3Ks these are uncharged sequences.[139,140]

Inhibitor Binding to PI3K Isoforms. As we have previously described, most of the data that can be retrieved regarding class II PI3K inhibitors relates to the assessment of class I inhibitors where the inhibition of class II PI3Ks is "off-target" activity[39] (Table 2). Binding models for inhibition of class II PI3Ks can be built with some confidence because several potent class II inhibitors (or close analogues) have been cocrystallized with class I enzymes. For example, one of the most potent PI3KC2α inhibitors is **15** (PIK90), which has been cocrystallized with both PI3Kγ and dsVps34.[47,139] Similarly, **16** (PI-103) has been cocrystallized with PI3Kα,[141] dsVps34,[139] and most recently mTOR.[131] The more recent success in solving structures of class III and class IV isoforms is particularly useful because in some respects those isoforms have more in common with class II than the class I isoforms do and in particular have common amino acid substitutions in known ligand binding sites.

The explanations for the observed potency and selectivity of PI3K inhibitors have been drawn from the identification of discrete binding motifs that are accessed by inhibitors as observed crystallographically. The inhibitor binding site has been subdivided into four regions on the basis of class I inhibitor interactions. These are the hinge region, the affinity pocket, the p-loop (or region 2), and region 1. In envisaging the

Table 2. PI3 Kinase Inhibition Data for Selected Inhibitors

| compd | PDB | IC$_{50}$ vs PI3K (µM) | | | | | |
		C2α	C2β	C2γ	class I[a]	Vps34	class IV[a]
3, GDC-0941	2WXP, 3DBS, 2Y3A	>10	0.59	nd	0.007 (δ)	>100	0.41 (mTOR)
6, NVP-BYL719, buparlisib[142]	4JPS	nd	nd	nd	0.005 (α)	inactive	>9.1
7, AZD6482[152,153]	4URK	>10	0.054	nd	0.01 (β)	3.4	0.54 (DNA-PK)
13, GS1101, idelalisib[158]	4XE0	nd	>1	nd	0.025 (δ)	978	6.7 (DNA-PK)
15, PIK90[47]	2X6I, 2CHX	0.047	0.064	nd	0.011 (α)	0.83	0.013 (DNA-PK)
16,[b] PI-103[47]	2X6K, 4JT6, 4L23	1.0	0.026		0.008 (α)	2300	0.002 (DNA-PK)
16,[b] PI-103[17]		>10	0.49	0.25	0.026 (α)	488	0.079 (mTOR)
17,[132]	4UWL	>10	n.d	>10	2.5 (γ)	0.002	>10 (mTOR)
18, PIK93[47]	2X6J, 2CHZ	16	0.14	nd	0.016 (γ)	0.32	0.064 (DNA-PK)
19, PIK124[47]		0.14	0.37	nd	0.023 (α)	10	1.5 (DNA-PK)
20, NVP-BEZ235[159]		0.034	0.044	nd	0.007 (α)	0.45	0.002 (mTOR)
21, ZSTK474[159]	2WXL	>100	0.18	nd	0.006 (δ)	>100	0.37 (mTOR)
22, AZD3147[146]		nd	nd	nd	0.92 (α)	nd	0.00015 (mTOR)
23[146]		nd	nd	nd	nd	nd	0.30 (mTOR)
24, PIK-587, gedatolisib[147]		nd	nd	nd	0.0004	nd	0.0016 (MOR)
25, PIK-III[134]	4PH4	nd	nd	nd	3.0 (γ)	0.018	>9.1
26, VPS34-IN1		>10	>10	>10	>10	0.076	>1
27, SAR405[150]	4OYS	>10	>10	>10	>10	0.0012	>10
28, MIPS-9922[155]		>10	>10	nd	0.063 (β)	nd	>10 (mTOR)
29, PI701[82]		nd	0.53	nd	>10	nd	>100
30, PI702[82]		nd	0.63	nd	>10	nd	>100
31, XL-147[156]		nd	nd	nd	0.023 (γ)	7.0	4.8 (DNA-PK)
32, AS-5[133]	2WXO	nd	nd	nd	0.090 (δ)	nd	nd
33, Freitag-26[157]		>10	29	0.34	>10	>10	n.d
34, Freitag-30[157]		>10	2.7	>10	>10	>10	nd

[a]Data refers to isoform for which inhibitor is most potent. [b]Data for **16** taken from separate references.
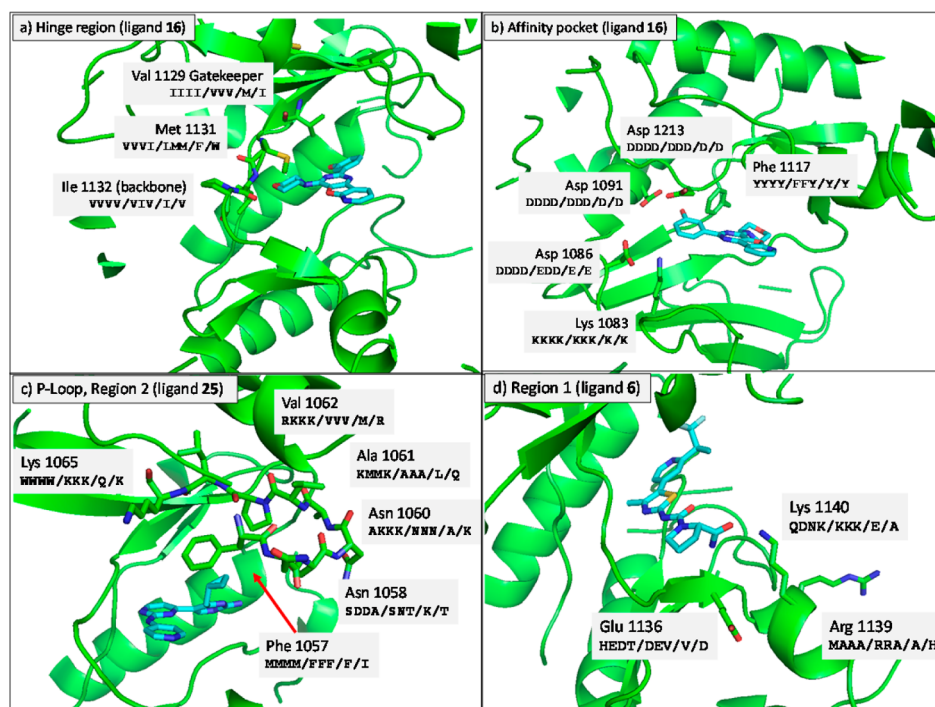
Figure 4. Views of PI3KC2β catalytic site (homology model) comparing residues at aligned positions. Key: class I$\alpha\beta\gamma\delta$/C2$\alpha\beta\gamma$/Vps34/mTOR. Ligands are modeled in from crystallographic poses.

development of potent, selective PI3KC2 inhibitors, these motifs are discussed in more detail with respect to non-conserved elements and the functional groups of PI3K inhibitors that target them (Figures 4 and 5).

Hinge and Gatekeeper. The most common binding element for inhibitors binding to PI3K is a hinge interaction between a backbone Val/Ile and a morpholine ring. This is true for many examples in class I isoforms, such as **3**, **7**, and **16**, and has been shown also recently for class III PI3K and mTOR.[131,139,141] The major driver of selective interactions in this region is the so-called "gatekeeper" residue which projects alongside the hinge amide. In the class I isoforms this is an Ile residue, while in class II it is a Val residue (Figure 4a). In Vps34, this is an unbranched Met residue. This difference has been exploited in the introduction of methyl-substituted morpholine group into compounds such as **17** (IC$_{50}$ vs Vps34, 2 nM) with hindered access to class I isoforms because of the branched group (IC$_{50}$ vs class I, >2 μM).[132]

One simple feature that seems difficult to reconcile is that morpholino compounds (**3**, **7**, **16**) are in general poor inhibitors of PI3KC2α, while the activity at PI3KC2β is preserved. The carbonylaminothiazoles **18** (PIK93) and **6**[47,142−144] are similarly PI3KC2β-preferring. In contrast, nonmorpholino class I inhibitors such as **15**, **19** (PIK124), and **20** (NVP-BEZ235) seem to have strong potency at both PI3KC2α and PI3KC2β isoforms and are potent also against class III PI3Ks and the class IV kinases. In crystal structures, **15** sits very deep in the catalytic pocket, tight against the hinge region.[47,139]

Affinity Pocket. The affinity pocket is a region of PI3K adjacent to the hinge region but not accessed by ATP and has been shown to accommodate a range of aryl substituents in inhibitors, and these have allowed for both pan-PI3K and dual PI3K/mTOR inhibitors to be developed. While largely conserved, a Phe for Tyr alteration is seen in PI3KC2α and

PI3KC2β and there is a Glu for Asp substitution in PI3KC2α, which has also been identified in mTOR.

The former variation would appear to hold some significance, as in class I PI3Ks the Tyr phenol has been identified as a contributor to affinity and isoform selectivity of inhibitors. Typically, the Tyr together with a nearby Asp residue makes a bifurcated interaction with polar functional groups of inhibitors (Figure 4b). This has been demonstrated with **16** as ligand in both PI3Kα (IC$_{50}$ = 8 nM) and mTOR (IC$_{50}$ = 80 nM).[131,141] Notably though, in dsVPS34[139] the phenol of **16** projects away from that grouping toward the conserved Lys residue, but potency is diminished (IC$_{50}$ = 2300 nM). It has been shown that the Tyr residue engages with other moieties such as indoles, indazoles, and aminopyridines creating modified hydrogen bonding networks that impart changes of selectivity within the class I isoforms.[145] The substitution of the Tyr for a Phe would be expected to change the ability of certain substituents to engage with the affinity pocket. Note that the pan-PI3K inhibitor **21** (ZSTK-474), which projects a difluorobenzimidazole group into the affinity pocket, does not utilize the Tyr residue but rather makes contact with the conserved Lys.[133]

The Glu for Asp change has been identified as a marker for targeting mTOR selectivity in the development of **22**, where a modeled interaction of an indole containing analogue, **23**, could interact with Glu but not Asp.[146] Venkatasan similarly identified this residue as influencing PI3Kα/mTOR selectivity in dual acting compounds such as **24** (PKI-587).[147]

P-Loop Region/Region 2/Specificity Pocket. The p-loop region would appear to provide a strong opportunity to make interactions with PI3KC2 that cannot be matched in the class I isoforms. It is essentially nonconserved between the two classes except for a Ser residue which binds β-phosphate of ATP and a proline residue. In each of the PI3KC2 isoforms the loop is bookended by a Phe and a Lys residue, in contrast to a Met and
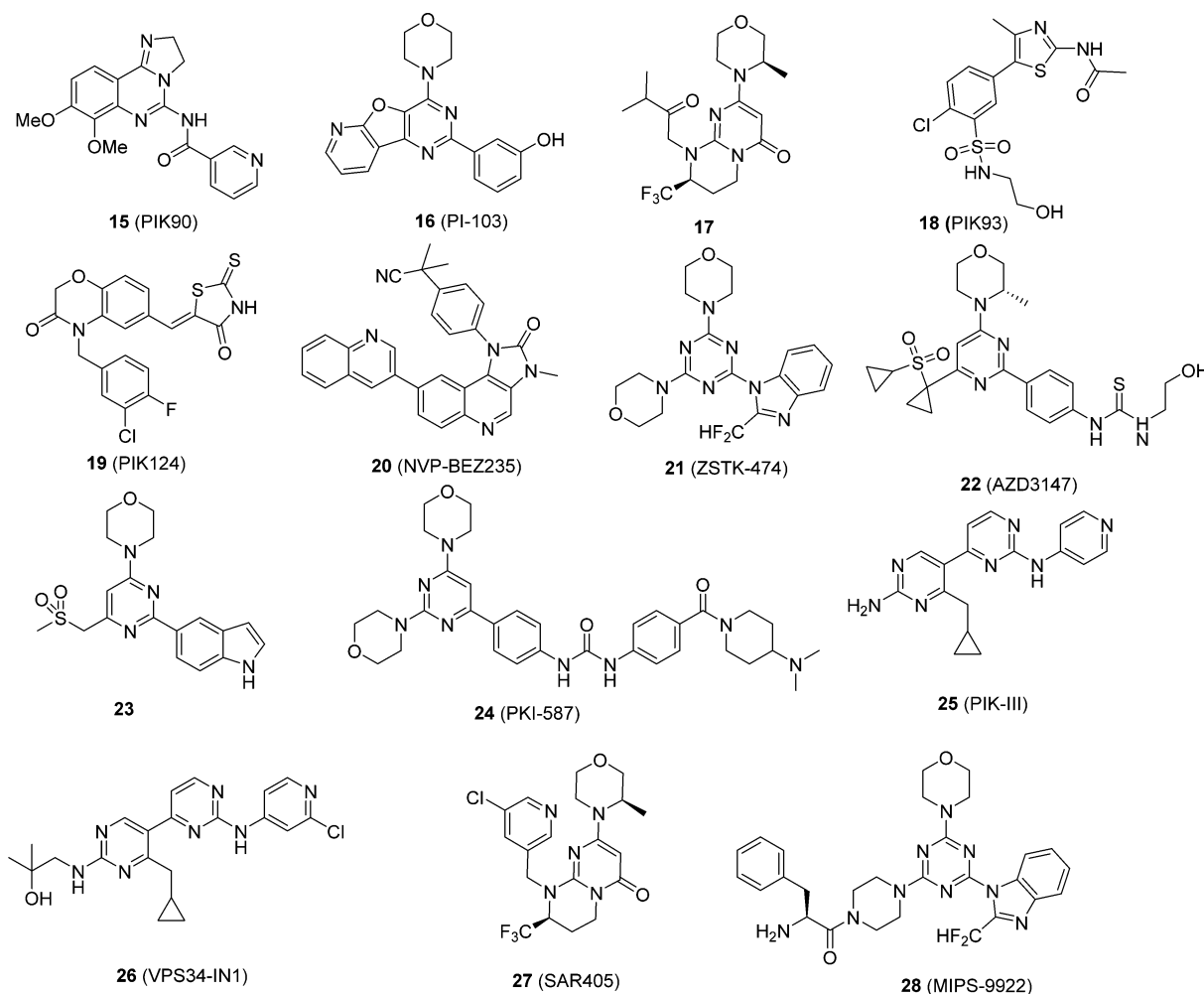
Figure 5. Structures of PI3K inhibitors **15–28** referred to in the text.

Trp in the class I isoforms; the intervening residues are basic in class I but neutral Asn-Ala-Val/Leu in class II PI3Ks. This architecture actually has much more in common with Vps34 (Ala-Leu-Met), and this principle has recently been exemplified in bis-aminopyrimidine Vps inhibitors **25** (PIK-III),[134] in which a cyclopropyl group (common to an analogous compound **26** (VPS34-IN1))[148] fits into a hydrophobic pocket, that also included the hinge phenylalanine (unique to PIKC3).[149] (Figure 4c). Similarly, trifluoromethyl substituents of Vps34 inhibitors **17**[132] and **27**[150] interact with the PIKC3 p-loop.

The difference in p-loop structures also may explain the generally poor PI3KC2 activity of the "propeller-style" inhibitors such as **13**.[151] These inhibitors utilize a cryptic or "specificity" pocket induced by a conformational change at Met which makes a pocket framed by a Trp residue. In the corresponding class II forms, such a pocket may not be accessible or will be very different. Interestingly, **7** is reported to show reasonably potent PI3KC2β inhibition, which may indicate a second binding mode that does not access the pocket.[152–154]

Region 1. The final region that has been shown to facilitate isoform selective interactions in class I isoforms is on the C-terminal side of the hinge region and describes a sequence termed region 1 that is variable across all PI3K isoforms. Selective inhibitors such as **6**[143] and **28** (MIPS-9922)[155] have been shown to specifically utilize Gln859 (PI3Kα) and the

corresponding Asp862 (PI3Kβ), respectively, to achieve selectivity (Figure 4d). In the class II isoforms, this residue is actually conserved; a lysine residue (also found in PI3Kγ) presents its side chain toward the binding pocket.

The First Class II Selective Inhibitors. The first isoform selective inhibitors of a class II PI3K have only recently been reported. These compounds have been identified from libraries of class I analogues series for which there are binding models. The PI3KC2β inhibitors, **29** (PI701), and **30** (PI702), were derived from a series developed by workers at Yamanouchi [Hayakawa et al. PCT Int. Appl. WO 2001083456, 2001], which is also where **16** was disclosed (Figure 6). The compounds have subsequently been described by Boller et al. as moderately potent (IC$_{50}$ of 0.5–0.6 μM) but selective inhibitors of PI3KC2β.[82]

Considered as analogues of **16**, it is difficult to explain the absolute PI3KC2β selectivity shown by **29** and **30**. It may be that these two compounds adopt a "flipped" pose where the acetamidophenyl group is placed in the affinity pocket[47] and the arylsulfonamide projects to the mouth of the binding site, but no SAR or structural data are available to test this hypothesis.

Freitag et al. recently described analogues of the pan-PI3K inhibitor **31** (XL147)[156] as inhibitors of PI3KC2γ and PI3KC2β.[157] The X-ray structure of the related compound **32** (AS5) showed a planar mode of binding to PI3Kδ where a

29, PI-701 (Ar = 2-Naphthyl)
30, PI-702 (Ar = Ph)

**31** (XL-147)

32 (AS-5)

33

34
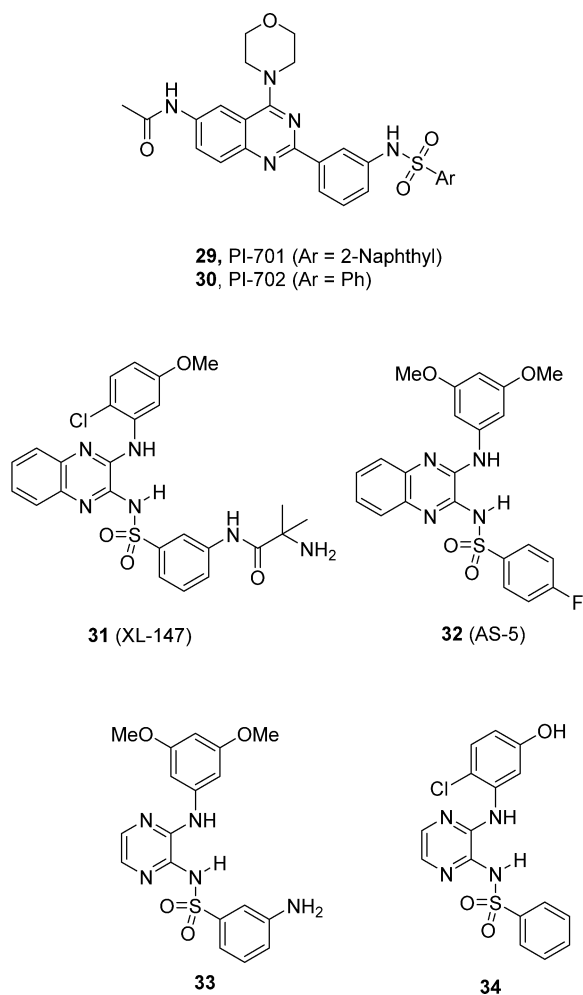
Figure 6. Structures of PI3K inhibitors **29**−**34**.

catechol ether occupied the hinge region and the sulfonamide mimicked the binding of the second phosphate of ATP to the p-loop Ser.[133] There was limited occupancy of the affinity pocket. The compounds including **33** and **34** are the only ones for which a comparison of the three class II isoforms can be made and there are clear differences between them. The hinge binding moiety influences selectivity, as does extension of the arylsulfonamide. As with ligands **29** and **30**, it is not obvious where the selectivity is derived from and it may well be that these ligands are adopting different poses to **32**, given the removal of the fused benzene ring from the scaffold. One striking feature is that compounds **29**−**34** all have an aryl sulfonamide moiety, suggesting that they may in fact have a common binding mode.

Upon the basis of the above data, it would seem that the lack of available selective class II inhibitors is not a function of the difficulty of achieving selectivity but rather the will to pursue them. The recent success in identifying mTOR and Vps34 selective inhibitors provides a strategic template to follow. There is an urgent need to identify isoform selective inhibitors of each of the class II PI3K isoforms so that the increasingly promising list of knock-out and knock-in phenotypes can be confirmed pharmacologically and potential therapeutic applications can be realized.

■ SUMMARY AND OUTLOOK

The overall focus of this review has been to provide a practical guide for researchers interested in the development and use of novel genetic and pharmacological tools to study class II PI3Ks. Isoform selective class II PI3K inhibitors are highly likely to be used well beyond the cell and animal studies described here. By analogy to selective class I PI3K inhibitors, these will be sought-after reagents for the conducting of cell biology research. The wide-ranging expression and function of class II PI3Ks predicts any inhibitors developed will be of value in different human diseases (Table 3). The expression and purification of class II enzymes will advance molecular and structural biology research of these enzymes also. Finally, advancement of class I inhibitors as clinical candidates has paid little heed to their effects on class II isoforms and a better knowledge of class II isoforms roles in cell functions will provide valuable information for researchers evaluating the clinical effects of these compounds.

The question of whether PI3K isoforms are redundant or whether they play distinct and nonoverlapping roles in cell signaling has received increasing attention, in particular with the development of isoform-specific PI3K inhibitors that require a clear understanding of the contribution of each PI3Ks for the evaluation of their safety and efficacy and their pharmacological potential. Studies on class II PI3Ks fit nicely into the current increasing interest in these enzymes and will both provide critical insight into their specific contribution to physiological and pathological conditions and validate these enzymes and signaling pathways specifically regulated by them, as novel potential therapeutic targets.

The limited existing knowledge on the function of class II PI3Ks suggests future research in this area has the potential to help define PI3K signaling and cell function, which to date has focused on class I isoforms. Given that each of the four class I PI3Ks has found a therapeutic application, it is possible that the findings from this basic research will lead to comparable translational benefit. In fact, the wide-ranging expression and function of class II PI3Ks predict the genetic models and pharmacological inhibitors developed in future will be of value well beyond the specific animal and cell lines studies investigated so far.

Table 3. Potential Clinical Utility of Isoform-Specific Class II PI3K Inhibitors

isoform	major known functions	relevant cells	expression level	potential clinical utility
PI3KC2α	Thrombosis[50,52]	Platelets	+	Arterial thrombosis
	Angiogenesis[49]	Endothelium	+++	Cancer (antiangiogenics)
PI3KC2β	Insulin signaling[54]	Hepatocytes	++	Diabetes
	Cell migration and invasion[99]	Prostate and breast cancer cells	Variable	Cancer (antimetastatics)
PI3KC2γ	Insulin signaling[127]	Hepatocytes	+++	Diabetes
	Lipid regulation[127]	Hepatocytes	+++	Steatosis

■ AUTHOR INFORMATION

Corresponding Author

*Phone +61 08 92669712. E-mail: marco.falasca@curtin.edu.au.

Author Contributions

The manuscript was written through contributions of all authors.

Notes

The authors declare no competing financial interest.

Biographies

Marco Falasca was educated in Italy. He then was involved in postdoctoral training at New York University from 1995 to 1998. Prof. Falasca took up a position as Head of the Unit of Physiopathology of Cell Signalling within the Consorzio Mario Negri Sud in 1998. In 2001 he moved to London where he was appointed as Principal Research Fellow at the University College London. In 2007 he was appointed as Professor of Molecular Pharmacology at the Queen Mary University of London. In 2014 he was appointed as Professor in Metabolism at the School of Biomedical Sciences, Curtin University, Perth, Australia. Research in his lab is mostly focused on intracellular signals regulated by specific lipids that act as "second messengers" such as those produced by PI3Ks.

Justin R. Hamilton obtained his Ph.D. in Pharmacology in 2001 from The University of Melbourne, Australia, and completed postdoctoral studies at The University of California, San Francisco, U.S., with Prof. Shaun Coughlin, from 2001 to 2006. He then moved back to Australia to establish a research group at The Australian Centre for Blood Diseases, Monash University, where he is currently a Future Fellow of the Australian Research Council and Head of the Platelets & Thrombosis Laboratory. His group studies the role of platelets in hemostasis, thrombosis, and inflammatory conditions, with a focus on intracellular signaling effectors such as class II PI3Ks.

Maria Selvadurai is a medical student and Ph.D. candidate at The Australian Centre for Blood Diseases, Monash University, under the supervision of Justin Hamilton. Maria is researching the cellular effects of class II PI3Ks and the biological implications of class II PI3K inhibitors. She has an interest in platelet biology, clinical platelet disorders, and the development of novel antiplatelet drugs for improved antithrombotic therapy and has previously studied at the Etablissement Francais du Sang (Alsace), Strasbourg, France, in the group of Prof. Christian Gachet.

Krithika Sundaram obtained her B.Sc. in Microbiology from Osmania University (India) and M.S. in Biotechnology from Victoria University (Australia). She obtained her Ph.D. degree from Monash University in May 2016. Her thesis was entitled "Structure-Based Studies in the Development of Anticancer Enzyme Inhibitors Including the Study of Class II PI3KC2β".

Aleksandra Adamska is a Ph.D. student at The Curtin Health Innovation Research Institute, School of Biomedical Sciences, Curtin University, where she is studying under the supervision of Prof. Marco Falasca. Aleksandra graduated from Wroclaw University of Technology (Wroclaw, Poland) in the field of pharmaceutical biotechnology. She also completed a 1-year internship at The University of Chicago in the group of Dr. Anthony Kossiakoff. Currently Aleksandra's interests are focused on the investigation of GPCRs and ABC transporters as potential targets in pancreatic cancer therapy.

Philip E. Thompson is an Associate Professor in Medicinal Chemistry at Monash University. He obtained his B.Sc.(Hons.) and Ph.D. from the University of Melbourne. In his research career, he has studied an array of topics with over 100 publications in international journals of diverse disciplines. He spent 5 years at the biotechnology company Kinacia, which developed the first PI3Kβ-selective inhibitors, and has continued to study PI3K in an academic setting. His other area of active interest is in peptide science with recent focus on polymyxin analogues and neuropeptide Y receptor ligands.

■ ABBREVIATIONS USED

Akt, protein kinase B (PKB), also known as Akt; AML, acute myeloid leukemia; CEM, human acute lymphoblastic leukemia cells; CLL, chronic lymphocytic leukemia; CRC, colorectal cancer; DNA-PK, DNA-dependent protein kinase; EMT, epithelial−mesenchymal transition; ESCC, esophageal squamous cell carcinoma; FcεRI, human Fc ε receptor I; GBM, glioblastoma; ITSN1, intersectin 1; KI, knock-in (mice); LPA, lysophosphatidic acid; MEK (MAPK), mitogen-activated protein kinase; miR, microRNA; mTOR, mammalian target of rapamycin; OCS, open canalicular system; OR, observed ratio; PCa, prostate cancer; PH, pleckstrin homology (domain); PtdIns, phosphatidylinositol; PtdIns4P, phosphatidylinositol 4-phosphate; PtdIns3P, phosphatidylinositol 3-phosphate; PtdIns(3,4)P2, phosphatidylinositol (3,4)-bisphosphate; PtdIns(3,4,5)P3, phosphatidylinositol (3,4,5)-trisphosphate; PTEN, phosphatase and tensin homologue; PX, phox homology (domain); siRNA (RNAi), silencer RNA; TP53, tumor protein 53; UTR, untranslated region; Vps, proteins involved in vesicle-mediated vacuolar protein sorting

■ REFERENCES

(1) Cantley, L. C. The phosphoinositide 3-kinase pathway. *Science* **2002**, *296*, 1655−1657.

(2) Jean, S.; Kiger, A. A. Classes of phosphoinositide 3-kinases at a glance. *J. Cell Sci.* **2014**, *127*, 923−928.

(3) Hawkins, P. T.; Anderson, K. E.; Davidson, K.; Stephens, L. R. Signalling through class I PI3Ks in mammalian cells. *Biochem. Soc. Trans.* **2006**, *34*, 647−662.

(4) Vanhaesebroeck, B.; Stephens, L.; Hawkins, P. PI3K signalling: the path to discovery and understanding. *Nat. Rev. Mol. Cell Biol.* **2012**, *13*, 195−203.

(5) Okkenhaug, K. Signaling by the phosphoinositide 3-kinase family in immune cells. *Annu. Rev. Immunol.* **2013**, *31*, 675−704.

(6) Ghigo, A.; Perino, A.; Hirsch, E. Phosphoinositides and cardiovascular diseases. *Curr. Top. Microbiol. Immunol.* **2012**, *362*, 43−60.

(7) Foukas, L. C.; Withers, D. J. Phosphoinositide signalling pathways in metabolic regulation. *Curr. Top. Microbiol. Immunol.* **2010**, *346*, 115−141.

(8) Falasca, M.; Maffucci, T. Regulation and cellular functions of class II phosphoinositide 3-kinases. *Biochem. J.* **2012**, *443*, 587−601.

(9) Vanhaesebroeck, B.; Guillermet-Guibert, J.; Graupera, M.; Bilanges, B. The emerging mechanisms of isoform-specific PI3K signalling. *Nat. Rev. Mol. Cell Biol.* **2010**, *11*, 329−341.

(10) Falasca, M.; Maffucci, T. Role of class II phosphoinositide 3-kinase in cell signalling. *Biochem. Soc. Trans.* **2007**, *35*, 211−214.

(11) Maffucci, T.; Falasca, M. New insight into the intracellular roles of class II phosphoinositide 3-kinases. *Biochem. Soc. Trans.* **2014**, *42*, 1378−1382.

(12) Rommel, C.; Camps, M.; Ji, H. PI3K delta and PI3K gamma: partners in crime in inflammation in rheumatoid arthritis and beyond? *Nat. Rev. Immunol.* **2007**, *7*, 191−201.

(13) Falasca, M. PI3K/Akt signalling pathway specific inhibitors: a novel strategy to sensitize cancer cells to anti-cancer drugs. *Curr. Pharm. Des.* **2010**, *16*, 1410−1410.

(14) Lam, K.; Carpenter, C. L.; Ruderman, N. B.; Friel, J. C.; Kelly, K. L. The phosphatidylinositol 3-kinase serine kinase phosphorylates IRS-1. Stimulation by insulin and inhibition by Wortmannin. *J. Biol. Chem.* **1994**, *269*, 20648−20652.

(15) Vlahos, C. J.; Matter, W. F.; Hui, K. Y.; Brown, R. F. A specific inhibitor of phosphatidylinositol 3-kinase, 2-(4-morpholinyl)-8-phenyl-4H-1-benzopyran-4-one (LY294002). *J. Biol. Chem.* **1994**, *269*, 5241−5248.

(16) Folkes, A. J.; Ahmadi, K.; Alderton, W. K.; Alix, S.; Baker, S. J.; Box, G.; Chuckowree, I. S.; Clarke, P. A.; Depledge, P.; Eccles, S. A.; Friedman, L. S.; Hayes, A.; Hancox, T. C.; Kugendradas, A.; Lensun, L.; Moore, P.; Olivero, A. G.; Pang, J.; Patel, S.; Pergl-Wilson, G. H.; Raynaud, F. I.; Robson, A.; Saghir, N.; Salphati, L.; Sohal, S.; Ultsch, M. H.; Valenti, M.; Wallweber, H. J.; Wan, N. C.; Wiesmann, C.; Workman, P.; Zhyvoloup, A.; Zvelebil, M. J.; Shuttleworth, S. J. The identification of 2-(1H-indazol-4-yl)-6-(4-methanesulfonyl-piperazin-1-ylmethyl)-4-morpholin-4-yl-t hieno[3,2-d]pyrimidine (GDC-0941) as a potent, selective, orally bioavailable inhibitor of class I PI3 kinase for the treatment of cancer. *J. Med. Chem.* **2008**, *51*, 5522−5232.

(17) Burger, M. T.; Pecchi, S.; Wagman, A.; Ni, Z.-J.; Knapp, M.; Hendrickson, T.; Atallah, G.; Pfister, K.; Zhang, Y.; Bartulis, S.; Frazier, K.; Ng, S.; Smith, A.; Verhagen, J.; Haznedar, J.; Huh, K.; Iwanowicz, E.; Xin, X.; Menezes, D.; Merritt, H.; Lee, I.; Wiesmann, M.; Kaufman, S.; Crawford, K.; Chin, M.; Bussiere, D.; Shoemaker, K.; Zaror, I.; Maira, S.-M.; Voliva, C. F. Identification of NVP-BKM120 as a potent, selective, orally bioavailable class I PI3 kinase inhibitor for treating cancer. *ACS Med. Chem. Lett.* **2011**, *2*, 774−779.

(18) Samuels, Y.; Wang, Z.; Bardelli, A.; Silliman, N.; Ptak, J.; Szabo, S.; Yan, H.; Gazdar, A.; Powell, S. M.; Riggins, G. J.; Willson, J. K.; Markowitz, S.; Kinzler, K. W.; Vogelstein, B.; Velculescu, V. E. High frequency of mutations of the PIK3CA gene in human cancers. *Science* **2004**, *304*, 554.

(19) So, L.; Yea, S. S.; Oak, J. S.; Lu, M.; Manmadhan, A.; Ke, Q. H.; Janes, M. R.; Kessler, L. V.; Kucharski, J. M.; Li, L. S.; Martin, M. B.; Ren, P.; Jessen, K. A.; Liu, Y.; Rommel, C.; Fruman, D. A. Selective inhibition of phosphoinositide 3-kinase p110alpha preserves lymphocyte function. *J. Biol. Chem.* **2013**, *288*, 5718−5731.

(20) Fritsch, C.; Huang, A.; Chatenay-Rivauday, C.; Schnell, C.; Reddy, A.; Liu, M.; Kauffmann, A.; Guthy, D.; Erdmann, D.; De Pover, A.; Furet, P.; Gao, H.; Ferretti, S.; Wang, Y.; Trappe, J.; Brachmann, S. M.; Maira, S. M.; Wilson, C.; Boehm, M.; Garcia-Echeverria, C.; Chene, P.; Wiesmann, M.; Cozens, R.; Lehar, J.; Schlegel, R.; Caravatti, G.; Hofmann, F.; Sellers, W. R. Characterization of the novel and specific PI3Kalpha inhibitor NVP-BYL719 and development of the patient stratification strategy for clinical trials. *Mol. Cancer Ther.* **2014**, *13*, 1117−1129.

(21) Stark, A.-K.; Sriskantharajah, S.; Hessel, E. M.; Okkenhaug, K. PI3K inhibitors in inflammation, autoimmunity and cancer. *Curr. Opin. Pharmacol.* **2015**, *23*, 82−91.

(22) Jackson, S. P.; Schoenwaelder, S. M.; Goncalves, I.; Nesbitt, W. S.; Yap, C. L.; Wright, C. E.; Kenche, V.; Anderson, K. E.; Dopheide, S. M.; Yuan, Y.; Sturgeon, S. A.; Prabaharan, H.; Thompson, P. E.; Smith, G. D.; Shepherd, P. R.; Daniele, N.; Kulkarni, S.; Abbott, B.; Saylik, D.; Jones, C.; Lu, L.; Giuliano, S.; Hughan, S. C.; Angus, J. A.; Robertson, A. D.; Salem, H. H. PI 3-kinase p110[beta]: a new target for antithrombotic therapy. *Nat. Med.* **2005**, *11*, 507−514.

(23) Schoenwaelder, S. M.; Ono, A.; Nesbitt, W. S.; Lim, J.; Jarman, K.; Jackson, S. P. Phosphoinositide 3-kinase p110 beta regulates integrin alpha IIb beta 3 avidity and the cellular transmission of contractile forces. *J. Biol. Chem.* **2010**, *285*, 2886−2896.

(24) Nylander, S.; Kull, B.; BjÖRkman, J. A.; Ulvinge, J. C.; Oakes, N.; Emanuelsson, B. M.; Andersson, M.; SkÄRby, T.; Inghardt, T.; FjellstrÖM, O.; Gustafsson, D. Human target validation of phosphoinositide 3-kinase (PI3K)*β*: effects on platelets and insulin sensitivity, using AZD6482 a novel PI3K*β* inhibitor. *J. Thromb. Haemostasis* **2012**, *10*, 2127−2136.

(25) Jackson, S. P.; Schoenwaelder, S. M. Antithrombotic phosphoinositide 3-kinase *β* inhibitors in humans: a 'shear' delight! *J. Thromb. Haemostasis* **2012**, *10*, 2123−2126.

(26) Schwartz, S.; Wongvipat, J.; Trigwell, C. B.; Hancox, U.; Carver, B. S.; Rodrik-Outmezguine, V.; Will, M.; Yellen, P.; De stanchina, E.; Baselga, J.; Scher, H. I.; Barry, S. T.; Sawyers, C. L.; Chandarlapaty, S.; Rosen, N. Feedback suppression of PI3K*α* signaling in PTEN-mutated tumors is relieved by selective inhibition of PI3K*β*. *Cancer Cell* **2015**, *27*, 109−122.

(27) Hancox, U.; Cosulich, S.; Hanson, L.; Trigwell, C.; Lenaghan, C.; Ellston, R.; Dry, H.; Crafter, C.; Barlaam, B.; Fitzek, M.; Smith, P. D.; Ogilvie, D.; D'Cruz, C.; Castriotta, L.; Wedge, Sr.; Ward, L.; Powell, S.; Lawson, M.; Davies, B.; Harrington, E.; Foster, E.; Cumberbatch, M.; Green, S.; Barry, S. Inhibition of PI3K beta signaling with AZD8186 inhibits growth of PTEN-deficient breast and prostate tumors alone and in combination with docetaxel. *Mol. Cancer Ther.* **2015**, *14*, 48−58.

(28) Bergamini, G.; Bell, K.; Shimamura, S.; Werner, T.; Cansfield, A.; Müller, K.; Perrin, J.; Rau, C.; Ellard, K.; Hopf, C.; Doce, C.; Leggate, D.; Mangano, R.; Mathieson, T.; O'Mahony, A.; Plavec, I.; Rharbaoui, F.; Reinhard, F.; Savitski, M. M.; Ramsden, N.; Hirsch, E.; Drewes, G.; Rausch, O.; Bantscheff, M.; Neubauer, G. A selective inhibitor reveals PI3K*γ* dependence of TH17 cell differentiation. *Nat. Chem. Biol.* **2012**, *8*, 576−582.

(29) Jin, M.; Zhou, Q.; Lee, E.; Dan, S.; Duan, H. Q.; Kong, D. AS252424, a PI3K*γ* inhibitor, downregulates inflammatory responsiveness in mouse bone marrow-derived mast cells. *Inflammation* **2014**, *37*, 1254−1260.

(30) Huang, L.; Sherchan, P.; Wang, Y.; Reis, C.; Applegate, R. L., 2nd; Tang, J.; Zhang, J. H. Phosphoinositide 3-kinase gamma contributes to neuroinflammation in a rat model of surgical brain injury. *J. Neurosci.* **2015**, *35*, 10390−10401.

(31) Hamada, K.; Sasaki, T.; Koni, P. A.; Natsui, M.; Kishimoto, H.; Sasaki, J.; Yajima, N.; Horie, Y.; Hasegawa, G.; Naito, M.; Miyazaki, J.-I.; Suda, T.; Itoh, H.; Nakao, K.; Mak, T. W.; Nakano, T.; Suzuki, A. The PTEN/PI3K pathway governs normal vascular development and tumor angiogenesis. *Genes Dev.* **2005**, *19*, 2054−2065.

(32) Hickey, F. B.; Cotter, T. G. BCR-ABL regulates phosphatidylinositol 3-kinase-p110*γ* transcription and activation and is required for proliferation and drug resistance. *J. Biol. Chem.* **2006**, *281*, 2441−2450.

(33) Edling, C. E.; Selvaggi, F.; Buus, R.; Maffucci, T.; Di Sebastiano, P.; Friess, H.; Innocenti, P.; Kocher, H. M.; Falasca, M. Key role of phosphoinositide 3-kinase class IB in pancreatic cancer. *Clin. Cancer Res.* **2010**, *16*, 4928−4937.

(34) Dituri, F.; Mazzocca, A.; Lupo, L.; Edling, C.; Azzariti, A.; Antonaci, S.; Falasca, M.; Giannelli, G. PI3K class IB controls the cell cycle checkpoint promoting cell proliferation in hepatocellular carcinoma. *Int. J. Cancer* **2012**, *130*, 2505−2513.

(35) Falasca, M.; Maffucci, T. Targeting p110gamma in gastrointestinal cancers: attack on multiple fronts. *Front. Physiol.* **2014**, *5*, 1−9.

(36) Evans, C. A.; Liu, T.; Lescarbeau, A.; Nair, S. J.; Grenier, L.; Pradeilles, J. A.; Glenadel, Q.; Tibbitts, T.; Rowley, A. M.; Dinitto, J. P.; Brophy, E. E.; O'hearn, E. L.; Ali, J. A.; Winkler, D. G.; Goldstein, S. I.; O'hearn, P.; Martin, C. M.; Hoyt, J. G.; Soglia, J. R.; Cheung, C.; Pink, M. M.; Proctor, J. L.; Palombella, V. J.; Tremblay, M. R.; Castro, A. C. Discovery of a selective phosphoinositide-3-kinase (PI3K)-gamma inhibitor (IPI-549) as an immuno-oncology clinical candidate. *ACS Med. Chem. Lett.* **2016**, *7*, 862.

(37) Furman, R. R.; Sharman, J. P.; Coutre, S. E.; Cheson, B. D.; Pagel, J. M.; Hillmen, P.; Barrientos, J. C.; Zelenetz, A. D.; Kipps, T. J.; Flinn, I.; Ghia, P.; Eradat, H.; Ervin, T.; Lamanna, N.; Coiffier, B.; Pettitt, A. R.; Ma, S.; Stilgenbauer, S.; Cramer, P.; Aiello, M.; Johnson,

D. M.; Miller, L. L.; Li, D.; Jahn, T. M.; Dansey, R. D.; Hallek, M.; O'Brien, S. M. Idelalisib and rituximab in relapsed chronic lymphocytic leukemia. *N. Engl. J. Med.* **2014**, *370*, 997−1007.

(38) Mazza, S.; Maffucci, T. Class II phosphoinositide 3-kinase C2alpha: what we learned so far. *Int. J. Biochem. Mol. Biol.* **2011**, *2*, 168−182.

(39) Mountford, S. J.; Zheng, Z. H.; Sundaram, K.; Jennings, I. G.; Hamilton, J. R.; Thompson, P. E. Class II but not second class-prospects for the development of class II PI3K inhibitors. *ACS Med. Chem. Lett.* **2015**, *6*, 3−6.

(40) Campa, C. C.; Franco, I.; Hirsch, E. PI3K-C2alpha: One enzyme for two products coupling vesicle trafficking and signal transduction. *FEBS Lett.* **2015**, *589*, 1552−1558.

(41) Vanhaesebroeck, B.; Guillermet-Guibert, J.; Graupera, M.; Bilanges, B. The emerging mechanisms of isoform-specific PI3K signalling. *Nat. Rev. Mol. Cell Biol.* **2010**, *11*, 329−341.

(42) Domin, J.; Pages, F.; Volinia, S.; Rittenhouse, S. E.; Zvelebil, M. J.; Stein, R. C.; Waterfield, M. D. Cloning of a human phosphoinositide 3-kinase with a C2 domain that displays reduced sensitivity to the inhibitor wortmannin. *Biochem. J.* **1997**, *326* (1), 139−147.

(43) Ktori, C.; Shepherd, P. R.; O'Rourke, L. TNF-alpha and leptin activate the alpha-isoform of class II phosphoinositide 3-kinase. *Biochem. Biophys. Res. Commun.* **2003**, *306*, 139−143.

(44) Turner, S. J.; Domin, J.; Waterfield, M. D.; Ward, S. G.; Westwick, J. The CC chemokine monocyte chemotactic peptide-1 activates both the class I p85/p110 phosphatidylinositol 3-kinase and the class II PI3K-C2alpha. *J. Biol. Chem.* **1998**, *273*, 25987−25995.

(45) Brown, R. A.; Domin, J.; Arcaro, A.; Waterfield, M. D.; Shepherd, P. R. Insulin activates the alpha isoform of class II phosphoinositide 3-kinase. *J. Biol. Chem.* **1999**, *274*, 14529−14532.

(46) Arcaro, A.; Zvelebil, M. J.; Wallasch, C.; Ullrich, A.; Waterfield, M. D.; Domin, J. Class II phosphoinositide 3-kinases are downstream targets of activated polypeptide growth factor receptors. *Mol. Cell. Biol.* **2000**, *20*, 3817−3830.

(47) Knight, Z. A.; Gonzalez, B.; Feldman, M. E.; Zunder, E. R.; Goldenberg, D. D.; Williams, O.; Loewith, R.; Stokoe, D.; Balla, A.; Toth, B.; Balla, T.; Weiss, W. A.; Williams, R. L.; Shokat, K. M. A pharmacological map of the PI3-K family defines a role for p110alpha in insulin signaling. *Cell* **2006**, *125*, 733−747.

(48) Harris, D. P.; Vogel, P.; Wims, M.; Moberg, K.; Humphries, J.; Jhaver, K. G.; DaCosta, C. M.; Shadoan, M. K.; Xu, N.; Hansen, G. M.; Balakrishnan, S.; Domin, J.; Powell, D. R.; Oravecz, T. Requirement for class II phosphoinositide 3-kinase C2alpha in maintenance of glomerular structure and function. *Mol. Cell. Biol.* **2011**, *31*, 63−80.

(49) Yoshioka, K.; Yoshida, K.; Cui, H.; Wakayama, T.; Takuwa, N.; Okamoto, Y.; Du, W.; Qi, X.; Asanuma, K.; Sugihara, K.; Aki, S.; Miyazawa, H.; Biswas, K.; Nagakura, C.; Ueno, M.; Iseki, S.; Schwartz, R. J.; Okamoto, H.; Sasaki, T.; Matsui, O.; Asano, M.; Adams, R. H.; Takakura, N.; Takuwa, Y. Endothelial PI3K-C2alpha, a class II PI3K, has an essential role in angiogenesis and vascular barrier function. *Nat. Med.* **2012**, *18*, 1560−1569.

(50) Mountford, J. K.; Petitjean, C.; Putra, H. W.; McCafferty, J. A.; Setiabakti, N. M.; Lee, H.; Tonnesen, L. L.; McFadyen, J. D.; Schoenwaelder, S. M.; Eckly, A.; Gachet, C.; Ellis, S.; Voss, A. K.; Dickins, R. A.; Hamilton, J. R.; Jackson, S. P. The class II PI 3-kinase, PI3KC2alpha, links platelet internal membrane structure to shear-dependent adhesive function. *Nat. Commun.* **2015**, *6*, 6535.

(51) Franco, I.; Gulluni, F.; Campa, C. C.; Costa, C.; Margaria, J. P.; Ciraolo, E.; Martini, M.; Monteyne, D.; De Luca, E.; Germena, G.; Posor, Y.; Maffucci, T.; Marengo, S.; Haucke, V.; Falasca, M.; Perez-Morga, D.; Boletta, A.; Merlo, G. R.; Hirsch, E. PI3K class II alpha controls spatially restricted endosomal PtdIns3P and Rab11 activation to promote primary cilium function. *Dev. Cell* **2014**, *28*, 647−658.

(52) Valet, C.; Chicanne, G.; Severac, C.; Chaussade, C.; Whitehead, M. A.; Cabou, C.; Gratacap, M. P.; Gaits-Iacovoni, F.; Vanhaesebroeck, B.; Payrastre, B.; Severin, S. Essential role of class II PI3K-C2alpha in platelet membrane morphology. *Blood* **2015**, *126*, 1128−1137.

(53) Harada, K.; Truong, A. B.; Cai, T.; Khavari, P. A. The class II phosphoinositide 3-kinase C2β is not essential for epidermal differentiation. *Mol. Cell. Biol.* **2005**, *25*, 11122−11130.

(54) Alliouachene, S.; Bilanges, B.; Chicanne, G.; Anderson, K. E.; Pearce, W.; Ali, K.; Valet, C.; Posor, Y.; Low, P. C.; Chaussade, C.; Scudamore, C. L.; Salamon, R. S.; Backer, J. M.; Stephens, L.; Hawkins, P. T.; Payrastre, B.; Vanhaesebroeck, B. Inactivation of the class II PI3K-C2beta potentiates insulin signaling and sensitivity. *Cell Rep.* **2015**, *13*, 1881−1894.

(55) Braccini, L.; Ciraolo, E.; Campa, C. C.; Perino, A.; Longo, D. L.; Tibolla, G.; Pregnolato, M.; Cao, Y.; Tassone, B.; Damilano, F.; Laffargue, M.; Calautti, E.; Falasca, M.; Norata, G. D.; Backer, J. M.; Hirsch, E. PI3K-C2gamma is a Rab5 effector selectively controlling endosomal Akt2 activation downstream of insulin signalling. *Nat. Commun.* **2015**, *6*, 7400.

(56) Maffucci, T.; Brancaccio, A.; Piccolo, E.; Stein, R. C.; Falasca, M. Insulin induces phosphatidylinositol-3-phosphate formation through TC10 activation. *EMBO J.* **2003**, *22*, 4178−4189.

(57) Falasca, M.; Hughes, W. E.; Dominguez, V.; Sala, G.; Fostira, F.; Fang, M. Q.; Cazzolli, R.; Shepherd, P. R.; James, D. E.; Maffucci, T. Role of phosphoinositide 3-kinase C2α in insulin signaling. *J. Biol. Chem.* **2007**, *282*, 28226−28236.

(58) Dominguez, V.; Raimondi, C.; Somanath, S.; Bugliani, M.; Loder, M. K.; Edling, C. E.; Divecha, N.; da Silva-Xavier, G.; Marselli, L.; Persaud, S. J.; Turner, M. D.; Rutter, G. A.; Marchetti, P.; Falasca, M.; Maffucci, T. Class II phosphoinositide 3-kinase regulates exocytosis of insulin granules in pancreatic β cells. *J. Biol. Chem.* **2011**, *286*, 4216−4225.

(59) Leibiger, B.; Moede, T.; Uhles, S.; Barker, C. J.; Creveaux, M.; Domin, J.; Berggren, P.-O.; Leibiger, I. B. Insulin-feedback via PI3K-C2α activated PKBα/Akt1 is required for glucose-stimulated insulin secretion. *FASEB J.* **2010**, *24*, 1824−1837.

(60) Leibiger, B.; Moede, T.; Paschen, M.; Yunn, N.-O.; Lim, H. H.; Ryu, S. H.; Pereira, T.; Berggren, P.-O.; Leibiger, I. B. PI3K-C2α knockdown results in rerouting of insulin signaling and pancreatic beta cell proliferation. *Cell Rep.* **2015**, *13*, 15−22.

(61) Alliouachene, S.; Bilanges, B.; Chaussade, C.; Pearce, W.; Foukas, L. C.; Scudamore, C. L.; Moniz, L. S.; Vanhaesebroeck, B. Inactivation of class II PI3K-C2alpha induces leptin resistance, age-dependent insulin resistance and obesity in male mice. *Diabetologia* **2016**, *59*, 1503−1512.

(62) Liu, T.; Li, H.; Ding, G.; Wang, Z.; Chen, Y.; Liu, L.; Li, Y. Comparative genome of GK and Wistar rats reveals genetic basis of type 2 diabetes. *PLoS One* **2015**, *10*, e0141859.

(63) Yuan, T. L.; Cantley, L. C. PI3K pathway alterations in cancer: variations on a theme. *Oncogene* **2008**, *27*, 5497−5510.

(64) Courtney, K. D.; Corcoran, R. B.; Engelman, J. A. The PI3K pathway as drug target in human cancer. *J. Clin. Oncol.* **2010**, *28*, 1075−1083.

(65) Wong, K. K.; Engelman, J. A.; Cantley, L. C. Targeting the PI3K signaling pathway in cancer. *Curr. Opin. Genet. Dev.* **2010**, *20*, 87−90.

(66) Weir, B.; Zhao, X.; Meyerson, M. Somatic alterations in the human cancer genome. *Cancer Cell* **2004**, *6*, 433−438.

(67) Guerreiro, A. S.; Fattet, S.; Fischer, B.; Shalaby, T.; Jackson, S. P.; Schoenwaelder, S. M.; Grotzer, M. A.; Delattre, O.; Arcaro, A. Targeting the PI3K p110α isoform inhibits medulloblastoma proliferation, chemoresistance, and migration. *Clin. Cancer Res.* **2008**, *14*, 6761−6769.

(68) Broderick, D. K.; Di, C.; Parrett, T. J.; Samuels, Y. R.; Cummins, J. M.; McLendon, R. E.; Fults, D. W.; Velculescu, V. E.; Bigner, D. D.; Yan, H. Mutations of PIK3CA in anaplastic oligodendrogliomas, high-grade astrocytomas, and medulloblastomas. *Cancer Res.* **2004**, *64*, 5048−5050.

(69) Ng, S. K. L.; Neo, S.-Y.; Yap, Y.-W.; Karuturi, R. K. M.; Loh, E. S. L.; Liau, K.-H.; Ren, E.-C. Ablation of phosphoinositide-3-kinase class II alpha suppresses hepatoma cell proliferation. *Biochem. Biophys. Res. Commun.* **2009**, *387*, 310−315.

(70) Elis, W.; Triantafellow, E.; Wolters, N. M.; Sian, K. R.; Caponigro, G.; Borawski, J.; Gaither, L. A.; Murphy, L. O.; Finan, P.

M.; Mackeigan, J. P. Down-regulation of class II phosphoinositide 3-kinase alpha expression below a critical threshold induces apoptotic cell death. *Mol. Cancer Res.* **2008**, *6*, 614−623.

(71) Zhou, J.; Wulfkuhle, J.; Zhang, H.; Gu, P.; Yang, Y.; Deng, J.; Margolick, J. B.; Liotta, L. A.; Petricoin, E., 3rd; Zhang, Y. Activation of the PTEN/mTOR/STAT3 pathway in breast cancer stem-like cells is required for viability and maintenance. *Proc. Natl. Acad. Sci. U. S. A.* **2007**, *104*, 16158−16163.

(72) Schepeler, T.; Holm, A.; Halvey, P.; Nordentoft, I.; Lamy, P.; Riising, E. M.; Christensen, L. L.; Thorsen, K.; Liebler, D. C.; Helin, K.; Orntoft, T. F.; Andersen, C. L. Attenuation of the beta-catenin/TCF4 complex in colorectal cancer cells induces several growth-suppressive microRNAs that target cancer promoting genes. *Oncogene* **2012**, *31*, 2750−2760.

(73) Nigorikawa, K.; Hazeki, K.; Guo, Y.; Hazeki, O. Involvement of class II phosphoinositide 3-kinase alpha-isoform in antigen-induced degranulation in RBL-2H3 cells. *PLoS One* **2014**, *9*, e111698.

(74) Petitjean, C.; Setiabakti, N. M.; Mountford, J. K.; Arthur, J. F.; Ellis, S.; Hamilton, J. R. Combined deficiency of PI3KC2alpha and PI3KC2beta reveals a nonredundant role for PI3KC2alpha in regulating mouse platelet structure and thrombus stability. *Platelets* **2016**, *27*, 402−409.

(75) Fyffe, C.; Buus, R.; Falasca, M. Genetic and epigenetic regulation of phosphoinositide 3-kinase isoforms. *Curr. Pharm. Des.* **2013**, *19*, 680−686.

(76) Rao, S. K.; Edwards, J.; Joshi, A. D.; Siu, I. M.; Riggins, G. J. A survey of glioblastoma genomic amplifications and deletions. *J. Neuro-Oncol.* **2010**, *96*, 169−179.

(77) Nobusawa, S.; Lachuer, J.; Wierinckx, A.; Kim, Y. H.; Huang, J.; Legras, C.; Kleihues, P.; Ohgaki, H. Intratumoral patterns of genomic imbalance in glioblastomas. *Brain Pathol.* **2010**, *20*, 936−944.

(78) Zhang, L.; Huang, J.; Yang, N.; Greshock, J.; Liang, S.; Hasegawa, K.; Giannakakis, A.; Poulos, N.; O'Brien-Jenkins, A.; Katsaros, D.; Butzow, R.; Weber, B. L.; Coukos, G. Integrative genomic analysis of phosphatidylinositol 3′-kinase family identifies PIK3R3 as a potential therapeutic target in epithelial ovarian cancer. *Clin. Cancer Res.* **2007**, *13*, 5314−5321.

(79) Talagas, M.; Marcorelles, P.; Uguen, A.; Redon, S.; Quintin-Roue, I.; Costa, S.; Ferec, C.; Morel, F.; Hieu, P. D.; De Braekeleer, M. Identification of a novel population in high-grade oligodendroglial tumors not deleted on 1p/19q using array CGH. *J. Neuro-Oncol.* **2012**, *109*, 405−513.

(80) Qian, Z.; Fernald, A. A.; Godley, L. A.; Larson, R. A.; Le Beau, M. M. Expression profiling of CD34+ hematopoietic stem/ progenitor cells reveals distinct subtypes of therapy-related acute myeloid leukemia. *Proc. Natl. Acad. Sci. U. S. A.* **2002**, *99*, 14925−14930.

(81) Chiaretti, S.; Li, X.; Gentleman, R.; Vitale, A.; Wang, K. S.; Mandelli, F.; Foa, R.; Ritz, J. Gene expression profiles of B-lineage adult acute lymphocytic leukemia reveal genetic patterns that identify lineage derivation and distinct mechanisms of transformation. *Clin. Cancer Res.* **2005**, *11*, 7209−7219.

(82) Boller, D.; Doepfner, K. T.; De Laurentiis, A.; Guerreiro, A. S.; Marinov, M.; Shalaby, T.; Depledge, P.; Robson, A.; Saghir, N.; Hayakawa, M.; Kaizawa, H.; Koizumi, T.; Ohishi, T.; Fattet, S.; Delattre, O.; Schweri-Olac, A.; Holand, K.; Grotzer, M. A.; Frei, K.; Spertini, O.; Waterfield, M. D.; Arcaro, A. Targeting PI3KC2beta impairs proliferation and survival in acute leukemia, brain tumours and neuroendocrine tumours. *Anticancer Res.* **2012**, *32*, 3015−3027.

(83) Knobbe, C. B.; Reifenberger, G. Genetic alterations and aberrant expression of genes related to the phosphatidyl-inositol-3′-kinase/protein kinase B (Akt) signal transduction pathway in glioblastomas. *Brain Pathol.* **2003**, *13*, 507−518.

(84) Liu, P.; Morrison, C.; Wang, L.; Xiong, D.; Vedell, P.; Cui, P.; Hua, X.; Ding, F.; Lu, Y.; James, M.; Ebben, J. D.; Xu, H.; Adjei, A. A.; Head, K.; Andrae, J. W.; Tschannen, M. R.; Jacob, H.; Pan, J.; Zhang, Q.; Van den Bergh, F.; Xiao, H.; Lo, K. C.; Patel, J.; Richmond, T.; Watt, M. A.; Albert, T.; Selzer, R.; Anderson, M.; Wang, J.; Wang, Y.; Starnes, S.; Yang, P.; You, M. Identification of somatic mutations in

non-small cell lung carcinomas using whole-exome sequencing. *Carcinogenesis* **2012**, *33*, 1270−1276.

(85) Arcaro, A.; Khanzada, U. K.; Vanhaesebroeck, B.; Tetley, T. D.; Waterfield, M. D.; Seckl, M. J. Two distinct phosphoinositide 3-kinases mediate polypeptide growth factor-stimulated PKB activation. *EMBO J.* **2002**, *21*, 5097−5108.

(86) Russo, A.; Okur, M. N.; Bosland, M.; O'Bryan, J. P. Phosphatidylinositol 3-kinase, class 2 beta (PI3KC2beta) isoform contributes to neuroblastoma tumorigenesis. *Cancer Lett.* **2015**, *359*, 262−268.

(87) Russo, A.; O'Bryan, J. P. Intersectin 1 is required for neuroblastoma tumorigenesis. *Oncogene* **2012**, *31*, 4828−4834.

(88) Chesler, L.; Schlieve, C.; Goldenberg, D. D.; Kenney, A.; Kim, G.; McMillan, A.; Matthay, K. K.; Rowitch, D.; Weiss, W. A. Inhibition of phosphatidylinositol 3-kinase destabilizes Mycn protein and blocks malignant progression in neuroblastoma. *Cancer Res.* **2006**, *66*, 8139−8146.

(89) Marone, R.; Cmiljanovic, V.; Giese, B.; Wymann, M. P. Targeting phosphoinositide 3-kinase: moving towards therapy. *Biochim. Biophys. Acta, Proteins Proteomics* **2008**, *1784*, 159−185.

(90) Ma, Y.; Wang, B.; Li, W.; Liu, X.; Wang, J.; Ding, T.; Zhang, J.; Ying, G.; Fu, L.; Gu, F. Intersectin1-s is involved in migration and invasion of human glioma cells. *J. Neurosci. Res.* **2011**, *89*, 1079−1090.

(91) Koutros, S.; Schumacher, F. R.; Hayes, R. B.; Ma, J.; Huang, W. Y.; Albanes, D.; Canzian, F.; Chanock, S. J.; Crawford, E. D.; Diver, W. R.; Feigelson, H. S.; Giovanucci, E.; Haiman, C. A.; Henderson, B. E.; Hunter, D. J.; Kaaks, R.; Kolonel, L. N.; Kraft, P.; Le Marchand, L.; Riboli, E.; Siddiq, A.; Stampfer, M. J.; Stram, D. O.; Thomas, G.; Travis, R. C.; Thun, M. J.; Yeager, M.; Berndt, S. I. Pooled analysis of phosphatidylinositol 3-kinase pathway variants and risk of prostate cancer. *Cancer Res.* **2010**, *70*, 2389−2396.

(92) Sato, N.; Fukushima, N.; Maitra, A.; Iacobuzio-Donahue, C. A.; van Heek, N. T.; Cameron, J. L.; Yeo, C. J.; Hruban, R. H.; Goggins, M. Gene expression profiling identifies genes associated with invasive intraductal papillary mucinous neoplasms of the pancreas. *Am. J. Pathol.* **2004**, *164*, 903−914.

(93) Marras, E.; Concari, P.; Cortellezzi, L.; Dondi, D.; De Eguileor, M.; Perletti, G. Involvement of PI3K in PKCepsilon-mediated oncogenic signal in rat colonic epithelial cells. *Int. J. Oncol.* **2001**, *19*, 395−399.

(94) Liu, Z.; Sun, C.; Zhang, Y.; Ji, Z.; Yang, G. Phosphatidylinositol 3-kinase-C2beta inhibits cisplatin-mediated apoptosis via the Akt pathway in oesophageal squamous cell carcinoma. *J. Int. Med. Res.* **2011**, *39*, 1319−1332.

(95) Waugh, M. G. Amplification of chromosome 1q genes encoding the phosphoinositide signalling enzymes PI4KB, AKT3, PIP5K1A and PI3KC2B in breast cancer. *J. Cancer* **2014**, *5*, 790−796.

(96) Chen, L. C.; Dollbaum, C.; Smith, H. S. Loss of heterozygosity on chromosome 1q in human breast cancer. *Proc. Natl. Acad. Sci. U. S. A.* **1989**, *86*, 7204−7207.

(97) Cruciger, Q. V.; Pathak, S.; Cailleau, R. Human breast carcinomas: marker chromosomes involving 1q in seven cases. *Cytogenet. Genome Res.* **1976**, *17*, 231−235.

(98) Orsetti, B.; Nugoli, M.; Cervera, N.; Lasorsa, L.; Chuchana, P.; Rougé, C.; Ursule, L.; Nguyen, C.; Bibeau, F.; Rodriguez, C.; Theillet, C. Genetic profiling of chromosome 1 in breast cancer: mapping of regions of gains and losses and identification of candidate genes on 1q. *Br. J. Cancer* **2006**, *95*, 1439−1447.

(99) Chikh, A.; Ferro, R.; Abbott, J.; Pineiro, R.; Buus, R.; Iezzi, M.; Ricci, F.; Bergamaschi, D.; Ostano, P.; Chiorino, G.; Lattanzio, R.; Broggini, M.; Piantelli, M.; Maffucci, T.; Falasca, M. Class II phosphoinositide 3-kinase C2 beta regulates a novel signaling pathway involved in breast cancer progression. *Oncotarget* **2016**, *7*, 18325−18345.

(100) Kawamoto, H.; Koizumi, H.; Uchikoshi, T. Expression of the G2-M checkpoint regulators cyclin B1 and cdc2 in nonmalignant and malignant human breast lesions: immunocytochemical and quantitative image analyses. *Am. J. Pathol.* **1997**, *150*, 15−23.

(101) Enerly, E.; Steinfeld, I.; Kleivi, K.; Leivonen, S. K.; Aure, M. R.; Russnes, H. G.; Ronneberg, J. A.; Johnsen, H.; Navon, R.; Rodland, E.; Makela, R.; Naume, B.; Perala, M.; Kallioniemi, O.; Kristensen, V. N.; Yakhini, Z.; Borresen-Dale, A. L. miRNA-mRNA integrated analysis reveals roles for miRNAs in primary breast tumors. *PLoS One* **2011**, *6*, e16915.

(102) Agarwal, R.; Gonzalez-Angulo, A. M.; Myhre, S.; Carey, M.; Lee, J. S.; Overgaard, J.; Alsner, J.; Stemke-Hale, K.; Lluch, A.; Neve, R. M.; Kuo, W. L.; Sorlie, T.; Sahin, A.; Valero, V.; Keyomarsi, K.; Gray, J. W.; Borresen-Dale, A. L.; Mills, G. B.; Hennessy, B. T. Integrative analysis of cyclin protein levels identifies cyclin b1 as a classifier and predictor of outcomes in breast cancer. *Clin. Cancer Res.* **2009**, *15*, 3654−3662.

(103) Nimeus-Malmstrom, E.; Koliadi, A.; Ahlin, C.; Holmqvist, M.; Holmberg, L.; Amini, R. M.; Jirstrom, K.; Warnberg, F.; Blomqvist, C.; Ferno, M.; Fjallskog, M. L. Cyclin B1 is a prognostic proliferation marker with a high reproducibility in a population-based lymph node negative breast cancer cohort. *Int. J. Cancer* **2010**, *127*, 961−967.

(104) Mavrommati, I.; Cisse, O.; Falasca, M.; Maffucci, T. Novel roles for class II phosphoinositide 3-kinase C2β in signalling pathways involved in prostate cancer cell invasion. *Sci. Rep.* **2016**, *6*, 23277.

(105) Taylor, B. S.; Schultz, N.; Hieronymus, H.; Gopalan, A.; Xiao, Y.; Carver, B. S.; Arora, V. K.; Kaushik, P.; Cerami, E.; Reva, B.; Antipin, Y.; Mitsiades, N.; Landers, T.; Dolgalev, I.; Major, J. E.; Wilson, M.; Socci, N. D.; Lash, A. E.; Heguy, A.; Eastham, J. A.; Scher, H. I.; Reuter, V. E.; Scardino, P. T.; Sander, C.; Sawyers, C. L.; Gerald, W. L. Integrative genomic profiling of human prostate cancer. *Cancer Cell* **2010**, *18*, 11−22.

(106) Wang, S.; Gao, J.; Lei, Q.; Rozengurt, N.; Pritchard, C.; Jiao, J.; Thomas, G. V.; Li, G.; Roy-Burman, P.; Nelson, P. S.; Liu, X.; Wu, H. Prostate-specific deletion of the murine Pten tumor suppressor gene leads to metastatic prostate cancer. *Cancer Cell* **2003**, *4*, 209−221.

(107) Sansal, I.; Sellers, W. R. The biology and clinical relevance of the PTEN tumor suppressor pathway. *J. Clin. Oncol.* **2004**, *22*, 2954−2963.

(108) Thiery, J. P. Epithelial-mesenchymal transitions in tumour progression. *Nat. Rev. Cancer* **2002**, *2*, 442−454.

(109) Gos, M.; Miloszewska, J.; Przybyszewska, M. [Epithelial-mesenchymal transition in cancer progression]. *Postepy Biochem.* **2009**, *55*, 121−128.

(110) Emadi Baygi, M.; Soheili, Z. S.; Essmann, F.; Deezagi, A.; Engers, R.; Goering, W.; Schulz, W. A. Slug/SNAI2 regulates cell proliferation and invasiveness of metastatic prostate cancer cell lines. *Tumor Biol.* **2010**, *31*, 297−307.

(111) Uygur, B.; Wu, W. S. SLUG promotes prostate cancer cell migration and invasion via CXCR4/CXCL12 axis. *Mol. Cancer* **2011**, *10*, 139.

(112) Maffucci, T.; Cooke, F. T.; Foster, F. M.; Traer, C. J.; Fry, M. J.; Falasca, M. Class II phosphoinositide 3-kinase defines a novel signaling pathway in cell migration. *J. Cell Biol.* **2005**, *169*, 789−799.

(113) Katso, R. M.; Pardo, O. E.; Palamidessi, A.; Franz, C. M.; Marinov, M.; De Laurentiis, A.; Downward, J.; Scita, G.; Ridley, A. J.; Waterfield, M. D.; Arcaro, A. Phosphoinositide 3-Kinase C2beta regulates cytoskeletal organization and cell migration via Rac-dependent mechanisms. *Mol. Biol. Cell* **2006**, *17*, 3729−3744.

(114) Domin, J.; Harper, L.; Aubyn, D.; Wheeler, M.; Florey, O.; Haskard, D.; Yuan, M.; Zicha, D. The class II phosphoinositide 3-kinase PI3K-C2beta regulates cell migration by a PtdIns3P dependent mechanism. *J. Cell. Physiol.* **2005**, *205*, 452−462.

(115) Kitatani, K.; Usui, T.; Sriraman, S. K.; Toyoshima, M.; Ishibashi, M.; Shigeta, S.; Nagase, S.; Sakamoto, M.; Ogiso, H.; Okazaki, T.; Hannun, Y. A.; Torchilin, V. P.; Yaegashi, N. Ceramide limits phosphatidylinositol-3-kinase C2beta-controlled cell motility in ovarian cancer: potential of ceramide as a metastasis-suppressor lipid. *Oncogene* **2015**, *21*, 1801−1812.

(116) van Leeuwen, F. N.; Giepmans, B. N.; van Meeteren, L. A.; Moolenaar, W. H. Lysophosphatidic acid: mitogen and motility factor. *Biochem. Soc. Trans.* **2003**, *31*, 1209−1212.

(117) Yamada, T.; Sato, K.; Komachi, M.; Malchinkhuu, E.; Tobo, M.; Kimura, T.; Kuwabara, A.; Yanagita, Y.; Ikeya, T.; Tanahashi, Y.; Ogawa, T.; Ohwada, S.; Morishita, Y.; Ohta, H.; Im, D. S.; Tamoto, K.; Tomura, H.; Okajima, F. Lysophosphatidic acid (LPA) in malignant ascites stimulates motility of human pancreatic cancer cells through LPA1. *J. Biol. Chem.* **2004**, *279*, 6595−6605.

(118) Stahle, M.; Veit, C.; Bachfischer, U.; Schierling, K.; Skripczynski, B.; Hall, A.; Gierschik, P.; Giehl, K. Mechanisms in LPA-induced tumor cell migration: critical role of phosphorylated ERK. *J. Cell Sci.* **2003**, *116*, 3835−3846.

(119) Pardo, O. E.; Castellano, L.; Munro, C. E.; Hu, Y.; Mauri, F.; Krell, J.; Lara, R.; Pinho, F. G.; Choudhury, T.; Frampton, A. E.; Pellegrino, L.; Pshezhetskiy, D.; Wang, Y.; Waxman, J.; Seckl, M. J.; Stebbing, J. miR-515−5p controls cancer cell migration through MARK4 regulation. *EMBO Rep.* **2016**, *17*, 570−584.

(120) Low, S.; Vougioukas, V. I.; Hielscher, T.; Schmidt, U.; Unterberg, A.; Halatsch, M. E. Pathogenetic pathways leading to glioblastoma multiforme: association between gene expressions and resistance to erlotinib. *Anticancer Res.* **2008**, *28*, 3729−3732.

(121) Iorns, E.; Lord, C. J.; Ashworth, A. Parallel RNAi and compound screens identify the PDK1 pathway as a target for tamoxifen sensitization. *Biochem. J.* **2009**, *417*, 361−370.

(122) Diouf, B.; Cheng, Q.; Krynetskaia, N. F.; Yang, W.; Cheok, M.; Pei, D.; Fan, Y.; Cheng, C.; Krynetskiy, E. Y.; Geng, H.; Chen, S.; Thierfelder, W. E.; Mullighan, C. G.; Downing, J. R.; Hsieh, P.; Pui, C. H.; Relling, M. V.; Evans, W. E. Somatic deletions of genes regulating MSH2 protein stability cause DNA mismatch repair deficiency and drug resistance in human leukemia cells. *Nat. Med.* **2011**, *17*, 1298−1303.

(123) Blajecka, K.; Marinov, M.; Leitner, L.; Uth, K.; Posern, G.; Arcaro, A. Phosphoinositide 3-kinase C2beta regulates RhoA and the actin cytoskeleton through an interaction with Dbl. *PLoS One* **2012**, *7*, e44945.

(124) Tibolla, G.; Piñeiro, R.; Chiozzotto, D.; Mavrommati, I.; Wheeler, A.; Norata, G.; Catapano, A.; Maffucci, T.; Falasca, M. Class II phosphoinositide 3-kinases contribute to endothelial cells morphogenesis. *PLoS One* **2013**, *8*, e53808.

(125) Rozycka, M.; Lu, Y. J.; Brown, R. A.; Lau, M. R.; Shipley, J. M.; Fry, M. J. cDNA cloning of a third human C2-domain-containing class II phosphoinositide 3-kinase, PI3K-C2gamma, and chromosomal assignment of this gene (PIK3C2G) to 12p12. *Genomics* **1998**, *54*, 569−574.

(126) Ono, F.; Nakagawa, T.; Saito, S.; Owada, Y.; Sakagami, H.; Goto, K.; Suzuki, M.; Matsuno, S.; Kondo, H. A novel class II phosphoinositide 3-kinase predominantly expressed in the liver and its enhanced expression during liver regeneration. *J. Biol. Chem.* **1998**, *273*, 7731−7736.

(127) Braccini, L.; Ciraolo, E.; Campa, C. C.; Perino, A.; Longo, D. L.; Tibolla, G.; Pregnolato, M.; Cao, Y.; Tassone, B.; Damilano, F.; Laffargue, M.; Calautti, E.; Falasca, M.; Norata, G. D.; Backer, J. M.; Hirsch, E. PI3K-C2[gamma] is a Rab5 effector selectively controlling endosomal Akt2 activation downstream of insulin signalling. *Nat. Commun.* **2015**, *6*, 7400.

(128) Daimon, M.; Sato, H.; Oizumi, T.; Toriyama, S.; Saito, T.; Karasawa, S.; Jimbu, Y.; Wada, K.; Kameda, W.; Susa, S.; Yamaguchi, H.; Emi, M.; Muramatsu, M.; Kubota, I.; Kawata, S.; Kato, T. Association of the PIK3C2G gene polymorphisms with type 2 DM in a Japanese population. *Biochem. Biophys. Res. Commun.* **2008**, *365*, 466−471.

(129) Li, A.; Chen, H.; Lin, M.; Zhang, C.; Tang, E.; Peng, J.; Wei, Q.; Li, H.; Yin, L. PIK3C2G copy number is associated with clinical outcomes of colorectal cancer patients treated with oxaliplatin. *Int. J. Clin. Exp. Med.* **2015**, *8*, 1137−1143.

(130) Williams, R.; Berndt, A.; Miller, S.; Hon, W. C.; Zhang, X. X. Form and flexibility in phosphoinositide 3-kinases. *Biochem. Soc. Trans.* **2009**, *37*, 615−626.

(131) Yang, H. J.; Rudge, D. G.; Koos, J. D.; Vaidialingam, B.; Yang, H. J.; Pavletich, N. P. mTOR kinase structure, mechanism and regulation. *Nature* **2013**, *497*, 217−223.

(132) Pasquier, B.; El-Ahmad, Y.; Filoche-Romme, B.; Dureuil, C.; Fassy, F.; Abecassis, P. Y.; Mathieu, M.; Bertrand, T.; Benard, T.; Barriere, C.; El Batti, S.; Letallec, J. P.; Sonnefraud, V.; Brollo, M.; Delbarre, L.; Loyau, V.; Pilorge, F.; Bertin, L.; Richepin, P.; Arigon, J.; Labrosse, J. R.; Clement, J.; Durand, F.; Combet, R.; Perraut, P.; Leroy, V.; Gay, F.; Lefrancois, D.; Bretin, F.; Marquette, J. P.; Michot, N.; Caron, A.; Castell, C.; Schio, L.; McCort, G.; Goulaouic, H.; Garcia-Echeverria, C.; Ronan, B. Discovery of (2S)-8[(3R)-3-methylmorpholin-4-yl]-1-(3-methyl-2-oxobutyl)-2-(trifluoromethyl)-3,4-dihydro-2H-pyrimido[1,2-a]pyrimidin-6-one: a novel potent and selective inhibitor of Vps34 for the treatment of solid tumors. *J. Med. Chem.* **2015**, *58*, 376−400.

(133) Berndt, A.; Miller, S.; Williams, O.; Le, D. D.; Houseman, B. T.; Pacold, J. I.; Gorrec, F.; Hon, W. C.; Liu, Y.; Rommel, C.; Gaillard, P.; Ruckle, T.; Schwarz, M. K.; Shokat, K. M.; Shaw, J. P.; Williams, R. L. The p110 delta structure: mechanisms for selectivity and potency of new PI(3)K inhibitors. *Nat. Chem. Biol.* **2010**, *6*, 117−124.

(134) Dowdle, W. E.; Nyfeler, B.; Nagel, J.; Elling, R. A.; Liu, S. M.; Triantafellow, E.; Menon, S.; Wang, Z. C.; Honda, A.; Pardee, G.; Cantwell, J.; Luu, C.; Cornella-Taracido, I.; Harrington, E.; Fekkes, P.; Lei, H.; Fang, Q.; Digan, M. E.; Burdick, D.; Powers, A. F.; Helliwell, S. B.; D'Aquin, S.; Bastien, J.; Wang, H.; Wiederschain, D.; Kuerth, J.; Bergman, P.; Schwalb, D.; Thomas, J.; Ugwonali, S.; Harbinski, F.; Tallarico, J.; Wilson, C. J.; Myer, V. E.; Porter, J. A.; Bussiere, D. E.; Finan, P. M.; Labow, M. A.; Mao, X. H.; Hamann, L. G.; Manning, B. D.; Valdez, R. A.; Nicholson, T.; Schirle, M.; Knapp, M. S.; Keaney, E. P.; Murphy, L. O. Selective VPS34 inhibitor blocks autophagy and uncovers a role for NCOA4 in ferritin degradation and iron homeostasis in vivo. *Nat. Cell Biol.* **2014**, *16*, 1069−1079.

(135) Fabbro, D.; Cowan-Jacob, S. W.; Moebitz, H. Ten things you should know about protein kinases: IUPHAR Review 14. *Br. J. Pharmacol.* **2015**, *172*, 2675−2700.

(136) Walker, E. H.; Pacold, M. E.; Perisic, O.; Stephens, L.; Hawkins, P. T.; Wymann, M. P.; Williams, R. L. Structural determinants of phosphoinositide 3-kinase inhibition by wortmannin, LY294002, quercetin, myricetin, and staurosporine. *Mol. Cell* **2000**, *6*, 909−919.

(137) Pirola, L.; Zvelebil, M. J.; Bulgarelli-Leva, G.; Van Obberghen, E.; Waterfield, M. D.; Wymann, M. P. Activation loop sequences confer substrate specificity to phosphoinositide 3-kinase alpha (PI3Kalpha). Functions of lipid kinase-deficient PI3Kalpha in signaling. *J. Biol. Chem.* **2001**, *276*, 21544−21554.

(138) Miller, M. S.; Schmidt-Kittler, O.; Bolduc, D. M.; Brower, E. T.; Chaves-Moreira, D.; Allaire, M.; Kinzler, K. W.; Jennings, I. G.; Thompson, P. E.; Cole, P. A.; Amzel, L. M.; Vogelstein, B.; Gabelli, S. B. Structural basis of nSH2 regulation and lipid binding in PI3Kalpha. *Oncotarget* **2014**, *5*, 5198−5208.

(139) Miller, S.; Tavshanjian, B.; Oleksy, A.; Perisic, O.; Houseman, B. T.; Shokat, K. M.; Williams, R. L. Shaping development of autophagy inhibitors with the structure of the lipid kinase Vps34. *Science* **2010**, *327*, 1638−1642.

(140) Walker, E. H.; Perisic, O.; Ried, C.; Stephens, L.; Williams, R. L. Structural insights into phosphoinositide 3-kinase catalysis and signalling. *Nature* **1999**, *402*, 313−320.

(141) Zhao, Y. L.; Zhang, X.; Chen, Y. Y.; Lu, S. Y.; Peng, Y. F.; Wang, X.; Guo, C. L.; Zhou, A. W.; Zhang, J. M.; Luo, Y.; Shen, Q. C.; Ding, J.; Meng, L. H.; Zhang, J. Crystal structures of PI3K alpha complexed with PI103 and its derivatives: new directions for inhibitors design. *ACS Med. Chem. Lett.* **2014**, *5*, 138−142.

(142) Furet, P.; Guagnano, V.; Fairhurst, R. A.; Imbach-Weese, P.; Bruce, I.; Knapp, M.; Fritsch, C.; Blasco, F.; Blanz, J.; Aichholz, R.; Hamon, J.; Fabbro, D.; Caravatti, G. Discovery of NVP-BYL719 a potent and selective phosphatidylinositol-3 kinase alpha inhibitor selected for clinical evaluation. *Bioorg. Med. Chem. Lett.* **2013**, *23*, 3741−3748.

(143) Zheng, Z.; Amran, S. I.; Zhu, J.; Schmidt-Kittler, O.; Kinzler, K. W.; Vogelstein, B.; Shepherd, P. R.; Thompson, P. E.; Jennings, I. G. Definition of the binding mode of a new class of phosphoinositide 3-kinase alpha-selective inhibitors using in vitro mutagenesis of non-

conserved amino acids and kinetic analysis. *Biochem. J.* **2012**, *444*, 529−535.

(144) Jamieson, S.; Flanagan, J. U.; Kolekar, S.; Buchanan, C.; Kendall, J. D.; Lee, W. J.; Rewcastle, G. W.; Denny, W. A.; Singh, R.; Dickson, J.; Baguley, B. C.; Shepherd, P. R. A drug targeting only p110 alpha can block phosphoinositide 3-kinase signalling and tumour growth in certain cell types. *Biochem. J.* **2011**, *438*, 53−62.

(145) Sutherlin, D. P.; Baker, S.; Bisconte, A.; Blaney, P. M.; Brown, A.; Chan, B. K.; Chantry, D.; Castanedo, G.; DePledge, P.; Goldsmith, P.; Goldstein, D. M.; Hancox, T.; Kaur, J.; Knowles, D.; Kondru, R.; Lesnick, J.; Lucas, M. C.; Lewis, C.; Murray, J.; Nadin, A. J.; Nonomiya, J.; Pang, J. D.; Pegg, N.; Price, S.; Reif, K.; Safina, B. S.; Salphati, L.; Staben, S.; Seward, E. M.; Shuttleworth, S.; Sohal, S.; Sweeney, Z. K.; Ultsch, M.; Waszkowycz, B.; Wei, B. Q. Potent and selective inhibitors of PI3K delta: Obtaining isoform selectivity from the affinity pocket and tryptophan shelf. *Bioorg. Med. Chem. Lett.* **2012**, *22*, 4296−4302.

(146) Pike, K. G.; Morris, J.; Ruston, L.; Pass, S. L.; Greenwood, R.; Williams, E. J.; Demeritt, J.; Culshaw, J. D.; Gill, K.; Pass, M.; Finlay, M. R. V.; Good, C. J.; Roberts, C. A.; Currie, G. S.; Blades, K.; Eden, J. M.; Pearson, S. E. Discovery of AZD3147: a potent, selective dual inhibitor of mTORC1 and mTORC2. *J. Med. Chem.* **2015**, *58*, 2326−2349.

(147) Venkatesan, A. M.; Dehnhardt, C. M.; Delos Santos, E.; Chen, Z. C.; Dos Santos, O.; Ayral-Kaloustian, S.; Khafizova, G.; Brooijmans, N.; Mallon, R.; Hollander, I.; Feldberg, L.; Lucas, J.; Yu, K.; Gibbons, J.; Abraham, R. T.; Chaudhary, I.; Mansour, T. S. Bis(morpholino-1,3,5-triazine) derivatives: potent adenosine 5′-triphosphate competitive phosphatidylinositol-3-kinase/mammalian target of rapamycin inhibitors: discovery of compound 26 (PKI-587), a highly efficacious dual inhibitor. *J. Med. Chem.* **2010**, *53*, 2636−2645.

(148) Bago, R.; Malik, N.; Munson, M. J.; Prescott, A. R.; Davies, P.; Sommer, E.; Shpiro, N.; Ward, R.; Cross, D.; Ganley, I. G.; Alessi, D. R. Characterization of VPS34-IN1, a selective inhibitor of Vps34, reveals that the phosphatidylinositol 3-phosphate-binding SGK3 protein kinase is a downstream target of class III phosphoinositide 3-kinase. *Biochem. J.* **2014**, *463*, 413−427.

(149) Honda, A.; Harrington, E.; Cornella-Taracido, I.; Furet, P.; Knapp, M. S.; Glick, M.; Triantafellow, E.; Dowdle, W. E.; Wiedershain, D.; Maniara, W.; Moore, C.; Finan, P. M.; Hamann, L. G.; Firestone, B.; Murphy, L. O.; Keaney, E. P. Potent, selective, and orally bioavailable inhibitors of VPS34 provide chemical tools to modulate autophagy in vivo. *ACS Med. Chem. Lett.* **2016**, *7*, 72−76.

(150) Ronan, B.; Flamand, O.; Vescovi, L.; Dureuil, C.; Durand, L.; Fassy, F.; Bachelot, M. F.; Lamberton, A.; Mathieu, M.; Bertrand, T.; Marquette, J. P.; El-Ahmad, Y.; Filoche-Romme, B.; Schio, L.; Garcia-Echeverria, C.; Goulaouic, H.; Pasquier, B. A highly potent and selective Vps34 inhibitor alters vesicle trafficking and autophagy. *Nat. Chem. Biol.* **2014**, *10*, 1013−1019.

(151) Somoza, J. R.; Koditek, D.; Villasenor, A. G.; Novikov, N.; Wong, M. H.; Liclican, A.; Xing, W. M.; Lagpacan, L.; Wang, R.; Schultz, B. E.; Papalia, G. A.; Samuel, D.; Lad, L.; McGrath, M. E. Structural, biochemical, and biophysical characterization of idelalisib binding to phosphoinositide 3-kinase delta. *J. Biol. Chem.* **2015**, *290*, 8439−8446.

(152) Giordanetto, F.; Barlaam, B.; Berglund, S.; Edman, K.; Karlsson, O.; Lindberg, J.; Nylander, S.; Inghardt, T. Discovery of 9-(1-phenoxyethyl)-2-morpholino-4-oxo-pyrido[1,2-a]pyrimidine-7-carboxamides as oral PI3K beta inhibitors, useful as antiplatelet agents. *Bioorg. Med. Chem. Lett.* **2014**, *24*, 3936−3943.

(153) Ni, J.; Liu, Q. S.; Xie, S. Z.; Carlson, C.; Von, T.; Vogel, K.; Riddle, S.; Benes, C.; Eck, M.; Roberts, T.; Gray, N.; Zhao, J. Functional characterization of an isoform-selective inhibitor of PI3K-p110 beta as a potential anticancer agent. *Cancer Discovery* **2012**, *2*, 425−433.

(154) Frazzetto, M.; Suphioglu, C.; Zhu, J.; Schmidt-Kittler, O.; Jennings, I. G.; Cranmer, S. L.; Jackson, S. P.; Kinzler, K. W.; Vogelstein, B.; Thompson, P. E. Dissecting isoform selectivity of PI3K

inhibitors: the role of non-conserved residues in the catalytic pocket. *Biochem. J.* **2008**, *414*, 383−390.

(155) Pinson, J. A.; Zheng, Z. H.; Miller, M. S.; Chalmers, D. K.; Jennings, I. G.; Thompson, P. E. L-aminoacyl-triazine derivatives are isoform-selective PI3K beta inhibitors that target nonconserved Asp862 of PI3K beta. *ACS Med. Chem. Lett.* **2013**, *4*, 206−210.

(156) Foster, P.; Yamaguchi, K.; Hsu, P. P.; Qian, F.; Du, X. N.; Wu, J. M.; Won, K. A.; Yu, P. W.; Jaeger, C. T.; Zhang, W. T.; Marlowe, C. K.; Keast, P.; Abulafia, W.; Chen, J.; Young, J.; Plonowski, A.; Yakes, F. M.; Chu, F.; Engell, K.; Bentzien, F.; Lam, S. T.; Dale, S.; Yturralde, O.; Matthews, D. J.; Lamb, P.; Laird, A. D. The selective PI3K inhibitor XL147 (SAR245408) inhibits tumor growth and survival and potentiates the activity of chemotherapeutic agents in preclinical tumor models. *Mol. Cancer Ther.* **2015**, *14*, 931−940.

(157) Freitag, A.; Prajwal, P.; Shymanets, A.; Harteneck, C.; Nurnberg, B.; Schachtele, C.; Kubbutat, M.; Totzke, F.; Laufer, S. A. Development of first lead structures for phosphoinositide 3-kinase-C2gamma inhibitors. *J. Med. Chem.* **2015**, *58*, 212−221.

(158) Lannutti, B. J.; Meadows, S. A.; Herman, S. E. M.; Kashishian, A.; Steiner, B.; Johnson, A. J.; Byrd, J. C.; Tyner, J. W.; Loriaux, M. M.; Deininger, M.; Druker, B. J.; Puri, K. D.; Ulrich, R. G.; Giese, N. A. CAL-101, a p110 delta selective phosphatidylinositol-3-kinase inhibitor for the treatment of B-cell malignancies, inhibits PI3K signaling and cellular viability. *Blood* **2011**, *117*, 591−594.

(159) Kong, D. X.; Dan, S. G.; Yamazaki, K.; Yamori, T. Inhibition profiles of phosphatidylinositol 3-kinase inhibitors against PI3K superfamily and human cancer cell line panel JFCR39. *Eur. J. Cancer* **2010**, *46*, 1111−1121.

Appendix II

REVIEW ARTICLE

Structure and function of the open canicular system – the platelet's specialized internal membrane network

Maria V. Selvadurai & Justin R. Hamilton ⓘ

Australian Centre for Blood Diseases, Monash University, Melbourne, Australia

Abstract

The open canicular system (OCS) is an internal membrane structure found in platelets. First identified 50 years ago, the OCS comprises a tunneling network of surface-connected channels that appear to play an important role in platelet function. Yet, our understanding of how the OCS forms, how it functions, and what might regulate its structure and behavior remains fairly rudimentary. Structural abnormalities of the OCS are observed in some human platelet disorders. Yet, because platelets from these patients display multiple defects, the specific contribution of any OCS dysregulation to the impaired platelet function is unclear. However, recent studies have begun to shed light on mechanisms that regulate the OCS structure and to understand what influence the OCS has on overall platelet function. Advances in cellular imaging techniques have allowed whole-cell visualization of the OCS, providing the opportunity for a more detailed structural examination. Furthermore, recent work indicates that the modulation of the OCS structure may be sufficient to impact *in vivo* platelet function, opening up the intriguing possibility of manipulating the OCS structure as an anti-thrombotic approach. On the 50th anniversary of its discovery, we review here what is known about OCS structure and function, and outline some of the key microscopy tools for studying this intriguing internal membrane system.

Introduction

The open canicular system (OCS) is a complex intracellular network of surface-connected membrane channels found in platelets. It is now 50 years since the OCS was first described by Olav Behnke in his early electron microscopy studies at The University of Copenhagen (1). Behnke used transmission electron microscopy to identify the existence of two distinct membrane systems in rat platelets: the dense tubular system (DTS) and the OCS – referred to at the time as the surface-connected system (SCS) (1). Apart from their distinguishing physical features on examination by electron microscopy, the main point of difference between these two internal membrane structures was their continuity (OCS) or lack thereof (DTS) with the plasma membrane. Soon after this initial description, the seminal work of James White demonstrated the existence of the OCS in human platelets and began to provide the first indications of its function (2). White's extensive study of the OCS revealed roles in the transport of substances into and out of the platelet (3) and provided insights into the involvement of the OCS in platelet activation – both as a membrane reserve for the expansion required during platelet shape change and spreading (4) and in facilitating the release of alpha granule contents to the cell's exterior (5). At the time of writing this article, 59 of the 226 articles in PubMed containing the term 'open canicular system' were authored by James White. Twenty-six percent!

More recent studies have begun to shed light on the molecular basis of some of the functions of the OCS, as well as some factors that may regulate the OCS structure and function. Advances in 3D imaging techniques have allowed whole-cell visualization of the OCS, providing the opportunity for a more detailed structural examination. Furthermore, very recent work has shown that modulation of the OCS can impact platelet function, raising the intriguing possibility of targeting the platelet internal membrane system as a therapeutic option and highlighting the need for further research into the factors regulating OCS structure and function. On the 50th anniversary of its discovery, we review here what is known regarding the structure and function of the platelet's internal membrane network.

Platelet production and the role of the DMS

Platelets are produced by megakaryocytes – large cells with characteristic multilobular nuclei residing predominantly in the bone marrow. Similar to platelets, megakaryocytes possess an internal membrane system, known as the demarcation membrane system (DMS). The DMS is a network of membrane channels made up of flattened cisternae and tubules (6). Similar to the platelet OCS, the megakaryocyte DMS is derived from and is continuous with the plasma membrane (6–8) – it is easily accessible from the extracellular space and is electrophysiologically contiguous with the plasma membrane (9). A recent study by Eckly et al. characterized the biogenesis of the DMS by using

---

Correspondence: Justin Hamilton Justin.Hamilton@monash.edu Australian Centre for Blood Diseases, Monash University, L2, AMREP Building, The Alfred, Commercial Rd, Melbourne, Victoria, 3004 Australia

confocal and electron microscopy to observe the DMS at various stages of its development (7). Here, it was observed that the DMS is produced via invaginations of the megakaryocyte plasma membrane that begin at a focal site. As the megakaryocyte matures, the membrane invaginations form a pre-DMS, which subsequently expands as the cell differentiates (7). Vesicular membrane for this expansion is delivered to the site of the growing DMS by Golgi complexes. Lipids may also be transferred to the DMS for *de novo* membrane synthesis, via the endoplasmic reticulum (7). The study by Eckly et al. also used focused ion beam-scanning electron microscopy (FIB-SEM) to visualize in three dimensions the intertwined, complex network of channels of the mature DMS (7). As discussed below, this approach has also been used to visualize and analyze the platelet's internal membranes.

The DMS functions as a membrane reservoir that provides a source of plasma membrane for the formation of platelets (10). During platelet production, long processes, termed proplatelets, are extended from the megakaryocyte into the vasculature and sheared off by the forces of flowing blood (11). Beaded and barbell-shaped proplatelets may be released into the blood, where they are further subdivided into individual platelets in the bloodstream (12). It is well known that the polymerization of microtubules into filaments and the sliding of overlapping microtubules are necessary for proplatelet elongation from mature megakaryocytes (13), whereas actin polymerization allows for the branching of proplatelets, which increases platelet production (14). Here, both microtubules and actin filaments associate with the DMS in the process of platelet production.

OCS structure

The OCS develops via invaginations of what will eventually become the platelet plasma membrane (15). Its lipid composition is identical to that of the plasma membrane (16), and surface glycoprotein receptors are present at similar levels across the two membranes (17,18). The final form of the OCS is a complex, anastomosing network of interconnected and surface-connected membrane channels that spans the platelet interior. The channels of the OCS vary in diameter within individual platelets, with vacuolar sections as well as thinner tubular sections (19), and there is also variation in the amount of OCS between platelets from any one individual. On average, the channels of the OCS in human platelets occupy approximately 3–4% of the total platelet volume, as estimated from 2D TEM images (20) (Figure 1).
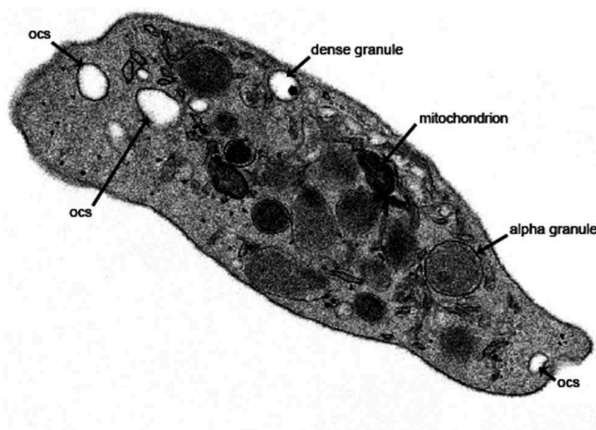

Figure 1. Anatomy of a platelet. TEM image of a human platelet, with the OCS, alpha granules, dense granules, and mitochondria visible. Scale bar, 0.5 μm.

Behnke's original study on platelet membrane systems also detailed the DTS, which is not linked to either the platelet plasma membrane or the OCS (1). In contrast to the OCS, subsequent studies of the DTS found that it is derived from the smooth endoplasmic reticulum of the megakaryocyte (21) and takes the form of long, thin tubules in resting platelets (22). The DTS regulates platelet behavior by either sequestering or releasing calcium, thus playing an important role in platelet activation (22). Although the DTS and OCS are not interconnected, they occasionally intertwine within the cell, forming membrane complexes that are present in the order of one to two per platelet (21).

Interestingly, not all mammalian platelets contain an OCS. Platelets from cow, horse, and camel all lack an internal membrane system (23–25), yet it is present in, among others, mouse, rat, rabbit, dog, and human platelets (1,2,26,27). This discrepancy does not appear to be related to evolutionary complexity, as an OCS-like structure is found in thrombocytes from lower vertebrates, including fish and frogs (28,29), as well as chickens (30). Why this variation between species exists and how it comes about remain unknown. Of note though, platelets without an OCS, including bovine, equine, and camelid platelets, have delayed responses to thrombin stimulation when compared to human platelets (31). Yet despite this, platelets from these species function relatively similarly to platelets from species with an OCS, raising the possibilities that the OCS is functionally redundant or that platelets lacking this internal membrane system have compensatory mechanisms to support any critical OCS functions.

OCS function

Uptake and release of platelet contents

A major function of the OCS is the transport of substances into and out of the platelet. Platelets have very little capacity for protein synthesis, so much of their cargo is taken up from plasma sources. This uptake largely occurs via the OCS, with a number of plasma proteins including fibrinogen (32) and tissue factor (33) taken up through channels of the OCS and then subsequently distributed to organelles within the platelet (e.g. alpha or dense granules). Behnke's early studies showed that particles added to platelet-rich plasma *in vitro*, or infused intravenously *in vivo*, were subsequently found in channels of the OCS, without any change in platelet morphology (1). White soon confirmed this finding and showed that thorium dioxide particles added to platelet-rich plasma were observed not only in OCS channels, but also in alpha granules – even when these granules had no visible physical association with the OCS (2). These early studies by the two pioneering researchers of OCS confirmed the 'open' nature of the OCS and revealed that these internal platelet channels are essentially exposed to the same medium as the platelet exterior.

The OCS also plays an important 'delivery' role in the release of substances stored in platelets to the cell exterior. Upon platelet activation, alpha and dense granules fuse with the OCS or plasma membrane, allowing release of their contents and potentiation of platelet activation (5,34). This process is regulated by SNARE proteins, a family of membrane-associated proteins that mediate membrane fusion. The distribution of SNARE proteins differs between granule membranes, and the plasma and OCS membranes, with the SNARE proteins VAMP 3 and 8 primarily found on granule membranes, SNAP-23 found on plasma and OCS membranes, and syntaxins 2 and 4 evenly distributed between both types of membrane (35). In the fusion of alpha and dense granules with OCS membranes, VAMP proteins on the granule surface interact with syntaxins 2 or 4 and SNAP-23 on the OCS membrane, linking tightly and forming an exocytic

core complex (36–38). This allows the two membranes to fuse, permitting the release of granule contents into the channels of the OCS and subsequently the platelet exterior. The rate of secretion of alpha granule contents has been shown to be dependent on both the concentration of the stimulating agonist and the time platelets are exposed to the stimulus (39). In platelets from species lacking an OCS, alpha granules fuse directly with the plasma membrane to release their contents (40). Intriguingly, a simple internal channel system appears to form in thrombin-activated bovine platelets (40). This *de novo* channel system, although much less extensive and complex than an OCS, connects to the exterior those granules not located at the plasma membrane and thereby facilitates release of the platelet's intracellular cargo (40).

More recently, it has also been suggested that the OCS plays a role in the regulation of platelet calcium signaling. Sage et al. found that the calcium signal in agonist-stimulated platelets was generated at, and propagated through, specific areas of the platelet, which matched the broad distribution and surface-linked nature of the OCS (41). Furthermore, impairment of the pericellular calcium signal reduced the magnitude of the agonist-induced cytosolic calcium signal as well as the rate of dense granule secretion. The authors thus proposed a model of pericellular calcium recycling, in which calcium released from the DTS following agonist stimulation moves into the OCS at specific locations – the membrane complexes where the DTS and OCS intertwine – from where it is recycled back into the platelet cytosol via calcium channels, to potentiate the calcium signal and trigger granule secretion (41).

Regulation of adhesion receptor levels

The OCS also functions as a storage site for platelet membrane receptors. Glycoprotein adhesion receptors on the membrane surface (most notably integrin $\alpha_{IIb}\beta_3$, the GPIb/XI/V complex, and GPVI) are particularly important for platelet function. It is notable then that the total pool of GPIb and inactive $\alpha_{IIb}\beta_3$ in a resting platelet is split evenly between the intracellular membranes of the OCS and the external plasma membrane (17,18). This large reserve of platelet adhesion receptors becomes important during platelet activation. For example, integrin $\alpha_{IIb}\beta_3$ levels at the cell surface increase in response to platelet activation, largely due to evagination of the OCS (4). Conversely, surface levels of the GPIb/XI/V complex are downregulated following platelet activation via sequestration into an intracellular pool on the OCS (42). In this way, the OCS appears to contribute to platelet activation by regulating levels of important cell surface adhesion receptors.

Membrane reserve

A further function of the OCS is to act as a membrane reserve for use during platelet activation (4). Following initial activation, platelets undergo a defined series of morphological changes – they lose their discoid shape and become spherical before extending filopodia, flattening, and spreading – all of which require additional membrane (43). Indeed, the surface area of a fully spread platelet is up to four-fold that of a resting platelet (44). The importance of the OCS in these processes is evidenced by bovine platelets, which lack an OCS and do not spread in response to surface activation (45). While bovine platelets do extend filopodia, the 'spreading' process does not proceed past this point, and flattened, spread platelets with lamellipodia are not observed (45) (Figure 2). Although possible that this could be attributable to differences in cytoskeletal organization between bovine and human platelets (45), the most likely explanation is a lack of membrane reserve.

OCS abnormalities in human platelets

Limited information on OCS function can be gleaned from human conditions. There are a number of clinical syndromes where abnormalities in the OCS have been documented, including some conditions that involve bleeding or thrombotic sequelae. However, platelets from patients with each of these conditions have a number of other structural abnormalities, making it difficult to ascertain the specific contribution of the OCS defect, if any, to any altered platelet function. For example, a dilated, hypertrophic OCS is seen in platelets from patients with Bernard–Soulier syndrome (BSS; Figure 3). BSS is the result of an abnormality in the gene encoding the GPIb (or occasionally GPIX) component of the GPIb/IX/V receptor complex and manifests as a bleeding disorder (46). More than 100 BSS-causing mutations in these genes have been identified, which impair either the expression of the receptor complex at the plasma membrane or the ability of the receptor to interact with von Willebrand factor (47). Yet, in addition to the OCS defect, platelets from these patients are also giant, exhibit disorganized microtubules, and have sparse or even absent granulation. A similar phenotype is observed in platelets from patients with MYH9-related disorders (e.g. May–Hegglin anomaly, Epstein syndrome, Fechtner syndrome). As with BSS, platelets from these patients exhibit not only a dilated and hypertrophic OCS, but also a pronounced macrothrombocytopenia and marked agranularity (17,48,49) (Figure 3). Intriguingly, Budd–Chiari syndrome, a rare prothrombotic condition characterized by hepatic vein or inferior vena cava thrombosis (50), also results in platelets with dilation and hypertrophy of the OCS (51). Yet, again, multiple other platelet ultrastructural defects are observed, including a general lack of organelle content (Figure 3). Finally, abnormal linkage of storage granules to the OCS has been implicated in alpha–delta platelet storage pool deficiency. In an ultrastructural study of multiple familial cases of the disease, it was found that alpha and dense granules were replaced by empty vacuolar structures in platelets from these patients, and that many of these vacuoles were connected to the OCS, suggesting that extraneous connections

Figure 2. Bovine platelets, which lack an OCS, fail to spread following surface activation. (A) Human platelets spread on a carbon-coated coverslip, showing spread platelets (SP) and 'dendritic'-looking platelets with numerous filopodia. (B) Bovine platelets under the same conditions, showing dendritic platelets (DPs) and resting platelets (RPs), but no spread platelets. Magnification x5000. Image reproduced with permission from ref 45.
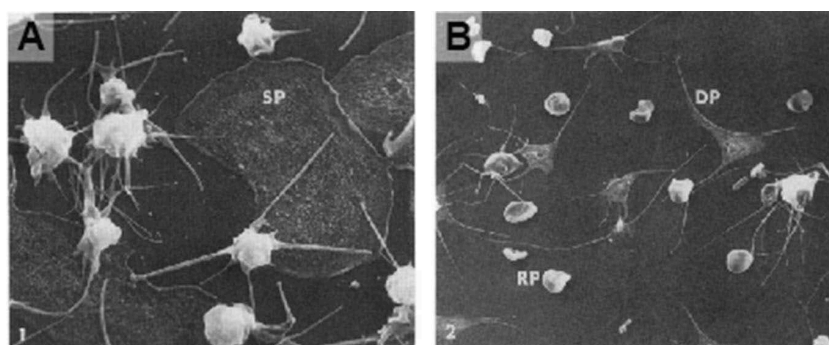
Figure 3. OCS abnormalities in human platelets. TEM images showing the ultrastructure of human platelets isolated from (A) healthy controls, or patients with (B) BSS, (C) Budd–Chiari syndrome, or (D) May–Hegglin anomaly. Note the dilated and hypertrophic OCS in the patients' platelets, but also the other structural abnormalities. All scale bars are 1 μm. Images reproduced with permission from refs 46 (B), 51 (C), and 17 (D).
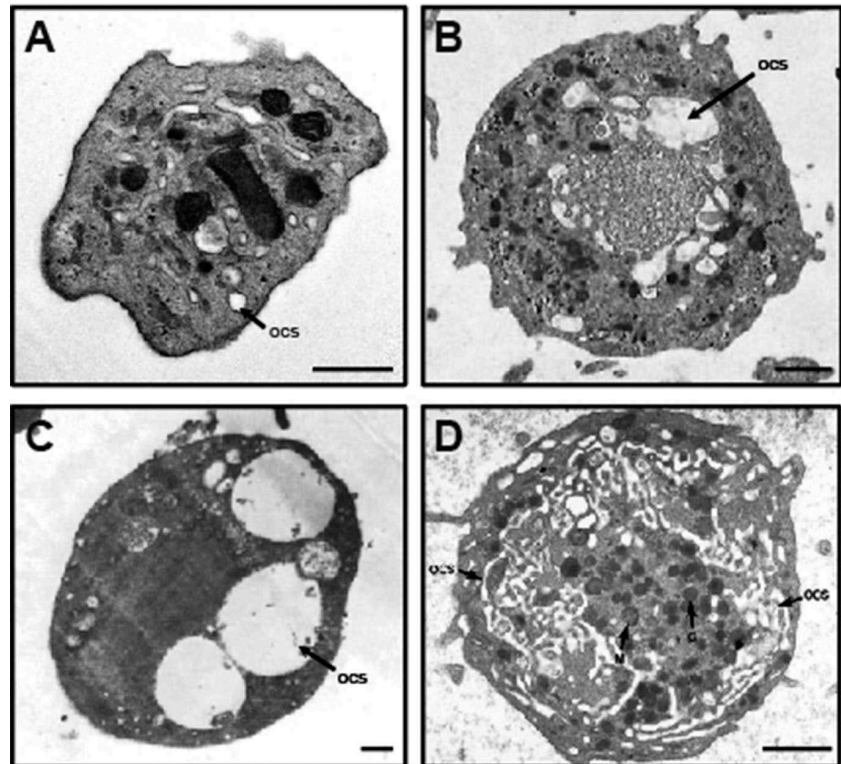
between the granules and OCS result in the loss of granule contents to the cell exterior in the absence of platelet activation (52). Given the lack of examples of a specific OCS defect in human platelets, direct evidence of OCS function has been limited to emerging information derived from genetically modified mouse models.

Regulation of OCS structure and function

Until recently, almost nothing was known about how the structure and function of the OCS might be regulated, apart from one study that suggested that cholesterol depletion of platelets with methyl-β-cyclodextrin may result in a collapse of the OCS (53). However, early clues on this came from studies implicating the phosphoinositide, PI(4,5)P$_2$, in the regulation of DMS structure and function. Schulze et al. found that the production of PI(4,5)P$_2$ by the phosphoinositide 4-kinase, PIP4Kα, contributes to megakaryocyte maturation and DMS organization, since depletion of PIP4Kα resulted in a loss of the largest, most mature cells in culture, and a lack of defined DMS (8). More recent work from Osman et al. showed that cationic amphiphilic drugs, such as the calmodulin inhibitor W-7, disrupt the DMS structure by binding to PI(4,5)P$_2$ and impairing its ability to interact with cytoskeletal proteins (54). For example, treatment of megakaryocytes with W-7 caused detachment of the DMS from the plasma membrane and collapse of the internal membrane network (54). Interestingly, W-7 similarly alters the structure of the platelet internal membrane system, with the surface area of the OCS (as visualized using TEM) significantly reduced following exposure of platelets to W-7 (54). These early studies hinted at a role for phosphoinositide regulation of the DMS and/or OCS structure and led to studies using mouse genetic models.

Following on from the pharmacological study by Osman et al. described above, two independent studies have shown that the class II phosphoinositide 3-kinase, PI3KC2α, appears to control the OCS structure. In the first of these studies, Mountford et al. used an inducible RNAi-based gene silencing approach to circumvent the early embryonic lethality of mice with a global PI3KC2α deficiency and essentially abolish PI3KC2α expression in mouse platelets. These PI3KC2α-deficient platelets had a specific structural defect in the OCS, manifesting as a dilation in TEM images and resulting in an increase in OCS surface area of approximately 40% compared with platelets from control mice (20). In contrast to all known clinical examples, the OCS defect in these platelets was not accompanied by any other structural abnormalities. Importantly though, the OCS structural defect was accompanied by impaired platelet function in the setting of thrombosis (delayed and unstable *in vivo* arterial thrombosis following electrolytic injury of the carotid artery) but not hemostasis (tail bleeding times were normal) (20). Interestingly, no alterations in PI3KC2α signaling were identified, with similar levels of all 3-phosphorylated phosphoinositides, the cellular products of PI3Ks, observed in platelets from both wild-type and PI3KC2α-deficient mice, potentially separating the changes in OCS structure from cellular activation status.

A subsequent study by Valet et al. used a distinct mouse model of PI3KC2α deficiency in which there was a kinase-inactivating point mutation in the PI3KC2α active site (55). Mice homozygous for this mutation were embryonically lethal, but heterozygous mice exhibited an approximate 50% reduction in PI3KC2α catalytic function. The authors confirmed the OCS structural defect and impaired *in vivo* thrombosis observed by Mountford et al. in these heterozygous PI3KC2α kinase-inactivated mice (55). Unlike the previous study, differences in PI3KC2α signaling were detected in platelets from these mice, with additional studies indicating that PI3KC2α regulates a basal pool of PI(3)P that may lead to impaired regulation of the platelet's cytoskeletal-membrane system, thereby identifying a potential mechanism by which the OCS structure may be controlled. Together, these initial studies suggest that regulating the structure and function of the OCS may have potential as a novel anti-thrombotic strategy and

highlight the value of continued research into factors affecting OCS structure and its function.

Tools for further study of the OCS

2D electron microscopy

Detailed study of the OCS structure is generally performed using electron microscopy. Indeed, the discovery of OCS was enabled by the advent of TEM. Standard TEM allows indications of the relative amount of OCS in a platelet, the size of the channels of the OCS, and can show surface openings, whereas the surface-linked nature of the OCS was determined using TEM imaging of platelets stained with cell-impermeable membrane dyes such as ruthenium red. SEM can also be used to image aspects of the OCS – specifically to look at OCS openings by examining the surface topology of the platelet's plasma membrane. However, there are a number of limitations of using two-dimensional imaging techniques to visualize the OCS. SEM provides only surface-level information and is therefore limited to examination of the number, size, and potential distribution of OCS openings, as well as general plasma membrane morphology. TEM provides only one slice through the platelet interior and at a random orientation, so does not infer what the entire internal membrane system in a given platelet may look like. As a result, changes in the distribution of the OCS or in the number or size of surface openings may be missed. These limitations in two-dimensional imaging techniques have led to more recent studies using three-dimensional approaches.

3D electron microscopy

The development of automated, serial-section, electron microscopy-based techniques has allowed a more sophisticated reconstruction of OCS structure in three dimensions and throughout the entire cell. The first of these methods to be used in platelet imaging, electron microscopy (EM) tomography, involves a series of images taken at different angular orientations of the sample, which are then aligned and merged to create a 3D representation of the sample (electron tomogram). Specific aspects within the sample, such as the OCS within a platelet, can be manually reconstructed from the tomogram. The first and most comprehensive EM tomography study of platelets to date was performed by van Nispen tot Pannerden et al., in which the authors used this technique to perform intricate reconstructions of OCS-DTS membrane complexes, as well as detailed analyses on the various subtypes of alpha granule present in the platelet (19). Although EM tomography can provide much useful information on platelet ultrastructure, limitations on the thickness of sections that can be imaged and the largely manual nature of the reconstruction limit

the capacity of this approach to produce accurate reconstructions of an entire platelet. For these reasons, with regard to the OCS, electron tomography may be the most useful for examining specific parts of the OCS within a platelet, as exploited to great effect by van Nispen tot Pannerden et al., such as its interactions with, or proximity to, other organelles.

A second 3D imaging technique, which is able to produce detailed whole-cell reconstructions of the platelet and its OCS, is FIB-SEM, as recently published by Eckly et al. (56). FIB-SEM is an automated microscopy technique involving the combined use of a scanning electron microscope and FIB technology (57) (Figure 4). This approach produces a series of sectional images, of comparable quality to traditional TEM, by sequentially using a gallium ion beam to remove thin layers of tissue from a sample and an electron beam to image each new block face (57,58). Components across these serial sections can be reconstructed to produce three-dimensional images of cell ultrastructure and sub-cellular structures. In the case of a platelet, these whole-cell 3D reconstructions produced using FIB-SEM show the entire OCS within any particular platelet, including both its network of connected channels within the cell and its openings at the plasma membrane (Figure 4). Organelles and smaller components can also be analyzed in detail. For example, Eckly et al. have, in addition to whole-cell platelet reconstruction, used FIB-SEM to show detailed changes in the ultrastructure of alpha and dense granules, and mitochondria, at various stages of platelet activation (56). As such, FIB-SEM provides more information than both traditional TEM and SEM combined, allowing quantitative information about the internal membranes of the whole cell, such as accurate determination of the total OCS volume. However, both the imaging and reconstructive analyses of FIB-SEM are very time consuming, making it impractical for analyzing large numbers of cells. A further limitation is the resolution of current approaches such that, as with TEM, particularly narrow channels of the OCS may be missed, resulting in a likely underestimation of the true interconnectivity of the system.

Conclusion

The OCS is a tunneling network of intracellular membrane channels found in platelets, which appears to play some important roles in platelet function. Yet, 50 years after its discovery, our understanding of how the OCS forms, how it functions, and what might regulate both its structure and its function remains fairly rudimentary. Structural abnormalities of the OCS occur in a number of human platelet function disorders – most of which are sufficient enough to cause significant clinical consequences – yet whether the OCS dysregulation per se contributes to the platelet function changes remains unknown. Recent studies in
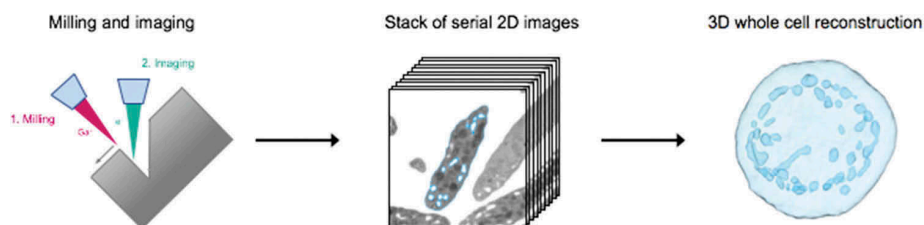

Figure 4. Whole-cell OCS analysis via FIB-SEM. FIB-SEM involves the resin-embedded sample being sequentially milled with a gallium ion beam and imaged with an electron beam. Each milling step removes 20 nm of embedded sample, and each image field for a platelet sample measures 15 μm x 15 μm. This stack of serial 2D images at 20 nm intervals is then segmented. Shown here is the segmentation of the OCS and plasma membrane of one platelet in cell suspension. A typical image stack for a whole-cell platelet reconstruction comprises 200–300 images. In this way, a whole-cell, 3D platelet reconstruction is produced. The reconstruction here shows the platelet plasma membrane and OCS. This image stack was produced at the Etablissement Français du Sang-Grand Est, Strasbourg, France, using a Helios NanoLab 600i FIB-SEM microscope. The reconstructed platelet was generated by MVS using 3D visualization software Amira.

mice indicate that modulation of the OCS structure may indeed be sufficient to impact *in vivo* platelet function and open up the intriguing possibility of manipulating the OCS structure as an anti-thrombotic approach. However, whether or not such an approach is achievable in human platelets in an acute fashion remains unknown. These studies, combined with recent advances in whole-cell microscopy, might help build on our understanding of this curious structure and determine whether manipulation of the OCS is a realistic therapeutic objective.

ORCID

Justin R. Hamilton ⓘ http://orcid.org/0000-0001-7554-6727

References

1. Behnke O. Electron microscopic observations on the membrane systems of the rat blood platelet. Anat Rec 1967;158(2):121–137.
2. White JG. The transfer of thorium particles from plasma to platelets and platelet granules. Am J Pathol 1968;53(4):567–575.
3. Escolar G, White JG. The platelet open canalicular system: A final common pathway. Blood Cells 1991;17(3):467–485. discussion 86-95.
4. Escolar G, Leistikow E, White JG. The fate of the open canalicular system in surface and suspension-activated platelets. Blood 1989;74(6):1983–1988.
5. White JG, Krumwiede M. Further studies of the secretory pathway in thrombin-stimulated human platelets. Blood 1987;69(4):1196–1203.
6. Behnke O. An electron microscope study of the megacaryocyte of the rat bone marrow. I. The development of the demarcation membrane system and the platelet surface coat. J Ultrastruct Res 1968;24(5):412–433.
7. Eckly A, Heijnen H, Pertuy F, Geerts W, Proamer F, Rinckel J-Y, et al. Biogenesis of the demarcation membrane system (DMS) in megakaryocytes. Blood 2014;123(6):921–930.
8. Schulze H, Korpal M, Hurov J, Kim SW, Zhang J, Cantley LC, et al. Characterization of the megakaryocyte demarcation membrane system and its role in thrombopoiesis. Blood 2006;107(10):3868–3875.
9. Mahaut-Smith MP, Thomas D, Higham AB, Usher-Smith JA, Hussain JF, Martinez-Pinna J, et al. Properties of the demarcation membrane system in living rat megakaryocytes. Biophys J 2003;84(4):2646–2654.
10. Radley JM, Haller CJ. The demarcation membrane system of the megakaryocyte: A misnomer? Blood 1982;60(1):213–219.
11. Junt T, Schulze H, Chen Z, Massberg S, Goerge T, Krueger A, et al. Dynamic visualization of thrombopoiesis within bone marrow. Science 2007;317(5845):1767–1770.
12. Thon JN, Macleod H, Begonja AJ, Zhu J, Lee K-C, Mogilner A, et al. Microtubule and cortical forces determine platelet size during vascular platelet production. Nat Commun 2012;3:852.
13. Patel SR, Richardson JL, Schulze H, Kahle E, Galjart N, Drabek K, et al. Differential roles of microtubule assembly and sliding in proplatelet formation by megakaryocytes. Blood 2005;106(13):4076–4085.
14. Rojnuckarin P, Kaushansky K. Actin reorganization and proplatelet formation in murine megakaryocytes: The role of protein kinase calpha. Blood 2001;97(1):154–161.
15. Choi E, Nichol J, Hokom M, Hornkohl A, Hunt P. Platelets generated in vitro from proplatelet-displaying human megakaryocytes are functional. Blood 1995;85(2):402–413.
16. Kosaki G. Platelet production by megakaryocytes: Protoplatelet theory justifies cytoplasmic fragmentation model. Int J Hematol 2008;88(3):255–267.
17. White JG, Krumwiede MD, Escolar G. Glycoprotein Ib is homogeneously distributed on external and internal membranes of resting platelets. Am J Pathol 1999;155(6):2127–2134.
18. Cramer EM, Savidge GF, Vainchenker W, Berndt MC, Pidard D, Caen JP, et al. Alpha-granule pool of glycoprotein IIb-IIIa in normal and pathologic platelets and megakaryocytes. Blood 1990;75(6):1220–1227.
19. van Nispen tot Pannerden H, de Haas F, Geerts W, Posthuma G, van Dijk S, Heijnen HF. The platelet interior revisited: Electron tomography reveals tubular alpha-granule subtypes. Blood 2010;116(7):1147–1156.
20. Mountford JK, Petitjean C, Putra HW, McCafferty JA, Setiabakti NM, Lee H, et al. The class II PI 3-kinase, PI3KC2alpha, links platelet internal membrane structure to shear-dependent adhesive function. Nat Commun 2015;6:6535.
21. White JG. Interaction of membrane systems in blood platelets. Am J Pathol 1972;66(2):295–312.
22. Ebbeling L, Robertson C, McNicol A, Gerrard JM. Rapid ultrastructural changes in the dense tubular system following platelet activation. Blood 1992;80(3):718–723.
23. Zucker-Franklin D, Benson KA, Myers KM. Absence of a surface-connected canalicular system in bovine platelets. Blood 1985;65(1):241–244.
24. Gader AG, Ghumlas AK, Hussain MF, Haidari AA, White JG. The ultrastructure of camel blood platelets: A comparative study with human, bovine, and equine cells. Platelets 2008;19(1):51–58.
25. Segura D, Monreal L, Perez-Pujol S, Pino M, Ordinas A, Brugues R, et al. Assessment of platelet function in horses: Ultrastructure, flow cytometry, and perfusion techniques. J Vet Intern Med 2006;20(3):581–588.
26. Kudo S, Onai H, Ogawa R. Response of blood cells to hemorrahagic shock in the dog. J Anesth 1987;1(1):51–61.
27. Liu LP, Shan CW, Liu XH, Xiao HC, Yang SQ. Effect of procainamide on ultrastructure of blood platelet in rabbits. Acta Pharmacol 1998;19(4):376–379.
28. Daimon T, Mizuhira V, Uchida K. Fine structural distribution of the surface-connected canalicular system in frog thrombocytes. Cell Tissue Res 1979;201(3):431–439.
29. Ferguson H. The ultrastructure of plaice (Pleuronectes platessa) leucocytes. J Fish Biol 1976;8(2):139–142.
30. Daimon T, Uchida K. Electron microscopic and cytochemical observations on the membrane systems of the chicken thrombocyte. J Anat 1978;125(Pt 1):11–21.
31. Choi W, Karim ZA, Whiteheart SW. Protein expression in platelets from six species that differ in their open canalicular system. Platelets 2010;21(3):167–175.
32. Harrison P, Wilbourn B, Debili N, Vainchenker W, Breton-Gorius J, Lawrie AS, et al. Uptake of plasma fibrinogen into the alpha granules of human megakaryocytes and platelets. J Clin Investig 1989;84(4):1320–1324.
33. Escolar G, Lopez-Vilchez I, Diaz-Ricart M, White JG, Galan AM. Internalization of tissue factor by platelets. Thromb Res 2008;122(Suppl 1):S37–41.
34. Fogelson AL, Wang NT. Platelet dense-granule centralization and the persistence of ADP secretion. Am J Physiol 1996;270(3 Pt 2):H1131–40.
35. Feng D, Crane K, Rozenvayn N, Dvorak AM, Flaumenhaft R. Subcellular distribution of 3 functional platelet SNARE proteins: Human cellubrevin, SNAP-23, and syntaxin 2. Blood 2002;99(11):4006.
36. Flaumenhaft R. Molecular basis of platelet granule secretion. Arterioscler Thromb Vasc Biol 2003;23(7):1152–1160.
37. Flaumenhaft R, Croce K, Chen E, Furie B, Furie BC. Proteins of the exocytotic core complex mediate platelet alpha-granule secretion. Roles Vesicle-Associated Membrane Protein, SNAP-23, Syntaxin 4 J Biol Chem 1999;274(4):2492–2501.
38. Polgár J, Chung S-H, Reed GL. Vesicle-associated membrane protein 3 (VAMP-3) and VAMP-8 are present in human platelets and are required for granule secretion. Blood 2002;100(3):1081.

39. White JG, Escolar G. The blood platelet open canalicular system: A two-way street. Eur J Cell Biol 1991;56(2):233–242.

40. White JG. The secretory pathway of bovine platelets. Blood 1987;69 (3):878–885.

41. Sage SO, Pugh N, Farndale RW, Harper AG. Pericellular Ca(2+) recycling potentiates thrombin-evoked Ca(2+) signals in human platelets. Physiol Rep 2013;1(5):e00085.

42. Hourdille P, Heilmann E, Combrie R, Winckler J, Clemetson KJ, Nurden AT. Thrombin induces a rapid redistribution of glycoprotein Ib-IX complexes within the membrane systems of activated human platelets. Blood 1990;76(8):1503–1513.

43. Hartwig JH. The platelet: Form and function. Semin Hematol 2006;43(1 Suppl 1):S94–100.

44. Blair P, Platelet FR. α-granules: Basic biology and clinical correlates. Blood Rev 2009;23(4):177–189.

45. Grouse LH, Rao GH, Weiss DJ, Perman V, White JG. Surface-activated bovine platelets do not spread, they unfold. Am J Pathol 1990;136(2):399–408.

46. Maldonado JE, Gilchrist GS, Brigden LP, Bowie EJ. Ultrastructure of platelets in Bernard-Soulier syndrome. Mayo Clin Proc 1975;50 (7):402–406.

47. Savoia A, Kunishima S, de Rocco D, Zieger B, Rand ML, Pujol-Moix N, et al. Spectrum of the mutations in Bernard-Soulier syndrome. Hum Mutat 2014;35(9):1033–1045.

48. Jantunen E. Inherited giant platelet disorders. Eur J Haematol 1994;53(4):191–196.

49. White JG. Giant platelet disorders. Haematologica 2002;87:85–92.

50. Ludwig J, Hashimoto E, McGill DB, Van Heerden JA. Classification of hepatic venous outflow obstruction: ambiguous terminology of the Budd-Chiari syndrome. Mayo Clin Proc 1990;65(1):51–55.

51. Dayal S, Pati HP, Pande GK, Sharma P, Saraya AK. Platelet ultra-structure study in Budd-Chiari syndrome. Eur J Haematol 1995;55 (5):294–301.

52. White JG, Keel S, Reyes M, Burris SM. Alpha–delta platelet storage pool deficiency in three generations. Platelets 2007; 18(1):1–10.

53. Grgurevich S, Krishnan R, White MM, Jennings LK. Role of in vitro cholesterol depletion in mediating human platelet aggregation. J Thromb Haemost 2003;1(3):576–586.

54. Osman S, Taylor KA, Allcock N, Rainbow RD, Mahaut-Smith MP. Detachment of surface membrane invagination systems by cationic amphiphilic drugs. Sci Rep 2016;6:18536.

55. Valet C, Chicanne G, Severac C, Chaussade C, Whitehead MA, Cabou C, et al. Essential role of class II PI3K-C2alpha in platelet membrane morphology. Blood 2015;126(9):1128–1137.

56. Eckly A, Rinckel JY, Proamer F, Ulas N, Joshi S, Whiteheart SW, et al. Respective contributions of single and compound granule fusion to secretion by activated platelets. Blood 2016;128 (21):2538–2549.

57. Merchan-Perez A, Rodriguez JR, Alonso-Nanclares L, Schertel A, Counting Synapses DJ. Using FIB/SEM microscopy: A true revolution for ultrastructural volume reconstruction. Front Neuroanat 2009;3:18.

58. Bennett AE, Narayan K, Shi D, Hartnell LM, Gousset K, He H, et al. Ion-abrasion scanning electron microscopy reveals surface-connected tubular conduits in HIV-infected macrophages. PLoS Pathog 2009;5(9):e1000591.